Self Cleaning Paint: Introduction of Photocatalytic Particles into a Paint System

Gunnarsson, Sverrir Grimur; Møller, Per; Poulsen, Søren; Ottosen, Lisbeth M.

Publication date:
2012

Document Version
Publisher's PDF, also known as Version of record

Self Cleaning Paint: Introduction of Photocatalytic Particles into a Paint System

PhD Thesis

Sverrir G. Gunnarsson

DYRUP

DTU Mechanical Engineering
Department of Mechanical Engineering

Preface

This thesis is submitted to fulfil the requirements for a PhD degree from the Technical University of Denmark. The work presented here has been carried out at DTU Mechanical Engineering section of Materials and Surface Engineering and at Dyrup A/S from May 2008 to September 2011. The work has been supervised by Professor Per Møller, Søren H. Poulsen of Dyrup A/S and co-supervised by Lars P. Nielsen of the Danish Technological Institute, Associate Professor Lisbeth M. Ottosen and Curt Sander of Danish Micro Engineering A/S.

Acknowledgements

First and foremost I would like to express my gratitude to Per Møller and Søren H. Poulsen for their supervision of the project, continued support and the numerous stimulating discussions. Without their contribution and steadfast dedication none of this would have been possible. Furthermore I would like to thank the co-supervisors Lars P. Nielsen and Lisbeth M. Ottosen for their contributions to the project.

I would like to thank all my colleagues at DTU Mechanical Engineering for their help and for making the past few years so enjoyable. I would especially like to thank John Troelsen and Lars Pedersen from the workshop at DTU Mechanical Engineering for all their help and outstanding craftsmanship.

I would like to thank everyone at the R&D department at Dyrup A/S. I feel very fortunate to have been able to learn from their expertise and professionalism. I would especially like to thank David Löf, Bent Samuelsen and Nina Axelsen for their help and for providing inspiration that has greatly contributed to the project.

Kenny Ståhl and Astrid Schøneberg, DTU Chemistry, are acknowledged for their help and guidance with XRD measurements.

I would like to thank Jiří Vrána, Vladimír Špaček, Luboš Kácovský and Josef Vraštil of Synpo for their hospitality and valuable help with DMA measurements

Guenther Kaupp of Eckart GmbH is acknowledged for his assistance with taking the first steps towards actualising the project.

The evaluations team at the Atlas South Florida Test Service is acknowledged for their professionalism in evaluating and reporting on outdoor exposures.

The people at GEA Niro are acknowledged for their help with the spray drying equipment.

Abstract

The current industrial PhD work was aimed at synthesising a photocatalytic composite material which could be used to give organic wood paint films self-cleaning and anti-microbial properties. The current PhD work was done in collaboration between Dyrup A/S and Technical University of Denmark.
The paint industry constantly faces updated restriction on toxic chemicals as for instance biocides which has prompted the search for alternative strategies for increasing the durability of their products. Photocatalysts are generally known to have adverse effects on organic coatings due to the highly reactive chemical species created by the photocatalytic reaction, which can damage the coating itself. The novel strategy for integrating the photocatalyst into the coating proposed in this work however offers most of the benefits of such self-cleaning coatings without the disadvantages.
The thesis consists of an introduction to relevant concepts and literature followed by results, presented as research papers, and a patent application. Four research papers are introduced as individual chapters. Chapter 4 discusses the synthesis and optimisation of anatase TiO_2 coated microspheres, chapter 5 discusses the self-cleaning properties and degradation mechanisms of photocatalytic organic coatings containing TiO_2 coated microspheres, chapter 6 discusses the rheological and mechanical properties of such coatings and chapter 7 discusses the durability and weather stability of photocatalytic self-cleaning coatings containing TiO_2 coated microspheres.
The results show that introducing a photocatalyst into an organic paint system as a coating on inert carrier particles results in durable and weather stable paint films. The paint films exhibit self-cleaning properties and are able to resist the attack of micro-organisms. The effect of the photocatalytic reaction on the organic binder is found to be minimal and the films are found to be more durable during outdoor exposure than conventional paint systems. The microspheres only influence the paint viscosity to a small degree and although the mechanical properties are generally degraded by the rigid filler the actual performance is improved by an altered mechanism for crack propagation in the films.
The project was funded by Dyrup A/S and the Danish Agency for Science and Innovation.

Resume (in Danish)

Denne erhvervs PhD afhandling har søgt at udvikle et fotokatalytisk kompositmateriale, som kan anvendes til at give en organisk træmalingsfilm selvrensende og antimikrobielle egenskaber. Projektet er et samarbejde mellem Dyrup A/S og DTU.
Malingsindustrien søger til stadighed at mindske brugen af potentielt skadelige tilsætningsstoffer, som f.eks. biocider, hvilket har bevirket at der søges alternative strategier til at forøge holdbarheden af malingsprodukter. Fotokatalysatorer er almindeligt kendt for at have uønskede effekter på organiske belægninger, idet de stærkt reaktive specier, der dannes ved de fotokatalytiske reaktioner, kan nedbryde malingsfilmen. En ny strategi for at integrere en fotokatalysator i en organisk malingsfilm er forsøgt i dette forskningsprojekt, hvorved de gavnlige virkninger fra fotokatalysatoren er bibeholdt, mens uønskede bivirkninger er minimeret.
Afhandlingen består af en introduktion til relevante begreber og mekanismer samt en introduktion til relevant litteratur. Resultaterne der er opnået i dette forskningsprojekt er præsenteret som fire individuelle videnskabelige artikler. Kapitel 4 angår syntese og optimering mikro-sfærer belagt med af anatase TiO_2. Kapitel 5 angår de selvrensende egenskaber af organiske malingsfilm, indeholdende mikro-sfærer belagt med anatase TiO_2, samt nedbrydningen af malingens binder, mens kapitel 6 angår de reologiske og mekanisk egenskaber af sådanne malingsfilm. Kapitel 7 angår holdbarheden og vejrbestandigheden af fotokatalytiske, selvrensende malingsfilm med TiO_2 belagte mikro-sfærer. Resultaterne viser, at introduktion af en fotokatalysator som belægning på inerte mikro-sfærer producerer holdbare og vejrbestandige malingsfilm. Det vises, at malingsfilmene udviser selvrensende egenskaber, og kan modstå angreb fra mikroorganismer. Nedbrydningen af malingsfilmens bindermateriale, grundet de fotokatalytiske reaktioner, er minimalt, og malingsfilmene er fundet at være mere modstandsdygtige overfor udendørs eksponering end konventionelle malingsfilm. Tilsætningen af de fotokatalytiske mikro-sfærer påvirker kun malingens viskositet i lav grad, mens de mekaniske egenskaber påvirkes i negativ retning. På trods af de forringede mekaniske egenskaber udviser den ny-udviklede malingsfilm forbedrede modstand over for revnedannelse, idet de inkorporerede fillerpartikler ændrer mekanismen for revneudbredelse.
Projektet er finansieret af Dyrup A/S og Ministeriet for Videnskab og Innovation.

List of abbreviations

ALD	Atomic Layer Deposition
CVD	Chemical Layer Deposition
DMA	Dynamic Mechanical Analysis
EDS	Electron Dispersive X-ray Spectroscopy
HGMS	Hollow Glass Microspheres
SEM	Scanning Electron Microscope
SGMS	Solid Glass Microspheres
SHE	Standard Hydrogen Electrode
TTIP	Titanium Tetra-Isopropoxide
UV	Ultra Violet
XRD	X-Ray Diffraction

Table of contents

1 Introduction

1.1 Background

For a number of years the coatings industry has been attempting to develop self-cleaning / easy-to-clean coatings with a long lasting effect. Such coatings require less maintenance and remain aesthetically pleasing for a longer period than a normal coating.
There are mainly two strategies for creating such surfaces, which are to either design a highly hydrophobic or highly hydrophilic surface [1]. A hydrophobic surface accomplishes the desired effect by repelling water droplets from a surface so instead of wetting the surface they roll off removing dirt particles in the process [2][3]. This is known as the lotus effect due to the lotus flowers unique ability to keep itself clean. The super-hydrophobicity is achieved by a special nano-structured surface, as shown in Fig. 1-1, which significantly reduces the contact area between the surface and a water droplet or immobilised dirt particle. The reduced contact area means that the adhesion force between a dirt particle and the surface is small and the dirt is therefore easily removed by a drop of water rolling off the surface. These surfaces have good self-cleaning properties but have limited application due to the sensitivity of the surface to mechanical wear which can alter the surface structure thereby negating the lotus effect [1].

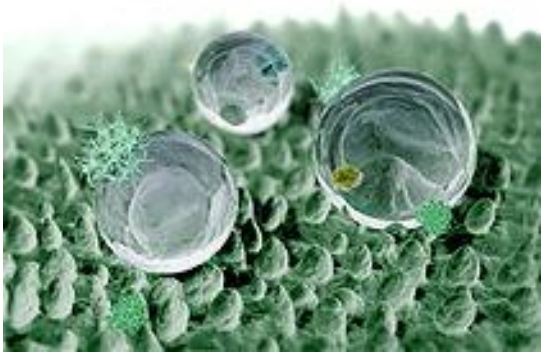

Fig. 1-1. Illustration of the surface structure of a lotus leaf [4].

Super-hydrophilic surfaces on the other hand accomplish a self-cleaning effect by retaining a thin film of water on the surface which prevents dirt from adhering to the surface. This strategy can be combined with photocatalysis due to the super-hydrophilic nature of photocatalytic TiO_2. The generation of highly reactive OH radicals is catalysed by the photocatalyst as it absorbs UV light. OH radicals have an extremely high oxidation potential and can therefore break down any organic material which has immobilised on the surface. The efficiency of photocatalytic materials for attaining self-cleaning properties has been known for many years. The technology has been used for cleaning glass and was first patented by Pilkington in 2002 and is sold under the brand name Pilkington Activ^{TM} [5]. The Pilkington patent is based on coating glass with photocatalytic anatase TiO_2, which is the most effective known photocatalyst [1]. Introducing such a material into an organic paint system is however very difficult because the strongly oxidizing OH radicals, generated as a results of UV exposure, can decompose the organic resin in the paint. The destructive effect of TiO_2 pigments on organic binders has for a long time been known to the paint industry [6][7] which is why most TiO_2 pigments today are stabilised to reduce their photoactivity [8].

Photocatalytic paints have mostly been formulated with anatase nano-particles due to the high photoactivity of such particles but these attempts have not been sufficiently successful due to the rapid degradation of the binder [9][10]. As a result of this it seems the coatings industry has mostly diverted its attention from photocatalytic paints.
Photocatalytic paints are however a very interesting option for paints intended for wood protection. In addition to making a surface self-cleaning the OH radicals can potentially keep the surface free of micro-organisms. Regulations regarding the use of toxic anti-microbial chemicals are constantly becoming stricter which limits the application of currently used solutions and makes it more expensive and difficult to introduce new chemicals. Photocatalysis is therefore an attractive strategy for keeping a surface free of dirt and micro-organisms because TiO_2 is non-toxic and has no environmental restrictions. Furthermore the effect is long lasting as the TiO_2 only functions as a catalyst and is therefore not used up in the reaction. It is however necessary to develop more robust photocatalytic organic paint where the effect of the photocatalyst on the binder is minimised.

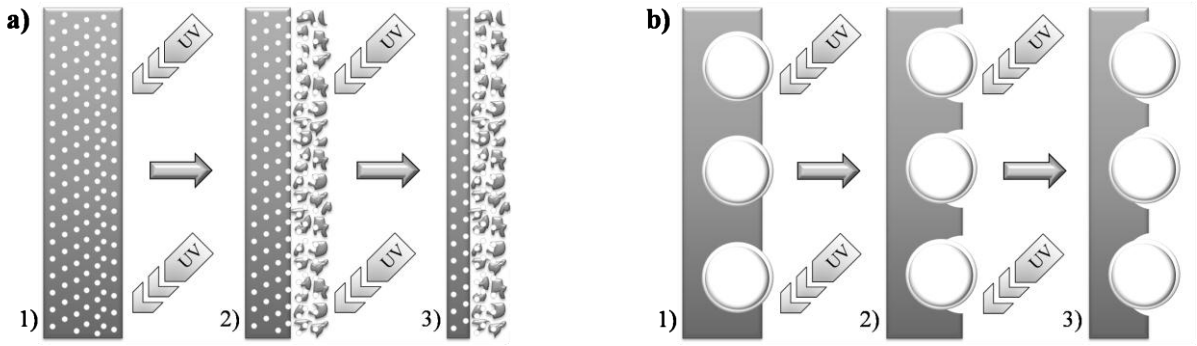

Fig. 1-2 a) shows a film with nano-particles constantly eroding from 1) to 3) during UV exposure. b) shows a film with photocatalytic carrier particles 1) Fresh film, 2) After initial exposure chalking has occurred, 3) Chalking has nearly ceased as UV radiation no longer reaches carrier particle/binder interface and the much slower photochemical degradation of the binder system becomes the predominant degradation process.

The aim of this work has been to develop such a system and this has been done by integrating the photocatalyst into the paint as a thin coating on hollow glass microsphere carrier particles. This greatly reduces the contact area between the photocatalyst and organic binder. The glass particles are inert to the photocatalytic reaction and provide a surface, away from the organic binder, for the photocatalytic reaction to take place. The proposed degradation mechanism of such a paint film versus a paint film containing nano-particles is illustrated in Fig. 1-2. Nano-particles will quickly degrade the binder surrounding them and separate from the film due to their small size. The next layer of particles is then exposed where the same process will be repeated resulting in fast erosion of the paint film. Micron sized particles are however embedded much deeper in the film so although the binder surrounding the particles in the surface region is degraded the particle remains in the film. It is limited how deep into the film UV light can penetrate so after the initial degradation the photocatalysis will seize to affect the binder. Furthermore, due to the extremely short lifetime of OH radicals [11] it is impossible for them to diffuse from the site of formation and attack the binder. The paint film therefore has self-cleaning properties and at the same time the degradation of the binder is minimised.

1.2 Photocatalysis

The photocatalytic mechanism was first described by Fujishima et al [12] in 1972 and since then a great deal of research has been done on the subject. Photocatalysts have found many different applications [13] and new ones are still being developed. Serpone et al [14] published an article explaining various terms and definitions regarding photocatalysis and several excellent review articles covering various aspects of the field have been published [15][16][17].
The photocatalytic mechanisms can be described by a Langmuir-Hinshelwood process [14] which can be broken down into the following steps.

1. $M + S \rightarrow M_{ads}$ (Adsorption of reagent M on surface S)
2. $M_{ads} \rightarrow M + S$ (Desorption of M on S)
3. $Cat + h\nu \rightarrow e^- + h^+$ (Photo-excitation of catalyst by UV-radiation)
4. $M_{ads} + h^+ \rightarrow M^+_{ads}$ (Positive hole creates radical)
5. $M^+_{ads} + e^- \rightarrow M_{ads}$ (Radical decays by receiving an electron)
6. $M^+_{ads} \rightarrow product + S$ (Final product and surface returns to unexcited state)

The first two steps establish an adsorption-desorption Langmuir equilibrium of the reagent at the surface of the catalyst. These steps can be very important for the overall reaction rate. If the kinetics of adsorption of the reagent on the photocatalyst are slow this step will be rate determining. The third step shows the photo-excited state of the catalyst where the UV-radiation combined with the photocatalyst creates a positive hole in the valence band by promoting an electron to the conduction band. The energy needed for this to happen depends on the band gap of the photocatalyst. The larger the band gap is the shorter the wavelength of the light needs to be. Step four describes the creation of a radical when the positive hole in the valence band oxidizes the reagent M and decays in the process. Step five represents the decay of the radical when it receives an electron and finally step six describes the product yielded by the radical and the catalyst surface returning to an unexcited state.
Water is the most typical adsorbate for the reaction due to the super-hydrophilic nature of the photocatalytic surface. The super-hydrophilicity of the surface is explained by an increase in surface hydroxyl density as a result of photo-excitation [18][19]. The most typical radical created is therefore the OH radical which is highly reactive and has been measured to have an oxidation potential of $E^0 = 2{,}72V$ vs. SHE [20].
The effectivity of a photocatalyst is determined by the dominant de-excitation pathway. Fig. 1-3 illustrates several mechanisms for the de-excitation of a photocatalyst following photo-excitation. (a) is the surface recombination of an electron and a positive hole, (b) is the recombination of an electron and a positive hole in the bulk material, (c) is the reduction of an electron acceptor, A, such as O_2 and (d) the oxidation of an electron donor, D, like for instance a surface hydroxyl [15].

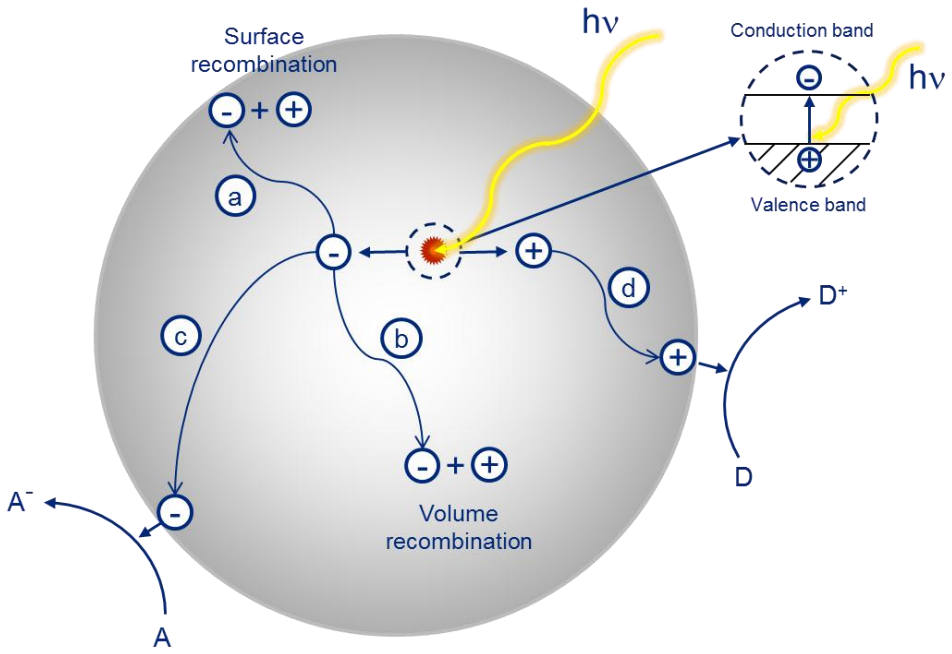

Fig. 1-3 Illustration of de-excitation pathways following photo-excitation.

The (a) and (b) mechanisms compete with the (c) and (d) mechanisms and the key to achieving high effectivity of the photocatalyst is to minimize (a) and (b). In order for adsorbate species to be oxidized the positive holes created in the bulk must migrate to the surface to create the radicals (D mechanism). The (c) pathway is also necessary to prevent a charge from building up on the surface because if the number of surface electrons, n_s, is much larger than positive holes at the surface, p_s, the recombination rate will be high and few positive holes left to oxidize the adsorbate. It has been shown that O_2 plays an important role as an electron scavenger that reduces surface recombination [21][22][15][23][24].

1.3 Titanium dioxide - TiO_2

Titanium dioxide is a naturally occurring oxide of titanium which is never found pure in nature. It is produced from $TiCl_4$ or $Ti(SO_4)_2$ precursors which are produced from titanium rich ore by the chloride process and sulphate process, respectively. TiO_2 is a very stable material which is used worldwide in large amounts mostly as pigment. Titanium dioxide is the most effective white pigment because of its high refractive index. Titanium dioxide can have three different crystal structures which are called brookite, anatase and rutile. Fig. 1-4 shows the crystal structure of rutile and anatase. Brookite is rare and isn't used for any industrial applications. Rutile is the most widely used white pigment as it has a slightly higher refractive index than anatase and is less photoactive.

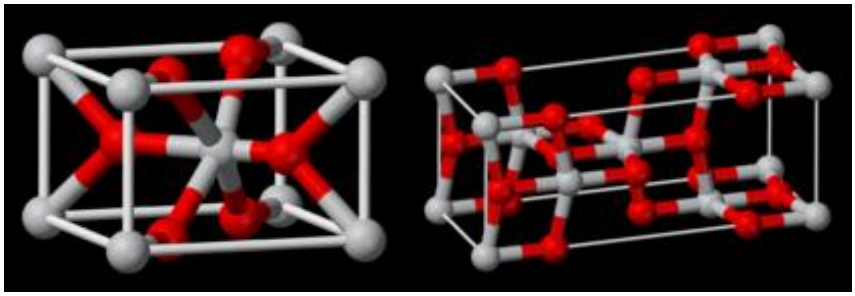

Fig. 1-4 Rutile crystal structure (left), anatase crystal structure (right). Red spheres represent oxygen atoms and grey titanium atoms.

Anatase can be formed over a wide range of temperatures depending on the process. Some report making anatase at temperatures below 100°C and up to 900°C. Generally though anatase is not thermally stable at high temperatures and is converted to rutile. This can happen over a range of temperatures of about 500 to 1000°C depending on the process. [25][26][27][28][29]

Both rutile and anatase are photocatalytic. TiO_2 is a good photocatalyst because the rate of recombination of electrons, freed by photo excitation, and positive holes is slow compared to other photocatalytic materials. Although rutile has a smaller band gap than anatase, and therefore absorbs a wider range of wavelengths, anatase is a much more effective photocatalyst due to a slower recombination rate [15].

1.4 Introduction to paint

Paint is any liquid material that can be applied to a substrate which after drying is converted to a thin opaque or transparent well adhering solid film. Paints are mainly used for decorative and/or protective purposes. This includes masonry coatings, wood stains, marine coatings etc. A wide variety of paints with special functionality are also used such as intumescent coatings, light reflective coatings, heat insulating coatings etc. Numerous types of binder systems exist for different applications but what most paints have in common is that they are made up of binder, pigment, filler, solvent and additives.
Paint is normally produced by mixing a liquid medium of binder(s) and solvents together with insoluble powders of pigments and extenders, plus sometimes additives, into a so-called premix. The pigments and extenders consist of primary particles agglomerated into small lumps that are divided and dispersed mechanically in a so-called grinding process. The grinding process evenly distributes and wets (with binder) pigments and extenders that secures the quality of the paint film. After the grinding process the paint can be thinned further.

The most important factors for high quality and long lifetime of paint systems are

- The substrate (steel, wood, concrete, plastics).
- Weather and working conditions (sunlight, rain, indoor, outdoor).
- Pre-treatment of the surface (sanding, abrasive blasting, cleaning etc.).
- Film quality.
- Choosing the right paint system for the application.
- Equipment and application.
- Film thickness.

1.4.1 Binder

The binder is the film forming component of the paint. It is generally viewed as the most important ingredient as the film quality is very dependent on the binder. The binder gives the coating adhesion to the substrate and cohesion between pigments and fillers. The physical properties of a paint film such as weather resistance, wear resistance, chemical and solvent resistance are highly dependent on the binder. Typical binders used for paints include both synthetic and natural resins like oils (tar), acrylics, polyesters, polyurethanes and epoxy.
Alkyd binders are commonly used for wood protection due to a combination of good properties for the application and relatively low price. Alkyds are oxidative cross linking paints which are cured by evaporation of solvents together with exposure to oxygen from the air. The binder contains drying oil that reacts with oxygen and causes the oil to polymerize and cross-link into large complex molecules, see Fig. 1-5.

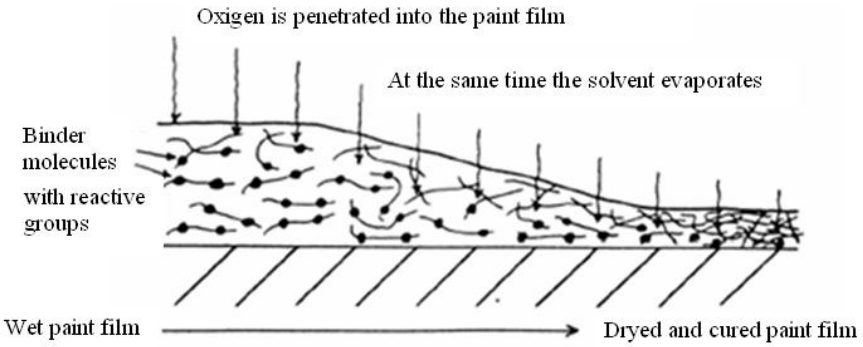

Fig. 1-5 Schematic of drying and curing mechanism of an oxidative cross-linking film [30].

The alkyd name is derived from the reaction of alcohol and acid or acid anhydride. Alkyds are typically manufactured by mixing appropriate amounts of acid anhydrides like phthalic acid anhydride or maleic anhydride with poly-alcohols like for instance glycerine. To get air drying properties the acid anhydrides and polyols are modified with drying oils. These drying oils are generally natural reaction products of glycerol and fatty acids like vegetable- or fish oil.
Amounts and type of drying oil in the polymer controls the oxygen reaction speed. Unsaturated fatty acids are able to polymerize and form a solid, coherent and adherent paint film. The air drying properties of the oils depends on the degree of unsaturated fatty acids together with organic metal salts driers of Co, Mn, and Zn which catalyse the cross-linking.
Alkyds are categorized by the relative fraction of drying oil components in the resin. These classes are called short, medium and long. Long oil alkyds contain over 60% fatty acids, medium about 40-60% and short contain less than 40%. Long and medium classes give softer and more flexible paint films; they dry slowly and have decent outdoor resistance, see Fig. 1-6. They are suitable for architectural and maintenance finish. Short oil alkyds are mainly used for industrial purposes. [31]

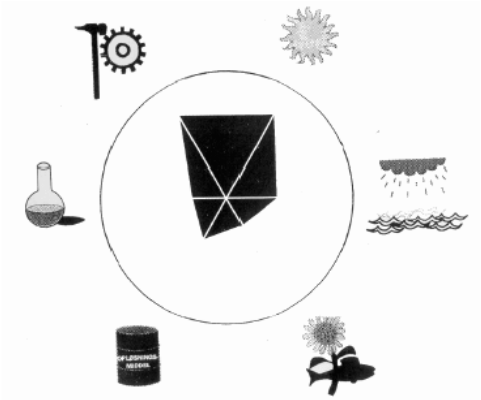

Fig. 1-6 Resistance property circle for medium oil alkyd binders [30]**.**

1.4.2 Pigment

Pigments are solid insoluble particles which give the paint film colour and hiding power. They also affect gloss, see Fig. 1-7, and flow in the paint film and the ability to protect the substrate from UV-light or water permeation. A wide variety of speciality pigments exists for applications such as corrosion protection, anti-fouling and more. Organic pigments normally give brighter colours and are more expensive than the inorganic pigments which give more matte earth toned colours.

Titanium dioxide is the worlds most used pigment as it is non-toxic and has excellent hiding power. [32]

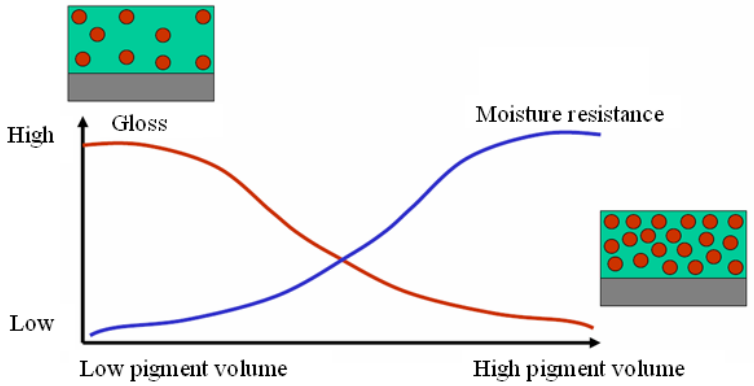

Fig. 1-7 Effect of pigment volume on gloss and moisture resistance [30].

1.4.3 Solvent (Vehicle)

Solvents are liquids with low viscosity which act as a carrier for the non-volatile paint components. They are used for adjusting the paints viscosity for easier application and flow control. Solvents play a large role in the film creation and control the drying time and flame point. They evaporate after application and are therefore not a part of the dried solid paint film. A wide range of solvents are used in paints such as alcohols, ketones, esters, glycol ethers, aliphatic or aromatic hydrocarbons and water [33].

1.4.4 Fillers

Fillers are normally opaque colour-neutral pigments which can serve to thicken the paint and adjust the gloss, mechanical- and applying properties. They are also used to give increased volume to the paint to lower finished product cost as fillers are normally inexpensive materials such as calcium carbonate, clay, talc and lime. [34]

1.4.5 Additives

All paints normally have a number of additives in small amounts. These additives have numerous different functions aimed at improving the properties of the paint. This can include pigments stability, wetting properties, control of foaming and skinning, reducing the drying- and curing time, fighting bacterial growth etc.

2 TiO_2 deposition on hollow glass microspheres

2.1 Properties of glass microspheres

Hollow glass microspheres (HGMS) were chosen as suitable carrier particles for the photocatalytic coating as they fulfil a number of the criteria deemed necessary. They can be added to paint in large quantities without having a large effect on the viscosity ,see chapter 6 , they are relatively inexpensive compared to other spherical fillers such as ceramic spheres, they have beneficial optical properties, see chapter 5, and most importantly they are inert to the photocatalytic reaction.
Several different types of both solid glass microspheres (SGMS) and HGMS were considered as possible candidates for use in the paint systems and they are listed in Table 2-1. Nevertheless only the HGMS were used for testing as their optical properties are preferred. The SGMS can however be interesting for the application as they have far higher strength and are available in smaller particle sizes. Fig. 2-1 shows an example of S38 type HGMS.

Product name	Type	Average size	Average density	Isostatic crush strength
iM30K	HGMS	15,5 µm	0,6 g/cm^3	193 MPa
S38	HGMS	40 µm	0,38 g/cm^3	28 MPa
Sphericel 60P18	HGMS	23 µm	0,6 g/cm^3	55 MPa
Sphericel 110P8	HGMS	11 µm	1,1 g/cm^3	67 MPa
Spheriglass 5000	SGMS	8,5 µm	2,5 g/cm^3	-
Spheriglass 7010	SGMS	4 µm	2,5 g/cm^3	-
Spheriglass 7025	SGMS	10,5 µm	2,5 g/cm^3	-

Table 2-1 Properties of glass microspheres.

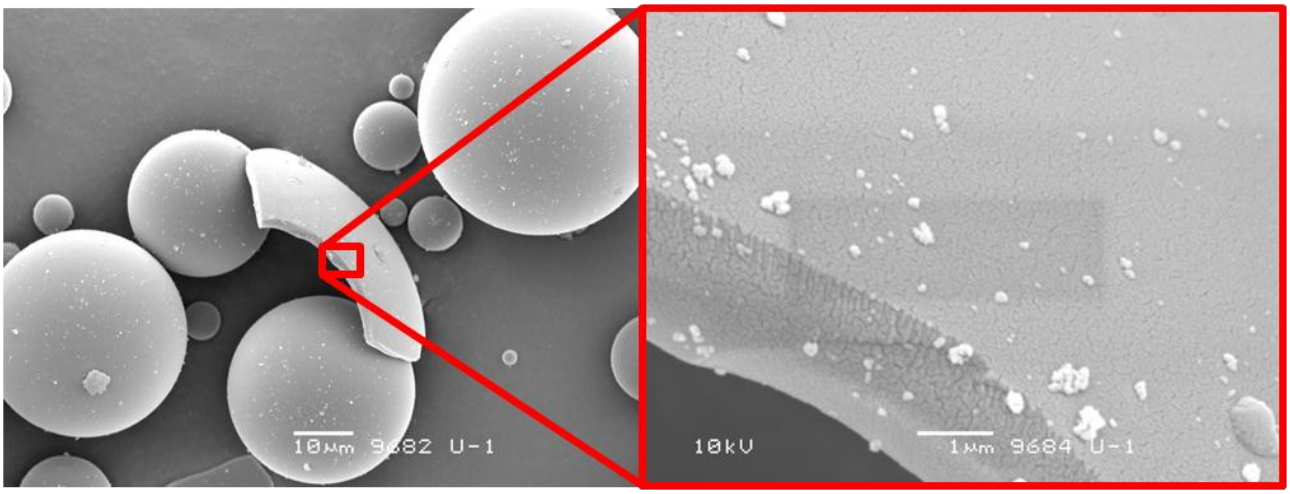

Fig. 2-1 Figure SEM images of uncoated S38 microspheres illustrating the smooth surface of the spheres.

The HGMS are made from soda-lime borosilicate glass and the solid microspheres from soda-lime glass. The approximate composition of the HGMS is:

- 70 -80 w/w% SiO_2

- 2 -6 w/w% B_2O_3
- 8 -15 w/w% CaO
- 3 -8 w/w% Na_2O
- 0 -10w/w% K_2O & Li_2O

The particle size distribution of the different types of HGMS and SGMS can be seen in Fig. 2-2 and Fig. 2-3, respectively

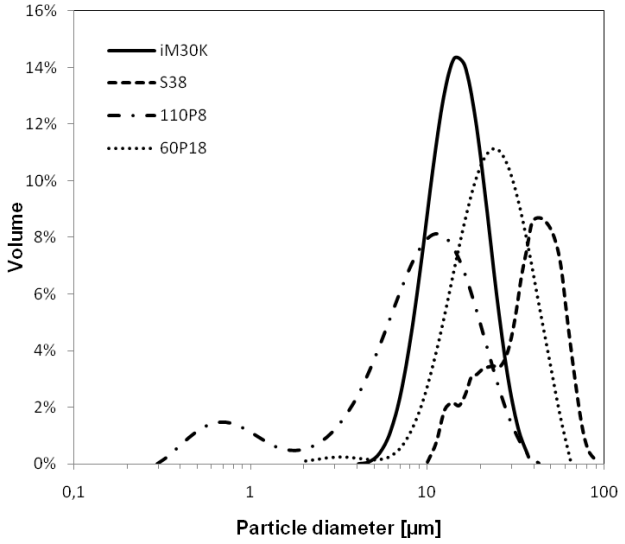

Fig. 2-2 Particle size distribution of hollow glass microspheres.

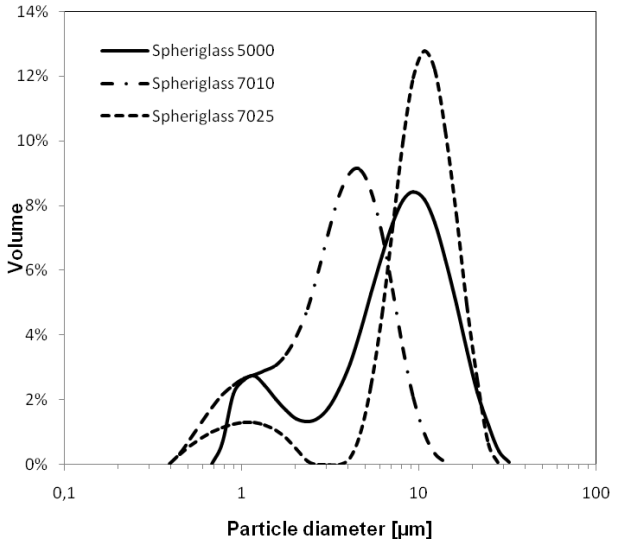

Fig. 2-3 Particle size distribution of solid glass microspheres.

2.2 Hollow glass microsphere surface

Glass is commonly considered chemically inert but that assumption is strictly speaking not correct. This assumption is based on the stability of glass and its high resistance to chemical attack but nevertheless there are reactive groups on the glass surface. Soda-lime borosilicate glass mostly consists of SiO_2 and various forms of hydroxyl groups can be found on the SiO_2 surface, often termed silanols. The different types of silanols are illustrated in Fig. 2-4 where a) is isolated silanols, b) is hydrogen bonded silanols and c) germinal silanols. Isolated silanols are single hydroxyl groups located too far from other groups to be able to interact with them. Hydrogen bonded silanols are hydroxyl groups in close proximity to one another and are therefore able to form hydrogen bonds. Geminal silanols are silanols where two hydroxyl groups are bound to a single silicon atom. These are however relatively rare and are believed to mostly exist at the end of chains of hydrogen bonded silanols [35]. Fig. 2-4 d) shows siloxane bridges which are formed when hydrogen bonded silanols condense as water on the surface. This has been shown to happen at temperatures above 190°C. The siloxane bridges are not very stable due to bond strain so the reaction is reversible unless the silica is heated above approximately 400°C where surface rearrangement can lower the bond strain [36]. Furthermore it has been shown that above 600°C only isolated silanols remain on the surface [35].

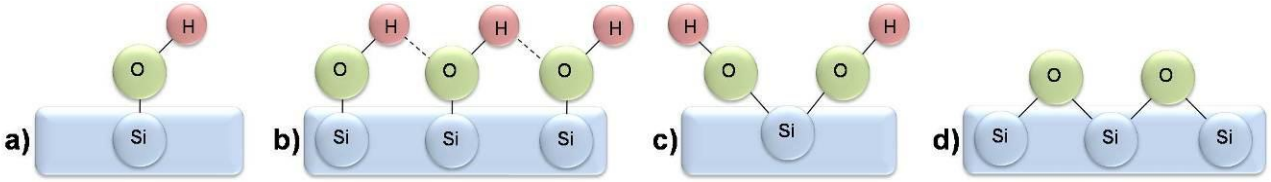

Fig. 2-4 Silanols on silica surface, a) isolated, b) hydrogen bonded, c) geminal and d) siloxane bridges.

Other oxides present in soda-lime borosilicate glass influence the hydroxyl concentration on the glass surface and for example Fry et al [37] and Rubio et al [38] have shown, by studying the adsorption isotherms of methanol on borosilicate glasses, that B_2O_3 decreases the hydroxyl concentration. However due to SiO_2 being the predominant constituent of the glass the reactions of titanium precursors with the glass will be discussed based on SiO_2 for simplification.

2.3 Titanium precursors

Three different types of titanium precursors were used for coating the microspheres. These were titanium tetra-isopropoxide, titanium tetra-chloride and titanium oxychloride which can be seen in Fig. 2-5.

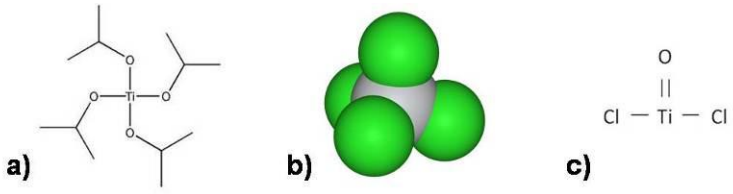

Fig. 2-5 Titanium precursors, a) TTIP, b) $TiCl_4$ and c) $TiOCl_2$.

Titanium-isopropoxide is a titanium alkoxide produced by reacting $TiCl_4$ with isopropanol, see Equation 2-1. It is a clear slightly viscous liquid which begins to hydrolyse when in contact with

atmospheric moisture. It isn't nearly as sensitive to water as $TiCl_4$ and is therefore a lot easier to handle. The hydrolysis reaction is shown in Equation 2-2.

$$TiCl_4 + 4(CH_3)_2CHOH \rightarrow Ti(OCH(CH_3)_2)_4 + 4HCl$$

Equation 2-1 $TiCl_4$ and isopropanol reaction

$$Ti(OCH(CH_3)_2)_4 + 2H_2O \rightarrow TiO_2 + 4(CH_3)_2CHOH$$

Equation 2-2 Hydrolysis of titanium isopropoxide.

Titanium tetra-chloride is a clear to slightly yellow liquid which is produced by chlorination of titanium ore with Cl_2 gas. It is extremely sensitive to water and the reaction is highly exothermic. When exposed to atmospheric moisture it gives off a thick white smoke which is a mixture of hydrochloric acid and TiO_2. Its reaction with water can be dangerous due to the highly concentrated hydrochloric acid released by the reaction. The hydrolysis reaction is shown in Equation 2-3.

$$TiCl_4 + 2H_2O \rightarrow TiO_2 + 4HCl$$

Equation 2-3 Hydrolysis reaction of titanium isopropoxide.

Titanium oxychloride is an aqueous solution of $TiCl_4$ which is highly acidic. It is a slightly yellow liquid that is prepared by partial hydrolysis of $TiCl_4$, see Equation 2-4, and it is only stable at very low pH. It is typically used for the production of TiO_2 pigments because it is less water sensitive than $TiCl_4$ and doesn't fume when exposed to atmospheric moisture. The hydrolysis reaction of titanium oxychloride can be seen in Equation 2-5.

$$TiCl_4 + H_2O \rightarrow TiOCl_2 + 2HCl$$

Equation 2-4 Partial hydrolysis of TiCl4.

$$TiOCl_2 + H_2O \rightarrow TiO_2 + 2HCl$$

Equation 2-5 Hydrolysis reaction of titanium oxychloride.

2.4 Reaction of titanium precursors with glass surface

The titanium precursors used for coating the microspheres all readily hydrolyse and can therefore react with silanols and form a covalent bond with the glass surface. Forming a covalent bond is important to ensure good adhesion of the TiO_2 coating to the substrate as shown in chapter 4. Srinivasan et al [39] investigated the interaction of TTIP with surface hydroxyls on silica. They investigated which sites act as the main adsorption sites for TTIP by studying the reactions on silica beads with different concentrations of silanols. They concluded that hydrogen bonded silanols are the main adsorption sites and that TTIP only weakly interacts with isolated silanols. The reaction of TTIP with hydrogen bonded silanols is illustrated in Fig. 2-6.

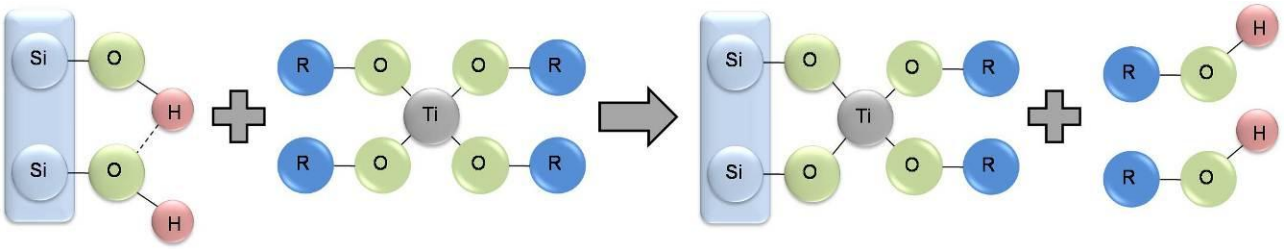

Fig. 2-6 Illustration of TTIP reaction with hydrogen bonded silanols

In order for TTIP to covalently bond with the glass surface the adsorption sites need to be free. Hair [40] and Young [41] have shown by studying the IR spectra of silica that hydrogen bonded silanols are also the main adsorption sites for water vapour. Therefore if physically adsorbed water isn't removed before coating the microspheres the titanium precursor is hydrolysed by adsorbed water rather than silanols. It is demonstrated in chapter 4 that failing to remove physically adsorbed water before coating the microspheres can result in poor adhesion while heat treating them above 100°C before further processing gives excellent adhesion.

2.5 Coating processes

2.5.1 Wet chemistry deposition of TTIP

A TiO_2 coating was deposited on S38, iM30K and 110P8 type microspheres in a wet chemistry process using TTIP as a precursor. In short the process consisted of dissolving TTIP in isopropanol and then dispersing the microspheres in the solution. After a short period of stirring de-ionised water was added to the solution to hydrolyse all remaining TTIP. This was followed by a filtration of the microspheres from the solution and mild heating to evaporate any remaining isopropanol. The next step was to crystallise the coating at high temperature after which another round of coating was applied to load more TiO_2 onto the spheres. Further details about the process can be found in chapters 4 and 5. This process worked well when coating the S38 microspheres as can be seen in Fig. 2-7 and no agglomeration of the microspheres was detected.

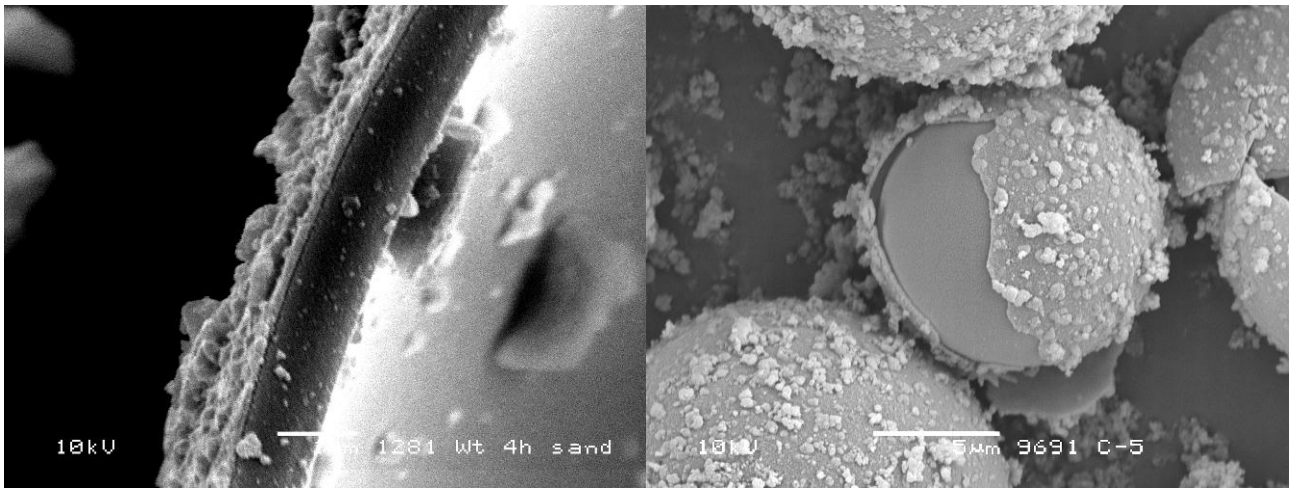

Fig. 2-7 Coated S38 microspheres. Sample heat treated before coating (left) and sample not heat treated before coating (right).

Attempting to coat smaller microspheres such as the iM30K and 110P8 types with the same process however resulted in large agglomerates forming as seen in Fig. 2-8. It was suspected that due to the smaller size the particles flocculated either during the filtration or drying phase and then formed inseparable agglomerates during calcination. This problem was later solved by returning the microspheres into the reaction vessel, after most of the isopropanol had been filtered off, and stirring continuously while heating mildly to allow the remaining alcohol to evaporate.

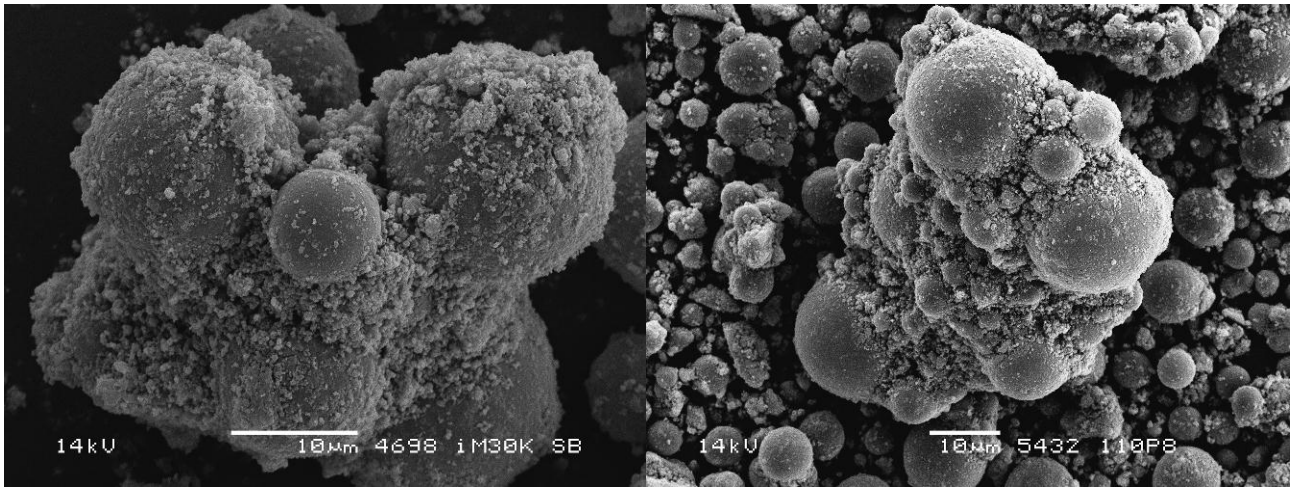

Fig. 2-8 Illustrates agglomerated microspheres after coating with unmodified TTIP process. iM30K (left), 110P8 (right).

To take steps towards realising industrial scale production of TiO_2 coated microspheres a company that produces pearlescent pigments, Eckart GmbH, was approached. Pearlescent pigments are produced by depositing a very uniform TiO_2 layer on mica flakes. Four different samples of coated 110P8 microspheres were received from Eckart. The precise details of the coating process are not known as it is a trade secret but it is believed to be done by hydrolysis of either titanium oxychloride or titanium oxysulfate as that is a common route for the synthesis [42]. Fig. 2-9 shows a comparison of the coating obtained on 110P8 microspheres by the TTIP wet chemistry process and the VP07 sample received from Eckart.

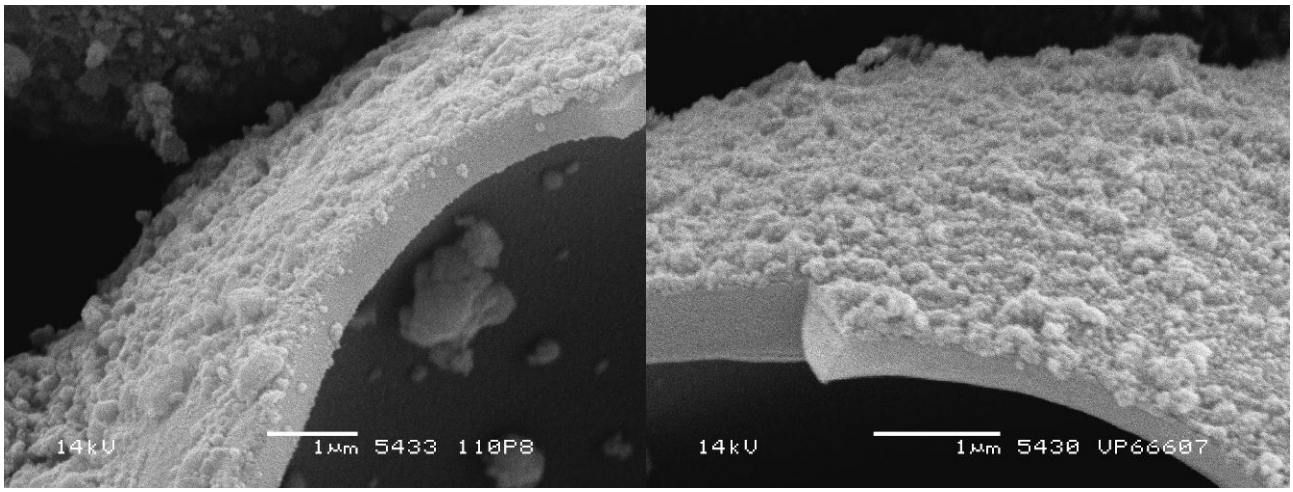

Fig. 2-9 Illustrates a microsphere coated with the TTIP wet chemistry process (left) and a microsphere coated at Eckart GmbH most likely by hydrolysis of either titanium oxychloride or titanium oxysulfate.

Two of the samples received from Eckart, VP07 and VP09, were intended to have the rutile structure and the other two, VP06 and VP08, the anatase structure. A thin layer of tin oxide is known to promote the formation of rutile on a mica substrate [42][43] and the VP07 and VP09 samples were therefore coated with SnO_2 before the TiO_2 layer was deposited. An XRD analysis of the samples however revealed that only one sample had the rutile structure and the others anatase, as shown in Fig. 2-10. This suggests that the microsphere surface promotes anatase formation.

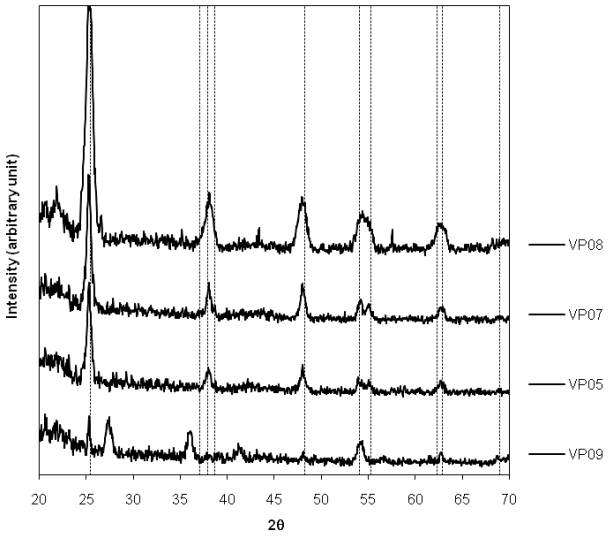

Fig. 2-10 XRD spectra of coated 110P8 samples received form Eckart. The broken lines show represent the peak positions for the anatase crystal structure.

SEM analysis of the microspheres coated by Eckart revealed some instances of poor adhesion which is believed to be due to physically adsorbed water on the microsphere surface as discussed in chapter 4. Fig. 2-11 shows the VP09 sample where large parts of the coating have disbonded.

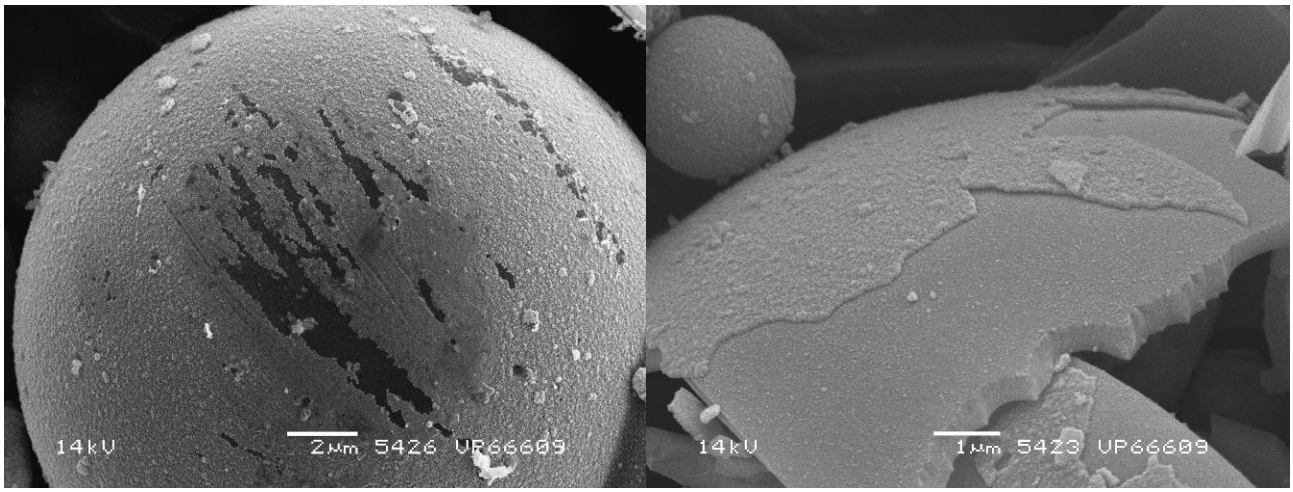

Fig. 2-11 Illustrates poor adhesion of TiO_2 coating on the VP09 sample received from Eckart GmbH.

2.5.2 Wet chemistry deposition of titanium oxychloride

Titanium alkoxides, such as TTIP, are far more expensive than titanium oxychloride or titanium oxysulfate and therefore have limited commercial interest. It was therefore attempted to deposit a TiO_2 coating on iM30K microspheres by thermal hydrolysis of titanium oxychloride. The process described by Ryu et al [44] was used with minor adjustments. 20g of iM30K microspheres were dispersed in 200ml de-ionised water and the pH adjusted to 1,6 by addition of HCl to prevent immediate precipitation of TiO_2 once introduced to the solution. A low pH is known to promote anatase formation whereas a high pH promotes amorphous TiO_2 [42]. The solution was heated to and maintained at 75°C during the entire process because temperatures of 65°C or lower are known to precipitate rutile [45][46]. 30ml of 5M titanium oxychloride was dispensed into the solution at a rate of 0,5ml/minute under continuous stirring. The solution was stirred for one hour and the pH slowly neutralised with aqueous ammonia. The slurry was filtered and thoroughly washed with de-ionised water to remove chlorides. Aqueous ammonia was chosen to neutralise the solution due to the reaction product ammonium chloride which decomposes at 338°C according to the reaction shown in Equation 2-6. The microspheres were calcined at 550°C which means any salt remaining after the washing phase would decompose into gases.

$$NH_4Cl \rightarrow NH_3 + HCl$$

Equation 2-6 Decomposition of NH4Cl above 338°C.

After the washing phase the water from the slurry was removed in a small test scale spray drying plant at GEA Niro to avoid agglomeration of the particles. GEA Niro is a Danish company which specialises in process equipment for spray drying, fluidised bed, freeze drying etc.
Fig. 2-12 shows a SEM analysis of the resulting TiO_2 coating on the microspheres. The process was clearly not successful as the microspheres were only partially coated. Furthermore large, approximately 1-3µm, precipitates were formed during the process which can be seen in Fig. 2-12. It is not entirely clear what happened as this process was not studied in detail. It is however believed that once the titanium precursor is introduced into the slurry and the hydrolysis begins to progress the solution becomes increasingly acidic thereby shifting the equilibrium towards a more stable titanium oxychloride. The solution pH was measured to drop under zero during the

hydrolysis which may have either slowed down or halted further hydrolysis. It is furthermore believed that once the ammonia is introduced into the solution and the pH rises sharply that the large precipitates, which were observed, are formed.

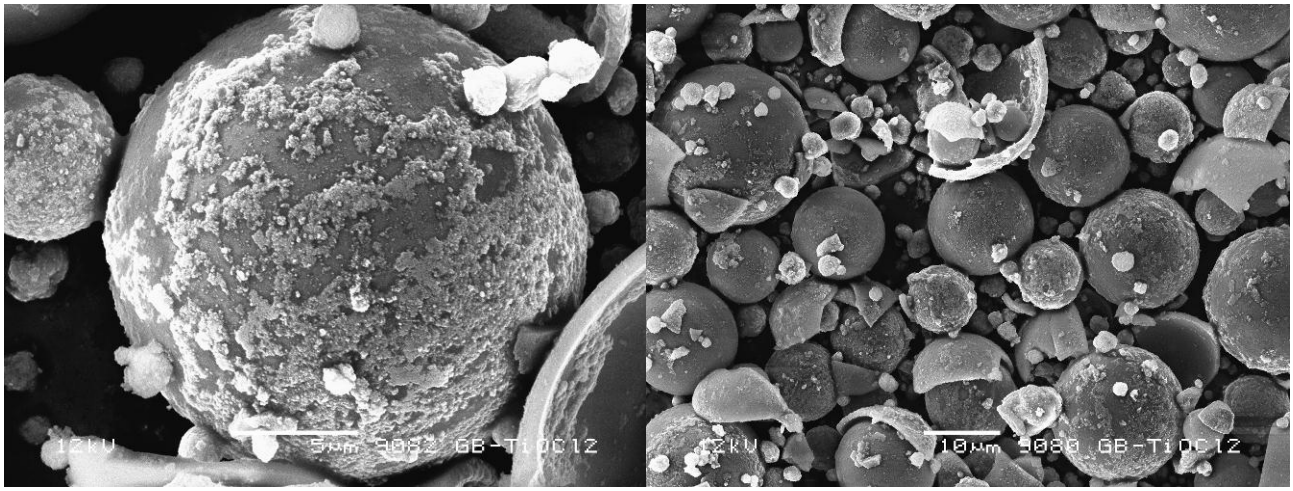

Fig. 2-12 Illustrates imperfect deposition on the microspheres and formation of approximately 1-3µm TiO_2 precipitates.

The crystal structure of TiO_2 coating and precipitates was analysed by XRD and found to be of the anatase structure. The spectrum is shown in Fig. 2-13.

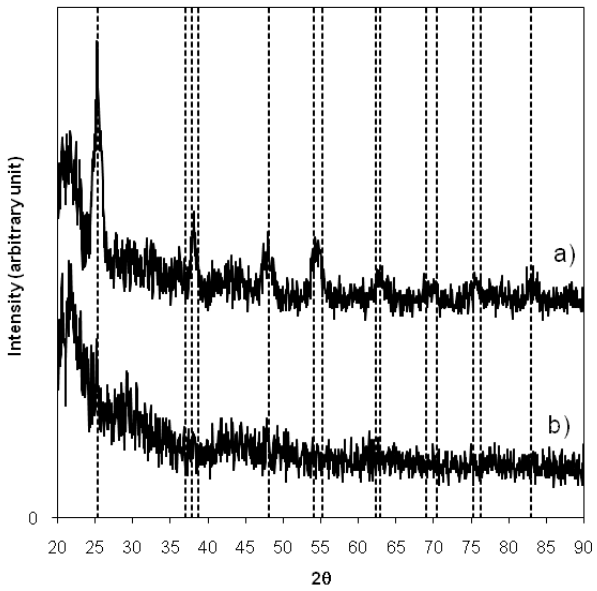

Fig. 2-13 Shows the XRD spectrum of a) the coated iM30K microspheres obtained by thermal hydrolysis of titanium oxychloride and b) of uncoated iM30K microspheres. The broken lines show represent the peak positions for the anatase crystal structure.

2.5.3 Chemical Vapour Deposition process (CVD)

To avoid difficulties with particle agglomeration in the wet chemistry processes an attempt was made to develop a coating process where the deposition was done on dry microsphere from a vapour phase. The concept behind the process was to slowly evaporate $TiCl_4$ by heating it close to its boiling point and to deliver it to the reaction vessel by an inert gas where it would adsorb on the microspheres. The gas stream would then be switched to a different branch of the system and flow through a chamber with controlled humidity delivering water vapour to hydrolyse the $TiCl_4$.
The CVD setup is illustrated in Fig. 2-14. Nitrogen with low water content was passed by a flow meter through silica gel to further dry the gas. The path of the gas was controlled by two T-junctions with three branches in total. Only one branch was open at any given time. One of the branches passed through a container with $TiCl_4$ which was immersed in paraffin oil which was heated to 115°C. Nitrogen was bubbled through the precursor to carry it into the reaction vessel. Teflon tubing connected the $TiCl_4$ container and the reaction vessel. Another branch passed through a water container with a saturated NaCl solution which maintained a relative humidity of 75%. The last branch was connected directly to the reaction vessel and was used for purging the vessel before dosing more $TiCl_4$ into the system. Purging is important to avoid a gas phase reaction. This process was repeated several times to build up a coating layer. The microspheres in the reaction vessel were continuously stirred by a mechanical stirrer. The waste gas was bubbled through water to remove any excess $TiCl_4$ or HCl released by a hydrolysis reaction.

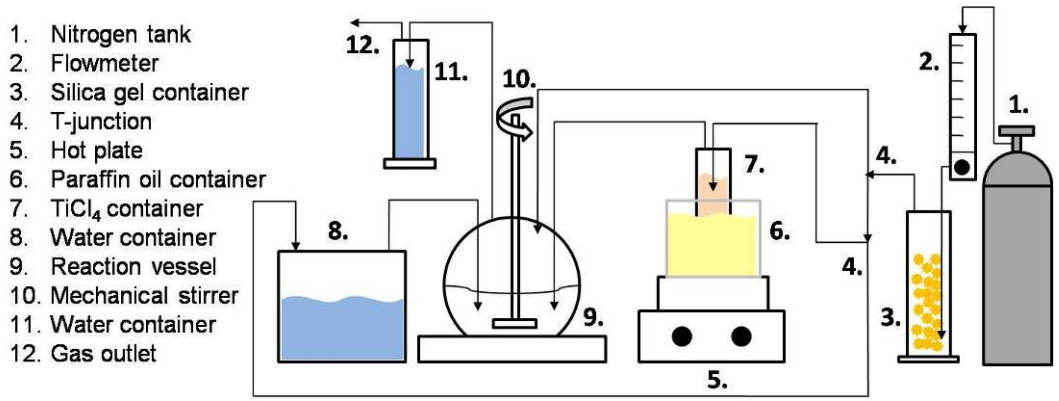

Fig. 2-14 CVD process setup schematic.

Fig. 2-15 and Table 2-2 show an EDS analysis of an iM30K microsphere coated in the CVD process. Very little titanium was found to be deposited on the microspheres, as shown in Figure F and Table T. Small particles were however detected in some cases and believed to be due to a gas phase reaction. Bypassing the purging step created a dense white fog in the reaction vessel so clearly the reactants were reaching the vessel. The slow rate of deposition can be explained by the reaction of $TiCl_4$ with a SiO_2 surface being self-limiting so only an extremely thin layer is deposited in each cycle.

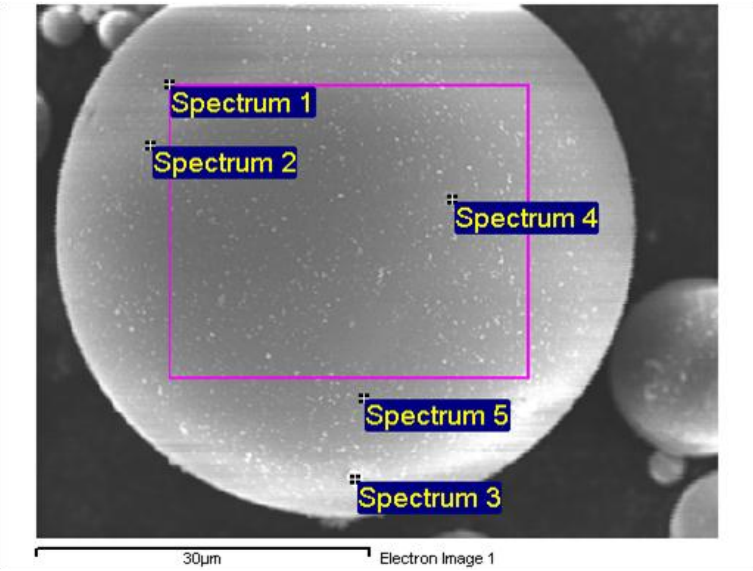

Fig. 2-15 iM30K microsphere coated with CVD process.

Spectrum	O	Na	Si	Cl	Ca	Ti
Spectrum 1	18.94	3.23	59.94		16.74	1.15
Spectrum 2	24.77	3.29	56.97		14.97	
Spectrum 3	12.94	2.30	44.99	1.27	17.09	21.42
Spectrum 4	17.62	3.10	61.54		17.74	
Spectrum 5	14.15	2.43	62.95		20.47	

Table 2-2 EDS analysis of the microsphere shown in Fig. 2-15. Results are in wt%.

2.5.4 Atomic Layer Deposition process (ALD)

Due to the self-limiting reaction of $TiCl_4$ with a SiO_2 surface the coating needs to be deposited by alternating pulses of $TiCl_4$ and H_2O vapour where effectively a monolayer is deposited in each cycle. A detailed study of the initial surface reactions was done by Hu et al [47] and the atomic layer deposition of TiO_2 has been studied extensively [48][49][50][51][52][53][54][55][56][57]. The setup built for the coating process is illustrated in Fig. 2-16. High purity nitrogen was passed through silica gel to remove traces of water and into two evaporation cells through a T-junction. Both branches were continually open to simplify the process control. The flow was equal through both evaporation cells and controlled by flowmeters. The evaporation cells were made from a block of aluminium, which was placed on a hot plate, and a glass container fastened to the aluminium block. A thermocouple was inserted into the aluminium block to control the temperature. The evaporation cells were fitted with programmable dispenser units that dosed both $TiCl_4$ and H_2O onto the aluminium block. A titanium plate covered the aluminium block in the $TiCl_4$ cell to avoid corrosion. The $TiCl_4$ cell was kept at 170°C. This temperature was chosen so the drop would evaporate in a few seconds. If the evaporation was too rapid the pressure surge caused backflow in the system. The H_2O cell was kept at 210°C for the same reason. The evaporation cells were insulated to avoid condensation on the cell walls which would cause a sudden pressure drop. 400g of iM30K microspheres were placed in the reaction vessel and stirred continuously. The coating cycle started by dispensing 0,2ml of $TiCl_4$ on to the titanium plate and purging the system for 3

minutes. Next 0,1ml of H2O was evaporated and the system purged for 3 minutes. This was to be repeated approximately 250 times to build up the TiO_2 layer.

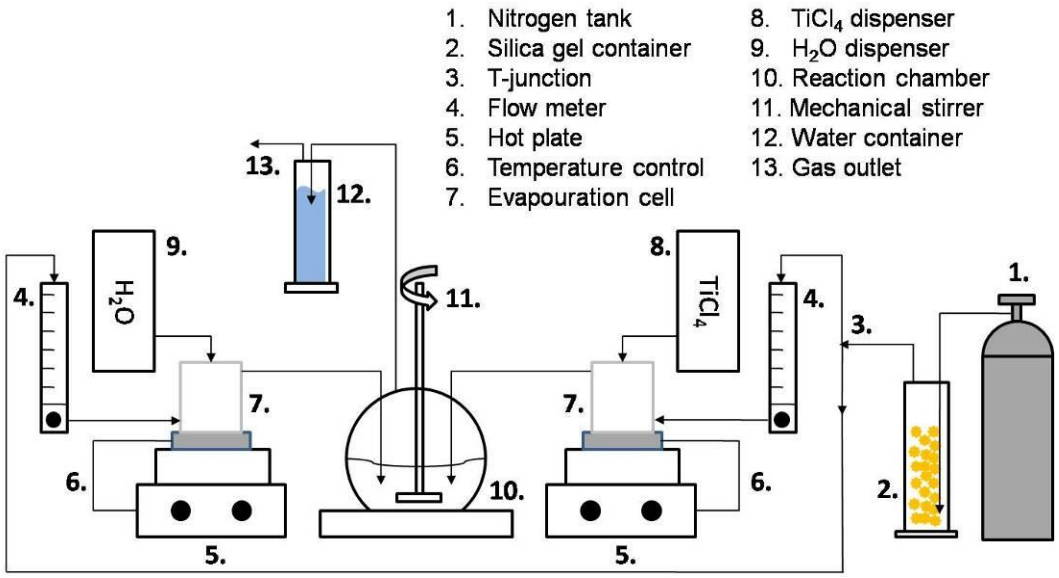

Fig. 2-16 Atomic layer deposition setup schematic.

It was however not possible to run the process for so many cycles due to the aggressive nature of the titanium precursor. The process broke down sporadically due to the precursor destroying the Teflon tubing, the flowmeter and the electronics in the dispenser unit. Due to consistent problems with the equipment the process was abandoned. The process setup can be seen in Fig. 2-17.

Fig. 2-17 ALD process setup (left). Evaporation cell (right)

3 Alternatives to hollow glass microspheres

3.1 Pearlescent pigment

Pearlescent pigments were considered as an alternative photocatalyst to TiO_2 coated microspheres. The main benefits are easy availability, lower material price and lower concentrations needed to get high surface coverage. A preliminary investigation of was made where two types of pearlescent pigments, supplied by Eckart, were tested in a transparent alkyd formulation. The tested types were PX-2000 and Prestige Green which both have the anatase structure and an average particle size of 11µm and 20µm, respectively. The films were exposed for 720 hours in QUV (for details on QUV exposure see chapter 5) and degradation of the binder investigated by SEM. Fig. 3-1 shows films with 0%; 1%; 2,5% and 5% PX-2000 pigment where it can be seen that at 5 wt% the surface coverage is very good. It seems the particles do not separate easily from the surface although most of the binder surrounding them has been degraded which indicates that the durability of the film is satisfactory. Further study of the degradation mechanism is however needed to confirm this. Fig. 3-2 shows films with the Prestige Green type pigment at 2,5 wt% and 5 wt%. Due to the larger particle size the same wt% results in much lower surface coverage similar to what is concluded about the relationship between particle size and surface coverage, regarding microspheres, in chapter 5.

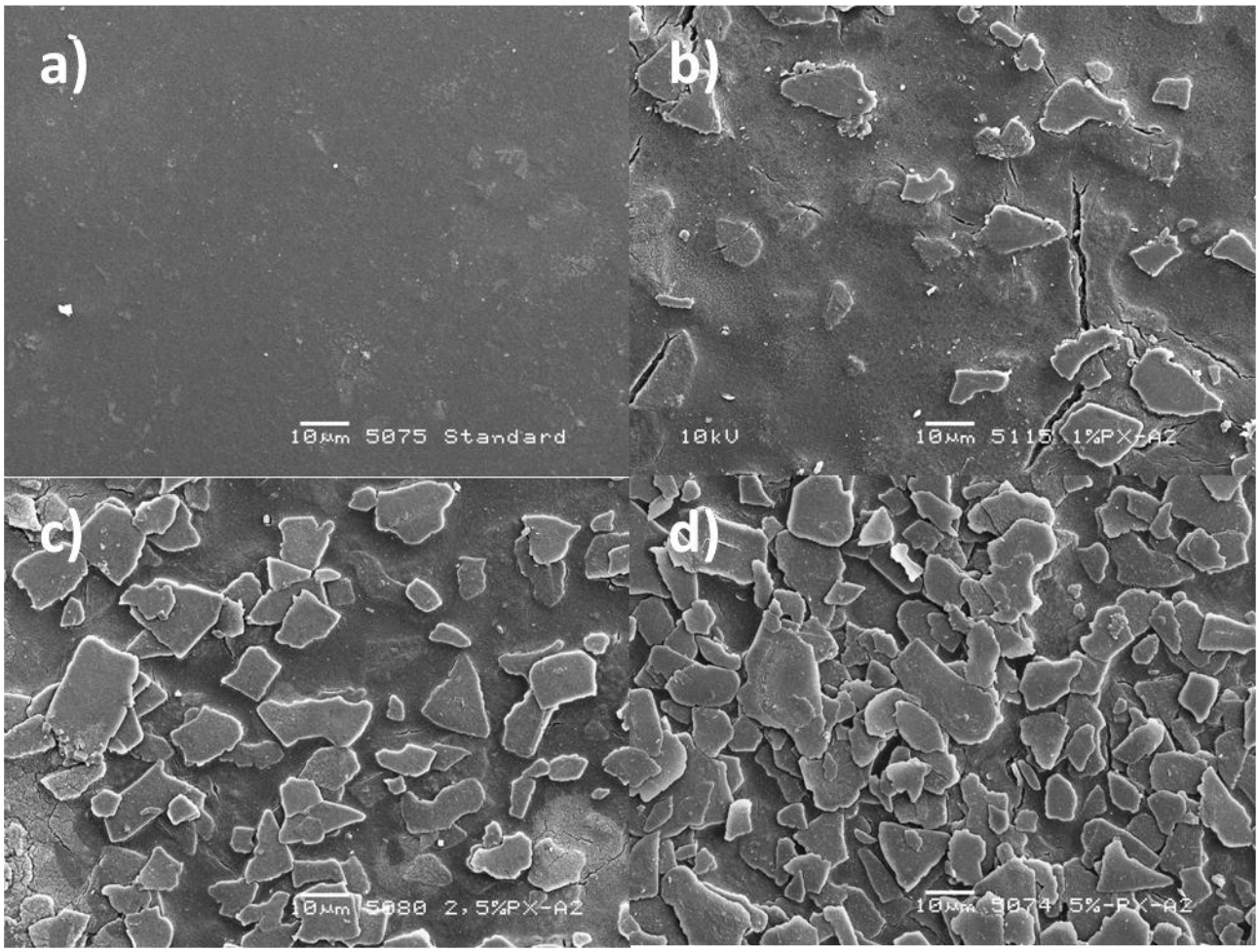

Fig. 3-1 Shows alkyd films after 720 hours of QUV exposure with a) no pigments, b) 1 wt% PX-2000, c) 2,5 wt% PX-2000 and d) 5 wt% PX-2000.

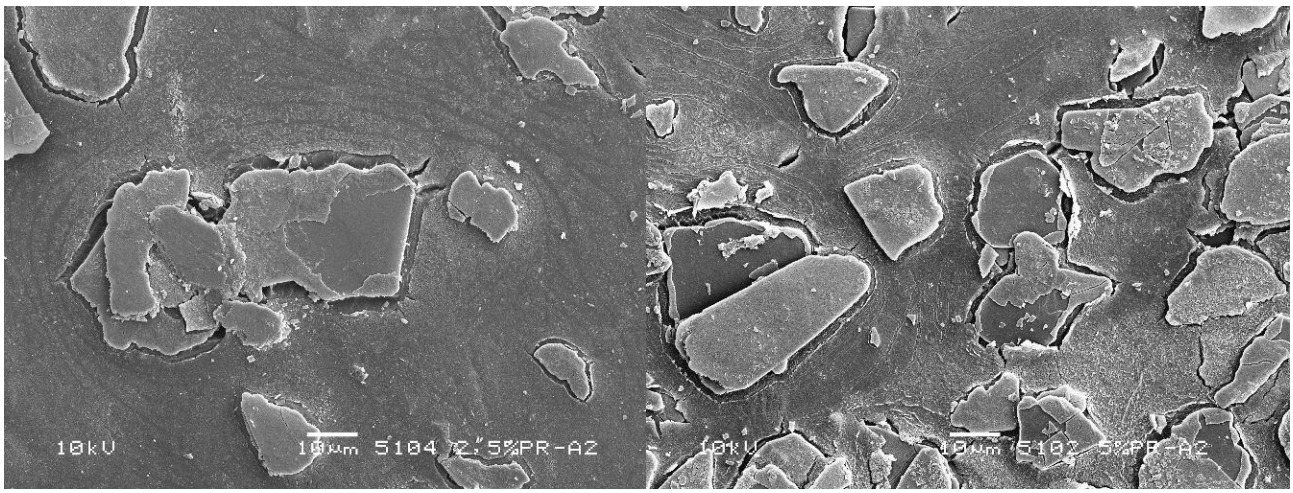

Fig. 3-2 Shows alkyd films after 720 hours of QUV exposure with 2,5 wt% Prestige Green (left) and 5 wt% PX-2000 (right).

A self-cleaning test was performed by putting a drop of 100µmol/L solution of methylene blue on the UV exposed area. The water was allowed to evaporate leaving a blue stain on the film. The

panels were then exposed in a QUV chamber for 24 hours before inspection. Fig. 3-3 shows a standard sample without pigment compared to a sample with 5 wt% PX-2000. The pigmented film is found to exhibit improved self-cleaning properties suggesting that pearlescent pigments may be a feasible alternative to TiO_2 coated microspheres.

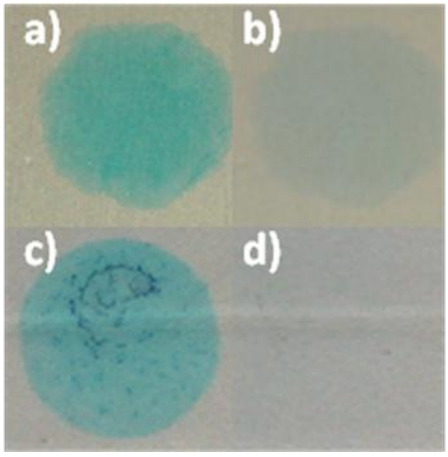

Fig. 3-3 Self-cleaning test of pearlescent pigment films. a) 0% film before QUV, b) 0% film after 24 hours QUV, c) 5 wt% PX-2000 film before QUV and d) 5 wt% PX-2000 film after 24 hours QUV

Although pearlescent pigments are a promising alternative they aren't believed to offer as good properties as the HGMS. Fig. 3-4 shows a with 1 wt% and 2,5 wt% Prestige Green pigment which have been exposed in a QUV chamber for 720 hours. A considerable amount of large cracks have developed in the surfaces which are observed to extend deep into the film. The particles are believed to act as crack initiation sites due to their irregular shape. Comparing these images with the water permeability films shown in chapter 5 it is clear that the crack resistance of films with microspheres is substantially better.

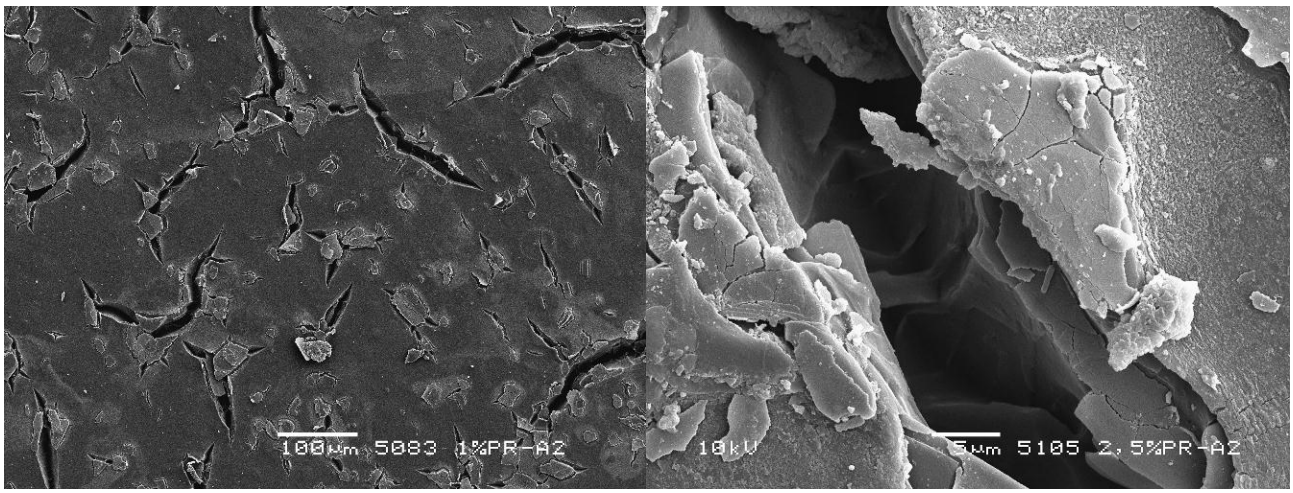

Fig. 3-4 Illustrates cracking, after 720 hours QUV exposure, in films containing Prestige Green pearlescent pigment with 1 wt% (left) and 2,5 wt% (right).

3.2 Fly ash

Fly ash was considered as an inexpensive alternative to HGMS. Fly ash is a waste product formed in coal power plants and therefore very cheap. One of the main uses is as filler in concrete but due to a very wide particle size distribution it generally isn't suitable for use in paint. It is however possible to find fly ash products with a narrower particle size distribution. Plasfill 5 is a fly ash product sold as filler for plastics which is made up of spherical particles mostly of Mullite (aluminium silicate) and SiO_2 that has an average particle size of 4,5µm. Fig. 3-5 and Table 3-1 show an EDS analysis of Plasfill 5 which shows the main ingredients in Mullite along with low concentrations of other elements which are mostly found in the smaller particles.

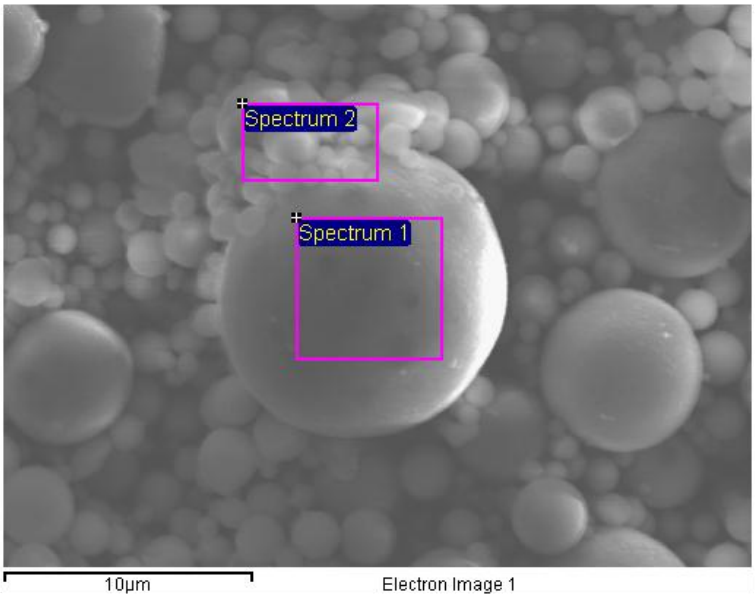

Fig. 3-5 EDS analysis of Plasfill 5 fly ash.

Spectrum	C	O	Mg	Al	Si	K	Ca	Ti	Fe
Spectrum 1		36.67		27.95	34.21	1.18			
Spectrum 2	16.31	36.51	0.56	16.40	25.50	0.67	1.80	0.96	1.30

Table 3-1 EDS analysis of Plasfill 5 fly ash shown in Fig. 3-5.

The larger particles are hollow, as seen in Fig. 3-6, and the smaller ones solid. Approximately 10% of the fly ash has a particle size of 10µm or more and small amounts large irregularly shaped particles can be found. These particles would have to be removed if the fly ash were to be used in paint formulations to avoid increasing the water permeability of the film.

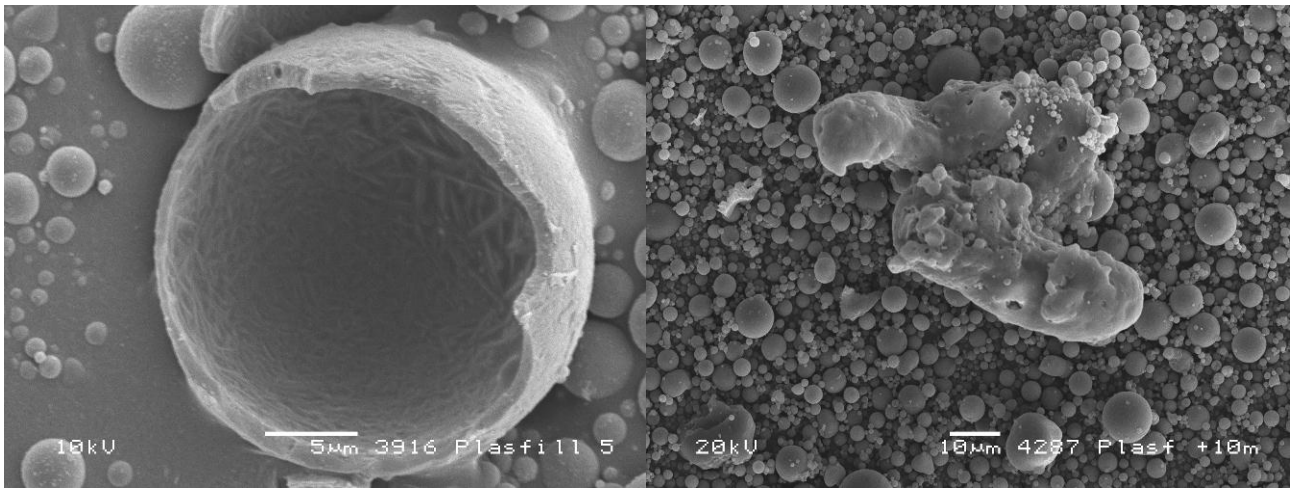

Fig. 3-6 Shows a hollow particle (left) and a large irregularly shaped particle (right)

The fly ash has a light grey colour and the effect of volume concentration on the colour of a rutile pigmented paint film is shown in Fig. 3-7. The large change in colour limits the use of fly ash in paint formulations to darker tones where the effect would be smaller. The material was therefore not considered suitable for the application.

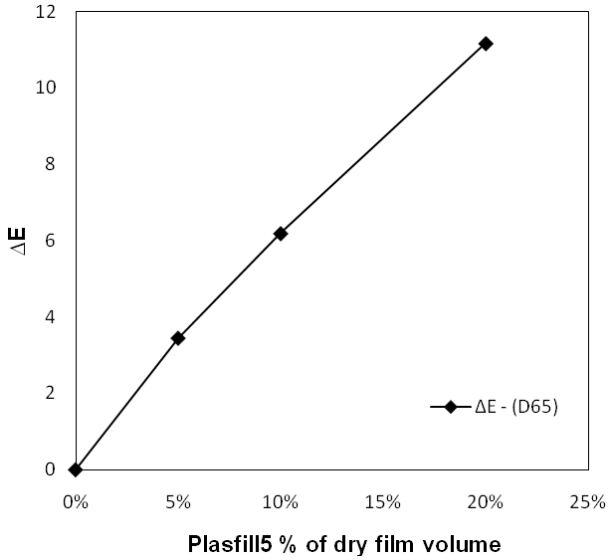

Fig. 3-7 shows the effect of Plasfill 5 volume concentration on the DE value (CIE Lab standard) compared to a standard white paint.

References

[1] I. P. Parkin and R. G. Palgrave, "Self-cleaning coatings," *Journal of Materials Chemistry*, vol. 15, no. 17, p. 1689, 2005.

[2] X.-M. Li, D. Reinhoudt, and M. Crego-Calama, "What do we need for a superhydrophobic surface? A review on the recent progress in the preparation of superhydrophobic surfaces," *Chem. Soc. Rev.*, vol. 36, no. 8, pp. 1350-1368, Jan. 2007.

[3] A. Marmur, "The Lotus Effect: Superhydrophobicity and Metastability," *Langmuir*, vol. 20, no. 9, pp. 3517-3519, 2004.

[4] W. Thielicke, *Lotus3.jpg*. .

[5] A. Mills, A. Lepre, N. Elliott, S. Bhopal, I. P. Parkin, and S. A. O'Neill, "Characterisation of the photocatalyst Pilkington Activ(TM): a reference film photocatalyst?," *Journal of Photochemistry and Photobiology A: Chemistry*, vol. 160, no. 3, pp. 213-224, Aug. 2003.

[6] G. KAEMPF, PAPENROT.W, and R. HOLM, "DEGRADATION PROCESSES IN TIO2-PIGMENTED PAINT FILMS ON EXPOSURE TO WEATHERING," *JOURNAL OF PAINT TECHNOLOGY*, vol. 46, no. 598, pp. 56-63, 1974.

[7] A. E. Jacobsen, "Titanium Dioxide Pigments: Correlation between Photochemical Reactivity and Chalking.," *Industrial & Engineering Chemistry*, vol. 41, no. 3, pp. 523-526, Mar. 1949.

[8] U. Gesenhues, "Al-doped TiO2 pigments: influence of doping on the photocatalytic degradation of alkyd resins," *Journal of Photochemistry and Photobiology A: Chemistry*, vol. 139, no. 2-3, pp. 243-251, Mar. 2001.

[9] N. S. Allen, M. Edge, G. Sandoval, J. Verran, J. Stratton, and J. Maltby, "Photocatalytic Coatings for Environmental Applications¶†," *Photochemistry and Photobiology*, vol. 81, no. 2, pp. 279-290, Mar. 2005.

[10] N. S. Allen et al., "Degradation and stabilisation of polymers and coatings: nano versus pigmentary titania particles," *Polymer Degradation and Stability*, vol. 85, no. 3, pp. 927-946, Sep. 2004.

[11] W. A. Pryor, "Oxy-Radicals and Related Species: Their Formation, Lifetimes, and Reactions," *Annual Review of Physiology*, vol. 48, no. 1, pp. 657-667, Oct. 1986.

[12] A. Fujishima and K. Honda, "Electrochemical Photolysis of Water at a Semiconductor Electrode," *Nature*, vol. 238, no. 5358, pp. 37-38, Jul. 1972.

[13] A. Fujishima, X. Zhang, and D. A. Tryk, "Heterogeneous photocatalysis: From water photolysis to applications in environmental cleanup," *International Journal of Hydrogen Energy*, vol. 32, no. 14, pp. 2664-2672, Sep. 2007.

[14] N. Serpone and A. V. Emeline, "Suggested terms and definitions in photocatalysis and radiocatalysis," *International Journal of Photoenergy*, vol. 4, pp. 91-131, 2002.

[15] A. L. Linsebigler, G. Lu, and J. T. Yates, "Photocatalysis on TiO2 Surfaces: Principles, Mechanisms, and Selected Results," *Chemical Reviews*, vol. 95, no. 3, pp. 735-758, May 1995.

[16] A. Fujishima, T. N. Rao, and D. A. Tryk, "Titanium dioxide photocatalysis," *Journal of Photochemistry and Photobiology C: Photochemistry Reviews*, vol. 1, no. 1, pp. 1-21, Jun. 2000.

[17] A. Mills and S. Le Hunte, "An overview of semiconductor photocatalysis," *Journal of Photochemistry and Photobiology A: Chemistry*, vol. 108, no. 1, pp. 1-35, Jul. 1997.

[18] J. Yu, X. Zhao, Q. Zhao, and G. Wang, "Preparation and characterization of super-hydrophilic porous TiO2 coating films," *Materials Chemistry and Physics*, vol. 68, no. 1-3, pp. 253-259, Feb. 2001.

[19] R. Wang, N. Sakai, A. Fujishima, T. Watanabe, and K. Hashimoto, "Studies of Surface Wettability Conversion on TiO2 Single-Crystal Surfaces," *J. Phys. Chem. B*, vol. 103, no. 12, pp. 2188-2194, 1999.
[20] H. A. Schwarz and R. W. Dodson, "Equilibrium between hydroxyl radicals and thallium(II) and the oxidation potential of hydroxyl(aq)," *J. Phys. Chem.*, vol. 88, no. 16, pp. 3643-3647, 1984.
[21] E. Carter, A. F. Carley, and D. M. Murphy, "Evidence for O2- Radical Stabilization at Surface Oxygen Vacancies on Polycrystalline TiO2," *J. Phys. Chem. C*, vol. 111, no. 28, pp. 10630-10638, 2007.
[22] A. M. Peiró, C. Colombo, G. Doyle, J. Nelson, A. Mills, and J. R. Durrant, "Photochemical Reduction of Oxygen Adsorbed to Nanocrystalline TiO2 Films: A Transient Absorption and Oxygen Scavenging Study of Different TiO2 Preparations," *J. Phys. Chem. B*, vol. 110, no. 46, pp. 23255-23263, 2006.
[23] H. Gerischer and A. Heller, "The role of oxygen in photooxidation of organic molecules on semiconductor particles," *J. Phys. Chem.*, vol. 95, no. 13, pp. 5261-5267, 1991.
[24] V. Sukharev and R. Kershaw, "Concerning the role of oxygen in photocatalytic decomposition of salicylic acid in water," *Journal of Photochemistry and Photobiology A: Chemistry*, vol. 98, no. 3, pp. 165-169, Aug. 1996.
[25] H. Kominami, M. Kohno, Y. Takada, M. Inoue, T. Inui, and Y. Kera, "Hydrolysis of Titanium Alkoxide in Organic Solvent at High Temperatures: A New Synthetic Method for Nanosized, Thermally Stable Titanium(IV) Oxide," *Ind. Eng. Chem. Res.*, vol. 38, no. 10, pp. 3925-3931, 1999.
[26] A. Hanprasopwattana, S. Srinivasan, A. G. Sault, and A. K. Datye, "Titania Coatings on Monodisperse Silica Spheres (Characterization Using 2-Propanol Dehydration and TEM)," *Langmuir*, vol. 12, no. 13, pp. 3173-3179, 1996.
[27] S. A. O'Neill, I. P. Parkin, R. J. H. Clark, A. Mills, and N. Elliott, "Atmospheric pressure chemical vapour deposition of titanium dioxide coatings on glass," *J. Mater. Chem.*, vol. 13, no. 1, pp. 56-60, Nov. 2002.
[28] Y. J. Yun, J. S. Chung, S. Kim, S. H. Hahn, and E. J. Kim, "Low-temperature coating of sol–gel anatase thin films," *Materials Letters*, vol. 58, no. 29, pp. 3703-3706, Nov. 2004.
[29] M. Okuya, K. Nakade, and S. Kaneko, "Porous TiO2 thin films synthesized by a spray pyrolysis deposition (SPD) technique and their application to dye-sensitized solar cells," *Solar Energy Materials and Solar Cells*, vol. 70, no. 4, pp. 425-435, Jan. 2002.
[30] P. Møller, *Overfladeteknologi*, First ed. Copenhagen, Denmark: Ingeniøren|bøger, 2003.
[31] D. Satas and A. A. Tracton, *Coatings Technology Handbook, Second Edition*, 2nd ed. CRC Press, 2000.
[32] D. A. Goldchmidt and D. H.-J. Streitberger, *Handbook on Basics of Coating Technology*, 1st ed. William Andrew Publishing, 2003.
[33] C. H. Hare, *Protective Coatings: Fundamentals of Chemistry and Composition*. Technology Pub. Co, 1994.
[34] T. Brock, M. Groteklaes, and P. Mischke, *European coatings handbook*. Vincentz Network GmbH & Co KG, 2000.
[35] J. P. Gallas, J. C. Lavalley, A. Burneau, and O. Barres, "Comparative study of the surface hydroxyl groups of fumed and precipitated silicas. 4. Infrared study of dehydroxylation by thermal treatments," *Langmuir*, vol. 7, no. 6, pp. 1235-1240, 1991.
[36] L. Diaz, C. M. Liauw, M. Edge, N. S. Allen, A. McMahon, and N. Rhodes, "Investigation of factors affecting the adsorption of functional molecules onto gel silicas: 1. Flow

microcalorimetry and infrared spectroscopy," *Journal of Colloid and Interface Science*, vol. 287, no. 2, pp. 379-387, Jul. 2005.
[37] Fry R.A., Mueller K.T., and Pantano C.G., "Effect of boron oxide on surface hydroxyl coverage of aluminoborosilicate glass fibres: a 19F solid state NMR study," *Physics and Chemistry of Glasses*, vol. 44, no. 2, pp. 64-68, 2003.
[38] F. Rubio, J. Rubio, and J. . Oteo, "Surface energy distributions on silicoborate glasses," *Colloids and Surfaces A: Physicochemical and Engineering Aspects*, vol. 139, no. 2, pp. 227-239, Aug. 1998.
[39] S. Srinivasan, A. K. Datye, M. H. Smith, and C. H. F. Peden, "Interaction of Titanium Isopropoxide with Surface Hydroxyls on Silica," *Journal of Catalysis*, vol. 145, no. 2, pp. 565-573, Feb. 1994.
[40] M. L. Hair, "Hydroxyl groups on silica surface," *Journal of Non-Crystalline Solids*, vol. 19, pp. 299-309, Dec. 1975.
[41] G. J. Young, "Interaction of water vapor with silica surfaces," *Journal of Colloid Science*, vol. 13, no. 1, pp. 67-85, Feb. 1958.
[42] T. G. Kim et al., "Phase Transformation of TiO_2 in the Preparation of Pearlescent Pigment," *Materials Science Forum*, vol. 544-545, pp. 99-102, 2007.
[43] B. B. Topuz, G. Gündüz, B. Mavis, and Ü. Çolak, "The effect of tin dioxide (SnO2) on the anatase-rutile phase transformation of titania (TiO2) in mica-titania pigments and their use in paint," *Dyes and Pigments*, vol. 90, no. 2, pp. 123-128, Aug. 2011.
[44] Y. C. Ryu et al., "Effect of substrate on the phase transformation of TiO2 in pearlescent pigment," *Journal of Industrial and Engineering Chemistry*, vol. 14, no. 2, pp. 213-218, Mar. 2008.
[45] S. D. Park, Y. H. Cho, W. W. Kim, and S.-J. Kim, "Understanding of Homogeneous Spontaneous Precipitation for Monodispersed TiO2 Ultrafine Powders with Rutile Phase around Room Temperature," *Journal of Solid State Chemistry*, vol. 146, no. 1, pp. 230-238, Aug. 1999.
[46] S. Kim, S. Park, Y. H. Jeong, and S. Park, "Homogeneous Precipitation of TiO2 Ultrafine Powders from Aqueous TiOCl2 Solution," *Journal of the American Ceramic Society*, vol. 82, no. 4, pp. 927-932, Apr. 1999.
[47] Z. Hu and C. H. Turner, "Initial Surface Reactions of TiO2 Atomic Layer Deposition onto SiO2 Surfaces: Density Functional Theory Calculations," *J. Phys. Chem. B*, vol. 110, no. 16, pp. 8337-8347, 2006.
[48] J. Aarik, A. Aidla, T. Uustare, and V. Sammelselg, "Morphology and structure of TiO2 thin films grown by atomic layer deposition," *Journal of Crystal Growth*, vol. 148, no. 3, pp. 268-275, Mar. 1995.
[49] J. Aarik, "Atomic-layer growth of TiO2-II thin films," *Philosophical Magazine Letters*, vol. 73, pp. 115-119, Mar. 1996.
[50] J. Aarik, A. Aidla, V. Sammelselg, and T. Uustare, "Effect of growth conditions on formation of TiO2-II thin films in atomic layer deposition process," *Journal of Crystal Growth*, vol. 181, no. 3, pp. 259-264, Nov. 1997.
[51] J. Aarik, A. Aidla, H. Mändar, and V. Sammelselg, "Anomalous effect of temperature on atomic layer deposition of titanium dioxide," *Journal of Crystal Growth*, vol. 220, no. 4, pp. 531-537, Dec. 2000.
[52] J. Aarik, A. Aidla, H. Mändar, and T. Uustare, "Atomic layer deposition of titanium dioxide from TiCl4 and H2O: investigation of growth mechanism," *Applied Surface Science*, vol. 172, no. 1-2, pp. 148-158, Mar. 2001.

[53] W. Gu and C. P. Tripp, “Role of Water in the Atomic Layer Deposition of TiO2 on SiO2,” *Langmuir*, vol. 21, no. 1, pp. 211-216, 2004.
[54] R. Matero, A. Rahtu, and M. Ritala, “In Situ Quadrupole Mass Spectrometry and Quartz Crystal Microbalance Studies on the Atomic Layer Deposition of Titanium Dioxide from Titanium Tetrachloride and Water,” *Chem. Mater.*, vol. 13, no. 12, pp. 4506-4511, 2001.
[55] M. Leskelä and M. Ritala, “Atomic layer deposition (ALD): from precursors to thin film structures,” *Thin Solid Films*, vol. 409, no. 1, pp. 138-146, Apr. 2002.
[56] M. A. Cameron, I. P. Gartland, J. A. Smith, S. F. Diaz, and S. M. George, “Atomic Layer Deposition of SiO2 and TiO2 in Alumina Tubular Membranes: Pore Reduction and Effect of Surface Species on Gas Transport,” *Langmuir*, vol. 16, no. 19, pp. 7435-7444, 2000.
[57] J. D. Ferguson, A. R. Yoder, A. W. Weimer, and S. M. George, “TiO2 atomic layer deposition on ZrO2 particles using alternating exposures of TiCl4 and H2O,” *Applied Surface Science*, vol. 226, no. 4, pp. 393-404, Mar. 2004.

Submitted papers

4 Paper 1: Synthesis and characterisation of photocatalytic TiO_2 coated hollow glass microspheres used for self cleaning organic paint

Sverrir G. Gunnarsson,*[a] Kári M. Guðmundsson[a], Per Møller*[a], Søren H. Poulsen[b] and Lars P. Nielsen[c]

Abstract

This paper proposes a new and novel way of integrating photocatalytic material into organic paint systems in order to make them self cleaning. The photocatalyst is coated onto micrometer sized carrier particles to minimize the exposure of the organic binder to the degrading photocatalytic reaction. Carrier particles (hollow glass microspheres) were coated with TiO_2 and characterized using SEM, EDS and XRD. The adhesion of the coating to the microspheres was optimized by pre-treating the microspheres before coating. The photocatalytic effectivity of the supported photocatalyst was estimated by measuring dye bleaching of methylene blue after exposure to UV radiation. Alkyd paint films with photocatalytic microspheres and untreated microspheres were prepared and their surface contaminated with methylene blue to test whether the organic dye would be degraded during UV exposure. The alkyd film comprising coated microspheres displayed self-cleaning properties while the film with untreated microspheres did not display any self-cleaning properties.

4.1 Introduction

Photocatalysis has shown great promise for a number of applications due to the high reactivity of the OH radicals created in the reaction, which can degrade even the most persistent organic pollutants (POP's) [1]. These applications include air purification [2], sterilization of water or surfaces [3] and making surfaces self-cleaning [4] just to exemplify a few of the potential applications discussed in the literature. The most commonly used photocatalyst is TiO_2 of the anatase or rutile structure, anatase being the more effective of the two. Furthermore TiO_2 is the most common pigment used in paints, where the rutile structure is favoured to the anatase structure due to slightly better optical properties and less photocatalytic activity. The photo-activity of TiO_2 pigments and consequent degradation of organic binders, often termed chalking, has been well known to the paint industry [5] since long before Fujishima and Honda published their paper on photolysis of water [6]. Controlled chalking was considered favourable as constant renewal of the surface served as a crude self-cleaning mechanism [5]. Today this photo-activity is much better understood which is why commercial titanium pigments currently are stabilised (doped or surface treated) with for example Al_2O_3 to suppress the creation of reactive hydroxyl radicals [7][8].
With increased understanding of the photocatalytic reaction a lot of work has been done to utilize and commercialize the technology where perhaps the best known example is the Pilkington Activ^{TM} self-cleaning window glass [9]. The trend is to use photocatalytic nano-particles because of the high effectivity attained with a large surface area. Inorganic paints comprising anatase nano-particles have been successfully commercialized but even though attempts have been made to develop such organic self-cleaning paints [10] they have not been successful due to the vulnerability of organic binders to the photocatalytic reaction. Inorganic binders are relatively expensive compared to

organic binders such as alkyds or acrylics and are not suitable for all applications making it interesting to further develop organic self-cleaning paints.
To be able to improve the design of organic self-cleaning paints it is necessary first to understand the degradation mechanism of paints comprising photocatalytic pigments. The mechanism is described in a paper by Kaempf et al [11] where the different effect of stabilised TiO2 pigment versus untreated pigments on alkyd binders are shown. In the paper a distinction is made between two degradation processes. Photochemical degradation of the binder due to absorption of UV-light and chalking which happens at the pigment/binder interface. The chalking mechanism is activated when photocatalytic pigment in the film surface is exposed to UV light and the particles become photoactive. The binder in the immediate vicinity of the particles is degraded by the hydroxyl radicals created and due to the small size of the particles very little material needs to be degraded before it is separated from the film. This mechanism causes films to slowly disintegrate or to put it in other words have much higher chalking rates compared to films with stabilised pigments. As mentioned above this can be interpreted as a self-cleaning mechanism as the surface continually renews itself but this approach has some serious disadvantages. The durability of the film will be very poor as it is in fact slowly self destructing and thereby rapidly loosing its protective properties. Substituting pigment sized particles (~ 0,25- 0,30µm) with nano-particles will increase the photocatalytic activity of the film and also greatly accelerate the rate of degradation of the film itself[10]. Furthermore as a result of a high chalking rate such a film would constantly release nano-particles to its surroundings. The effect of photocatalytic nano-particles on people has not yet been fully studied but investigations suggest they may have adverse health effects [12]. Due to the small size of the particles they are both highly active and may be able to penetrate the outermost skin layers and reach living cells.

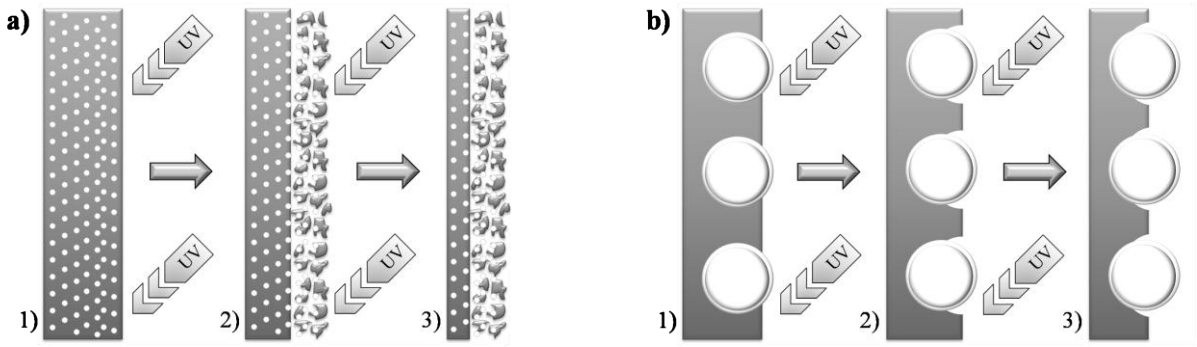

Fig. 4-1 a) shows a film with nano-particles constantly eroding from 1) to 3) during UV exposure. b) shows a film with photocatalytic carrier particles 1) Fresh film, 2) After initial exposure chalking has occurred, 3) Chalking has nearly ceased as UV radiation no longer reaches carrier particle/binder interface and the much slower photochemical degradation of the binder system becomes the predominant degradation process.

Instead of formulating organic paints with nano-particles this paper proposes an alternative strategy applying supported photocatalysts where nano-crystalline anatase TiO_2 is coated onto carrier particles in the micrometer size-range which are made of material inert to the photocatalytic reaction. This can dramatically reduce the effect on the organic binder since the contact area between photocatalyst and binder is much smaller and due to the extremely short half life of OH radicals [13] they cannot diffuse away from the site of creation. Therefore the binder should only be degraded in the immediate vicinity of the carrier particles. The particles need to be large enough to be embedded deep enough in the film so that UV light doesn't activate the buried part of the particle. Initially there will be chalking around the particles in the surface region but not over the

entire particle/binder interface and therefore separation of carrier particles from the film can be minimised or even totally avoided contrary to the case of unsupported nano-particles. Once the initial chalking has ceased the degradation process will be governed by the much slower photochemical degradation. Only after an extended period of weathering can the chalking around the carrier particles resume. This way of integrating a photocatalyst into the film should slow down the chalking instead of increasing it and still yield enough photocatalytic activity to make the surface self-cleaning as the carrier particles offer an area, unaffected by the photocatalytic reaction, on the film surface for the self-cleaning effect to take place. The different film degradation mechanisms are illustrated in Fig. 4-1 which shows cross sections of the films. The figures do not represent the full film thickness.
Hollow glass microspheres were chosen as suitable carrier particles because they fulfil a number of the specifications deemed necessary. Most importantly they are made of borosilicate glass which is inert to the photocatalytic reaction and also due to their spherical shape a large amount of them can be dispersed in paint without having a too severe effect on viscosity and other important properties. It is important to add a large volume of carrier particles in order to get a sufficiently high concentration in the surface because otherwise the resulting self-cleaning effect can be poor.
This work was done to characterize and investigate the effect of several factors on the preparation and photocatalytic effectivity of the carrier particles. A 2k-factorial design of experiments (DOE) was employed to estimate the effect of the different factors and to investigate if there were any interacting factors. The most effective coated carrier particles were then used to formulate a paint to test whether the film could be self-cleaning.

4.2 Experimental

4.2.1 Materials and equipment

The hollow glass microspheres (HGMS) used were S38 Glass Bubbles from 3M. The average density of the microspheres is 0,38g/cm3, the average diameter of the particles is 40µm and the size distribution can be seen in Fig. 4-2. The spheres can withstand temperatures up to 600°C. According to the producer the microspheres are made from the following materials:

- 70 -80 w/w% SiO2
- 2 -6 w/w% B2O3
- 8 -15 w/w% CaO
- 3 -8 w/w% Na2O
- 0 -10w/w% K2O & Li2O

The titanium-tetraisopropoxide (TTIP) used to coat the microspheres was VERTEC® TIPT, 97+% from Alfa Aesar and the methylene blue (MB) used for the photocatalytic efficiency experiments was 0,05 wt% in H_2O from Sigma Aldrich.
Electron microscopy was done using a JEOL model JSM-5900 electron microscope with a LaB_6 filament. The x-ray diffraction analysis was done using a Huber Guinier G670 diffractometer with CuKα1 radiation. The UV-Vis spectrometer used was a Shimadzu UV-mini 1240 and the UV lamp a Dymax 5000-EC. The emission spectrum can be seen in Fig. 4-4 b). Particle size was measured with a Malvern Mastersizer 2000.

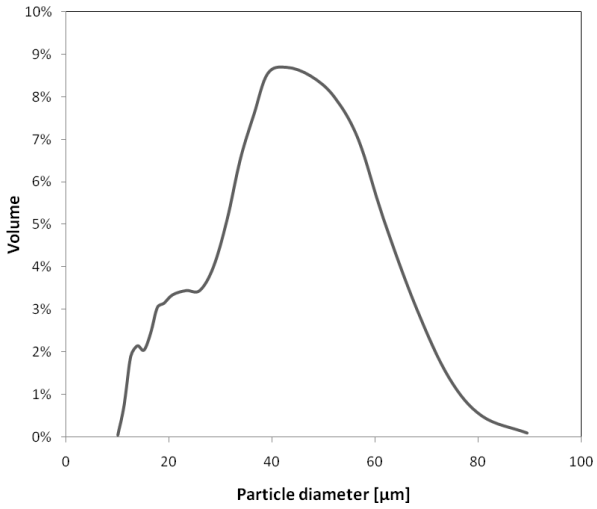

Fig. 4-2 S38 glass bubbles size distribution.

4.2.2 Coating process

The HGMS were coated using the method described below. The HGMS were pre-treated at a fixed temperature for 24 hours. TTIP, see Fig. 4-3, was mixed with isopropanol and stirred for 20 minutes. 1g of microspheres was added to the solution for every 10 ml isopropanol and the mixture stirred for 20 minutes. Then de-ionized water, 1 ml for every 1g of microspheres, was added to the solution and stirred for 10 minutes. The solution was then filtered and heated to dryness at 110˚C. Then the coated microspheres were calcined to crystallize the TiO_2. The process was repeated once more to load more TiO_2 on the microspheres. After the second round of coating the microspheres were sonicated in de-ionized water for 20 minutes and separated from all unbound TiO_2. Finally the coated microspheres were heated to dryness at 110˚C. 10g of HGMS were coated each time and further details about TTIP to isopropanol ratio, calcining temperature etc. can be found in the next section on experimental design.

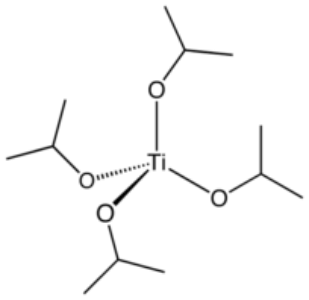

Fig. 4-3 Titanium tetraisopropoxide structure.

4.2.3 Experimental design

The aim of this study was to investigate different factors in the process of coating glass spheres with TiO_2 and how they affect the photocatalytic activity of the coating. Four parameters in the coating

process were investigated and a 2^4 factorial experimental design used to investigate the effect on the photocatalytic effectivity. The gathered data was analyzed using ANOVA and regression analysis.
In the 2^k factorial design methodology k factors are tested at two different levels, high and low, respectively, and a total of 2^k measurements made for each replicate. The benefit of this methodology is that it measures the effect of interactions between factors as well as the effect of the factors themselves. The main drawback is that it assumes that the response variable behaves linearly with regard to the factors since they are only tested at two levels.
The tested factors are listed in Table 4-1. Factor A, the ratio between TTIP and HGMS [ml/g], was chosen as it was expected to affect the amount of TiO_2 deposited on the spheres. Factor B, the calcining temperature, and factor C, the calcining time, were chosen because of their expected effect on the crystallinity of the coating. Factor D, the temperature of the HGMS before being coated, was chosen to investigate whether the pre-treatment had an effect on the deposition of the coating or its effectivity.
The factors are denoted by capital letters and the treatment combinations by lower case letters where the letters indicate which factors are at high level. This means that a sample with A at high level and B at low level is denoted as "a" and a sample with both at high level as "ab". The combination with all factors at low level is denoted as "1".

Factor	Description	High	Low	Unit
A:	TTIP to microsphere ratio	1:1	1:4	ml/g
B:	Calcining temperature	550	400	˚C
C:	Calcining time	5	3	hours
D:	Pre-heating temp.	150	20	˚C

Table 4-1 Coating process factors and their levels

4.2.4 Photocatalytic effectivity experiment

The photocatalytic effect of the coated microspheres was tested by measuring the degradation of an organic dye, methylene blue, as a function of time under UV exposure (intensity 225mW/cm^2) using a UV-visible spectrometer.
The experimental setup consisted of a cylindrical pyrex reactor placed on a magnetic stirrer and under the UV source. The reactor was cooled with a fan during UV exposure. The inner diameter of the Pyrex reactor was 4,6cm.
The experiment was carried out by dispersing 60mg of coated microspheres in a 30ml solution of MB. The solution was stirred and allowed to reach equilibrium in the dark for 24 hours. Once at equilibrium the MB concentration was measured and the value recorded as the initial concentration. The initial concentration of the samples was 100±5µmol/dm^3. Next the solution was placed in the reactor and irradiated for 5 min under continuous stirring. After exposure the solution was left in the dark for 24 hours before the MB concentration was measured in the spectrometer. This was done to both let the solution reach equilibrium and because the spheres float to the surface of the solution due to their low density. This is important so a sample for measurement can be drawn from the solution without any microspheres which would affect the measured spectrum. The procedure was repeated until the solution had been exposed to UV light for 20 minutes.

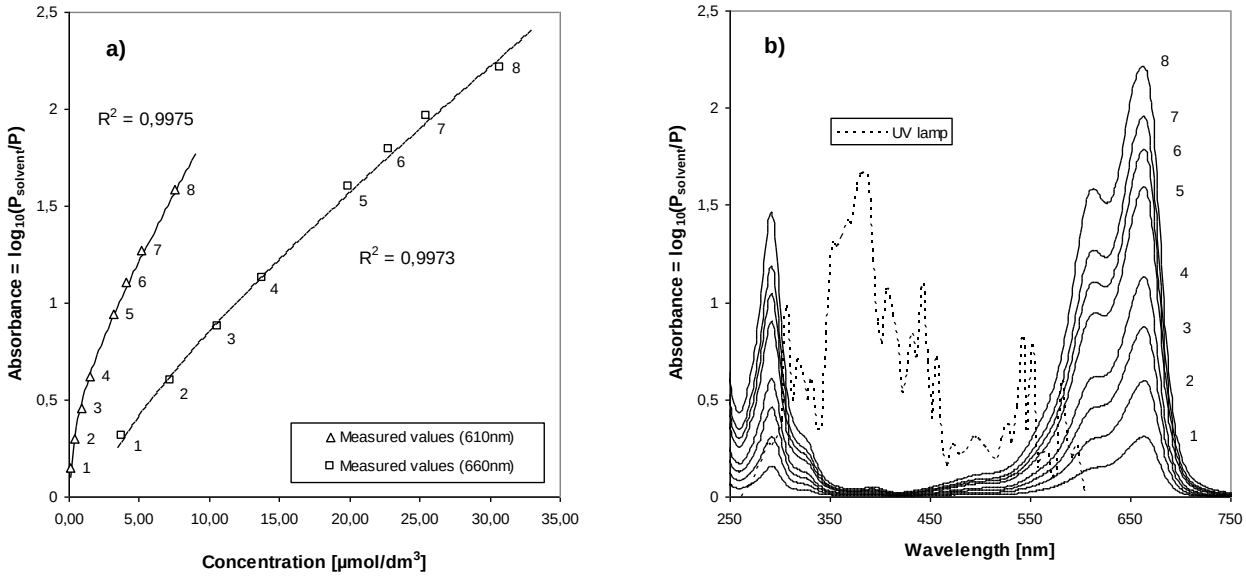

Fig. 4-4 a) Modelled light absorption of MB monomer and dimer. b) UV-Vis spectra of known concentrations and UV lamp emission spectrum.

4.2.5 Calibration of photocatalytic effectivity measurement

The calibration of the MB concentration was done by measuring the spectrum of solutions with known concentrations. MB does not aggregate further than to dimers at concentrations between 10^{-5} and 10^{-3}M in aqueous solution and in the visible part of the spectrum the absorption peaks are at 660nm and 610nm, which are due to the monomer and dimer respectively [14]. To correctly calibrate both peaks in the concentration range 10^{-5} to 10^{-3}M it is therefore necessary to know the equilibrium between monomer and dimer, which can be calculated with Equation 4-1 [15], where K_{eq} = 3970dm^{3}mol^{-1} according to the literature [16], [MB] is the monomer concentration and $[MB]_{Tot}$ is the total concentration of methylene blue.

$$2 \cdot K_{eq}[MB]^2 + [MB] - [MB]_{Tot} = 0$$

Equation 4-1

MB does not obey Beer's law although calibration curves can be close to linear within a certain concentration range. Due to the concentration dependence of the ratio of mono- and dimer a calibration of the corresponding peaks will not behave linearly within the concentration range used in this work so Beer's law can not be directly applied. Adding a constant and a term with the logarithm of the concentration to Beer's law, Equation 4-2, gives a good fit within the concentration range used as can be seen in Fig. 4-4 a). The calibration curves were determined by measuring the absorption of monomer and dimer for known concentrations, labelled 1-8, and determining the concentration of monomer and dimer with Equation 4-1. The measured values were then modelled with Equation 4-2, where A is absorption and c concentration, yielding the constants α,β and γ, see Table 4-2.

$$\begin{bmatrix} A_1 \\ \vdots \\ A_n \end{bmatrix} = \alpha + \beta \cdot \begin{bmatrix} c_1 \\ \vdots \\ c_n \end{bmatrix} + \gamma \cdot \begin{bmatrix} \ln(c_1) \\ \vdots \\ \ln(c_n) \end{bmatrix}$$

Equation 4-2

Constant	610nm peak	660nm peak
α	0,40192	-0,21912
β	0,11868	0,05583
γ	0,13631	0,22474

Table 4-2 Model constants for 610nm and 660nm peaks, respectively.

The effect of the light source on the MB concentration during exposure also has to be taken into account. In Fig. 4-4 b) the MB spectrum is compared to the emission spectrum of the UV source used. There is some overlapping of the two spectra which means the light source can cause some dye bleaching.

4.2.6 Self-cleaning test of paint films

In order to test whether a paint film comprising the photocatalytic carrier particles has self-cleaning functionality alkyd paints comprising both uncoated and coated HGMS were prepared. The approximate formulation for the alkyd paint can be seen in Table 4-3**Error! Reference source not found.**. Films were applied on panels and exposed in a Q-Lab QUV chamber, equipped with QUV-A340 UV lamps, for 3500 hours with alternating 4 hours of UV-exposure and 4 hours water condensation according to ISO 11507. The self-cleaning test was done by applying 0,3 ml drop of 100 µmol/dm^3 aqueous MB to the surface and allowing it to dry out. The panels were then exposed in a QUV chamber and photographed after 28 and 52 hours of exposure.

Raw material	Weight %
Alkyd binder	~30
Glass microspheres	~6,5
Rutile TiO2 pigment	~20
Solvents and additives	~43,5

Table 4-3 Approximate alkyd formulation.

4.3 Results and discussion

4.3.1 TiO_2 Coating

Fig. 4-5 shows a comparison of a) uncoated microspheres versus coated samples, both the b) "1" and c) "abcd" treatment combinations. The surface of the uncoated microspheres is very smooth in contrast to the coated ones so clearly the treatments have modified the surface. Both coatings can be described as a thin layer covering the whole surface with larger clusters spread randomly on the surface. Nevertheless due to the treatment differences the morphology of the coatings is quite

different. Fig. 4-5 d) shows the cross section of a broken microsphere which has been coated with the "abcd" treatment where the thin coating can be seen.

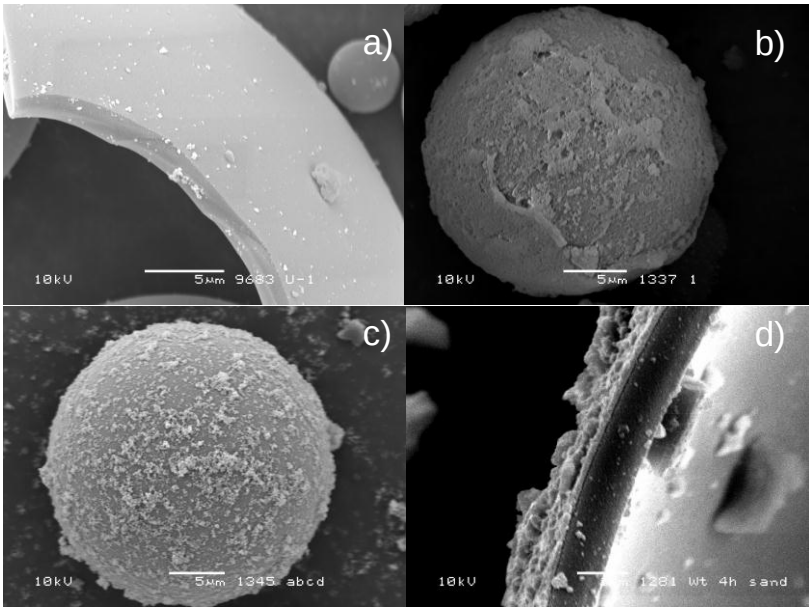

Fig. 4-5 a) Uncoated microsphere fragment. b) Microsphere coated with the "1" treatment combination. c) Microsphere coated with the "abcd" treatment combination. d) Wear tested microsphere fragment coated with the "abcd" treatment combination.

To verify that the coating was TiO_2 and furthermore of the anatase crystal structure an EDS and XRD analysis were made. Fig. 4-6 and Table 4-4 show the results of an EDS analysis of a coated microsphere in weight percent. Spectrum 1 is an area scan of an area that has no large particle clusters and spectrum 2 is a point scan of a large particle cluster. The area scan shows 2,2 wt% titanium indicating a thin coating containing titanium. The other elements make up all the main ingredients in borosilicate glass. The microspheres contain boron and may contain potassium and/or lithium but boron and lithium are however not detectable with EDS. The point scan shows 35,4 wt% titanium as well as a high concentration of oxygen and the clusters are therefore identified as being an oxide of titanium.

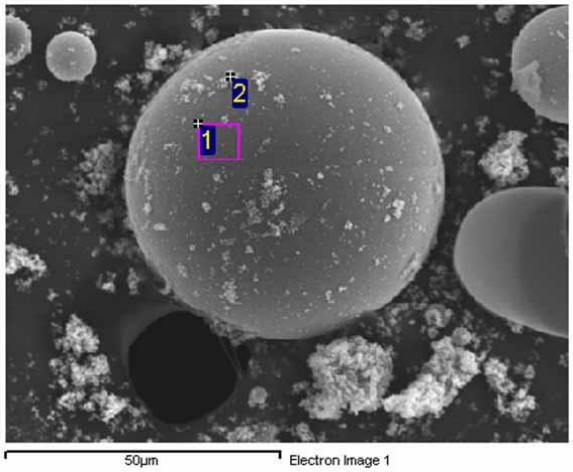

Fig. 4-6 Microsphere coated with the "abc" treatment combination analysed with EDS.

Spectrum	O	Na	Si	Ca	Ti
	wt%	wt%	wt%	wt%	wt%
1	39,3	3,7	44,0	10,8	2,2
2	37,6	2,5	19,4	5,1	35,4

Table 4-4 EDS analysis of "abc" coated microsphere. All results are in wt%

An XRD analysis of all the different coating treatment combinations is shown in Fig. 4-7 where the anatase peak positions are marked by broken lines. Generally the peaks are not so pronounced which can be attributed to the amorphous glass dominating the spectrum. This can be seen in Fig. 4-8 which shows a comparison of spectra, from Fig. 4-7 a), b), c) and d) and the spectrum of uncoated spheres (labelled 0), where the background signal has not been removed.

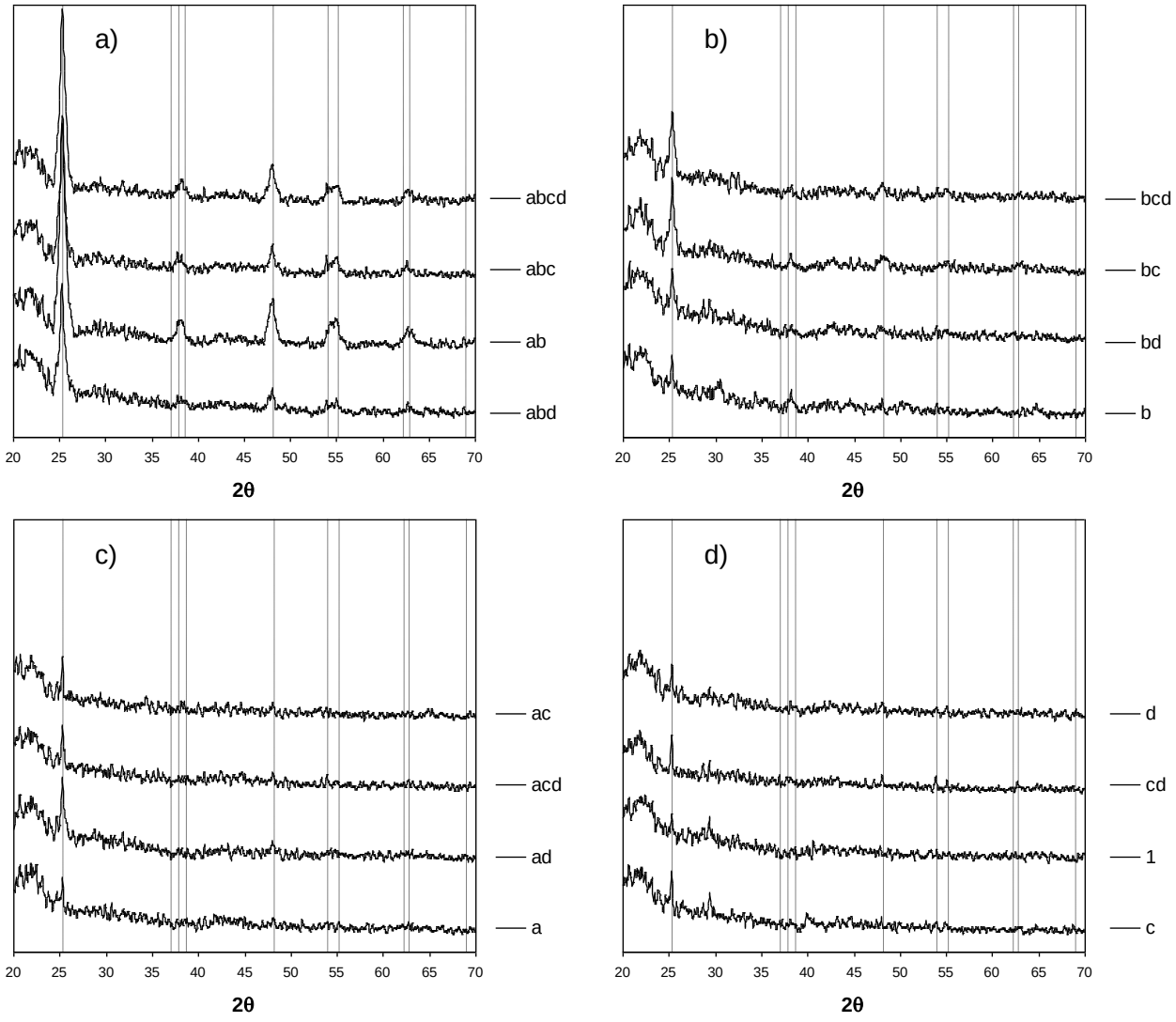

Fig. 4-7 XRD spectra HGMS coated with different treatment combinations. a) "A" and "B" at high level, b) "B" at high level "A" at low, c) "A" at high level "B" at low, d) neither "A" nor "B" at high level. The lines correspond to the anatase peak positions.

From comparing the spectra in Fig. 4-7 it is clear that the combinations with "A" and "B" at high level are the most crystalline of all the samples and the peak positions are consistent with anatase.

In the remaining spectra only the peak at 2θ ~26° can be detected and treatment combinations with "B" at high level exhibit the largest peaks of those. The crystal size for the samples with "A" and "B" at high level was determined by applying Rietveld refinement on the spectra and found to be 11nm. It was however not possible to determine the crystal size of the other samples.

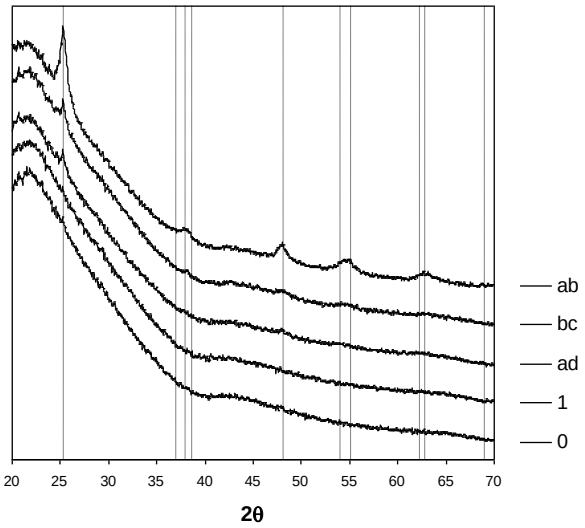

Fig. 4-8 XRD spectra with background.

4.3.2 Coating adhesion

An important property of the anatase coating is its adhesion to the HGMS. Pigments and fillers need to be dispersed in paint for it to be homogenous and this is generally done by stirring. This exposes the particles to shear forces and the anatase coating needs to be robust enough to handle such processing. This can be achieved by forming a covalent bond between the coating and substrate which should give excellent adhesion. The microspheres are predominantly made of silica which has OH groups (silanols) on the surface and because TTIP is readily hydrolyzed a covalent bond can be formed by reacting TTIP with silanols as shown in Fig. 4-9. However, this can only be achieved if TTIP has access to surface hydroxyls. It has been shown that out of the different types of silanols TTIP reacts mainly with hydrogen bonded silanols[17] and furthermore that hydrogen bonded silanols are the main adsorption sites for physically adsorbed water[18]-[19]. Therefore if physically adsorbed water isn't removed before coating the TTIP may be hydrolyzed before reaching the silanols causing poor adhesion. Fig. 4-10 a), b) and c) shows examples where the adhesion of the coating was poor. The coating is obviously not covalently bound to the glass surface as large shell like pieces break off the microsphere. This was found in all the samples where the microspheres had not been heat treated before being coated. Poor adhesion of a TiO_2 coating to glass microspheres and subsequent loss of coating due to mechanical processing has been reported elsewhere[20]. This indicates that the mechanical stability and durability of coated spheres, which aren't heat treated before coating, may be unsatisfactory.
Heat treating the microspheres above 100°C will remove physically adsorbed water and should therefore allow TTIP to react directly with hydrogen bonded silanols but the treatment temperature should not exceed 165°C as silanols can start to evaporate from the surface[18]-[21]. Poor adhesion, as seen in Fig. 4-10 a), b) and c), was not detected in the samples which were heat treated before coating.

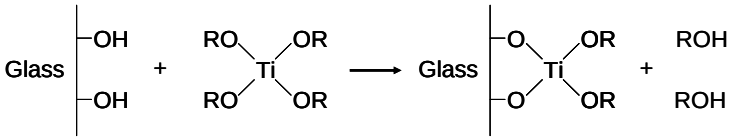

Fig. 4-9 Schematic illustration of the reaction of TTIP with a glass surface.

To further test the adhesion of the coating to the microspheres a simple wear test was devised to investigate how the coating on the microspheres which had been heat treated would perform under harsh conditions. Microspheres coated with the "abcd" treatment combination were subjected to a wear test. The test was made by mixing 0,25g of coated microspheres with 10g of quartz sand, average particle size 0,5mm, in a small plastic bottle. The bottle was then attached to a horizontal rotating axle and allowed to rotate at 60rpm for 4 hours. This treatment was severe enough so that only a small portion of the microspheres remained unbroken but the coating on the ones that were was intact. Furthermore investigation of sphere fragments revealed that the coating on the fragments was still intact and that the coating fractured along the same line as the glass. Examples of this can be seen in Fig. 4-5 d) and Fig. 4-10 d). The heat treatment of the microspheres before coating therefore seems to greatly improve the adhesion of the coating to the glass.

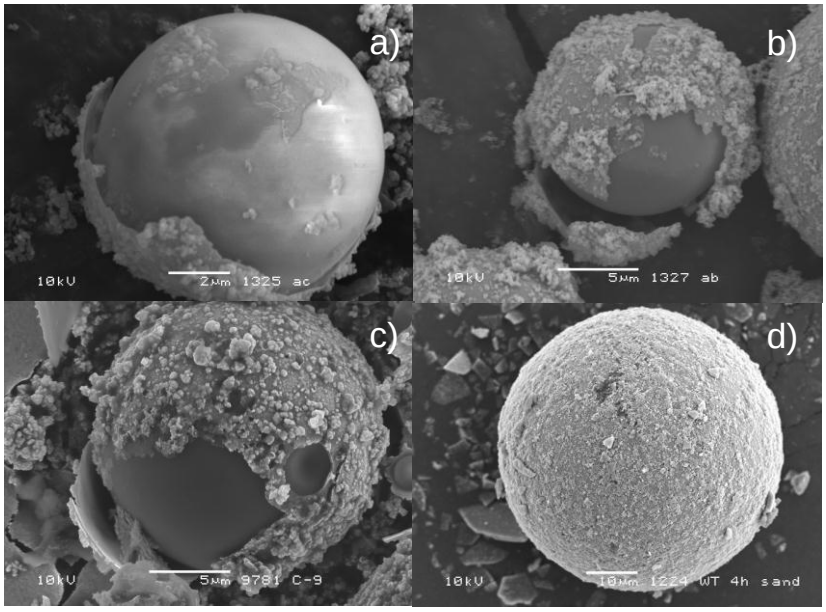

Fig. 4-10 Poor adhesion detected in treatment combinations a) "ac" b) "ab" c) "abc". Good adhesion to microsphere coated with the d) "abcd" treatment combination even after wear testing.

4.3.3 Photocatalytic effectivity

The photocatalytic effectivity of the coated microspheres was investigated by measuring the dye bleaching of MB as a function of UV irradiation time. The structure of methylene blue can be seen in Fig. 4-11 and the reaction when MB is totally mineralised by a photocatalyst is:

$$C_{16}H_{18}N_3SCl + 25\frac{1}{2}O_2 \xrightarrow[h\nu \geq 3,2eV]{TiO_2} HCl + H_2SO_4 + 3HNO_3 + 16CO_2 + 6H_2O$$

Equation 4-3

The photocatalytic degradation pathway of MB in water has been investigated in more detail by Houas et al [22]. It should be made clear that measuring dye bleaching is not a measurement of the total mineralisation reaction but instead of the partial breakdown of the molecules. Measurement of dye bleaching is therefore not a suitable method for estimating the true quantum yield of a photocatalytic reaction but is a useful and quick method for comparing the effectivity of samples.

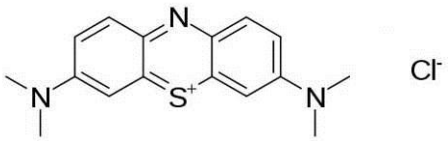

Fig. 4-11 Methylene blue structure.

The results of the photocatalytic effectivity measurements of all the treatment combinations are shown in Fig. 4-12 a) and b). The figures show the concentration change as a function of time. The results fall into three groups with regards to effectivity. The first group is made up of the four most effective combinations which have both factors "A" and "B" at high level. The second most effective group is the four combinations that have "B" at high and "A" at low. The third and least effective group is the eight combinations which have "B" at low level.

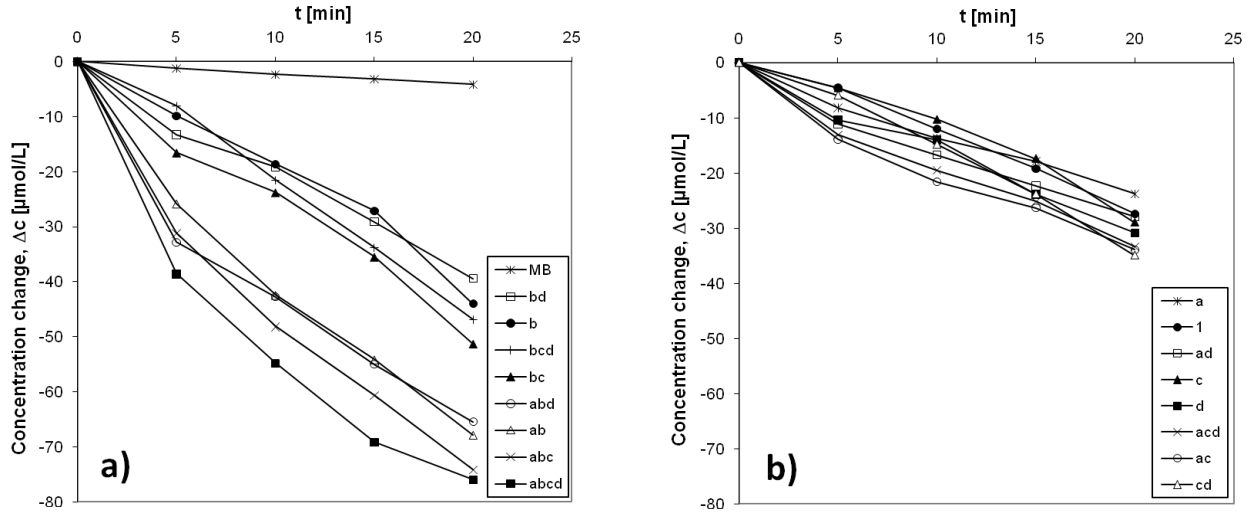

Fig. 4-12 Measured concentration decrease of different treatment combinations. a) The most effective treatments including a clean sample only with methylene blue solution, labelled MB. b) The least effective treatment combinations.

The effectivity is calculated using equation Equation 4-4 [23] where Δc is the concentration change in [µmol/l], V is the solution volume [l], I is the radiation intensity [W/cm^2], s is irradiated solution surface area [cm^2], t is time [s] and E is effectivity [µmol/J].

$$E = \frac{\Delta c \cdot V}{I \cdot s \cdot t}$$

Equation 4-4

To determine the significance of the individual factors in the coating process on the photocatalytic effectivity the factors were analysed using analysis of variance (ANOVA).
The results of the ANOVA analysis are presented in Table 4-5 and they illustrate that there are at least 4 factors that influence the photocatalytic activity. In can be asserted with high confidence that "A", "B", "AB" and "C" are all influential but the "AC" interaction is borderline significant, given a 95% confidence interval. The most influential factor is "B", calcining temperature, followed by the "AB" interaction and "A", TTIP to HGMS ratio. This is in good agreement with the results which show the treatment combinations with both "A" and "B" at high level are both the most effective and most crystalline. The second most effective and crystalline group of samples have "B" at high level and the rest show considerably less effectivity and crystallinity. Intuitively "A" is significant because using a high TTIP vs. HGMS ratio in the coating process will result in more TiO_2 on the glass surface. "B" and "C" increase the photocatalytic effectivity because high temperature and long annealing time results in better crystallization due to a higher diffusion rate and longer diffusion time, respectively. Therefore the significance of the "AB" and "AC" interactions can be explained by the temperature and calcining time having a larger effect when there is more material to crystallize. "D", heat treating the microspheres before coating, doesn't seem to have any significant effect on the photocatalytic activity but as shown earlier improves the adhesion of the coating.

Factor	Effect	Sum sq.	Mean sq.	F_0	P-value (α)
A	9,62E-05	3,70E-08	3,70E-08	183,11	3,9·10-5
B	1,69E-04	1,15E-07	1,15E-07	567,31	2,4·10-6
AB	1,06E-04	4,47E-08	4,47E-08	221,02	2,5·10-5
C	3,59E-05	5,14E-09	5,14E-09	25,46	0,0039
AC	1,84E-05	1,36E-09	1,36E-09	6,72	0,0488
BC	1,35E-05	7,27E-10	7,27E-10	3,6	0,1164
ABC	-1,15E-05	5,27E-10	5,27E-10	2,61	0,1672
D	1,52E-05	9,19E-10	9,19E-10	4,55	0,0862
AD	-9,89E-06	3,91E-10	3,91E-10	1,93	0,2229
BD	-8,46E-06	2,86E-10	2,86E-10	1,42	0,2874
ABD	1,43E-06	8,16E-12	8,16E-12	0,04	0,8486
CD	6,61E-07	1,75E-12	1,75E-12	0,01	0,9295
ACD	-1,53E-06	9,39E-12	9,39E-12	0,05	0,8378
BCD	8,63E-06	2,98E-10	2,98E-10	1,47	0,2788
ABCD	6,48E-06	1,68E-10	1,68E-10	0,83	0,404
Error		1,01E-09	2,02E-10		
Total		2,06E-07			

Table 4-5 ANOVA table for factorial experiment.

An F-test was used to determine the significance of the factors. The F-test is very sensitive to non-normality of the dataset so to ensure the reliability of the model it is necessary to check whether the non-significant factors and the residuals are normally distributed. Fig. 4-13 shows a normal probability plot of the calculated effects and Fig. 4-14 residual plots of the model. The four most significant factors are not normally distributed while the non-significant factors and the residuals are. None of the high order interactions seem to be significant and they are therefore added together as the sum of squares error. Judging from the residual plots in Fig. 4-14 the residuals seem to be normally distributed and the model therefore accepted.

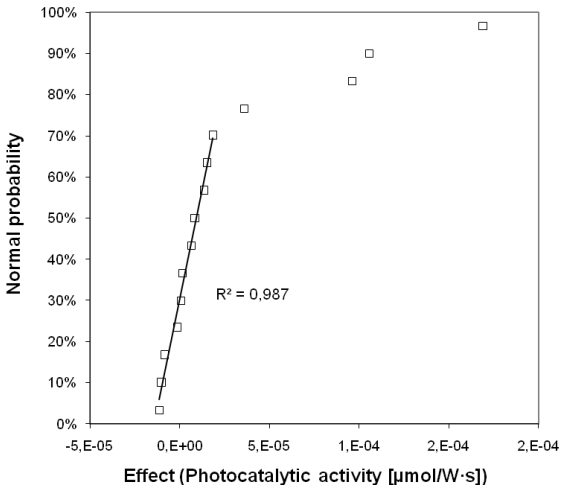

Fig. 4-13 Normal probability plot of effects.

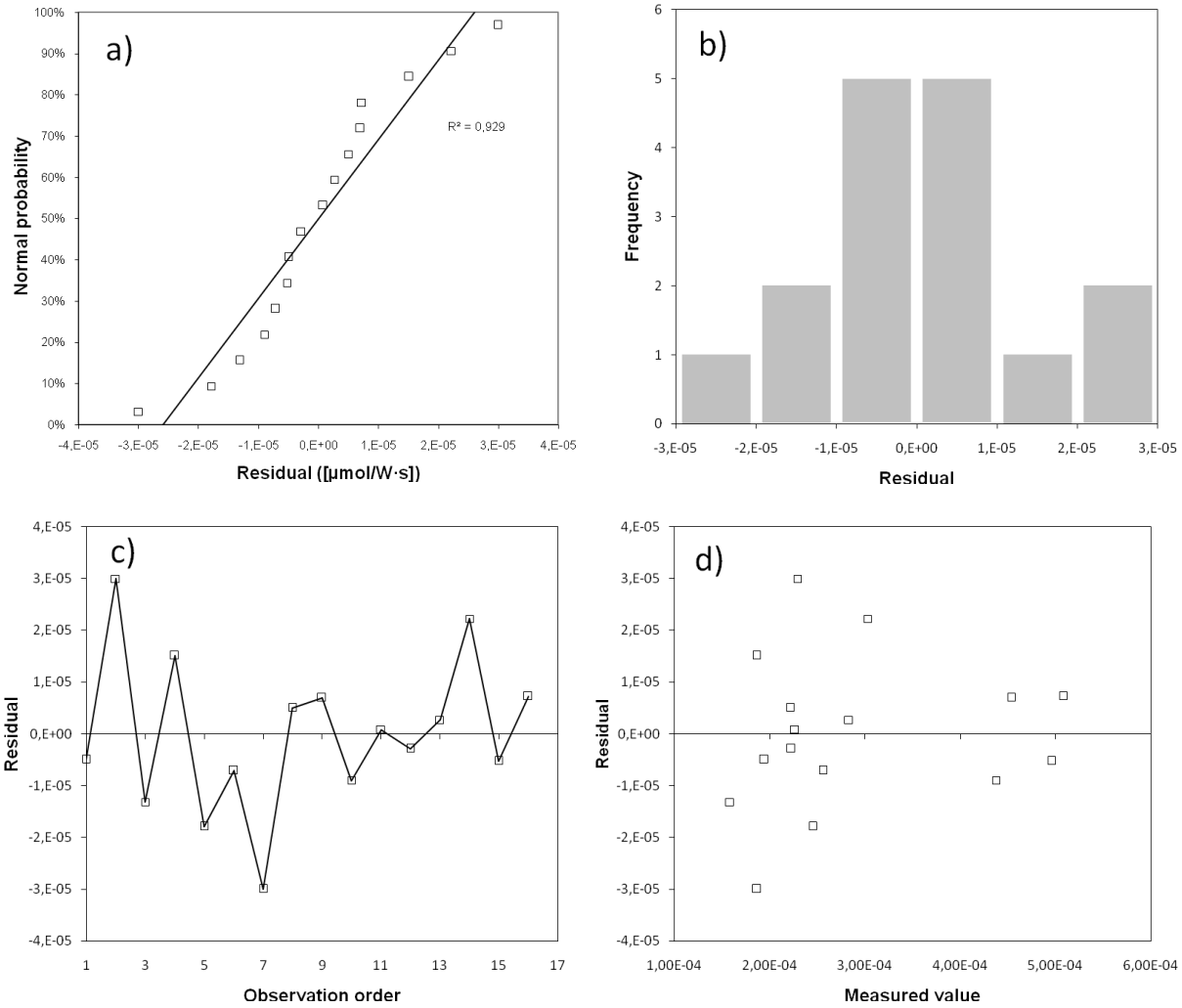

Fig. 4-14 Residual plots. a) Normal probability plot of residuals. b) Residual histogram. c) Residuals versus observation order. d) Residuals versus measured values.

Coefficient	Value
β_0	2,882E-04
β_A	9,62E-05
β_B	1,693E-04
β_C	3,59E-05
β_{AB}	1,057E-04
β_{AC}	1,84E-05

Table 4-6 Regression model coefficients.

The regression model for photocatalytic effectivity based on the five significant factors is shown in Equation 4-5 and the model constants are in Table 4-6.

$$Y = \beta_0 + \beta_A \cdot x_A + \beta_B \cdot x_B + \beta_C \cdot x_C + \beta_{AB} \cdot x_A \cdot x_B + \beta_{AC} \cdot x_A \cdot x_C + \varepsilon$$

Equation 4-5

4.3.4 Self-cleaning effect

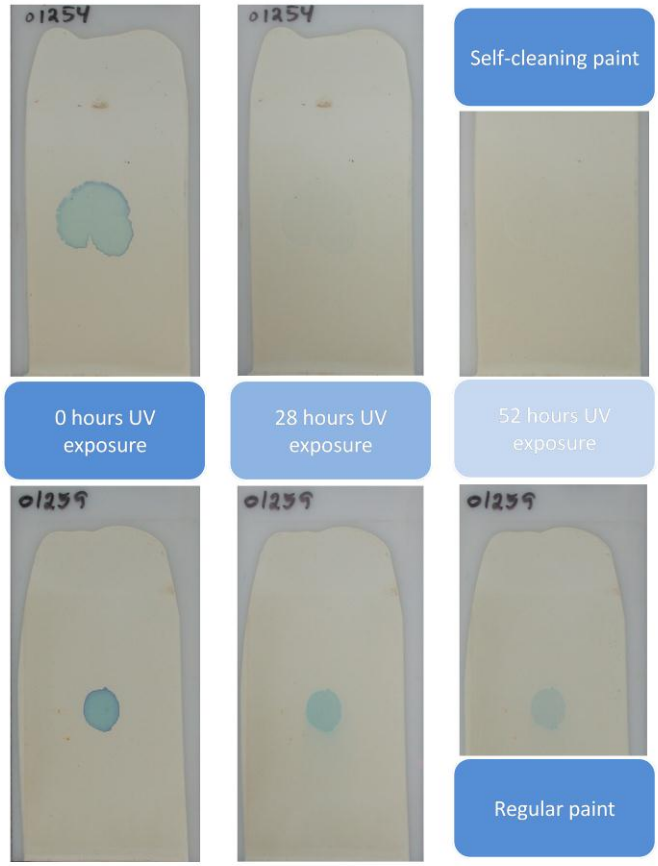

Fig. 4-15 Self cleaning test of alkyd paint films with uncoated microspheres and anatase coated microspheres.

The results of the self-cleaning test are presented in Fig. 4-15 which shows a comparison of two paint films comprising uncoated and coated microspheres. Both films had been exposed for 3500 hours in an accelerated weathering test chamber simulating sunlight and water condensation. Even

after this long period of exposure there was no visible evidence of the photocatalytic film being further degraded than the other film and there weren't any signs of excessive chalking. The dye colour on the film with uncoated microspheres did fade somewhat as a result of water condensation and UV exposure but can not be considered to have self cleaning properties. The film with coated microspheres on the other hand showed very positive results as the stain had nearly disappeared after 28 hours of exposure. After 52 hours there was very little trace of the stain left. It is interesting to note that the drop spread over a much larger area on the self-cleaning film. This is most likely due to the hydrophilic nature of the photocatalyst.

4.4 Conclusion

Hollow glass microspheres were coated with TiO_2 under different conditions and the coatings characterized. The performance of the coating was evaluated based on its photocatalytic activity and adhesion to the substrate.
The calcining temperature was found to be very important for the photocatalytic activity. The coatings that were calcined at 400°C exhibited very little crystallinity and therefore a lot less photocatalytic activity as compared to the samples calcined at 550°C. The temperature resistance of the microspheres is a limiting factor as they can start to change shape at 600°C so the calcining temperature should be as close as possible to maximize the photocatalytic effectivity.
Heat treating the glass microspheres before coating did not have any effect on the photocatalytic activity but was shown to have a positive effect on the adhesion of the coating to the substrate.
Paint formulated with anatase coated microspheres display excellent self-cleaning properties along with excellent UV stability.

Acknowledgements

The authors would like to express their gratitude to Kenny Ståhl and Astrid Schøneberg; DTU Chemistry, Technical University of Denmark; for their help with XRD measurements and analysis. Furthermore we thank Dyrup A/S and the Danish Agency for Science and Innovation for financial support.

References

[1] L. Li, W. Zhu, P. Zhang, Q. Zhang, and Z. Zhang, "TiO2/UV/O3-BAC processes for removing refractory and hazardous pollutants in raw water," *Journal of Hazardous Materials*, vol. 128, no. 2-3, pp. 145-149, Feb. 2006.
[2] J. Zhao and X. Yang, "Photocatalytic oxidation for indoor air purification: a literature review," *Building and Environment*, vol. 38, no. 5, pp. 645-654, May 2003.
[3] A. Fujishima, X. Zhang, and D. A. Tryk, "Heterogeneous photocatalysis: From water photolysis to applications in environmental cleanup," *International Journal of Hydrogen Energy*, vol. 32, no. 14, pp. 2664-2672, Sep. 2007.
[4] I. P. Parkin and R. G. Palgrave, "Self-cleaning coatings," *Journal of Materials Chemistry*, vol. 15, no. 17, p. 1689, 2005.
[5] A. E. Jacobsen, "Titanium Dioxide Pigments: Correlation between Photochemical Reactivity and Chalking.," *Industrial & Engineering Chemistry*, vol. 41, no. 3, pp. 523-526, Mar. 1949.
[6] A. Fujishima and K. Honda, "Electrochemical Photolysis of Water at a Semiconductor Electrode," *Nature*, vol. 238, no. 5358, pp. 37-38, Jul. 1972.

[7] U. Gesenhues, “Al-doped TiO2 pigments: influence of doping on the photocatalytic degradation of alkyd resins,” *Journal of Photochemistry and Photobiology A: Chemistry*, vol. 139, no. 2-3, pp. 243-251, Mar. 2001.
[8] P. A. Christensen, A. Dilks, T. A. Egerton, E. J. Lawson, and J. Temperley, “Photocatalytic oxidation of alkyd paint films measured by FTIR analysis of UV generated carbon dioxide,” *Journal of Materials Science*, vol. 37, no. 22, pp. 4901-4909, 2002.
[9] A. Mills, A. Lepre, N. Elliott, S. Bhopal, I. P. Parkin, and S. A. O’Neill, “Characterisation of the photocatalyst Pilkington Activ(TM): a reference film photocatalyst?,” *Journal of Photochemistry and Photobiology A: Chemistry*, vol. 160, no. 3, pp. 213-224, Aug. 2003.
[10] N. S. Allen, M. Edge, G. Sandoval, J. Verran, J. Stratton, and J. Maltby, “Photocatalytic Coatings for Environmental Applications¶†,” *Photochemistry and Photobiology*, vol. 81, no. 2, pp. 279-290, Mar. 2005.
[11] G. KAEMPF, PAPENROT.W, and R. HOLM, “DEGRADATION PROCESSES IN TIO2-PIGMENTED PAINT FILMS ON EXPOSURE TO WEATHERING,” *JOURNAL OF PAINT TECHNOLOGY*, vol. 46, no. 598, pp. 56-63, 1974.
[12] W. G. Wamer, J.-J. Yin, and R. R. Wei, “Oxidative Damage to Nucleic Acids Photosensitized by Titanium Dioxide,” *Free Radical Biology and Medicine*, vol. 23, no. 6, pp. 851-858, 1997.
[13] W. A. Pryor, “Oxy-Radicals and Related Species: Their Formation, Lifetimes, and Reactions,” *Annual Review of Physiology*, vol. 48, no. 1, pp. 657-667, Oct. 1986.
[14] E. Rabinowitch and L. F. Epstein, “Polymerization of Dyestuffs in Solution. Thionine and Methylene Blue1,” *Journal of the American Chemical Society*, vol. 63, no. 1, pp. 69-78, Jan. 1941.
[15] A. Mills and J. Wang, “Photobleaching of methylene blue sensitised by TiO2: an ambiguous system?,” *Journal of Photochemistry and Photobiology A: Chemistry*, vol. 127, no. 1-3, pp. 123-134, Oct. 1999.
[16] W. Spencer and J. R. Sutter, “Kinetic study of the monomer-dimer equilibrium of methylene blue in aqueous solution,” *The Journal of Physical Chemistry*, vol. 83, no. 12, pp. 1573-1576, Jun. 1979.
[17] S. Srinivasan, A. K. Datye, M. H. Smith, and C. H. F. Peden, “Interaction of Titanium Isopropoxide with Surface Hydroxyls on Silica,” *Journal of Catalysis*, vol. 145, no. 2, pp. 565-573, Feb. 1994.
[18] M. L. Hair, “Hydroxyl groups on silica surface,” *Journal of Non-Crystalline Solids*, vol. 19, pp. 299-309, Dec. 1975.
[19] G. J. Young, “Interaction of water vapor with silica surfaces,” *Journal of Colloid Science*, vol. 13, no. 1, pp. 67-85, Feb. 1958.
[20] M. Koopman et al., “Titania-coated glass microballoons and cenospheres for environmental applications,” *Journal of Materials Science*, vol. 44, no. 6, pp. 1435-1441, Sep. 2008.
[21] L. Diaz, C. M. Liauw, M. Edge, N. S. Allen, A. McMahon, and N. Rhodes, “Investigation of factors affecting the adsorption of functional molecules onto gel silicas: 1. Flow microcalorimetry and infrared spectroscopy,” *Journal of Colloid and Interface Science*, vol. 287, no. 2, pp. 379-387, Jul. 2005.
[22] A. Houas, H. Lachheb, M. Ksibi, E. Elaloui, C. Guillard, and J.-M. Herrmann, “Photocatalytic degradation pathway of methylene blue in water,” *Applied Catalysis B: Environmental*, vol. 31, no. 2, pp. 145-157, May 2001.
[23] S. Preis, M. Krichevskaya, Y. Terentyeva, A. Moiseev, and J. Kallas, “Treatment of Phenolic and Aromatic Amino Compounds in Polluted Waters by Photocatalytical Oxidation,” *Journal of Advanced Oxidation Technologies*, vol. 5, pp. 77-84, Jan. 2002.

5 Paper 2: Self-cleaning efficiency and degradation mechanism of alkyd paint comprising photocatalytic TiO2 coated hollow glass microspheres

Sverrir G. Gunnarsson,*a Per Møller*a and Søren H. Poulsenb

Abstract

Hollow glass microspheres (HGMS) were coated with photocatalytic TiO_2 and characterised with SEM, EDS and XRD. The coated microspheres were integrated into an alkyd paint system with the purpose of making the films self-cleaning. The effect of the photocatalyst on the degradation of the paint film was investigated and found to be minimal. The self-cleaning efficiency of paint films with 0%, 10%, 20% and 30% microspheres by volume was studied by measuring the degradation rate of methylene blue (MB) and found to be dependent on the surface concentration of coated microspheres. The liquid and vapour permeability of the films was investigated and the microspheres found to greatly improve the barrier properties not only due to a increase in water diffusion length but also because of increased crack resistance.

5.1 Introduction

Photocatalysis has shown great promise for a number of applications due to the high reactivity of the OH radicals created in the reaction, which can degrade even the most persistent organic pollutants (POP's) [1]. These applications include air purification [2], sterilization of water or surfaces [3] and making surfaces self-cleaning [4] just to exemplify a few of the potential applications discussed in the literature. The most commonly used photocatalyst is TiO_2 of the anatase or rutile structure, anatase being the more effective of the two [5]. Furthermore TiO_2 is the most common pigment used in paints; where the rutile structure is favoured to the anatase structure due to slightly better optical properties and less photocatalytic activity. The photo-activity of TiO_2 pigments and consequent degradation of organic binders, often termed chalking, has been well known to the paint industry [6] since long before Fujishima and Honda published their paper on photolysis of water [7]. Controlled chalking was considered favourable as constant renewal of the surface served as a crude self-cleaning mechanism [6]. Today this photo-activity is much better understood which is why commercial titanium pigments currently are stabilised (surface treated) with for example Al_2O_3 to suppress the creation of reactive hydroxyl radicals [8][9].
With increased understanding of the photocatalytic reaction a lot of work has been done to utilize and commercialize the technology where perhaps the best known example is the Pilkington Activ^{TM} self-cleaning window glass [10]. The trend is to use photocatalytic nano-particles because of their high effectivity attained with a large surface area. Inorganic paints comprising anatase nano-particles have been successfully commercialized but even though attempts have been made to develop such organic self-cleaning paints [11] they have not been successful due to the vulnerability of organic binders to the photocatalytic reaction. Inorganic binders are relatively expensive compared to organic binders such as alkyds or acrylics and are not suitable for all applications making it interesting to further develop organic self-cleaning paints.
To be able to improve the design of organic self-cleaning paints it is necessary first to understand the degradation mechanism of paints comprising photocatalytic pigments. The mechanism is described in a paper by Kaempf et al [12] where the different effect of stabilised TiO_2 pigment

versus untreated pigments on alkyd binders are shown. In the paper a distinction is made between two degradation processes. Photochemical degradation of the binder due to absorption of UV-light and chalking which happens at the pigment/binder interface. The chalking mechanism is activated when photocatalytic pigment in the film surface is exposed to UV light and the particles become photoactive. The binder in the immediate vicinity of the particles is degraded by the hydroxyl radicals created and due to the small size of the particles very little material needs to be degraded before it is separated from the film. This mechanism causes films to slowly disintegrate or to put it in other words have much higher chalking rates compared to films with stabilised pigments. As mentioned above this can be interpreted as a self-cleaning mechanism as the surface continually renews itself but this approach has some serious disadvantages. The durability of the film will be very poor as it is in fact slowly self-destructing and thereby rapidly losing its protective properties. Substituting pigment sized particles (~ 0,25- 0,30µm) with nano-particles will increase the photocatalytic activity of the film and also greatly accelerate the rate of degradation of the film itself [11]. Furthermore as a result of a high chalking rate such a film would constantly release nano-particles to its surroundings. The effect of photocatalytic nano-particles on people has not yet been fully studied but investigations suggest they may have adverse health effects [13]. Due to the small size of the particles they are both highly active and may be able to penetrate the outermost skin layers and reach living cells.

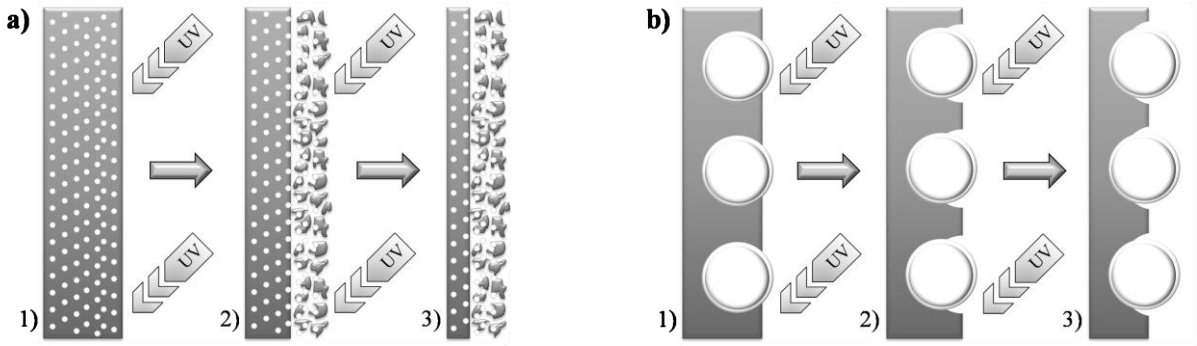

Fig. 5-1 a) shows a film with nano-particles constantly eroding from 1) to 3) during UV exposure. b) shows a film with photocatalytic carrier particles 1) Fresh film, 2) After initial exposure chalking has occurred, 3) Chalking has nearly ceased as UV radiation no longer reaches carrier particle/binder interface and the much slower photochemical degradation of the binder system becomes the predominant degradation process.

Instead of formulating organic paints with nano-particles the photocatalytic nano-crystalline anatase TiO_2 was coated onto micrometer sized carrier particles made from a material inert to the photocatalytic reaction. This can dramatically reduce the effect on the organic binder since the contact area between photocatalyst and binder is much less and due to the extremely short half-life of OH radicals[14] they cannot diffuse away from the site of formation. Therefore the binder should only be degraded in the immediate vicinity of the carrier particles. The particles need to be large enough to be embedded deep enough in the film so that UV light doesn't activate the buried part of the particle. Initially there will be chalking around the particles in the surface region but not over the entire particle/binder interface and therefore separation of carrier particles from the film can be minimized or even totally avoided contrary to the case of unsupported nano-particles. Once the initial chalking has ceased the degradation process will be governed by the much slower photochemical degradation. Only after an extended period of weathering can the chalking around the carrier particles resume. This way of integrating a photocatalyst into the film should slow down the chalking instead of increasing it and still yield enough photocatalytic activity to make the

surface self-cleaning as the carrier particles offer an area, unaffected by the photocatalytic reaction, on the film surface for the self-cleaning effect to take place.
The different film degradation mechanisms are illustrated in Fig. 5-1 which shows cross sections of the films. The figures do not represent the full film thickness.
Hollow glass microspheres were chosen as suitable carrier particles because they fulfil a number of the specifications deemed necessary. Most importantly they are made of borosilicate glass which is inert to the photocatalytic reaction and also due to their spherical shape a large amount of them can be dispersed in paint without having a too severe effect on viscosity and other important properties. It is important to add a large volume of carrier particles in order to get a sufficiently high concentration in the surface because otherwise the resulting self-cleaning effect can be poor.
This work was done to investigate the degradation mechanism during weathering of an alkyd paint film comprising photocatalytic TiO_2 coated microspheres and to determine the effects of different volume concentrations on self-cleaning efficiency and barrier properties.

5.2 Experimental

5.2.1 Materials and equipment

The hollow glass microspheres (HGMS) used for the self-cleaning efficiency test were iM30K Glass Bubbles from 3M. The microspheres are from borosilicate glass and have an average density of 0,6g/cm^3. The size distribution can be seen in Fig. 5-2 and the average diameter of the particles is measured to be 15,5µm. The spheres can withstand temperatures up to 600°C.

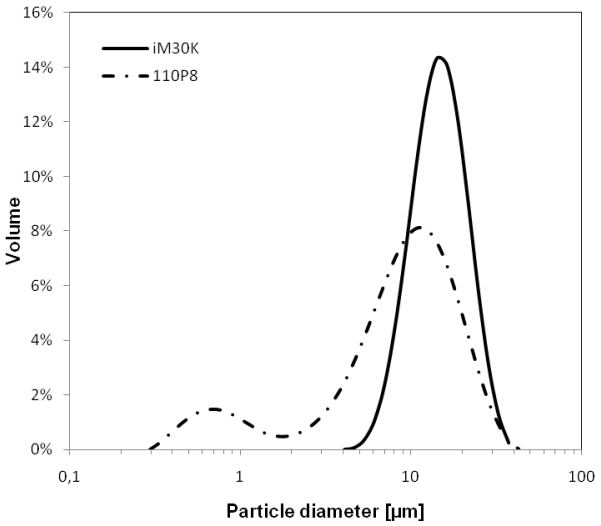

Fig. 5-2 iM30K and Sphericell 110P8 HGMS particle size distribution.

The HGMS used for the water permeability test were Sphericel 110P8 from Potters Industries. The average density is 1,1g/cm3 and the mean particle size 11µm. The size distribution can be seen in Fig. 5-2.

The titanium-tetraisopropoxide (TTIP) used to coat the microspheres was VERTEC® TIPT, 97+% from Alfa Aesar and the methylene blue (MB) used for the photocatalytic efficiency experiments 0,05% weight in H_2O from Sigma Aldrich.
Artificial weathering of samples was done in a Q-lab QUV artificial weathering chamber, equipped with QUV-A340 UV lamps, according to EN 927-6:2006 where the samples were exposed to alternating periods of 2,5 hours of UV exposure and 0,5 hours water spray for six days followed by 1 day of water condensation.
Electron microscopy was done using a JEOL model JSM-5900 electron microscope with a LaB_6 filament. The x-ray diffraction analysis was done using a Huber Guinier G670 diffractometer with $Cu_{K\alpha 1}$ radiation and particle size was measured with a Malvern Mastersizer 2000.

5.2.2 Coating process

The HGMS were coated using the method described below. The microspheres were pre-treated at 150°C for 24 hours to remove physically adsorbed water. Titanium tetra isopropoxide (TTIP), see Fig. 5-3, was mixed with isopropanol with a ratio of 1:10 and stirred for 20 minutes. 1g (iM30K) or 1,8g (Sphericel 110P8) of microspheres was added to the solution for every 10 ml isopropanol and the mixture stirred for 20 minutes. Then de-ionized water, 1 ml for every 1ml of TTIP, was added to the solution and stirred for 10 minutes. The solution was then filtered to remove most of the isopropanol and then heated to 70°C and continously stirred to avoid agglomeration while the remaining isopropanol evapourated. Once dry the coated microspheres were calcined at 550°C for 5 hours to crystallize the TiO_2. The process was repeated once more to load more TiO_2 on the microspheres. After the second round of coating the microspheres were separated from all unbound TiO_2 by sonication.

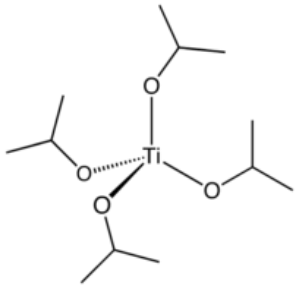

Fig. 5-3 Titanium tetraisopropoxide structure.

5.2.3 Paint formulations

Both opaque and transparent air drying alkyd paints were formulated with 0, 10, 20 and 30% of the solids volume as coated microspheres. Coated iM30K microspheres were used in the opaque paints and Sphericel 110P8 microspheres in the transparent paints. The microspheres were dispersed in the binder at 1000rpm and mixed with a rutile pigment paste. The approximate formulations can be seen in Table 5-1.

	Dry film HGMS vol.%	Binder	HGMS	Rutile	Solvents and additives
Opaque	0%	~31%	0%	~22%	~47%
	10%	~30%	~4%	~21,5%	~44,5%
	20%	~28%	~9%	~21%	~42%
	30%	~26%	~15%	~20%	~39%
Transparent	0%	~40%	0%	-	~60%
	10%	~37%	~5%	-	~58%
	20%	~35%	~10%	-	~55%
	30%	~33%	~16%	-	~51%

Table 5-1 Approximate alkyd formulations in wt%

5.2.4 Photocatalytic activity test

The self-cleaning efficiency of the paint films was estimated by measuring the dye bleaching of methylene blue (MB) as a function of UV radiation exposure time. The degradation pathway of methylene blue in water has been studied by others [15].
Alkyd paints were formulated with 0, 10, 20 and 30% of the solids volume as coated microspheres and applied on stainless steel panels. After drying the panels were exposed in a QUV chamber for 0, 473, 924, 1224 and 1675 hours. After exposure 5x5cm samples were cut out and placed in a 20µm MB solution for 1 hour to allow MB to pre-adsorb on the surface. The samples were then placed in a flow cell, the setup can be seen Fig. 5-4. The samples sat on a cooling plate and were held in place by a PTFE plate with a conical hole in the centre exposing an area with a diameter of 37mm. A cylindrical glass cell, with a quartz plate on top, was placed above the hole in the PTFE plate. 30ml of 20µmol MB solution was circulated in the cell at 12,5cm^3/min. The MB concentration was allowed to reach equilibrium in the dark and the solution was aerated before UV exposure began. The samples were then exposed to UV for 140 minutes and the absorbance of the solution at 660nm was measured every 10 minutes with a Shimadzu UV-mini 1240 UV-Vis spectrometer. The UV source used was a Philips CLEO HPA 400S, see spectrum in Fig. 5-15, which was placed approximately 40cm from the sample surface. The solution temperature was kept constant at 35°C with a thermostat which pumped water through the cooling plate.

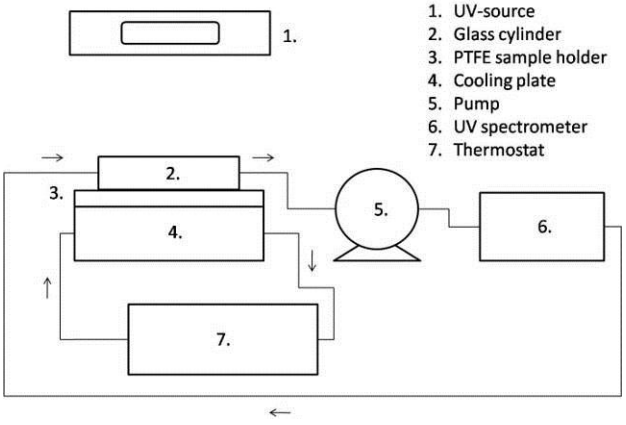

Fig. 5-4 Setup schematic for photocatalytic activity test.

After measuring the self-cleaning efficiency the same samples
were again placed under the UV source to confirm that the remaining MB on the surface could be bleached. The 1224 hour QUV exposure samples were placed in polystyrene Petri dishes on top of small PTFE blocks and 5ml of demineralised water added to provide high humidity. The samples

were not in direct contact with liquid water. The samples were then exposed to UV radiation for a total of 5 hours and photographed at 1 hour intervals.

5.2.5 Water permeability test

The water permeability of paint films with microsphere concentrations of 0, 10, 20 and 30% of the solid volume was measured by the cup method according to ISO 7783:2008. 0,7mm thick pinewood veneer was used as a substrate for the paint films. The permeability of the films was measured before QUV exposure and after 10, 20 and 30 days of exposure. The formulated paints were transparent (un-pigmented) to make them more sensitive to UV exposure. This was done to shorten the exposure time needed to measure changes in the film properties as it is limited how long such a thin substrate can withstand the aggressive environment of a QUV chamber. Great care was taken to spread the film evenly on the veneer and the film thickness was controlled by measuring the weight of the paint applied to a known area. The films were allowed to dry for 2 weeks at 23°C and 50%RH before being exposed in QUV. After the exposure the paint films were kept in a climate chamber at 23°C and 50%RH for 4 days before testing began. Uncoated veneer samples were also measured to determine the permeability of the substrate. Three specimens were measured for each sample.
The cups used were made from standard 1 ¼" x 40mm PVC adapter unions with PVC plugs which were sealed with glue. The cups were filled with de-ionized water up to a rim 1,7cm from the paint film. 5cm diameter samples were cut from the veneer and placed in the cups with the painted side inside the cup. The exposed area of the samples was 3,2cm in diameter. The cups were kept in a climate chamber at 23°C and 50%RH and weighed twice per week to keep track of water evaporation. The cups were placed upright to measure water vapour permeability and down with the water in contact with the paint films to measure liquid water permeability.

5.3 Results and discussion

5.3.1 TiO_2 Coating

The coated iM30K microspheres were characterized by SEM, EDS and XRD. Fig. 5-5 shows the coating on the surface of a broken microsphere. The coating is approximately 150nm thick with large clusters randomly placed on the surface.

Spectrum	O wt%	Na wt%	Si wt%	Ca wt%	Ti wt%
1	43.8	2.7	35.7	10.4	7.4
2	40.3	2.2	13.7	2.9	40.9
3	42.6	2.2	21.8	5.5	27.9

Table 5-2 EDS analysis of coated microsphere shown in Fig. 5-5.

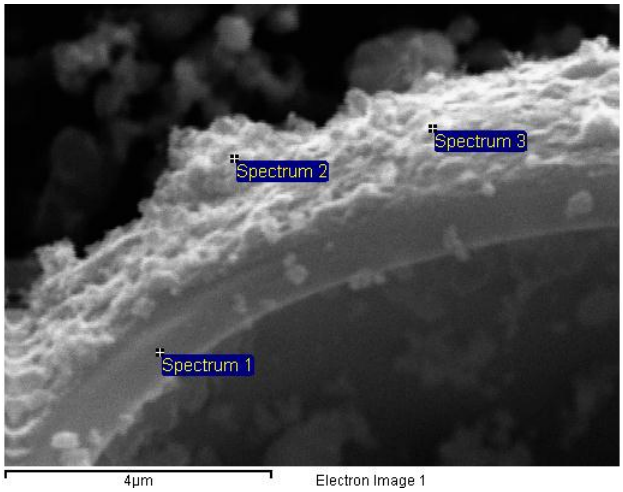

Fig. 5-5 Broken microsphere with TiO_2 coating on surface

The results of the EDS analysis of the coating in Fig. 5-5 is shown in Table 5-2. Spectrum 1 as expected shows a high content of the elements found in borosilicate glass. Spectrum 2 and 3 show a high Ti and O content indicating an oxide of titanium on the microsphere surface. This was confirmed with an XRD analysis of the coated microspheres compared with uncoated spheres. The microspheres were found to be amorphous while the coated spheres were crystalline. The spectra can be seen in Fig. 5-6 where the peak positions of anatase are represented by vertical broken lines. The peaks match an anatase TiO_2 structure and a Rietveld refinement of the spectrum indicated a crystal size of 14nm.

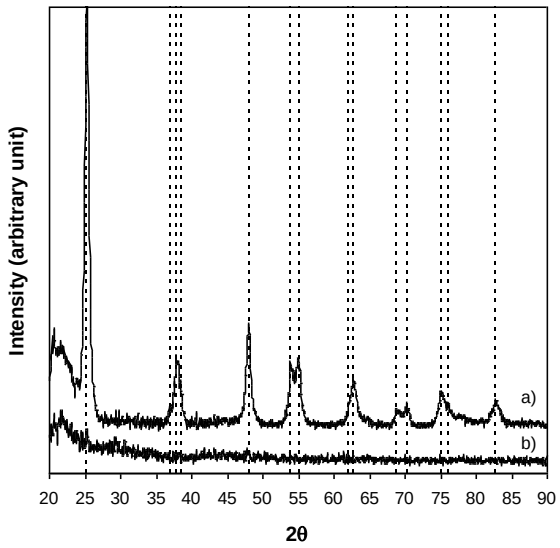

Fig. 5-6 XRD spectrum of a) coated microspheres and b) uncoated microspheres. The broken lines represent anatase TiO_2 peak positions.

5.3.2 Particle size and surface coverage

For a paint film with photocatalytic particles to be self-cleaning it is necessary that the concentration of particles in the surface is high and that the surface coverage is good. If large areas

in the paint film surface are without photocatalytic microspheres discolouration of the paint, due to some macroscopic areas being clean and others not, can affect the visual appearance of the film. This means that the average distance between the particles is of similar importance as volume concentration with regards to surface coverage. A very high volume percentage will of course result in short distances between particles but it is also highly dependent on particle size.
Nearest neighbour distance was first described by Hertz[16] and also discussed by Chandrasekhar[17]. According to this model the average distance between the centres of two particles, D, is

$$D = \frac{\Gamma\left(\frac{4}{3}\right)}{\left(\frac{4}{3}\pi \cdot n\right)^{\frac{1}{3}}}$$

Equation 5-1

where Γ represents the Gamma function and n is the average number of particles per unit volume. It can however be shown that this model doesn't describe the average distance well at high volume fractions. The number of particles per unit volume, n, can also be written as the volume percentage of solid particles, f_{solid}, divided by the volume of a spherical particle with radius r.

$$n = \frac{f_{solid}}{\frac{4}{3}\pi \cdot r^3}$$

Equation 5-2

Inserting Equation 5-2 into Equation 5-1 gives

$$D = \frac{\Gamma\left(\frac{4}{3}\right)}{f_{solid}^{\frac{1}{3}}} \cdot r$$

Equation 5-3

and as mentioned earlier D represents the distance between particle centres so to insert the particle size into the model we introduce $d_{average}$ as the distance between the surfaces of two equally large particles. D can therefore be written as

$$D = d_{average} + 2r$$

Equation 5-4

And by inserting Equation 5-4 into Equation 5-3 we get

$$d_{average} + 2r = \frac{\Gamma\left(\frac{4}{3}\right)}{f_{solid}^{\frac{1}{3}}} \cdot r$$

Equation 5-5

If the assumption is made that the particles cannot overlap, i.e. the spheres are tightly packed, the maximum solid volume concentration can be calculated by setting $d_{average}$ equal to zero which yields

$$\frac{\Gamma\left(\frac{4}{3}\right)}{f_{solid}^{1/3}} = 2$$

Equation 5-6

Solving Equation 5-6 for f_{solid} results in the maximum solid volume concentration of the model which is

$$f_{solid} = \left(\frac{1}{2} \cdot \Gamma\left(\frac{4}{3}\right)\right)^3 \approx 8{,}9\%$$

Equation 5-7

This result is far lower than the value proven by Gauss [18] to be the highest volume percentage possible for mono-sized spheres which brings us to the conclusion that the model doesn't adequately describe the average distance between particles at least at high loadings.

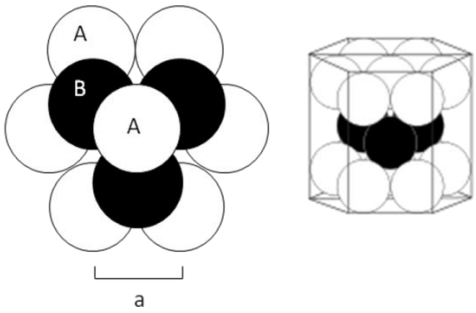

Fig. 5-7 HCP unit cell structure.

To derive the average distance between particles it is useful to assume that the particles are perfectly distributed so that the distance from the centre of each particle to the centre of all its neighbours is equal. At high volume fractions some structuring of the particles becomes necessary and it is therefore convenient to describe the system with the hexagonal close packing structure (hcp), as seen in Fig. 5-7, in which each particle has twelve neighbours all equally spaced and the highest possible packing ratio. The volume V of a hcp unit cell is

$$V_{hcp,unitcell} = 3 \cdot \sqrt{2} \cdot a^3$$

Equation 5-8

where a represents the side length, as seen in Fig. 5-7. Each unit cell contains 6 equally sized particles so the solid ratio of the unit cell is

$$f_{solid} = \frac{6 \cdot V_{sphere}}{V_{hcp,unitcell}} = \frac{8 \cdot \pi \cdot r^3}{3 \cdot \sqrt{2} \cdot a^3}$$

Equation 5-9

where r is particle radius. The side length, a, equals the sum of two times the particle radius and the distance between two particles, $d_{average}$.

$$a = d_{average} + 2r$$

Equation 5-10

Therefore when $d_{average} = 0$ we get a = 2r and by inserting into Equation 5-9 the highest possible packing ratio is found.

$$f_{solid} = \frac{\pi}{3 \cdot \sqrt{2}}$$

Equation 5-11

Isolating "a" in Equation 5-9 gives

$$a = \left(\frac{8 \cdot \pi}{3 \cdot \sqrt{2} \cdot f_{solid}} \right)^{\frac{1}{3}} \cdot r$$

Equation 5-12

and by inserting eEquation 5-10 into Equation 5-12 and solving for $d_{average}$ we get the relation

$$d_{average} = \left(\left(\frac{8 \cdot \pi}{3 \cdot \sqrt{2} \cdot f_{solid}} \right)^{\frac{1}{3}} - 2 \right) \cdot r$$

Equation 5-13

which describes the dependancy of average distance between particles on particle radius and solid ratio.

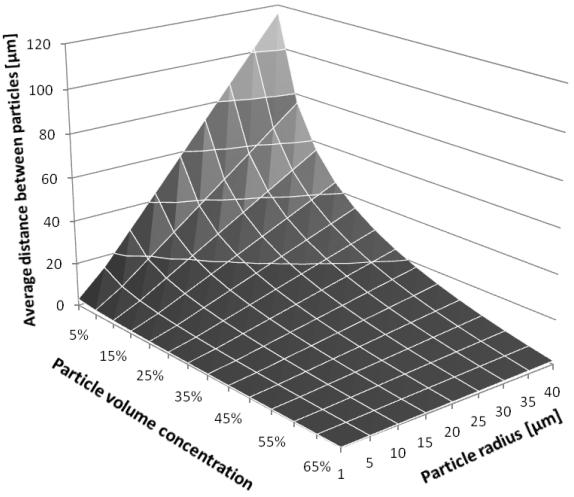

Fig. 5-8 Average distance between particles as a function of volume concentration and particle radius.

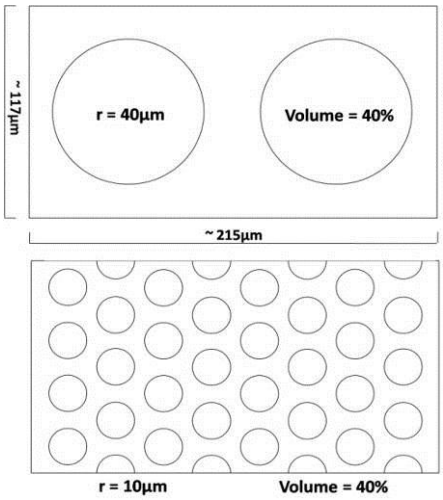

Fig. 5-9 Illustration of surface coverage with different particle sizes but same area ratio.

Fig. 5-8 shows a plot of the function for a solid ratio between 5% and 70% and particle radius from 1 to 40µm. The figure shows that at very high loadings, or close to the maximum, the particle size has nearly no effect on the average distance between particles but a much more significant effect at lower volume concentrations. Fig. 5-9 illustrates the potential difference in surface coverage of equal volume concentration of particles with radius 10 and 40µm. Using smaller micropsheres is therefore beneficial as similar coverage can in theory be attained with less material but it does however not mean that it is desirable to go to very low concentrations by using very small particles. This will cause them to separate quickly from the film when they are exposed to UV radiation just as described in the introduction. The correct microsphere size has to be chosen based on a number of factors. A large volume of microspheres can cause the PVC of the paint to be too high and cause reduce flexibility. Furthermore the size of the spheres must be considerably smaller than the film thickness to ensure low water permeability. Too small particles can reduce the durability as they will separate from the film after much less exposure.

5.3.3 Film degradation mechanism

The UV degradation mechanism of alkyd paint films comprising anatase coated microspheres was investigated to determine how and to what degree the photocatalytic activity affects the organic binder. This was done by exposing alkyd films with different concentrations of coated microspheres in a QUV chamber and analysing the film morphology by SEM. The microsphere concentrations were 0, 10, 20 and 30% of the solid volume and the films were exposed for 0, 473, 924, 1224 and 1675 hours in QUV.

Fig. 5-10 a) shows that the microspheres in the unexposed samples are initially covered with a layer of binder. This layer is removed relatively quickly as a result of chalking once exposure begins. After 473 hours of QUV exposure the binder layer covering the coated microspheres has disappeared off of the most prominent spheres in the surface and the ones embedded slightly deeper are beginning to surface as shown in Fig. 5-10 b). This initial chalking happens relatively quickly compared to what follows. After 924 hours of exposure a slightly larger concentration has built up in the surface and a thin gap is starting to form around the spheres, Fig. 5-10 c). After 1224 hours very little difference can be seen indicating that the chalking has become very slow, Fig. 5-10 d). The concentration in the surface continues to build slowly and after 1675 hours of QUV exposure the gap around the spheres has become larger, see Fig. 5-10 e). It is not certain how deep into the film the gap reaches but only a very small fraction of the spheres has separated from the surface at this point. Fig. 5-10 f) shows a film with uncoated microspheres which has been exposed for 1000 hours where clearly there is still binder covering the particle. If these images are compared with Fig. 5-19 c) and d), which illustrate a transparent film with 30% coated microspheres after 720 hours QUV exposure, it is evident that rutile pigment significantly contributes to the UV stability of the film as the transparent film is much further degraded than the pigmented films. Despite that the film is further degraded only a few microspheres have separated from the surface. The surface concentration of microspheres in the transparent film is much higher and the due to the smaller size of the particles the average distance between them is shorter.

The degradation mechanism of the binder surrounding the microspheres is the same for all the different concentrations but the observed surface concentrations are very different. The 10% films have very low surface coverage, as can be seen in Fig. 5-11 a), and may therefore not be sufficiently self-cleaning. The films with 20% and 30% naturally have a much higher concentration as shown in Fig. 5-11 d) and c), respectively. Measuring the area of exposed coated spheres reveals the surface concentration to be far lower than the volume concentration. Table 5-3 summarizes the measured values which show a slow increase in concentration with UV exposure time. This result confirms that the chalking becomes very slow after the initial exposure and no indication of a large amount of spheres separating from the film can be seen. After 1224 and 1675 hours of exposure only a very small fraction of the microspheres has separated from the film (marked by a red circle) as shown in Fig. 5-11 c) and d). Furthermore comparing the films comprising microspheres with the neat film, Fig. 5-11 b), shows no indication of the photocatalytic reaction affecting the film surface except in the immediate vicinity of the spheres.

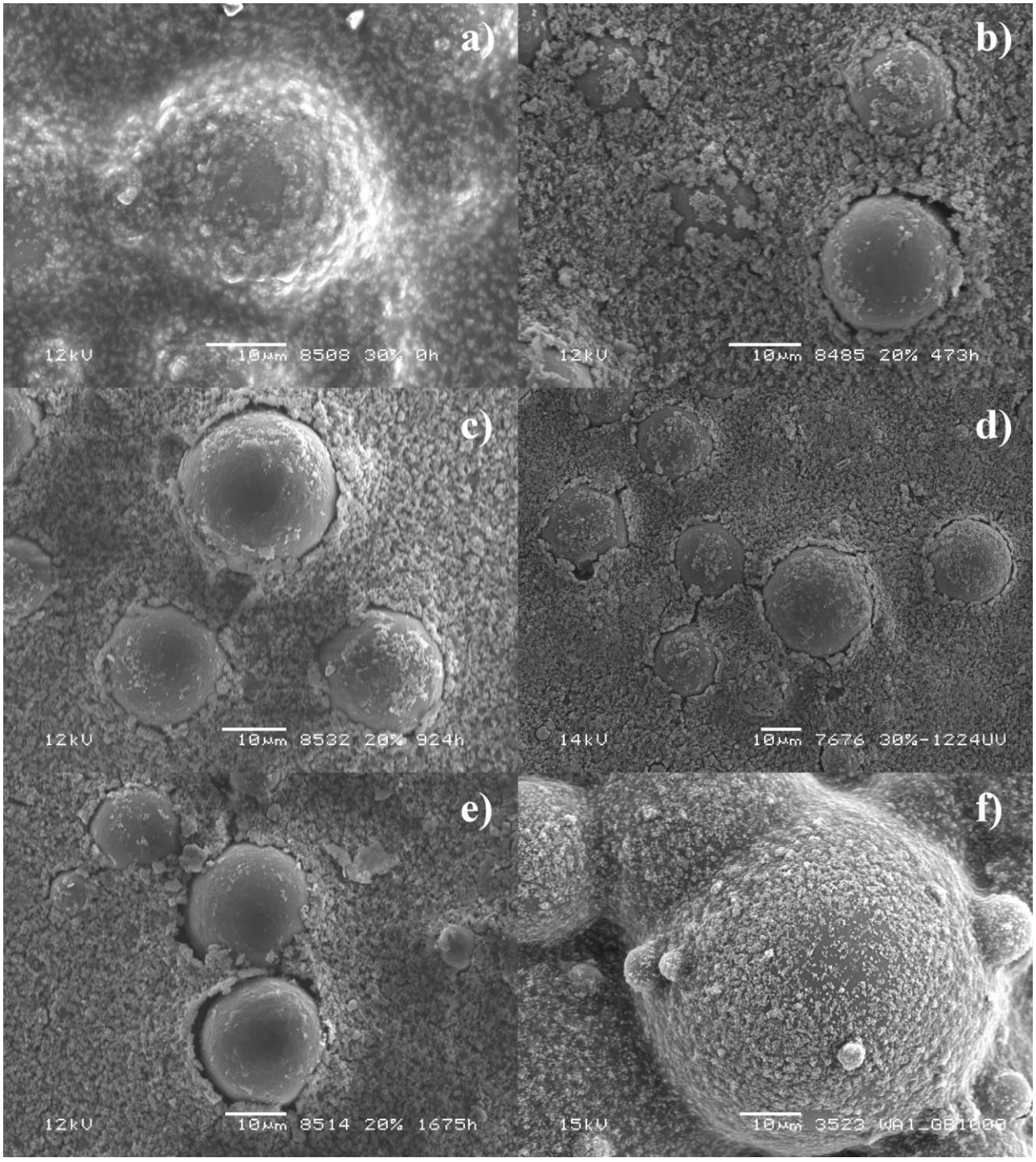

Fig. 5-10 SEM images showing binder degradation after QUV exposure a) 0 hours (30%), b) 473 hours (20%), c) 924 hours (20%), d) 1224 hours (30%), e) 1675 hours (20%) and f) film with uncoated microspheres after 1000 hours exposure (30%).

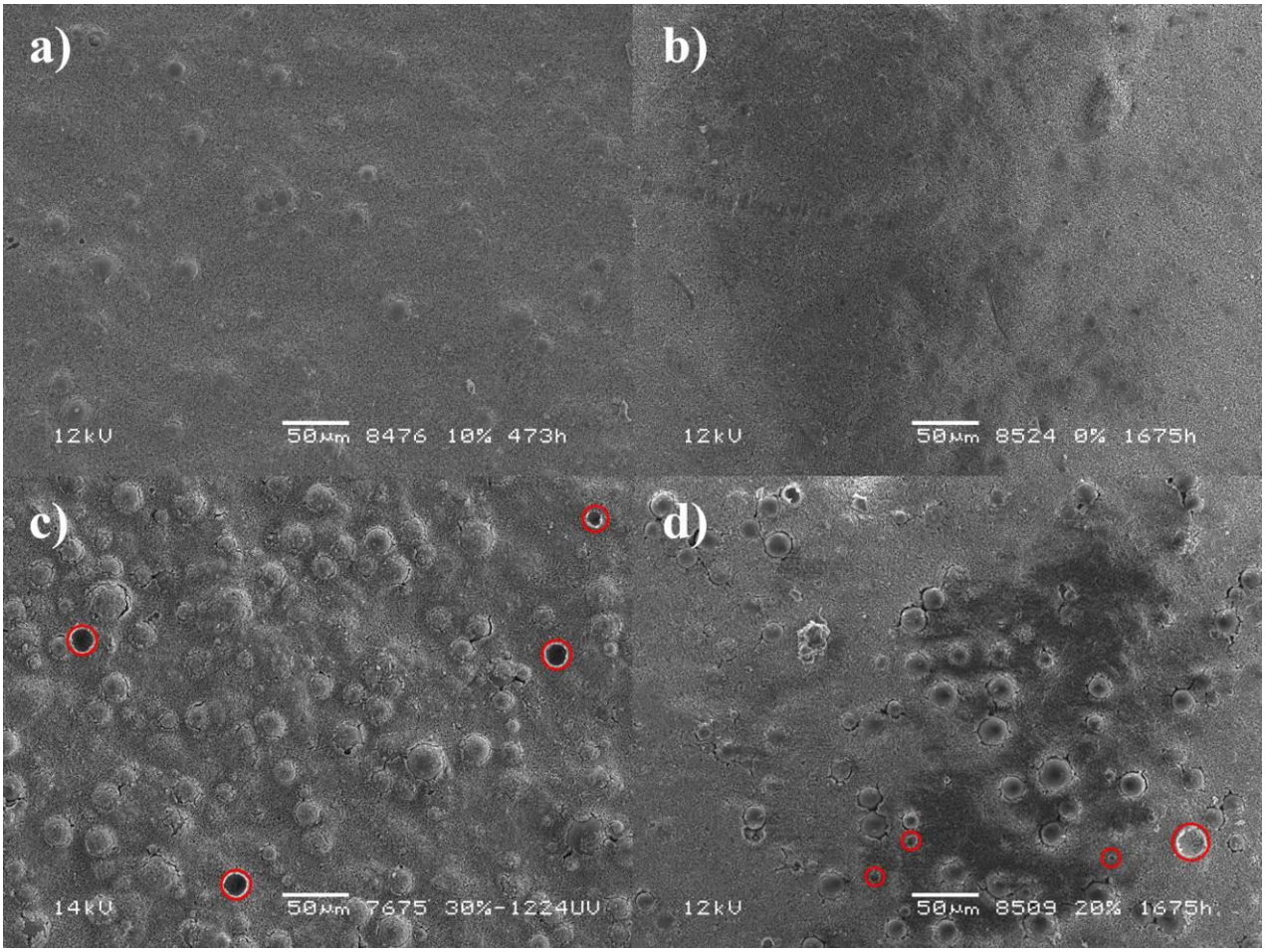

Fig. 5-11 SEM images of films with different concentrations after different exposure times a) 10% after 473 hours, b) 0% after 1675 hours, c) 30% after 1224 hours and d) 20% after 1675 hours.

	QUV exposure time [hours]							
	473		924		1224		1675	
Microsphere vol.% of solids	Conc. [%]	$d_{average}$ [µm]	Conc. [%]	$d_{average}$ [µm]	Conc. [%]	$d_{average}$ [µm]	Conc. [%]	$d_{average}$ [µm]
10%	2,7	30,3	4,6	23	5,1	21,7	5,6	20,5
20%	8,0	16,5	9,6	14,7	10,5	13,8	11,3	13,1
30%	14,4	10,9	15,7	10,2	17,2	9,4		

Table 5-3 Measured values for surface concentration of microspheres and corresponding calculated values for average distance between particles.

Table 5-3 shows the average distance between particles calculated with Equation 5-13 for the different films. Due to the slow chalking of the films the surface concentration has only reached approximately half of the volume concentration in the period between 924 and 1224 hours of UV exposure and therefore the actual average distance between particles in the surface is higher than indicated by Equation 5-13 for a given particle size and volume concentration. It therefore seems necessary to have a relatively large volume concentration to get adequate surface coverage.
The observed degradation mechanism is in agreement with the description given in the introduction where after the initial chalking the process severely slows down and the microspheres remain embedded in the film. This shows that it is possible to integrate photocatalytic material into an organic paint film without causing excessive chalking and poor durability.

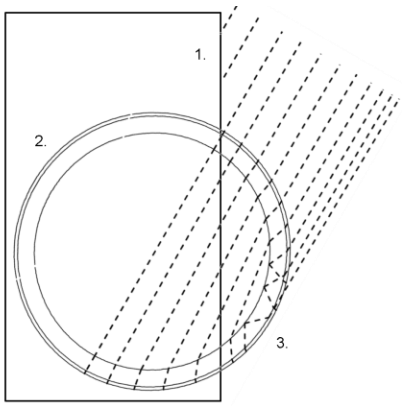

Fig. 5-12 Illustration of light interaction with microsphere in paint film surface. 1) Area where UV-light is absorbed by pigment, 2) Area where no UV-light reaches, 3) Area where UV-light is reflected back towards the surface.

It is not unlikely that the films will exhibit better UV stability in outdoor applications than as demonstrated with the films exposed in a QUV chamber. In a QUV chamber the panels are placed in front of the UV-lamps so the UV light strikes them at a relatively low angle of incidence. Outdoors however most painted surfaces are vertical so UV radiation from sunlight hits the surface with a high angle of incidence, especially at midday when the intensity is high. Fig. 5-12 illustrates a coated microsphere in the surface of paint film and shows that under these conditions a large portion of the microsphere surface will not be activated. The area marked "1" will absorb UV, especially if stabilised TiO_2 pigment is present, and prevent activation of the photocatalyst. Very little UV light will reach the area of the microsphere marked "2" which should substantially delay the separation of the particle from the film. Area "3" shows an interesting property of the hollow microspheres which is that the incident light can be totally reflected. The general rule when light hits a surface is that a part of it is reflected and part is refracted. The higher the angle of incidence the more light is reflected. However when light passes from a material and into another with a lower refractive index there is a critical angle where the all the light with this incident angle or higher is reflected. This is known as total internal reflection and the critical angle equals

$$\theta_{cr} = \arcsin\left(\frac{n_1}{n_2}\right)$$

Equation 5-14

Where n_2 is the higher refractive index (glass) and n_1 the lower (air). If the TiO_2 coating was on a flat piece of glass so that all the surfaces were parallel it is easily shown using Snell's law that the angle of incidence from glass to air is equal to

$$\theta_{glass-air} = \arcsin\left(\frac{n_{air}}{n_{glass}} \cdot \sin\theta_i\right)$$

Equation 5-15

where n is refractive index and θ_i is the initial angle of incidence when the light hits the TiO_2 coating. From this we can see that total internal reflection is impossible as Equation 5-14 and Equation 5-15 are only equal if the initial angle of incidence equals 90°. However due to the curved surfaces of the microsphere more light will be reflected and total internal reflection becomes

possible because the angle of incidence at the glass-air interface inside the sphere is higher as shown in Fig. 5-13. The angle increase equals ϕ which is the angle between the normals for θ_1 and θ_2. This means that the microspheres guide more of the incident UV light to the TiO_2 coating in the paint film surface where it is wanted rather than deeper in the film where it is unwanted.

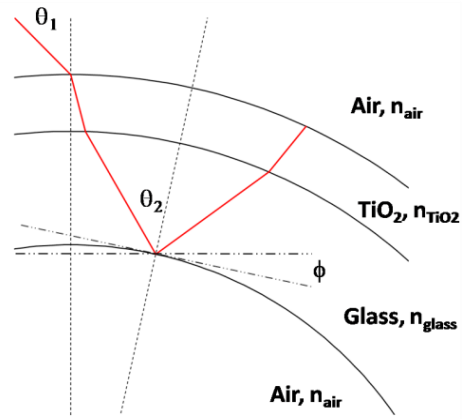

Fig. 5-13 Illustration of increase in angle of incidence at glass-air interface for a spherical surface.

5.3.4 Photocatalytic activity of paint films

The photocatalytic activity of paint films with different concentrations of coated microspheres after different UV exposure times was evaluated by measuring the bleaching of MB as a function of time. The results are shown in Fig. 5-14 where it can be seen that there is some bleaching measured on a film without coated microspheres. This bleaching is caused by the UV source used for the test which is due to an overlap of the UV source emission spectrum and the MB spectrum as shown in Fig. 5-15.

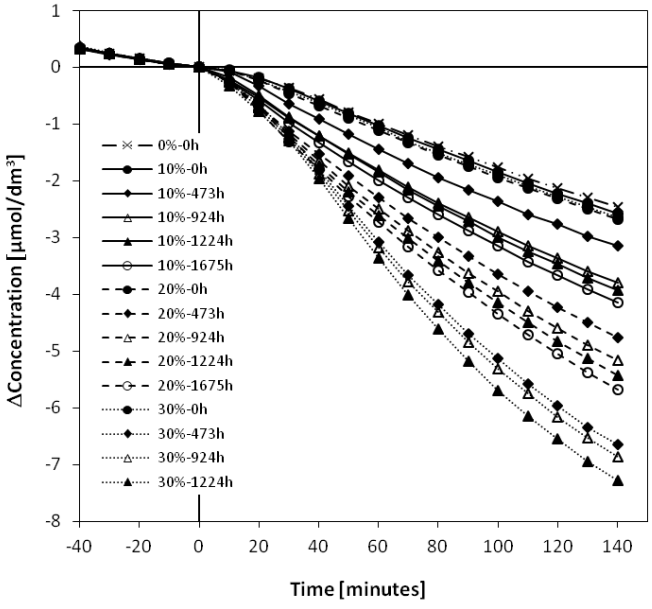

Fig. 5-14 Concentration change as a function of UV exposure time.

Equilibrium was assumed to be reached once the absorbance change measured was equal to or less than 0,005 per 10 minutes, which equals a concentration change of 0,007µmol/dm^3. The starting concentration for the samples when the UV source was turned on was 10,5 ± 0,5µmol/dm^3. It was important to measure at this low concentration because at concentrations above 10µmol/dm^3 MB can dimerise [19]. For this experiment the 660nm absorption peak was measured but the dimer has an absorption maximum at 610nm. Since the monomer-dimer equilibrium isn't linearly dependant a calibration curve of the 660nm peak strictly speaking doesn't follow Beer's law at concentrations above 10µmol/dm^3.
The unexposed samples all had very similar degradation rates regardless of microsphere concentration which is in agreement with the SEM analysis of the films which showed that the microspheres in the film surface are initially covered by a thin layer of binder. Furthermore the 0% samples which had been exposed to UV did not show any significant difference in degradation rates. The degradation measured for these films is therefore considered to be due to the UV-source. After 473 hours exposure the films with coated microspheres however showed a large increase in the degradation rate except perhaps the 10% film where the increase is more modest. The efficiency of the samples is clearly related to the concentration of microspheres and the 30% samples exhibit the highest degradation rate. The length of QUV exposure increases the degradation rate which again is in good agreement with the observed surface concentrations from the SEM analysis.

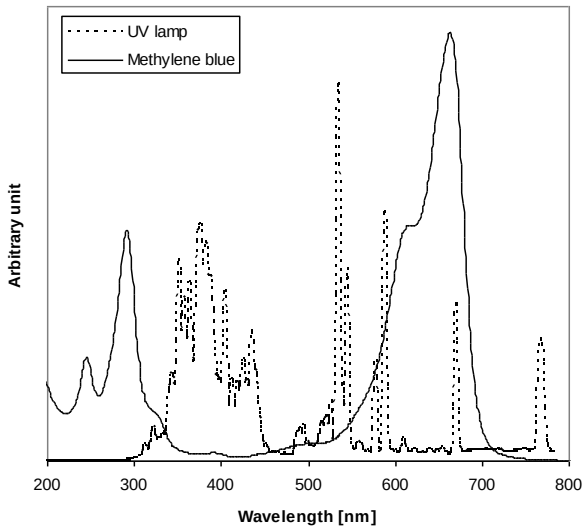

Fig. 5-15 Comparison of UV source emission spectrum and MB spectrum.

After measuring the self-cleaning efficiency of the samples the bleaching of the remaining adsorbed MB during UV exposure was investigated to document whether the films could remove the discolouration or not. The initial intensity of the blue colour was clearly different between samples as can be seen in Fig. 5-16, where the 0% sample has the highest intensity and the 30% sample the lowest. This is due to the different concentrations of the MB solutions at the end of the self-cleaning efficiency test which leads to different amounts of adsorbed MB on the surfaces. Despite the initial differences it can be seen that the bleaching rate is clearly increases with the concentration of coated microspheres. Very little bleaching is observed on the 0% sample and the slight colour change is attributed to MB absorbing radiation from the UV source. The blue colour on the 30% sample has however become very faint after just 1 hour of exposure and no traces of it can be seen after 3

hours. The 10% sample still has a faint blue colour after 5 hours of exposure and the 20% sample only a slight trace. It therefore seems that although the surface concentration of coated microspheres is low the surface is able to clean itself at least in the case of water soluble substances. The importance of microsphere concentration with regard to degrading substances insoluble in water has not been investigated yet but is expected to be more significant.

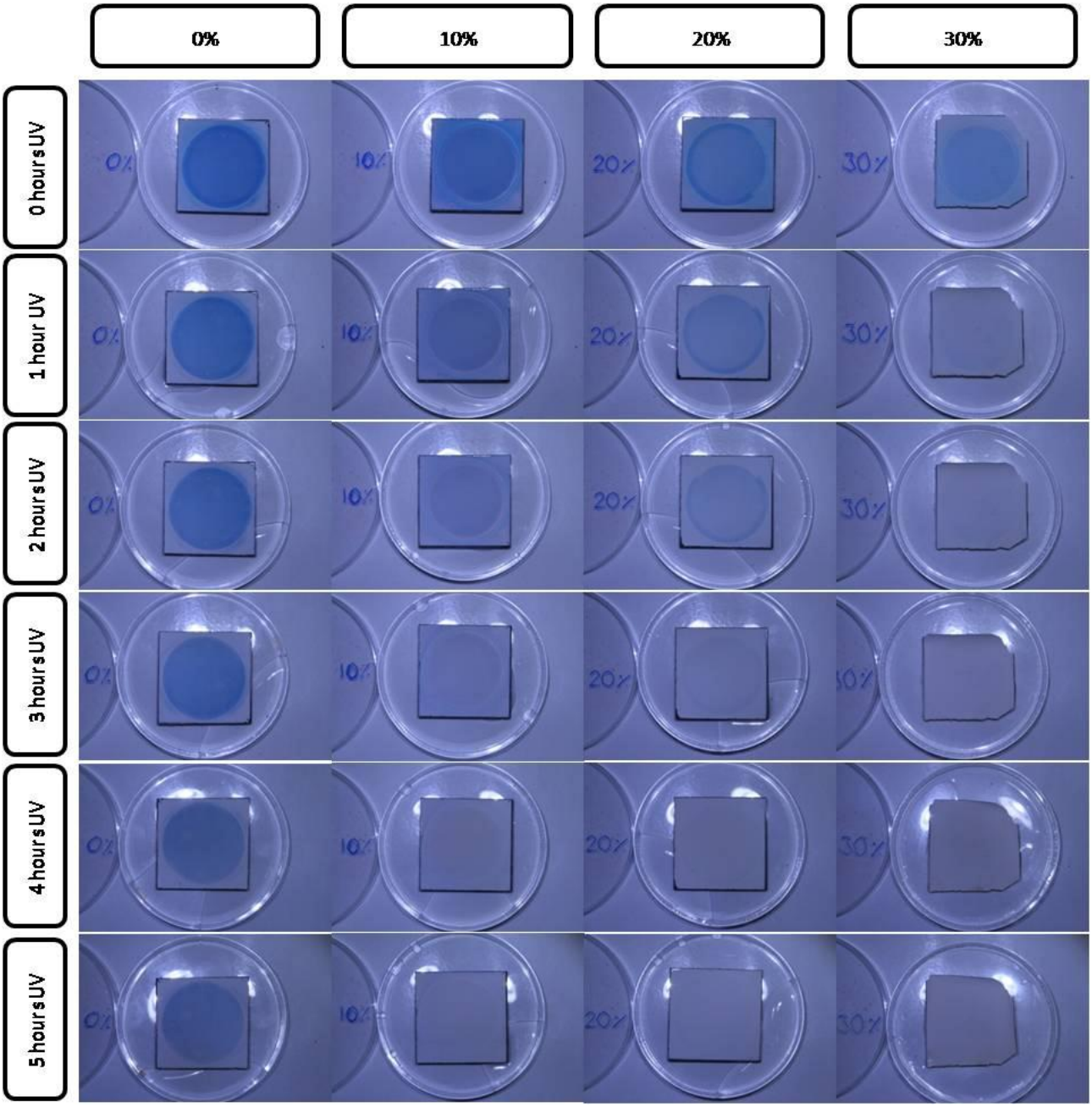

Fig. 5-16 Self-cleaning test of paint films. Left to right 0% to 30% film microsphere volume and top to bottom 0 hours to 5 hours UV exposure.

5.3.5 Water permeability of paint films

The cup test measures the steady state permeability of a paint film. The driving force for the permeation is the difference in partial pressure on both sides of the film and the barrier consists of different resistances such as the coating, substrate, external air gap and internal air gap for an upright cup. If the cup is kept in a climate chamber there is no resistance due to an external air gap and the internal air gap is insignificant for alkyd coatings due to their low permeability [20].
The water transmission rate of the coating, V_c, can be described by the equation

$$V_c = \frac{G_{cs} \cdot G_s}{(G_s - G_{cs}) \cdot A}$$

Equation 5-16

where A is the area of permeation, G_s is the mass change per time measured for the substrate and G_{cs} is the mass change per time for a coated substrate. The permeability coefficient, δ, is then calculated with the equation

$$\delta = \frac{V_c \cdot d}{\Delta p}$$

Equation 5-17

where d is the coating thickness and Δp is the vapour pressure difference between the inside and outside of the cup. The Δp was calculated to be 1320Pa.

	Microsphere vol.% of solids			
	0%	10%	20%	30%
Average thickness [µm]	99,7	102,2	105,8	110,6
Standard deviation	1,1	0,8	3,1	1,0

Table 5-4 Calculated thickness of applied films.

The values used to calculate the permeability constants were the calculated average thickness of the films as shown in Table 5-4 and the water transmission rates which were determined once the rate had reached a steady state.
The water vapour permeability coefficients are shown in Fig. 5-17 and the liquid water permeability coefficients in Fig. 5-18. At all stages the films without microspheres have the highest water vapour permeability coefficient followed by the 10% films. The 20% and 30% films have very similar coefficients. It was not unexpected to initially measure lower permeability coefficients for the films with microspheres as the effective diffusion length for water molecules is longer with a higher concentration of impermeable particles. The fact that these films maintain lower permeability coefficients after UV exposure however illustrates the UV stability of the films. The water vapour permeability coefficient was counter-intuitively observed to decrease with QUV exposure up until 20 days of exposure and the standard deviation of the measurements is relatively low. This is believed to be because of the elevated temperatures the films are exposed to in the QUV chamber. Alkyds are oxidative drying and therefore they continue to cure for a long time after application which could explain the drop in permeability. During UV exposure the temperature reaches approximately 60°C followed by rapid cooling. This temperature cycling should speed up the drying of the film and since the temperature reaches above T_g during each cycle followed by cooling it may contribute to a denser film through a higher degree of crystallinity. The T_g of polymers is known to be indicative of crosslinking density [21] so the T_g of sample films after 0, 12

and 25 days of QUV exposure was measured by DMA to investigate whether the QUV exposure accelerated the drying of the film. The measurement showed an increase in Tg from approximately 19°C, before exposure, to 37°C after 12 days of exposure. Further exposure increased the Tg slightly to approximately 40°C. This is similar to the relatively large drop in permeabilty of the films after 10 days of exposure and the following lower drop after 20 days. After 30 days of QUV exposure the trend of lower permeability turned and especially the permeability of the films without coated spheres increased drastically. At this stage the UV exposure has taken its toll on binder but it seems the microspheres significantly contribute to the UV stability of the film. Unfortunately not enough samples were available to measure the vapour permeability of the 20% films after 30 days of exposure due to cracks in the veneer substrate and due to the large increase in standard deviation of the measurements after this exposure time it is believed that the sensitivity of such a thin substrate to the QUV conditions contributes to the observed increase in permeability.

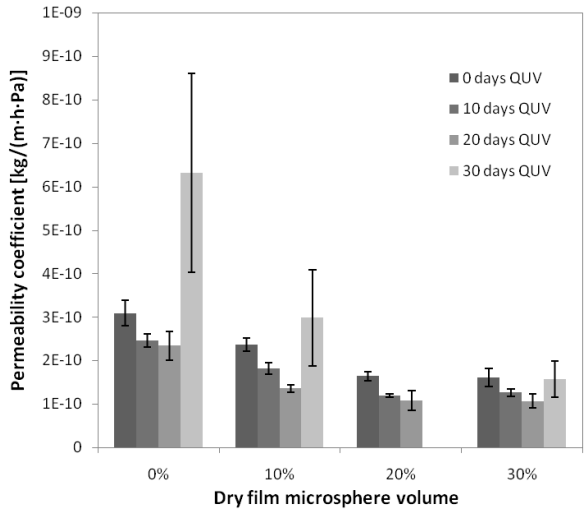

Fig. 5-17 Water vapour permeability coefficients of paint films with different concentrations of coated microspheres after different QUV exposure times. The error bars show the standard deviation.

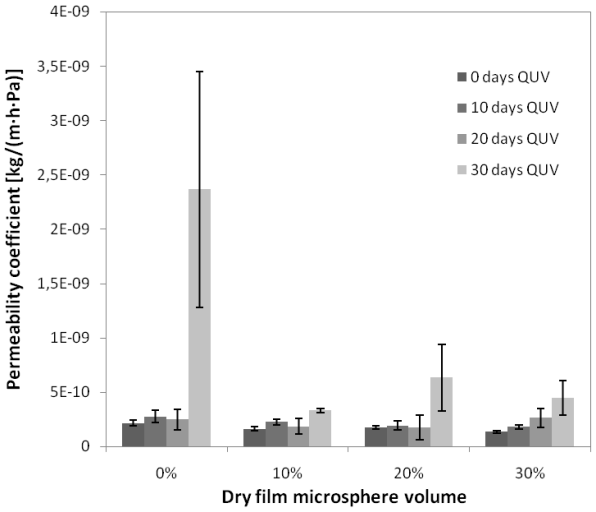

Fig. 5-18 Liquid water permeability coefficients of paint films with different concentrations of coated microspheres after different QUV exposure times. The error bars show the standard deviation.

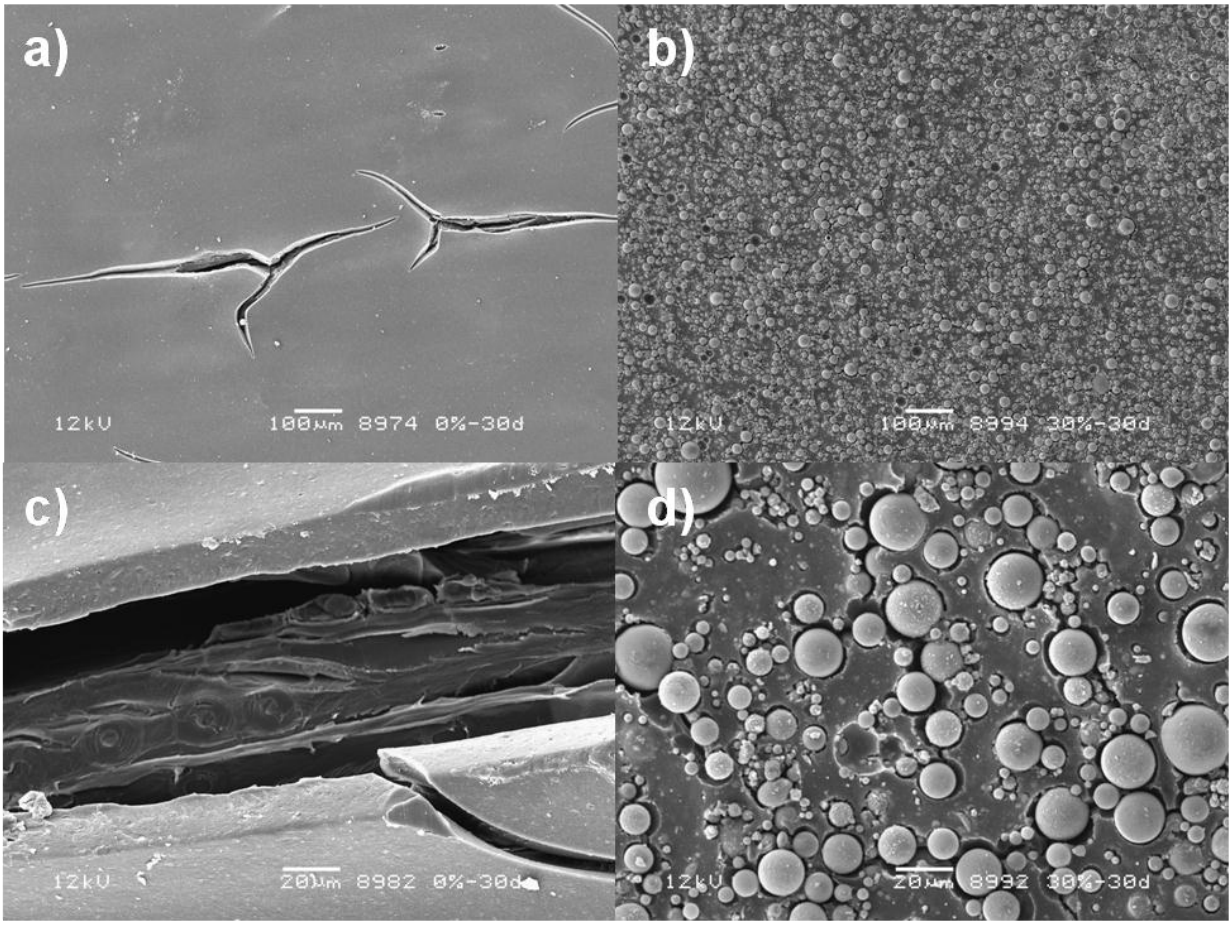

Fig. 5-19 Illustrates the surface of a transparent alkyd films painted on veneer after 30 days of exposure in QUV, a) and c) 0% film with large cracks in surface, b) and d) 30% film with small cracks over entire surface. Both films are shown with the same magnification.

Initially the liquid water permeability of the films is slightly lower than the vapour permeability but once exposure starts it increases and after 10 days it has become higher. As with the vapour permeability the 0% films exhibit the highest liquid permeability with only one exception. After 20 days of exposure the 30% films have slightly higher permeability. Generally the permeability doesn't increase significantly until after 30 days of exposure and similar to the results above the 0% films exhibit by far the largest increase. This sudden increase in permeability after 30 days of exposure can be attributed to crack formation in the film as shown in Figure F which shows the surfaces of 0% and 30% samples which had been exposed for 30 days. It is interesting to observe that although the entire surface of the 30% sample is covered with cracks the liquid water permeability is far less than for the 0% sample. The reason for this difference is the mechanism by which cracks propagate in material. Once a crack is initiated it can grow due to high stress concentrated around the crack tip. This high stress causes the material to fail and thereby the crack to propagate through the material as the crack tip advances. This can be seen in the 0% sample where the cracks have become long and deep and as seen in Fig. 5-19 c), where a wood fiber can be seen under the paint film. Such a catastrophic failure of the film naturally causes a large increase in the permeability especially the liquid permeability. Cracks in a film with microspheres on the other hand behave differently. After a crack has initiated and started to propagate the crack tip will hit a particle causing a reduction in the stress intensity at the tip. This mechanism is called crack pinning[22] and can either stop the advance of the crack tip or deflect it into another direction which increases the energy needed for its growth. This mechanism causes numerous small and

superficial cracks to form in a film with microspheres, see Fig. 5-19 d) and d), while a few catastrophic cracks form in a film without microspheres. It is impossible to avoid cracking in an alkyd film painted on wood which is exposed to the elements but it seems that the durability may be significantly enhanced by the addition of microspheres.
These results further illustrate the UV stability of films with photocatalytically active microspheres. Even though the films do not contain any rutile pigment that protects the film from UV light the degradation due to the microspheres doesn't significantly decrease the protective properties of the film but rather seem to enhance it.

5.4 Conclusion

It has been illustrated that the novel idea of integrating photocatalytic TiO_2 into paint as a coating on carrier particles is a promising method for making a long lasting self-cleaning paint based on an organic binder system. The films exhibit excellent self-cleaning properties, improved crack resistance and lower water permeability. Furthermore it has been found that the influence of the photocatalytic reaction on the organic binder is minimal and that therefore the UV stability is excellent for a photocatalytically active paint.

Acknowledgements

The authors would like to express their gratitude to Bent Samuelsen, Dyrup A/S, for guidance with the water permeability measurements and Kenny Ståhl and Astrid Schøneberg; DTU Chemistry, Technical University of Denmark; for their help with XRD measurements and analysis. Furthermore we thank Dyrup A/S and the Danish Agency for Science and Innovation for financial support.

References

[1] L. Li, W. Zhu, P. Zhang, Q. Zhang, and Z. Zhang, "TiO2/UV/O3-BAC processes for removing refractory and hazardous pollutants in raw water," *Journal of Hazardous Materials*, vol. 128, no. 2-3, pp. 145-149, Feb. 2006.

[2] J. Zhao and X. Yang, "Photocatalytic oxidation for indoor air purification: a literature review," *Building and Environment*, vol. 38, no. 5, pp. 645-654, May 2003.

[3] A. Fujishima, X. Zhang, and D. A. Tryk, "Heterogeneous photocatalysis: From water photolysis to applications in environmental cleanup," *International Journal of Hydrogen Energy*, vol. 32, no. 14, pp. 2664-2672, Sep. 2007.

[4] I. P. Parkin and R. G. Palgrave, "Self-cleaning coatings," *Journal of Materials Chemistry*, vol. 15, no. 17, p. 1689, 2005.

[5] J. Augustynski, "The role of the surface intermediates in the photoelectrochemical behaviour of anatase and rutile TiO2," *Electrochimica Acta*, vol. 38, pp. 43-46, Jan. 1993.

[6] A. E. Jacobsen, "Titanium Dioxide Pigments: Correlation between Photochemical Reactivity and Chalking.," *Industrial & Engineering Chemistry*, vol. 41, no. 3, pp. 523-526, Mar. 1949.

[7] A. Fujishima and K. Honda, "Electrochemical Photolysis of Water at a Semiconductor Electrode," *Nature*, vol. 238, no. 5358, pp. 37-38, Jul. 1972.

[8] U. Gesenhues, “Al-doped TiO2 pigments: influence of doping on the photocatalytic degradation of alkyd resins,” *Journal of Photochemistry and Photobiology A: Chemistry*, vol. 139, no. 2-3, pp. 243-251, Mar. 2001.
[9] P. A. Christensen, A. Dilks, T. A. Egerton, E. J. Lawson, and J. Temperley, “Photocatalytic oxidation of alkyd paint films measured by FTIR analysis of UV generated carbon dioxide,” *Journal of Materials Science*, vol. 37, no. 22, pp. 4901-4909, 2002.
[10] A. Mills, A. Lepre, N. Elliott, S. Bhopal, I. P. Parkin, and S. A. O’Neill, “Characterisation of the photocatalyst Pilkington Activ(TM): a reference film photocatalyst?,” *Journal of Photochemistry and Photobiology A: Chemistry*, vol. 160, no. 3, pp. 213-224, Aug. 2003.
[11] N. S. Allen, M. Edge, G. Sandoval, J. Verran, J. Stratton, and J. Maltby, “Photocatalytic Coatings for Environmental Applications¶†,” *Photochemistry and Photobiology*, vol. 81, no. 2, pp. 279-290, Mar. 2005.
[12] G. KAEMPF, PAPENROT.W, and R. HOLM, “DEGRADATION PROCESSES IN TIO2-PIGMENTED PAINT FILMS ON EXPOSURE TO WEATHERING,” *JOURNAL OF PAINT TECHNOLOGY*, vol. 46, no. 598, pp. 56-63, 1974.
[13] W. G. Wamer, J.-J. Yin, and R. R. Wei, “Oxidative Damage to Nucleic Acids Photosensitized by Titanium Dioxide,” *Free Radical Biology and Medicine*, vol. 23, no. 6, pp. 851-858, 1997.
[14] W. A. Pryor, “Oxy-Radicals and Related Species: Their Formation, Lifetimes, and Reactions,” *Annual Review of Physiology*, vol. 48, no. 1, pp. 657-667, Oct. 1986.
[15] A. Houas, H. Lachheb, M. Ksibi, E. Elaloui, C. Guillard, and J.-M. Herrmann, “Photocatalytic degradation pathway of methylene blue in water,” *Applied Catalysis B: Environmental*, vol. 31, no. 2, pp. 145-157, May 2001.
[16] P. Hertz, “ber den gegenseitigen durchschnittlichen Abstand von Punkten, die mit bekannter mittlerer Dichte im Raume angeordnet sind,” *Mathematische Annalen*, vol. 67, pp. 387-398, Sep. 1909.
[17] S. Chandrasekhar, “Stochastic Problems in Physics and Astronomy,” *Reviews of Modern Physics*, vol. 15, no. 1, p. 1, Jan. 1943.
[18] C. F. Gauss, “Besprechung des Buchs von L.A. Seeber: Intersuchungen über die Eigenschaften der positiven ternären quadratischen Formen usw,” *Göttingsche Gelehrte Anzeigen*, 1831.
[19] E. Rabinowitch and L. F. Epstein, “Polymerization of Dyestuffs in Solution. Thionine and Methylene Blue1,” *Journal of the American Chemical Society*, vol. 63, no. 1, pp. 69-78, Jan. 1941.
[20] Charles M. Hansen, “Potential Errors in Water/Water Vapor Permeation Measurements Using the Cup Method,” *Färg och Lack*, vol. 39, no. 3, pp. 57-60, 1993.
[21] T. FOX and S. LOSHAEK, “INFLUENCE OF MOLECULAR WEIGHT AND DEGREE OF CROSSLINKING ON THE SPECIFIC VOLUME AND GLASS TEMPERATURE OF POLYMERS,” *JOURNAL OF POLYMER SCIENCE*, vol. 15, no. 80, pp. 371-390, 1955.
[22] A. J. Kinloch, D. L. Maxwell, and R. J. Young, “The fracture of hybrid-particulate composites,” *Journal of Materials Science*, vol. 20, pp. 4169-4184, Nov. 1985.

6 Paper 3: Characterisation of the mechanical and rheological properties of hollow glass microsphere filled alkyd paints

Sverrir G. Gunnarsson[a*], Per Møller[a], Søren H. Poulsen[b]

Abstract

The rheological properties of a solvent borne alkyd and water borne acrylic paints with different concentrations of hollow glass microspheres were characterised. The microspheres were found to have a minor effect on the viscosity profiles of the paints at high shear. The effect of the microspheres on the mechanical properties of alkyd films was studied and found to generally have a negative effect for the desired application. Despite this the overall performance of the paint films was improved by the microspheres due to elevated crack resistance of the films. The crack front pinning mechanism observed in the microsphere containing films caused numerous small and superficial cracks to form instead of large and deep crack as witnessed in the unfilled films.

6.1 Introduction

Photocatalysis has shown great promise for a number of applications where self-cleaning surfaces are one of them [1][2]. Attempts have been made to integrate photocatalytic material into organic paints [3], either as anatase pigment or anatase nano-particles, but such attempts have not yielded sufficiently good results due to the aggressive nature of the OH radicals created by the photocatalytic reaction. The photo-activity of TiO_2 pigments and consequent degradation of organic binders, often termed chalking, has been well known to the paint industry [4][5] for a long time and most TiO_2 pigments today are therefore stabilized to minimize chalking [6][7]. The authors have however shown [unpublished work] that it is possible to integrate photocatalytic material into an organic paint system without it causing excessive chalking. This is achieved by the novel approach of coating the photocatalyst onto hollow glass microspheres which are dispersed in the paint. This reduces the interfacial area between the photocatalyst and the binder and provides an inert surface for the photocatalytic reaction to take place. Fig. 6-1 shows the different degradation mechanism for a paint film with photocatalytic nano-particles compared to a film with coated microspheres. The binder surrounding photocatalytic nano- or pigment sized particles in the film surface will quickly degrade when exposed to UV-light which causes the particles to separate from the film, i.e. chalking. This effect has been interpreted as self-cleaning due to the constant renewal of the surface but it has some serious disadvantages as the film rapidly loses its protective properties. Furthermore as a result of a high chalking rate such a film would constantly release particles to its surroundings. The effect of photocatalytic nano-particles on people has not yet been fully studied but investigations suggest they may have adverse health effects [8]. Microspheres on the other hand are embedded much deeper in the film so although the binder is degraded at the surface UV-light doesn't reach the binder-particle interface deeper in the film. A thin gap has been observed to form around the particles in the surface but nevertheless the particles do not separate from the film prematurely. The glass particles therefore provide an area for the photocatalysis to take place which is unaffected by the reaction. Furthermore due to the exceptionally short lifetime of the OH radical [9] it is impossible for it to diffuse away from the site of creation and attack binder which isn't in direct contact with the photocatalyst.

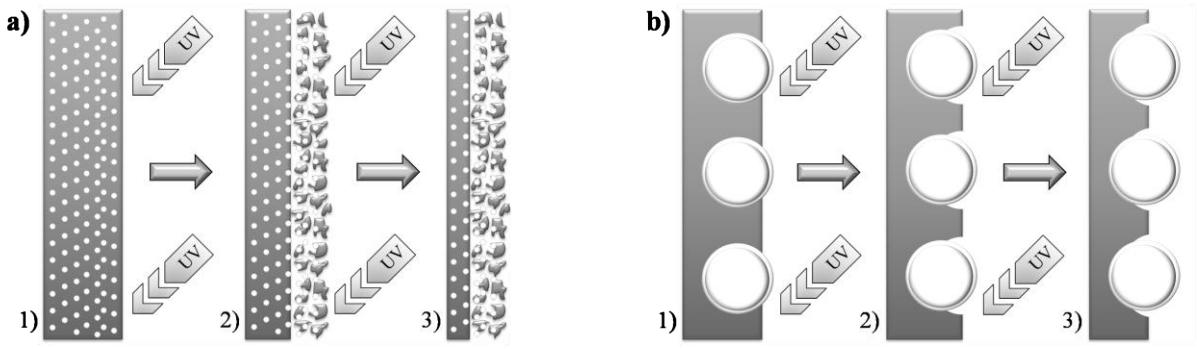

Fig. 6-1 a) shows a film with nano-particles constantly eroding from 1) to 3). b) shows a film with photocatalytic carrier particles 1) Fresh film, 2) After initial exposure chalking has occurred, 3) Chalking has nearly ceased as UV radiation no longer reaches carrier particle/binder interface and the much slower photochemical degradation of the binder becomes the predominant process. The figures do not represent the full film thickness.

In order to make the surface sufficiently self-cleaning it is necessary to have a large concentration of coated microspheres in the surface so they need to be a substantial part of the formulation volume. It is therefore important to investigate the effect microspheres have on important properties such as the rheological and mechanical properties of the paint. A lot of work has been done on the effect of spherical fillers on the mechanical properties of epoxy composites [10]-[17] but to our knowledge no such work has been done on thin films such as alkyd paints. The effect of spherical particles on viscosity has also been studied [18] but because of the complex rheological properties of paints; due to surfactants, thickeners and other additives; it is necessary to investigate each system individually.

6.2 Experimental

6.2.1 Materials and equipment

The hollow glass microspheres (HGMS) used for the rheology and mechanical measurements were iM30K Glass Bubbles from 3M. The average density of the microspheres is 0,6g/cm^3, the average diameter of the particles is 15,5µm and the size distribution can be seen in Fig. 6-2. The HGMS used for the water permeability test were Sphericel 110P8 from Potters Industries. The average density is 1,1g/cm^3 and the mean particle size 11µm. The size distribution can be seen in Fig. 6-1.

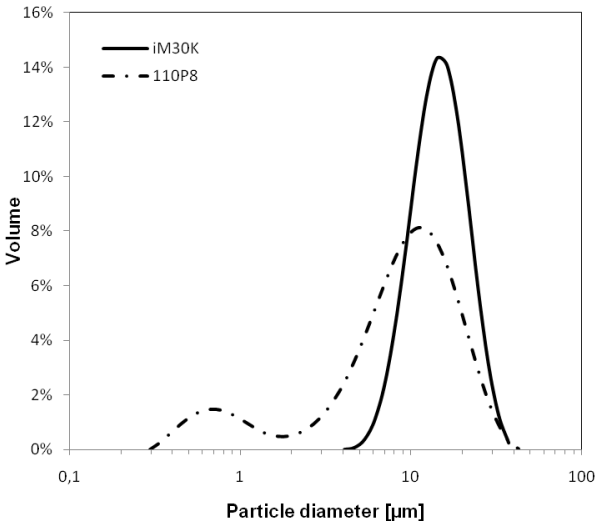

Fig. 6-2 iM30K and Sphericel 110P8 HGMS particle size distribution.

Paint film drying time was measured with a Horus® film formation analyzer, particle size was measured with a Malvern Mastersizer 2000 and electron microscopy was done with a JEOL model JSM-5900 electron microscope with a LaB_6 filament.
Artificial weathering of samples was done in a Q-lab QUV artificial weathering chamber, equipped with QUV-A340 UV lamps, according to EN 927-6:2006 where the samples were exposed to alternating periods of 2,5 hours of UV exposure and 0,5 hours water spray for six days followed by 1 day of water condensation.

6.2.2 Coating process

The Spericel 110P8 HGMS were coated using the method described below. The microspheres were pre-treated at 150°C for 24 hours to remove physically adsorbed water. Titanium tetra isopropoxide (TTIP) was mixed with isopropanol with a ratio of 1:10 and stirred for 20 minutes. 1,8g HGMS was added to the solution for every 10 ml isopropanol and the mixture stirred for 20 minutes. Then de-ionized water, 1 ml for every 1ml of TTIP, was added to the solution and stirred for 10 minutes. The solution was then filtered to remove most of the isopropanol and then heated to 70°C and continously stirred to avoid agglomeration while the remaining isopropanol evapourated. Once dry the coated microspheres were calcined at 550°C for 5 hours to crystallize the TiO_2. The process was repeated once more to load more TiO_2 on the microspheres. After the second round of coating the microspheres were separated from all unbound TiO_2 by sonication.

6.2.3 Paint formulations

Solvent borne air drying alkyd paints and water borne acrylic paints were formulated with different HGMS loadings. The approximate formulations can be seen in Table 6-1 where “other solids” represent binder, rutile pigment and fillers. The solvent borne paints were prepared by dispersing the microspheres in the binder at 1000rpm which was then mixed with a rutile pigment paste along

with solvents and additives. The water borne paints were prepared by dispersing the microspheres at 1000rpm in a ready made product.

Binder type	HGMS % of total solids	HGMS vol.%	Other solids vol%	Solvents and additives vol%
Alkyd	0	0,0	40,1	59,9
Alkyd	5	2,1	39,3	58,6
Alkyd	10	4,3	38,4	57,3
Alkyd	15	6,6	37,5	55,9
Alkyd	20	9,1	36,5	54,4
Alkyd	25	11,8	35,4	52,8
Alkyd	30	14,7	34,2	51,1
Alkyd	40	21,1	31,7	47,2
Alkyd	50	28,6	28,6	42,7
Acrylic	0	0,0	31,7	68,3
Acrylic	5	1,6	31,2	67,2
Acrylic	10	3,4	30,6	66,0
Acrylic	20	7,3	29,4	63,3
Acrylic	30	12,0	27,9	60,1
Acrylic	40	17,4	26,2	56,4
Acrylic	50	24,1	24,1	51,8

Table 6-1 Approximate paint formulations in vol.%.

6.2.4 Rheology measurements

Rheology measurements were done on a TA Instruments AR-G2 rheometer. The following procedure was used to investigate the rheological properties of the paints. The linear viscoelastic region (LVR) was determined by an oscillatory stress sweep from 0,01-100Pa at 1Hz and 25°C. Next the viscosity profiles were measured as a function of shear rate at temperatures of 5, 15, 25 and 35°C. The shear rate sweep of the alkyd paints was separated into two ramps where the change in shear rate per time was slower in the first ramp than the second. This was done because of the thixotropic behaviour of the alkyd to capture more points at the lower shear rates. The first ramp from 0,01-50Hz was measured over a period of 30 minutes and the second ramp from 50-4000Hz was measured over a period of 40 minutes. The shear rate sweep of the acrylic paints was also separated into two ramps where the change in shear rate per time was slower in the first ramp than the second. The first ramp from 0,01-50Hz was measured over a period of 15 minutes and the second ramp from 50-4000Hz was measured over a period of 15 minutes. Finally he non-Newtonian behaviour of the paints was investigated by breaking down the structure of the paints by exposing them to a shear rate of $2000s^{-1}$, which was chosen from the viscosity profiles, for 1 minute followed by an oscillatory time sweep at 25°C, 1Pa and 1Hz, which is within the LVR. The shear storage and loss moduli, G´and G´´, were recorded.

6.2.5 Mechanical measurements

The stress-strain curves of dry paint films were acquired with an Instron 3343 tensile testing machine with a 100N Instron load cell. Free films were prepared by applying the paint on PTFE panels with a wet thickness of 400µm. The films were allowed to dry for 2 months at 23°C and 50% relative humidity before testing. The films were cut into 10x60mm strips and the gauge length of the specimens tested was 40mm. The results are calculated as an average of at least 5 samples and all samples that broke at the grips were discarded. The films were tested at strain rates of 0,001 and $0{,}0001s^{-1}$. Tangential Young's moduli were determined from the initial parts of the stress strain curves. The stress relaxation of the films was measured on the same Instron tensile testing machine at 1% strain and the characteristic relaxation time was calculated as an average of 5 samples.
The stress intensity factor was determined by introducing a 2mm crack in the films before stressing them in an Instron tensile testing machine. The films were tested at a strain rate of 0,001s-1 and the stress intensity factor calculated from the stress at which the crack began to propagate.
The dynamic mechanical analysis was done using a Rheometric Scientific ARES torsional rheometer. The prepared samples were 10x40mm and the gauge length of the specimens tested was 23mm. For the creep measurement the films were exposed to a shear stress of 1MPa for 10 minutes at 20°C after which the stress was released and the recovery measured. The dynamic viscoelasticity versus temperature of the dry alkyd films was measured at 1Hz and a strain of 0,1% over the temperature range -30 to 85°C.

6.2.6 Water permeability test

The water permeability of paint films with microsphere concentrations of 0, 10, 20 and 30% of the solid volume was measured by the cup method according to ISO 7783:2008. 0,7mm thick pinewood veneer was used as a substrate for the paint films. The formulated paints were transparent (un-pigmented) to decrease the UV stability of the samples. This was done to shorten the exposure time needed to measure changes in the film properties as it is limited how long such a thin substrate can withstand the rapid temperature and relative humidity changes. Great care was taken to spread the film evenly on the veneer and the film thickness was controlled by measuring the weight of the paint applied to a known area. The films were allowed to dry for 2 weeks at 23°C and 50%RH before being exposed to UV radiation in a QUV chamber for 0, 10, 20 and 30 days. After the exposure the paint films were kept in a climate chamber at 23°C and 50%RH for 4 days before testing began. Uncoated veneer samples were also measured to determine the permeability of the substrate. Three specimens were measured for each sample.
The cups used were made from standard 1 ¼" x 40mm PVC adapter unions with PVC plugs which were sealed with glue. The cups were filled with de-ionized water up to a rim 1,7cm from the paint film. 5cm diameter samples were cut from the veneer and placed in the cups with the painted side inside the cup. The exposed area of the samples was 3,2cm in diameter. The cups were kept in a climate chamber at 23°C and 50%RH and weighed twice per week to keep track of water evaporation. The cups were placed downwards on a wire mesh with the water in contact with the paint films to measure the liquid water permeability.

6.3 Results and discussion

6.3.1 Drying time

The drying time of alkyd paint films with microspheres; 0, 5, 10, 20, 30, 40 and 50% dry film volume; was measured with Multiple Speckle Diffusing Wave Spectroscopy (MS-DWS) [19]. The films were applied on glass plates with a wet thickness of 120µm. The technique measures the motion of particles in the surface and the drying time can therefore be determined from the curves when a steep drop in surface activity is measured.
Mixing microspheres into the paint was found to greatly reduce the time until the films were "touch dry" as seen in Fig. 6-3. At 50% loadings the drying time is approximately half of that of the 0% film and at even very low loadings the gain is substantial.

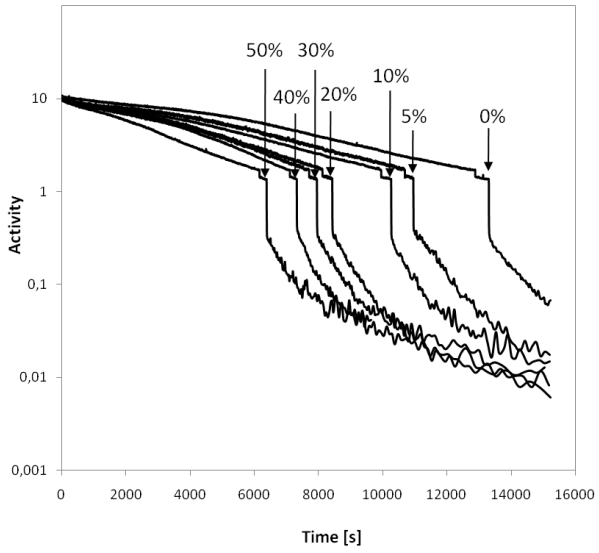

Fig. 6-3 Drying time of alkyd paints with different concentrations of glass micropsheres.

6.3.2 Viscosity of alkyd paints

The viscosity of both alkyd and acrylic paints with seven different concentrations of microspheres were measured at four different temperatures to investigate the effect of microsphere loading for both a solvent borne system and a water borne system.
The alkyd paints contain thixotropic agents which gives them a gel like consistency when they are not subjected to shear forces. The high viscosity in this state contributes to the stability of the pigments with regards to flocculation and the thixotropy gives the paint special application properties. The initial high viscosity prevents the paint from dripping from the applicator and once application begins the viscosity drops due to the structure of the paint being broken down by the shear forces and the paint becomes more workable. When shearing ends the structure starts to rebuild and the viscosity increases which means a thicker layer can be applied in each coat without the paint sagging. Shear thinning paints exhibit similar behaviour when shear is applied but their response is not time dependant which means that they immediatly regain viscosity when shearing ceases. If the paint is applied by brush this fast increase in viscosity can prevent the brush marks from leveling out while due to the time delay in the viscosity increase of a thixotropic paint the surface can level out due to surface tension [20] making brush marks disappear.

Fig. 6-4 shows the oscillatory stress sweep of alkyd paints with 0 and 40% HGMS of the solids volume. The LVR extends to approximately 10Pa for both paints so an oscillatory stress of 1Pa can be used for the oscillatory time sweep.

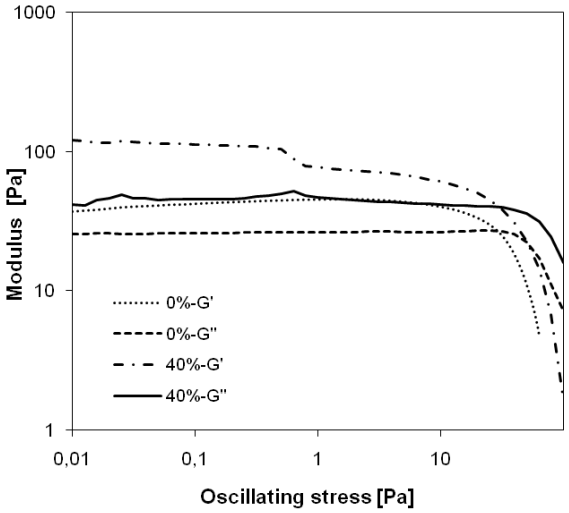

Fig. 6-4 Oscillatory stress sweep of alkyd paint with 0 and 40% HGMS.

Fig. 6-5 show the viscosity profiles of the alkyd paints with different concentrations of microspheres at different temperatures. The measured viscosity at low shear rates may seem inconsistent but this is due to the thixotropic nature of the alkyd which makes it very difficult to measure the true viscosity at low shear rates. Placing a sample in the instrument introduces enough shear force to alter the viscosity and it takes a long time for the sample to reach steady state. The measured viscosity values at low shear rates should therefore not be considered representative of the true low shear viscosity. It is however the viscosity at high shear which is of interest as this determines the application properties of the paint. At all concentrations and temperatures the viscosity profiles have virtually the same shape and show the same response to shear. The change in the slope at a shear rate of $50s^{-1}$ is due to the difference of the shear rate change per time of the ramps, as explained in the experimental section, which illustrates the time dependant behaviour of the paint. There is a clear shift to higher viscosity at high microsphere loadings but at low concentrations; 0, 5 and 10%; the profiles are nearly identical. These results however show that the viscosity increase at high loadings is very small considering the increase in solid content.
Fig. 6-6 shows a comparison of the measured viscosity of the alkyd paints at a shear rate of $2500s^{-1}$. This figure illustrates that at low microsphere concentrations the viscosity is relatively the same as the 0% alkyd but increases somewhat at higher loadings. The broken lines represent the model for viscosity put forward by Einstein [21].

$$\mu^* = \mu(1 + 2{,}5 \cdot C_f)$$

Equation 6-1

where μ^* is the viscosity of the dispersion, μ the viscosity of the solvent and C_f represents the filler concentration. The results fit the model surprisingly well considering that it is derived for dilute solutions where no interactions are between the particles. As expected the viscosity increases with decreasing temperature and it can be seen that at high loadings the paints are more temperature sensitive as the viscosity increase at low temperatures is much higher.

It should be possible to formulate the paints to have an even smaller difference in viscosity if that is desired. The paints contain thickening agents and their concentrations could be adjusted slightly to lower the viscosity.

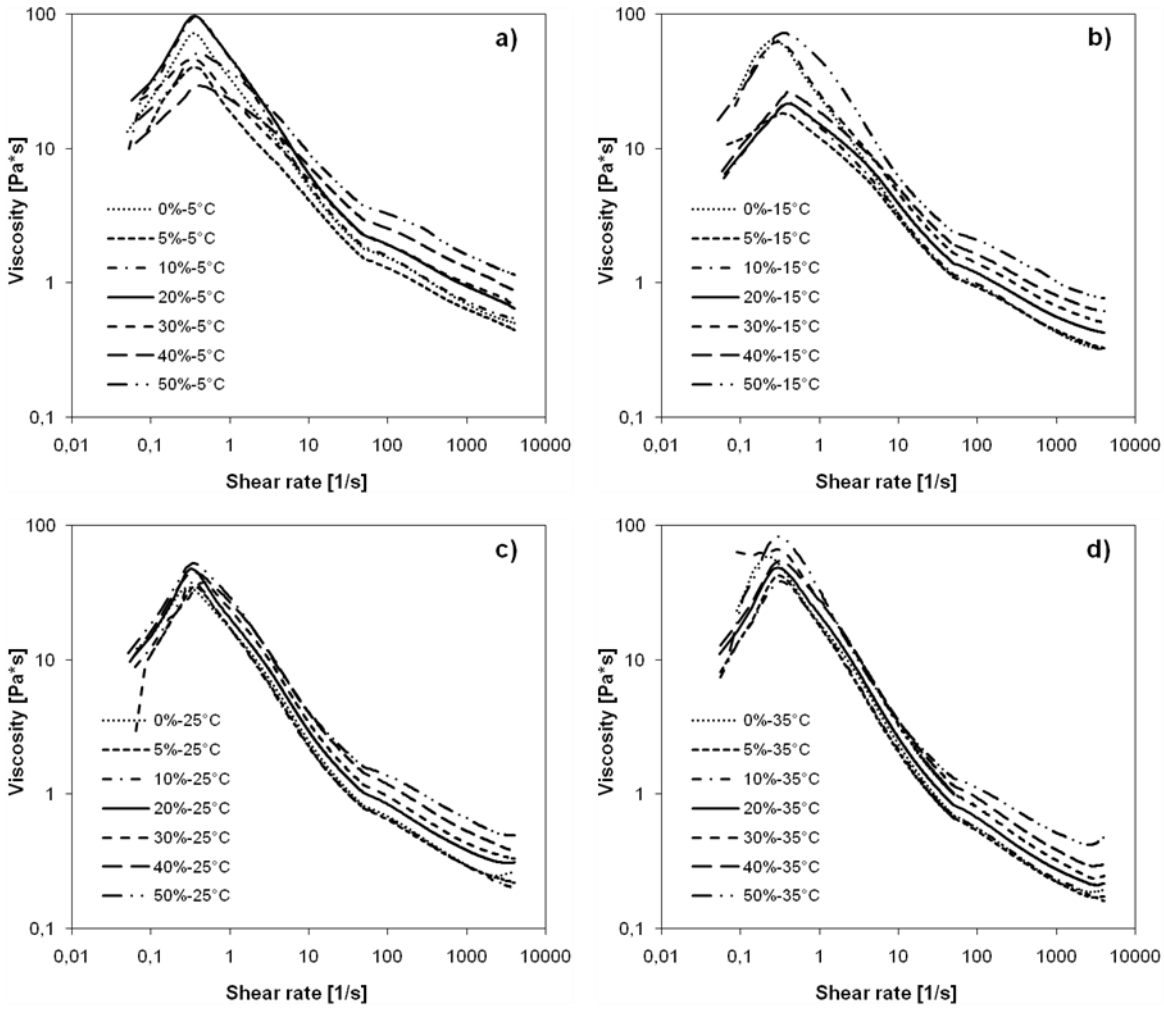

Fig. 6-5 Viscosity profile of alkyd paints at a) 5°C, b) 15°C, c) 25°C and d) 35°C.

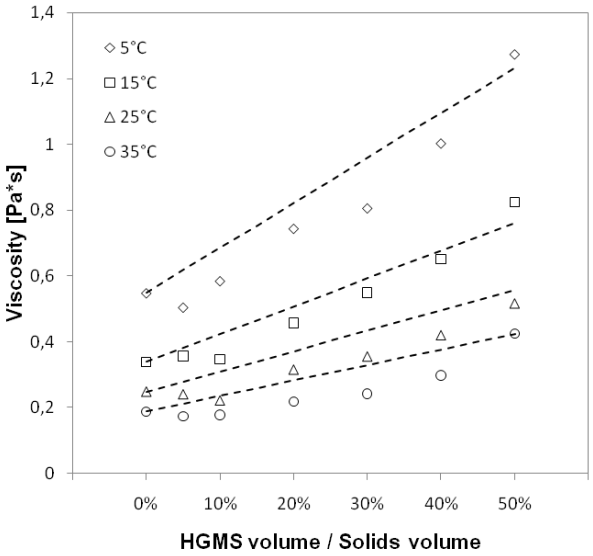

Fig. 6-6 Viscosity of alkyd paints at a shear rate of 2500 s^{-1} at different temperatures. The broken lines show the Einstein model.

The thixotropy of the paints was evaluated by pre-shearing the samples and then monitoring the rebuilding of the structure with an oscillating time sweep. After shearing the samples exhibit more viscous behaviour than elastic where the loss modulus is larger than the storage modulus which results in a large phase angle between the applied stress and the measured strain. As the structure rebuilds the storage modulus will increase faster than the loss modulus over time which decreases the phase angle. The changes in G´ and G´´ over time were therefore measured, see Fig. 6-7, and the paints compared on the time it took for the storage and loss moduli to become equal, or in other words for the phase angle to become 45°. The measured times as a function of microsphere loading are shown in Fig. 6-8 which shows that the microspheres significantly slow down the structure rebuilding except at very low loadings. A maximum in the rebuilding time is reached at microsphere loadings between 20 and 30% of the solids volume and at higher loadings the rebuilding time decreases again which is believed to be due to the high amount of solid content.

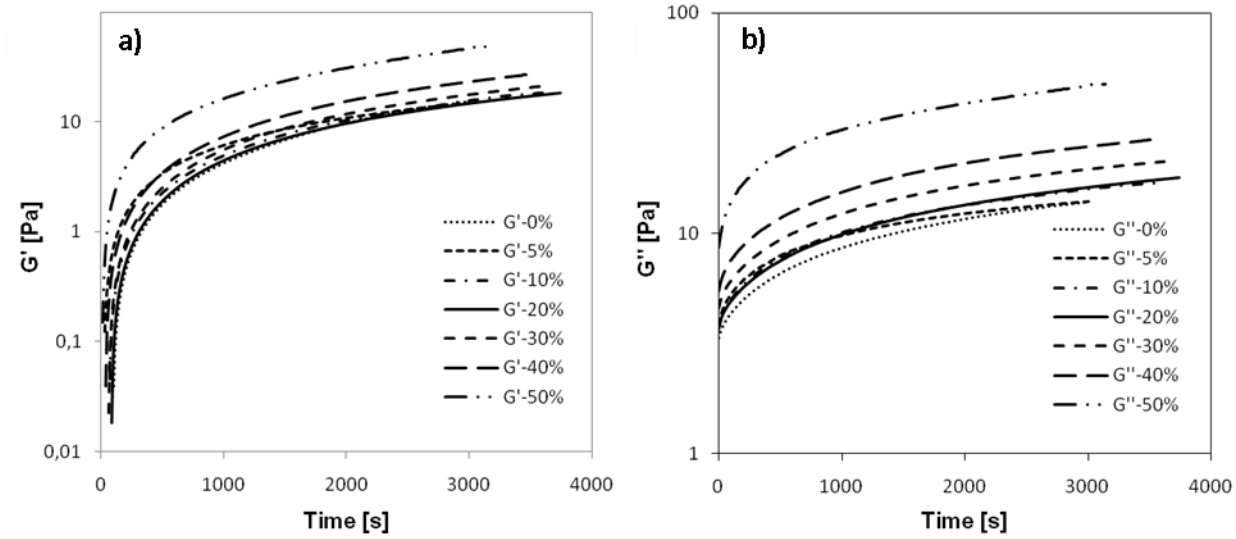

Fig. 6-7 a) G' and b) G'' during oscillation time sweep of alkyd paints.

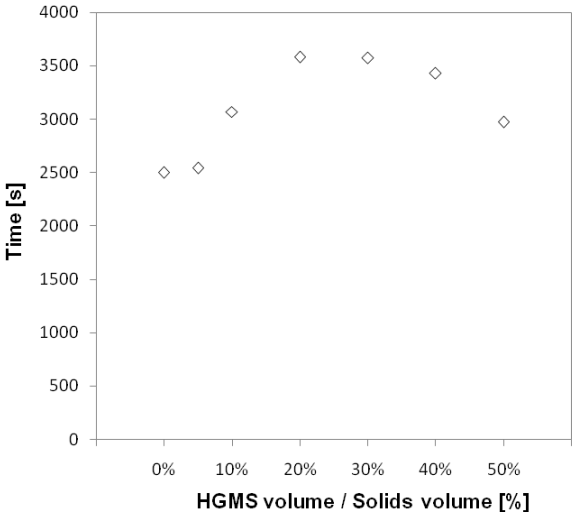

Fig. 6-8 Rebuilding time after shearing of samples. The storage and loss moduli are measured to be equal at this time.

6.3.3 Viscosity of acrylic paints

Fig. 6-9 show the measured viscosity profiles of acrylic paints with different concentrations of microspheres at different temperatures. The profiles exhibit a similar response to shear at all concentrations and temperatures. Generally the microspheres increase the viscosity of the paint and especially at low shear the increase is considerable. The profiles however converge at high shear which makes the application properties of the paints similar. The shear rate sweep was seperated into two ramps with different shear rate changes per time as with the alkyd paints. There is however no noticeable change in the slope at a shear rate of $50s^{-1}$ because the acrylic paints are pseudo-plastic and therefore do not exhibit time dependant behaviour.
Figure Fig. 6-10 shows a comparison of the measured viscosity of the acrylic paints at a shear rate of $2500s^{-1}$. The increase in viscosity as a function of microsphere loading is less than measured for the alkyds and the high solid paints are less sensitive to lower temperatures than the alkyds. The viscosity of the 20% paint is somewhat higher than what the general trend observed from the other samples would suggest. This is seen at all different temperatures and is therefore unlikely to be an artifact and is probably due to imperfect mixing of the sample. At lower temperatures the measured viscosity is significantly lower than the Einstein model suggest which is an interesting result considering that improved models [18][22] derived for more concentrated dispersions predict much higher viscosities at high filler loadings. Water based paints are however highly complex dispersions which are difficult to model.

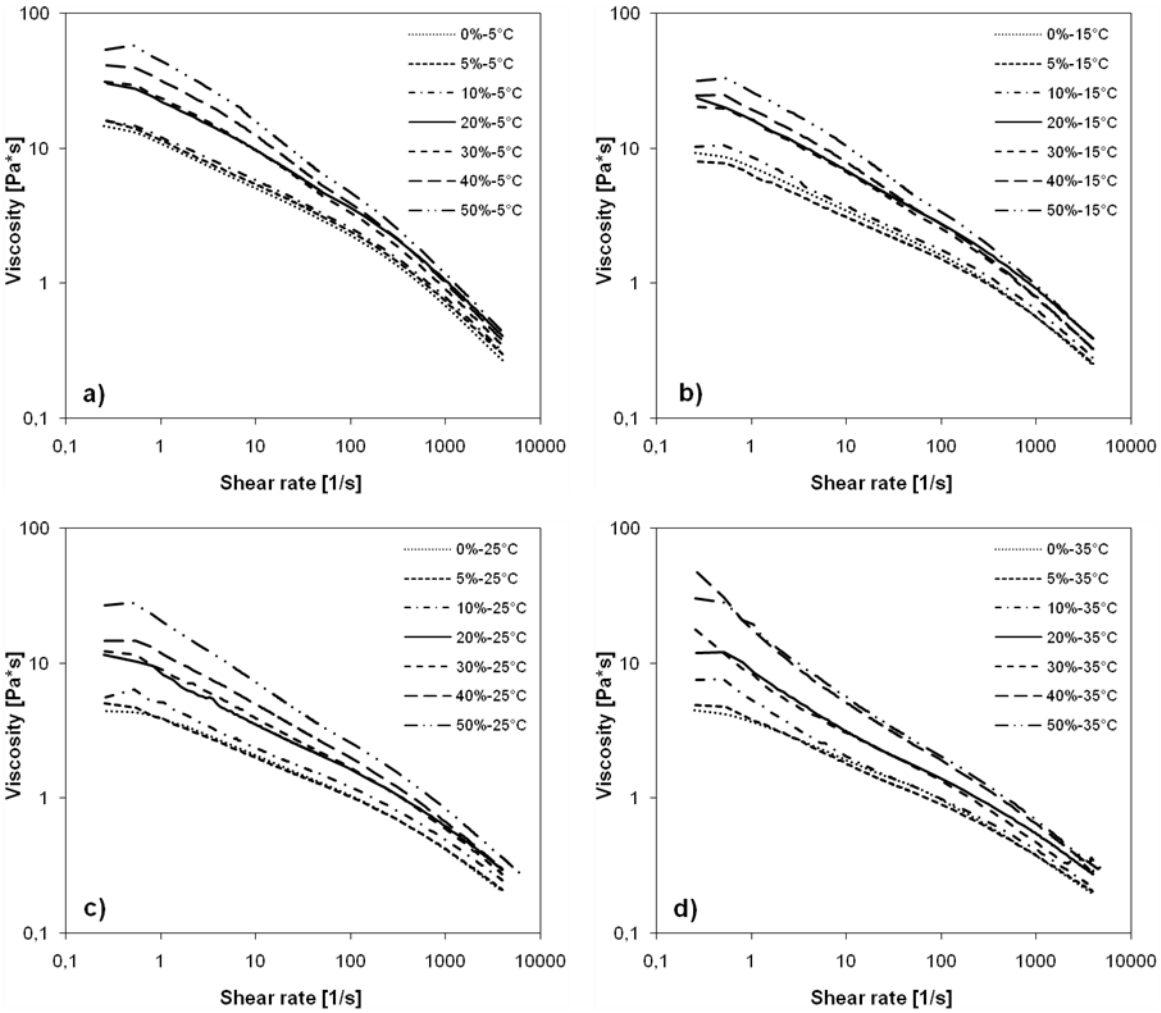

Fig. 6-9 Viscosity of acrylic paints at a) 5°C, b) 15°C, c) 25°C and d) 35°C.

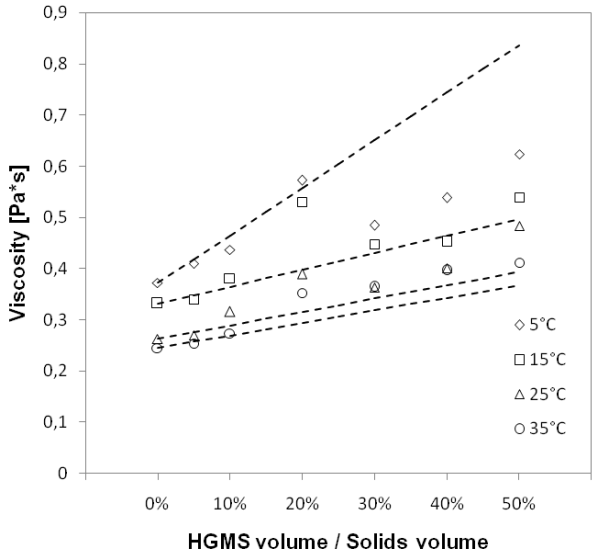

Fig. 6-10 Viscosity of acrylic paints at a shear rate of 2500 s^{-1} at different temperatures. The broken lines show the Einstein model.

An oscillating time sweep measurement of the acrylic paints was done at 1Pa and 1Hz as with the alkyds. The paints did not exhibit time dependant behaviour and the storage and loss moduli immediately reached steady state after shearing stopped, as shown in Fig. 6-11.

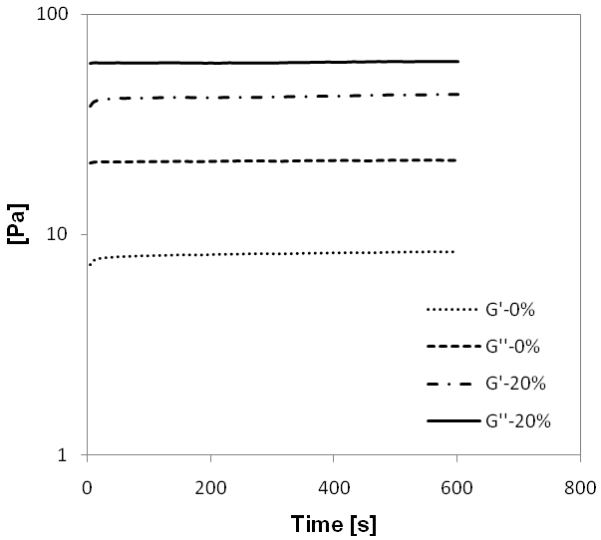

Fig. 6-11 Oscillatory time sweep of acrylic paints.

6.3.4 Mechanical Properties

The dynamic viscoelastic properties of dry alkyd films comprising microspheres were investigated by measuring the dependence of the shear storage and loss moduli, G´ and G´´, on temperature before and after QUV exposure.

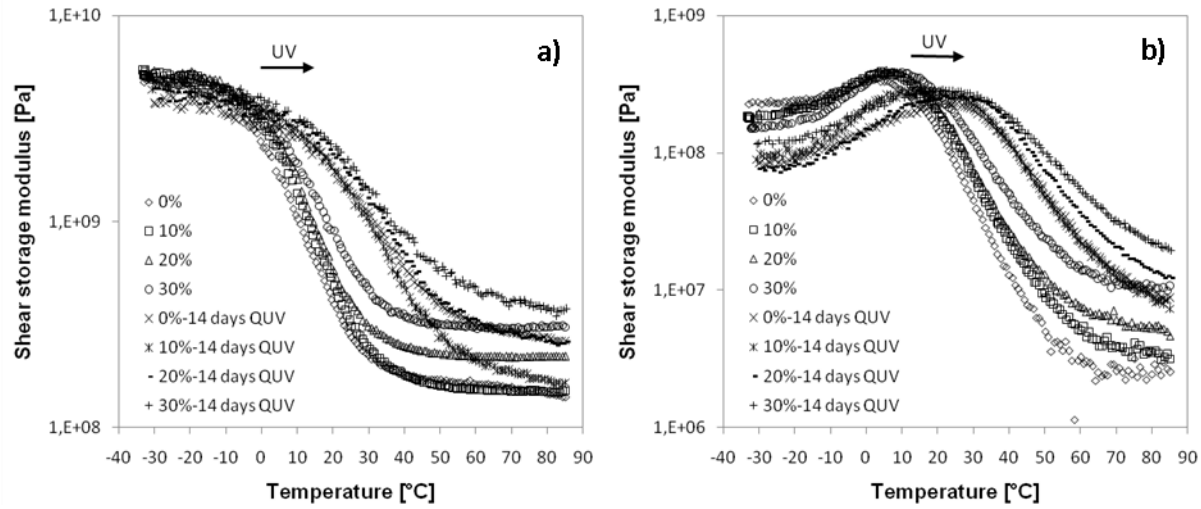

Fig. 6-12 shows G´ where it can be seen that before UV exposure the storage modulus increases with microsphere loading suggesting more elastic behaviour of the films containing microspheres. The increase in the glassy region is small while the increase in the rubbery region is far more pronounced which has also been observed in filled epoxies [23]. This is due to particle interactions in agglomerates which behave differently in glassy polymers compared to rubbery [24]. This can be

seen more clearly in Fig. 6-13 a) which shows the G´ of the filled alkyds relative to the 0% alkyd. The relative modulus of the films is just slightly above unity at temperatures below the T_g, which is 19°C as shown in Fig. 6-14, and begins to grow around T_g. The observed increase is very sharp at high loadings but at low loadings where the likelihood of agglomerates is small the increase is far less. Exposing the films to UV for two weeks increases the T_g to 36°C due to further curing. The filled films have a Tg about 1°C higher at low loadings and 2°C at high. The storage and loss modulus, Fig. 6-12, increase in the rubbery region after UV exposure but only slightly for the filled films while the change is significant for the 0% alkyd. It is possible that the coated microspheres offer increased UV protection [25] but it is also possible that the strain history of the films is different after exposure in the QUV chamber where they are exposed to rapid temperature and moisture changes. This has not been fully studied yet but clearly the relative modulus for filled films is measured to be much lower after UV exposure as seen in Fig. 6-13 b).

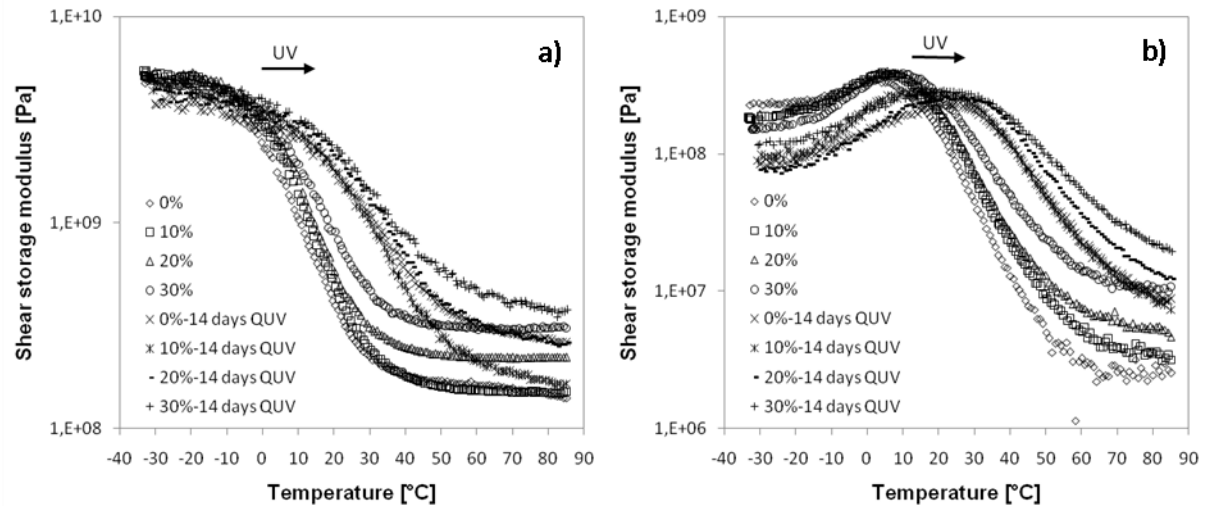

Fig. 6-12 a) Shear storage moduli and b) shear loss moduli of alkyd films without UV exposure and after 14 days exposure in QUV.

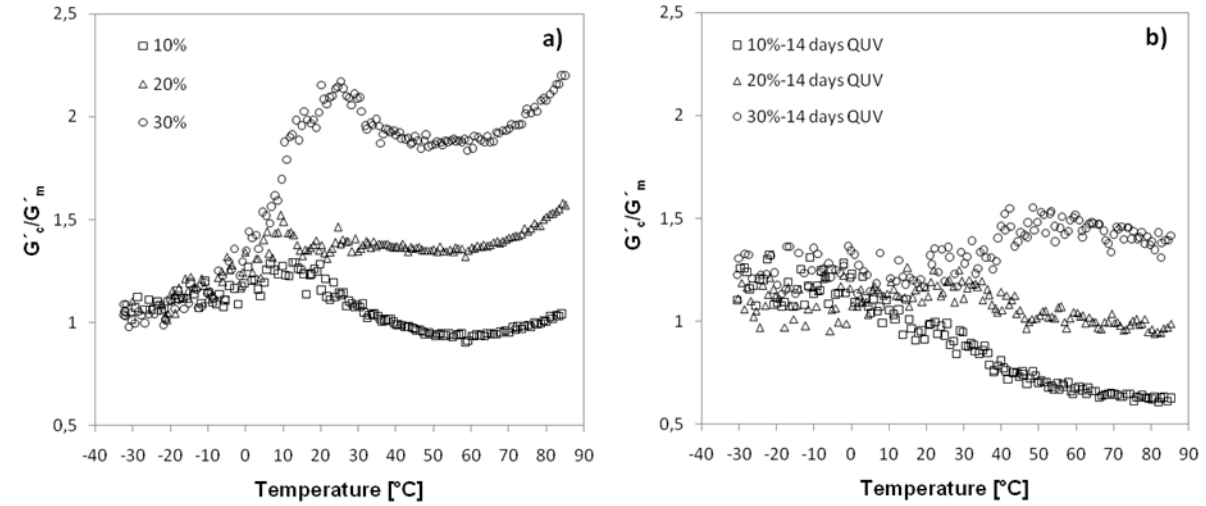

Fig. 6-13 G´ of the composite films relative to G´ of the 0% alkyd a) without UV exposure and b) after 14 days QUV exposure.

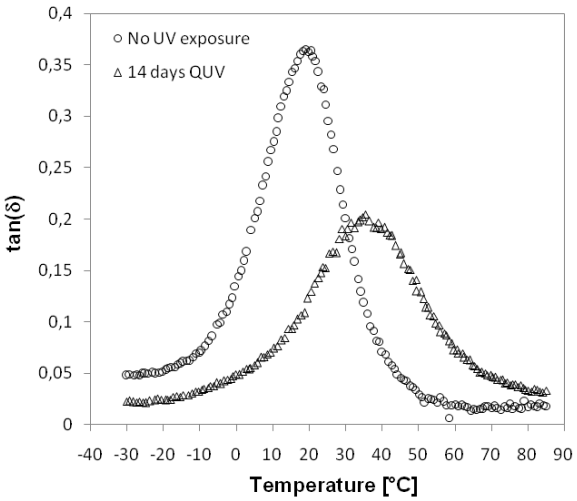

Fig. 6-14 tan(δ) of 0% alkyd films without UV exposure and after 14 days exposure in QUV.

6.3.5 Creep of alkyd films

Creep complicance can be analyzed from a mechanical model consisting of an elastic spring connected to a Voigt element; with a parallel spring, E_d, and dashpot, η_d; which is connected to a dashpot, η. This model is described by the equation

$$J(t) = J_0 + J_d\left(1 - e^{-\frac{E_d \cdot t}{\eta_d}}\right) + \frac{t}{\eta}$$

Equation 6-2

where the first term, J_0, represents the spring (i.e. the elastic component); the second and third terms the Voigt element (viscous component) and the last term the dashpot (flow component) [26]. The equilibrium compliance J_e, which is found from J_0 and J_d, as well as the creep viscosity, η, can be estimated from the tangent of the creep curve once steady state is reached [27][28] as shown in Fig. 6-15. The creep viscosity equals

$$\eta = \frac{1}{tan\theta}$$

Equation 6-3

and the equilibrium compliance equals the intersection of the tangent with the y-axis.
The measured creep compliance of alkyd films with 0, 10, 20 and 30% microspheres by volume can be seen in Fig. 6-15. Both the instantaneous and the delayed compliance of the films in the creep zone was found to decrease with microsphere loading which is due to the reinforcing effect of the microspheres. This decrease is reflected in the calculated equilibrium compliance which is shown in Fig. 6-16. Furthermore at higher loadings the microspheres were found to increase the creep viscosity which is a measure of the resistance of a material under stress to creep, see Fig. 6-16. High creep viscosity and low compliance are qualities that are perhaps more suitable for load bearing applications but in the case of wood paint the film needs to be able to withstand cyclic expansion and contraction of the substrate. High creep compliance and low creep viscosity can therefore be

viewed as positive as it can prevent the buildup of stress in the film and ultimately prevent crack formation.

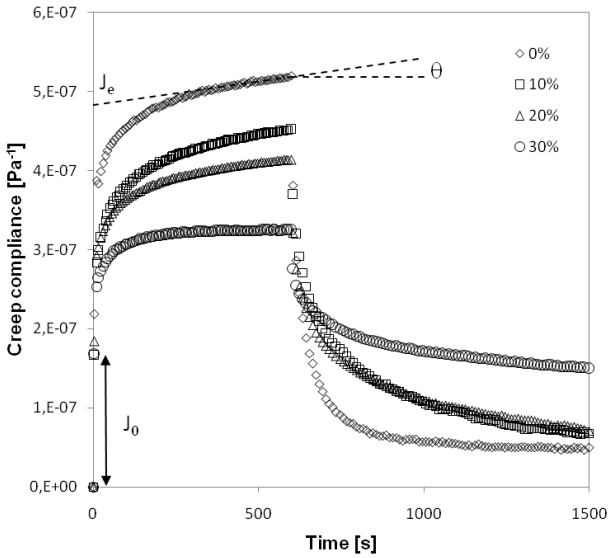

Fig. 6-15 Creep compliance of alkyd films.

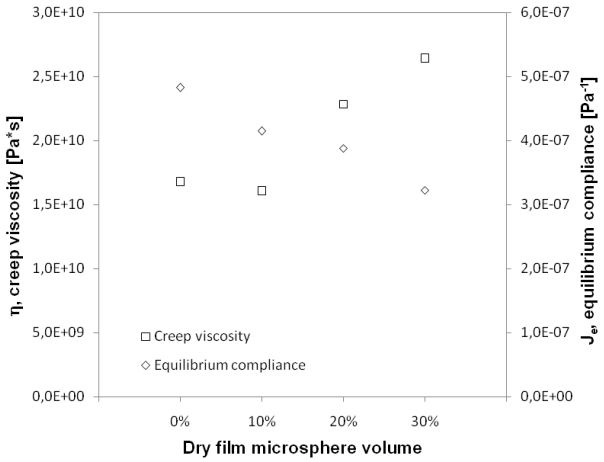

Fig. 6-16 Creep viscosity and equilibrium compliance of alkyd films as a function of microsphere loading.

The creep recovery of the film is however a more important property for the performance of wood paint than compliance or creep viscosity. A film that exhibits good strain recovery develops less permanent strain and can therefore follow the movement of the wood better without cracking or disbonding resulting in improved resistance to cyclic strain.
The equilibrium recoverable compliance, J_{er}, can be calculated by the equation [28].

$$J_{er}(t) = \frac{\gamma_c - \gamma_r(t)}{\sigma_c}$$

Equation 6-4

where γ_c is the maximum strain during loading, $\gamma_r(t)$ is the time dependant strain in the recovery zone and σ_c the stress applied in the creep zone. The equilibrium recoverable compliance becomes significantly lower with microsphere loading, see Fig. 6-17, and especially at 30% loading it is very low suggesting that permanent strain is more easily developed in the composite films.

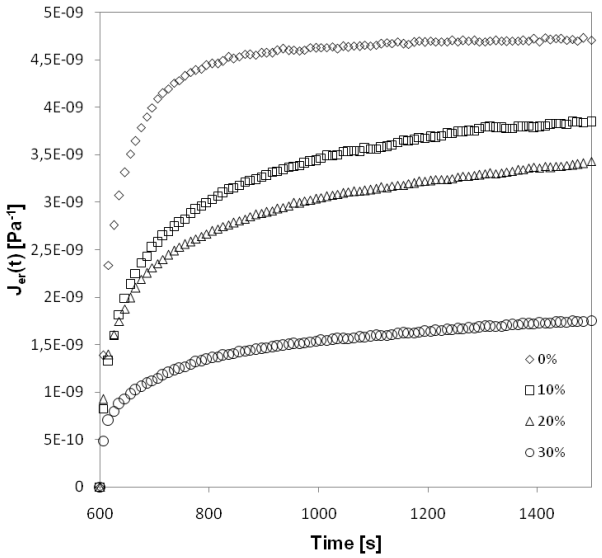

Fig. 6-17 Equilibrium recoverable compliance of alkyd films at 0%, 10%, 20% and 30% microsphere loadings.

6.3.6 Stress relaxation of alkyd films

The measured relaxation moduli of the alkyd paints at 1% strain are shown in Fig. 6-18. The films all have a similar reaction to near instantaneous strain but the relaxation modulus increases with microsphere loading and the rate of relaxation becomes slower. The modulus increase was expected as rigid filler will increase the stiffness of the composite [29] and the slower rate of relaxation can be explained by particle-matrix interactions reducing the mobility of the polymer [13]. The slower relaxation rate is considered negative for the intended application as the ability of the composite to dissipate stored energy is decreased. The decrease is however not thought to be severe enough to seriously affect the performance of wood coatings containing microspheres as the films will generally only be exposed to relatively slow strain rates due to temperature and moisture changes in wood.

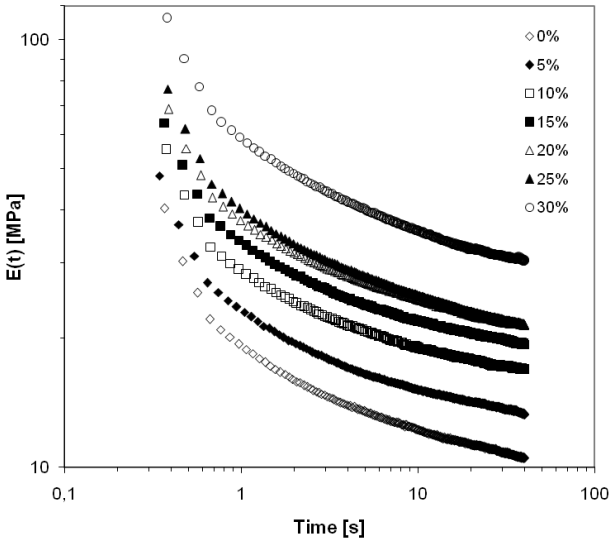

Fig. 6-18 Relaxation moduli of microsphere filled alkyd paints.

A calculation of the characteristic relaxation time, τ, based on the Maxwell model shows a linear increase with microsphere loading up to 20% where a maximum is reached as shown in Fig. 6-19. The time is calculated from the equation

$$\sigma(t) = \sigma_0 \cdot e^{\left(-\frac{t}{\tau}\right)}$$

Equation 6-5

where σ_0 is the instantaneous stress. The characteristic relaxation time is found when t equals τ and the measured stress is

$$\sigma(t_{t=\tau}) = \frac{\sigma_0}{e}$$

Equation 6-6

The observed decrease in relaxation time above 20% loading is however not believed to be due to relaxation of the polymer matrix but rather due to defects at the particle-matrix interface such as incomplete wetting of pigment and fillers. This is supported by the large increase in standard deviation with microsphere loading despite the low deviation of the 30% sample which could be explained by the concentration of defects being large enough for them to be equally distributed. The PVC of the 30% sample is close to 50%, as it also contains rutile pigment and other fillers, which can be very close to the critical PVC [30].

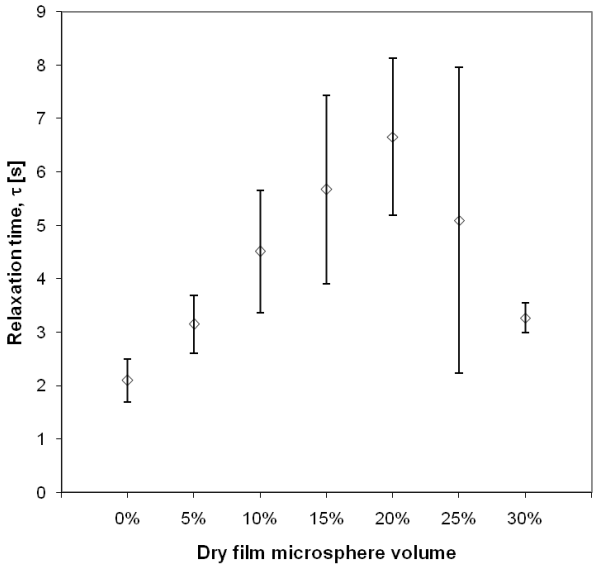

Fig. 6-19 Characteristic relaxation times of microsphere filled alkyd paints. The error bars show the standard deviation of the measurements.

6.3.7 Tensile test of alkyd films

The average values of the measured Young‘s moduli of alkyd films with HGMS at two different strain rates is shown in Fig. 6-20. Increased microsphere loading increases the modulus which is in agreement with results obtained by others [14][16][17]. The results are in good agreement with the model proposed by Ishai & Cohen [29] for rigid fillers in an epoxy matrix and the values fall within the upper and lower boundaries set by the model for both strain rates except for the 5% samples. The upper boundary in the case of rigid fillers is given by the equation

$$\frac{E_c}{E_m} = \frac{1}{1 - C_f^{1/3}}$$

Equation 6-7

where C_f is the filler concentration and E_c and E_m are the Young’s modulus of the composite and matrix, respectively. The lower boundary is given by the equation

$$\frac{E_c}{E_m} = 1 + \frac{C_f}{1 - C_f^{1/3}}$$

Equation 6-8

An increase in paint film stiffness can in no way contribute to a lower induced strain due to moisture changes in the wood substrate and therefore a higher Young’s modulus is not considered positive for the application as it will only result in higher stress in the film.

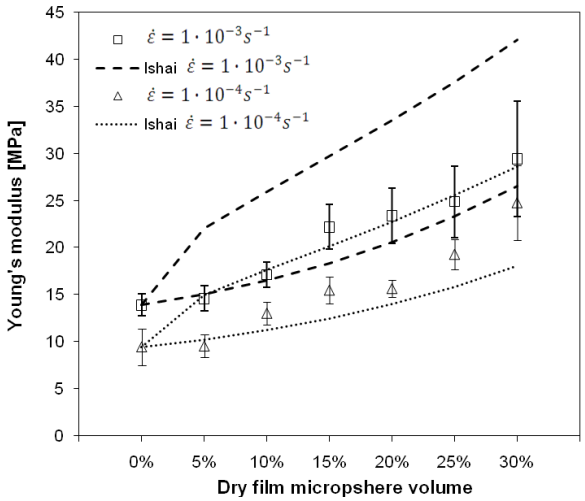

Fig. 6-20 Young's modulus as a function of micropshere loading at two different strain rates. The broken lines show the upper and lower boundaries of the Ishai model for both strain rates and the error bars show the standard deviation of the measurements.

It has been shown that fillers reduce the fatigue resistance of a material by acting as crack initiation sites. Fillers are however a necessity and are found in almost all paints. Glass beads however have been shown to improve the fatigue resistance [10] by restricting crack propagation through a mechanism called crack front pinning [31][32][33][34]. Crack front pinning occurs when a propagating crack hits a rigid particle and can not continue to grow in the same direction. The crack must therefore bow out past the particle effectively lengthening the crack and thereby increasing the crack surface which requires more energy. The toughening effect of crack front pinning has been shown to increase with shorter interparticle distances [17] and to increase with particle size [11].
The toughening effect can be estimated from the critical stress intensity factor which is given by the equation

$$K_{IC} = \sigma^0 \cdot \sqrt{\pi \cdot a} \cdot f\left(\frac{a}{W}\right)$$

Equation 6-9

Where K_{IC} is the stress intensity factor, σ^0 is the stress at which the crack begins to propagate, a is the length of the introduced crack, W is the width of the sample and f(a/W) is the geometric function which for this case is given by [35].

$$f\left(\frac{a}{W}\right) = \left(\frac{2 \cdot W}{\pi \cdot a} \cdot \tan\left(\frac{\pi \cdot a}{2 \cdot W}\right)\right)^{1/2} \cdot \left(\cos\left(\frac{\pi \cdot a}{2 \cdot W}\right)\right)^{-1} \cdot \left(0{,}752 + 2{,}02 \cdot \left(\frac{a}{W}\right) + 0{,}37 \cdot \left(1 - \sin\left(\frac{\pi \cdot a}{2 \cdot W}\right)\right)^3\right)$$

Equation 6-10

The measured relative stress intensity factor ($K_{IC,comp}/K_{IC,\ matrix}$) for the filled alkyd films is shown in Fig. 6-21 and the measured increase in the stress intensity factor is quite modest compared to the results of others [11][12][15][16][17]. Their work was however done on microsphere filled epoxy so a likely explanation for the difference is the low cross link density of an alkyd compared to an epoxy. That means that although the cracks develop a larger surface area the energy difference is

small due to the low cross linking density. The stress strain curves of the filled alkyd films exhibit modest signs of stick/slip crack propagation [12], indicative of crack front pinning, which can be seen in Fig. 6-22 by the kinks in the curves after the maximum stress is reached. The curve for the 0% film does not show this behaviour and looking at the crack surface, shown in Fig. 6-23, the mechanism for crack propagation is clearly different.

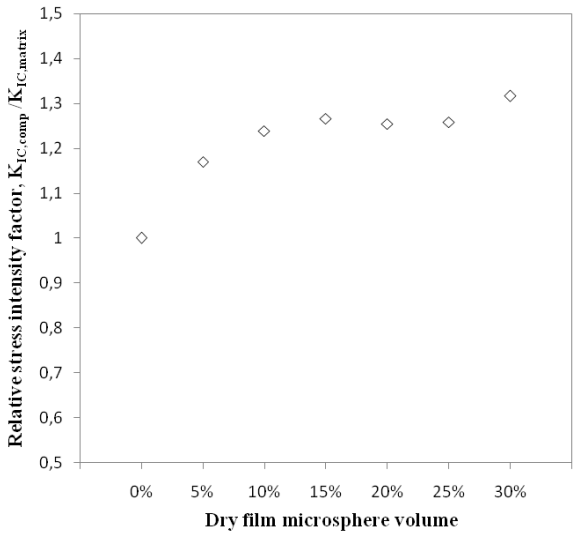

Fig. 6-21 Measured relative stress intensity factor of alkyd films.

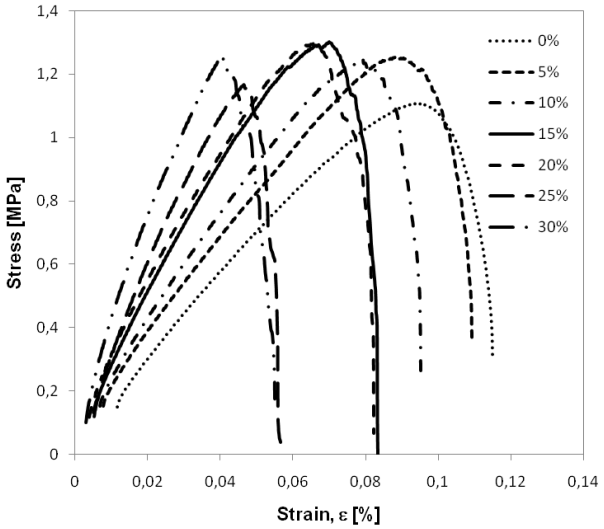

Fig. 6-22 Stress strain curves exhibiting stick/slip crack propagation.

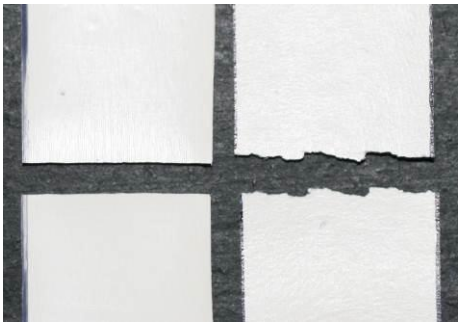

Fig. 6-23 Crack surfaces of 0% alkyd film (left) and 30% film (right).

Fig. 6-24 illustrates the measured elongation at break of the alkyd films as a function of microsphere loading at two different strain rates. The elongation at break is significantly reduced with microsphere loading and the elongation of the 30% films is less than one third of the elongation of the 0% films. Highly ductile films are generally considered good for application on wood as they can better withstand the movement of the substrate. Paint films can be subjected to large strains on a wood surface especially at the interface between earlywood and latewood and as the film ages and is exposed to the elements it loses ductility. Decreasing the strain rate results in less elongation at break and the difference is most pronounced for the 0% films. The relatively small small change in ductility for the filled films is believed to be related to the crack front pinning mechanism.

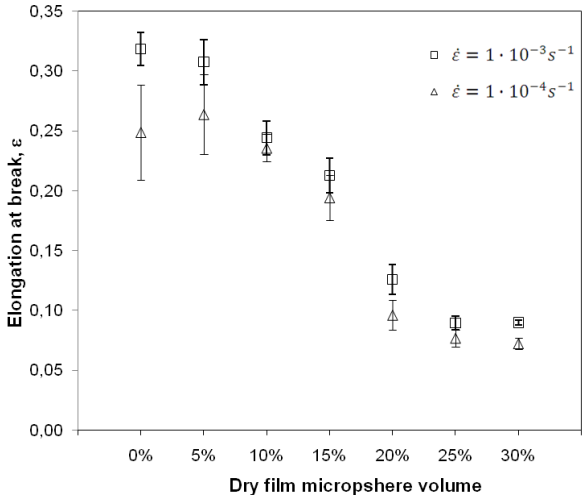

Fig. 6-24 Measured elongation at break of alkyd films at different microsphere loadings.

6.3.8 Water permeability

The cup test measures the steady state permeability of a paint film. The driving force for the permeation is the difference in partial pressure on both sides of the film and the barrier consists of different resistances such as the coating, substrate and external air gap. If the cup is kept in a climate chamber there is no resistance due to an external air gap [36].
The water transmission rate of the coating, V_c, can be described by the equation

$$V_c = \frac{G_{cs} \cdot G_s}{(G_s - G_{cs}) \cdot A}$$

Equation 6-11

where A is the area of permeation, G_s is the mass change per time measured for the substrate and G_{cs} is the mass change per time for a coated substrate. The permeability coefficient, δ, is then calculated with the equation

$$\delta = \frac{V_c \cdot d}{\Delta p}$$

Equation 6-12

where d is the coating thickness and Δp is the vapour pressure difference between the inside and outside of the cup. The Δp was calculated to be 1320Pa.

The liquid water permeability coefficients are shown in Fig. 6-25. It was not unexpected to initially measure lower permeability coefficients for the films with microspheres as the effective diffusion length for water molecules is longer with a higher concentration of impermeable particles. It was however originally believed that the permeability of the filled films would quickly become higher than for the 0% film because of degradation caused by the photocatalyst and generally poorer mechanical properties. The fact that these films maintain lower permeability coefficients after all stages of UV exposure however indicates good UV stability of the films. What is most interesting though is the sudden increase in permeability of the 0% films after 30 days of QUV exposure. A SEM analysis of the films revealed that after 30 days few large cracks had formed in the 0% films while the filled films had small superficial cracks covering a large part of the surface as seen in Fig. 6-26. Some of the cracks in the 0% film reached all the way down to the substrate revealing the wood fibers as seen in Fig. 6-26 c). This shows that although the mechanical properties of the 30% films are measured to be inferior compared to the 0% films the performance of the 30% films is better due to a different cracking mechanism. Once cracks are initiated in the 0% films they can propagate relatively unhindered and therefore become long and deep. This allows micro-organism to gain a foothold which will lead to the wood rotting and ultimately disbondment of the paint film. In the 30% films on the other hand numerous small and, judging from the relatively small increase in permeability, superficial cracks are formed as a result of the crack front pinning mechanism. The mechanical energy from stresses in the film is released over a much larger area so the film retains more of its protective properties. Only a few of the coated microspheres have separated from the surface showing that the photocatalyst is not active deep in the film. Furthermore no indications can be seen of the photocatalytic reaction having an effect elsewhere than in the immediate vicinty of the microspheres. It is therefore concluded that the coated micropsheres can improve the protective properties of the paint films rather than degrade it.

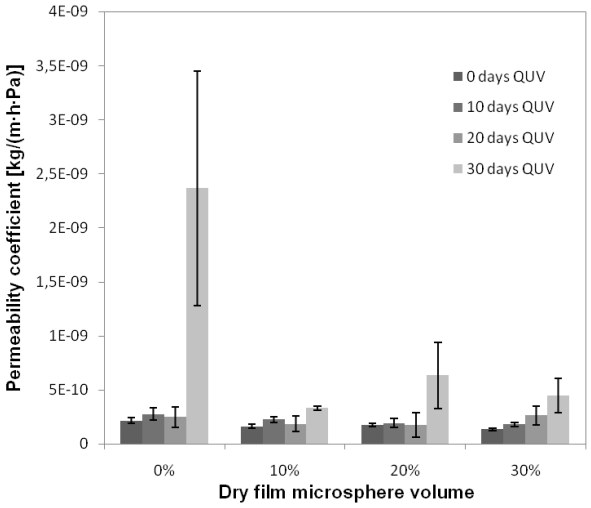

Fig. 6-25 Liquid water permeability coefficients of paint films with different concentrations of coated microspheres after different QUV exposure times. The error bars show the standard deviation.

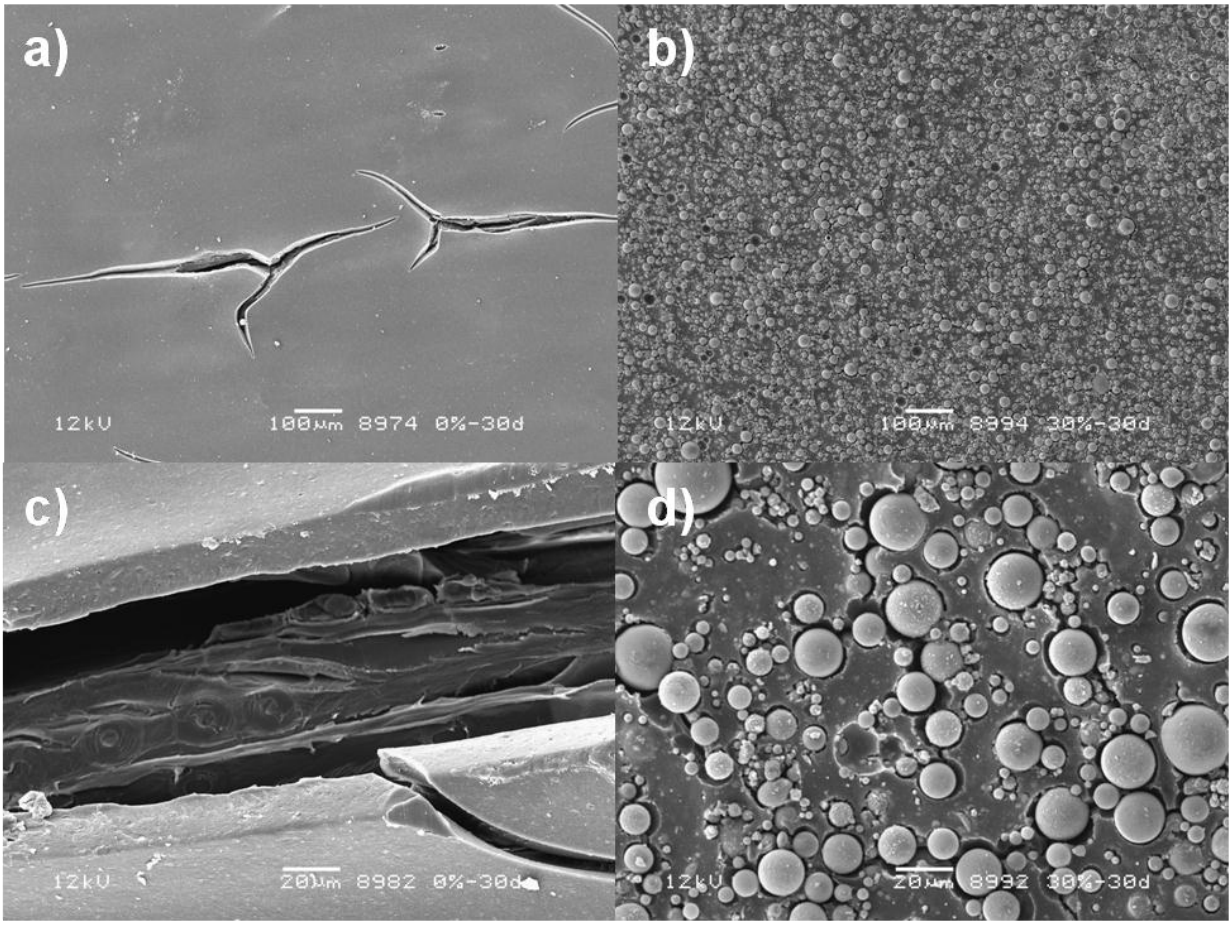

Fig. 6-26 Illustrates the surface of transparent alkyd films painted on veneer after 30 days of exposure in QUV, a) and c) 0% film with large cracks in surface, b) and d) 30% film with small cracks over entire surface. Both films are shown with the same magnification.

6.4 Conclusion

It has been shown that solvent borne alkyds and water borne acrylic paints can be formulated with high concentrations of microspheres without affecting the viscosity at high shear to a large extent. The microspheres were found to have a negative effect on the mechanical properties of alkyd films but nevertheless the overall performance of the films were found to improve with regard to water permeability and crack resistance.

Acknowledgements

The authors would like to express their gratitude to David Löf, Dyrup A/S, for guidance with the rheology measurements, Bent Samuelsen, Dyrup A/S, for guidance with the water permeability measurements and Luboš Kácovský and Vladimír Špaček, Synpo, for assistance with the dynamic mechanical measurements. Furthermore we thank Dyrup A/S and the Danish Agency for Science and Innovation for financial support.

References

[1] A. Mills, A. Lepre, N. Elliott, S. Bhopal, I. P. Parkin, and S. A. O'Neill, "Characterisation of the photocatalyst Pilkington Activ(TM): a reference film photocatalyst?," *Journal of Photochemistry and Photobiology A: Chemistry*, vol. 160, no. 3, pp. 213-224, Aug. 2003.
[2] I. P. Parkin and R. G. Palgrave, "Self-cleaning coatings," *Journal of Materials Chemistry*, vol. 15, no. 17, p. 1689, 2005.
[3] N. S. Allen, M. Edge, G. Sandoval, J. Verran, J. Stratton, and J. Maltby, "Photocatalytic Coatings for Environmental Applications¶†," *Photochemistry and Photobiology*, vol. 81, no. 2, pp. 279-290, Mar. 2005.
[4] A. E. Jacobsen, "Titanium Dioxide Pigments: Correlation between Photochemical Reactivity and Chalking.," *Industrial & Engineering Chemistry*, vol. 41, no. 3, pp. 523-526, Mar. 1949.
[5] G. KAEMPF, PAPENROT.W, and R. HOLM, "DEGRADATION PROCESSES IN TIO2-PIGMENTED PAINT FILMS ON EXPOSURE TO WEATHERING," *JOURNAL OF PAINT TECHNOLOGY*, vol. 46, no. 598, pp. 56-63, 1974.
[6] U. Gesenhues, "Al-doped TiO2 pigments: influence of doping on the photocatalytic degradation of alkyd resins," *Journal of Photochemistry and Photobiology A: Chemistry*, vol. 139, no. 2-3, pp. 243-251, Mar. 2001.
[7] P. A. Christensen, A. Dilks, T. A. Egerton, E. J. Lawson, and J. Temperley, "Photocatalytic oxidation of alkyd paint films measured by FTIR analysis of UV generated carbon dioxide," *Journal of Materials Science*, vol. 37, no. 22, pp. 4901-4909, 2002.
[8] W. G. Wamer, J.-J. Yin, and R. R. Wei, "Oxidative Damage to Nucleic Acids Photosensitized by Titanium Dioxide," *Free Radical Biology and Medicine*, vol. 23, no. 6, pp. 851-858, 1997.
[9] W. A. Pryor, "Oxy-Radicals and Related Species: Their Formation, Lifetimes, and Reactions," *Annual Review of Physiology*, vol. 48, no. 1, pp. 657-667, Oct. 1986.
[10] H. Sautereau, A. Maazouz, J. F. Gerard, and J. P. Trotignon, "Fatigue behaviour of glass bead filled epoxy," *Journal of Materials Science*, vol. 30, pp. 1715-1718, 1995.
[11] Y. Nakamura, M. Yamaguchi, M. Okubo, and T. Matsumoto, "EFFECT OF PARTICLE-SIZE ON THE FRACTURE-TOUGHNESS OF EPOXY-RESIN FILLED WITH SPHERICAL SILICA," *Polymer*, vol. 33, no. 16, pp. 3415-3426, 1992.
[12] A. J. Kinloch, D. L. Maxwell, and R. J. Young, "The fracture of hybrid-particulate composites," *Journal of Materials Science*, vol. 20, pp. 4169-4184, Nov. 1985.
[13] N. Amdouni, H. Sautereau, and J. F. Gerard, "Epoxy composites based on glass beads. I. Viscoelastic properties," *Journal of Applied Polymer Science*, vol. 45, no. 10, pp. 1799-1810, Aug. 1992.
[14] N. Amdouni, H. Sautereau, and J. F. Gerard, "Epoxy composites based on glass beads. II. Mechanical properties," *Journal of Applied Polymer Science*, vol. 46, no. 10, pp. 1723-1735, Dec. 1992.
[15] A. C. Moloney, H. H. Kausch, and H. R. Stieger, "The fracture of particulate-filled epoxide resins," *Journal of Materials Science*, vol. 19, pp. 1125-1130, Apr. 1984.
[16] J. Spanoudakis and R. J. Young, "Crack propagation in a glass particle-filled epoxy resin," *Journal of Materials Science*, vol. 19, pp. 473-486, Feb. 1984.
[17] J. Spanoudakis and R. J. Young, "Crack propagation in a glass particle-filled epoxy resin," *Journal of Materials Science*, vol. 19, pp. 487-496, Feb. 1984.
[18] M. Mooney, "The viscosity of a concentrated suspension of spherical particles," *Journal of Colloid Science*, vol. 6, no. 2, pp. 162-170, Apr. 1951.

[19] A. Brun, H. Dihang, and L. Brunel, “Film formation of coatings studied by diffusing-wave spectroscopy,” *Progress in Organic Coatings*, vol. 61, no. 2-4, pp. 181-191, Feb. 2008.
[20] O. Cohu and A. Magnin, “The levelling of thixotropic coatings,” *Progress in Organic Coatings*, vol. 28, no. 2, pp. 89-96, Jun. 1996.
[21] A. Einstein, “Eine neue Bestimmung der Moleküldimensionen,” *Annalen der Physik*, vol. 324, no. 2, pp. 289-306, Jan. 1906.
[22] E. Guth, “Theory of Filler Reinforcement,” *Journal of Applied Physics*, vol. 16, no. 1, p. 20, 1945.
[23] S. N. Goyanes, P. G. König, and J. D. Marconi, “Dynamic mechanical analysis of particulate- filled epoxy resin,” *Journal of Applied Polymer Science*, vol. 88, no. 4, pp. 883-892, Apr. 2003.
[24] B.-L. Lee and L. E. Nielsen, “Temperature dependence of the dynamic mechanical properties of filled polymers,” *Journal of Polymer Science: Polymer Physics Edition*, vol. 15, no. 4, pp. 683-692, Apr. 1977.
[25] J.-W. Kim et al., “Titanium dioxide/poly(methyl methacrylate) composite microspheres prepared by in situ suspension polymerization and their ability to protect against UV rays,” *Colloid & Polymer Science*, vol. 280, no. 6, pp. 584-588, Jun. 2002.
[26] K. Ueda, H. Kanai, and T. Amari, “Viscoelastic properties of paint films and formability in deep drawing of pre-painted steel sheets,” *Progress in Organic Coatings*, vol. 45, no. 1, pp. 15-21, Sep. 2002.
[27] K. Ueda, H. Kanai, and T. Amari, “Formability of polyester/melamine pre-painted steel sheets from rheological aspect,” *Progress in Organic Coatings*, vol. 45, no. 2-3, pp. 267-272, Oct. 2002.
[28] J. M. Dealy and R. G. Larson, *Structure and rheology of molten polymers: from structure to flow behavior and back again*. Hanser Verlag, 2006.
[29] O. Ishai and L. J. Cohen, “Elastic properties of filled and porous epoxy composites,” *International Journal of Mechanical Sciences*, vol. 9, no. 8, pp. 539-546, Aug. 1967.
[30] H. Panda, *Alkyd Resins Technology Handbook*. Asia Pacific Business Press Inc., 2010.
[31] A. G. Evans, “The strength of brittle materials containing second phase dispersions,” *Philosophical Magazine*, vol. 26, pp. 1327-1344, Dec. 1972.
[32] F. F. Lange and K. C. Radford, “Fracture energy of an epoxy composite system,” *Journal of Materials Science*, vol. 6, pp. 1197-1203, Sep. 1971.
[33] D. J. Green, P. S. Nicholson, and J. D. Embury, “Fracture of a brittle particulate composite,” *Journal of Materials Science*, vol. 14, pp. 1413-1420, Jun. 1979.
[34] D. J. Green, P. S. Nicholson, and J. D. Embury, “Fracture of a brittle particulate composite,” *Journal of Materials Science*, vol. 14, pp. 1657-1661, Jul. 1979.
[35] H. Tada, P. C. Paul, and G. R. Irwin, *The Stress Analysis of Cracks Handbook*, First ed. Hellertown, PA: Del Research Corporation, 1973.
[36] Charles M. Hansen, “Potential Errors in Water/Water Vapor Permeation Measurements Using the Cup Method,” *Färg och Lack*, vol. 39, no. 3, pp. 57-60, 1993.

7 Paper 4: Durability and performance of photocatalytic self-cleaning alkyd paint during outdoor exposure

Sverrir G. Gunnarsson, Per Møller, Søren H. Poulsen and Lisbeth M. Ottosen

Abstract

Hollow glass microspheres were coated with photocatalytically active anatase TiO_2. Both transparent and opaque alkyd paints with different concentrations of coated and uncoated microspheres were prepared and applied on wood panels which were exposed outdoors to investigate the durability of the paint films. The microspheres were found to improve the durability of the paint films and to help keep micro-organisms from immobilising on the surface. The liquid water permeability of the films was investigated and the microspheres found to greatly improve the barrier properties not only due to an increase in water diffusion length but also because of increased crack resistance.

7.1 Introduction

Photocatalysis has shown great promise for a number of applications where self-cleaning surfaces are one of them [1][2]. Attempts have been made to integrate photocatalytic material into organic paints [3], either as anatase pigment or anatase nano-particles, but such attempts have not yielded sufficiently good results due to the aggressive nature of the OH radicals created by the photocatalytic reaction. The photo-activity of TiO_2 pigments and consequent degradation of organic binders, often termed chalking, has been well known to the paint industry [4][5] for a long time and most TiO_2 pigments today are therefore stabilized to minimize chalking [6][7]. The authors have however shown [unpublished work] that it is possible to integrate photocatalytic material into an organic paint system without it causing excessive chalking. This is achieved by the novel approach of coating the photocatalyst onto hollow glass microspheres which are dispersed in the paint. This reduces the interfacial area between the photocatalyst and the binder and provides an inert surface for the photocatalytic reaction to take place. Fig. 7-1 shows the different degradation mechanism for a paint film with photocatalytic nano-particles compared to a film with coated microspheres. The binder surrounding photocatalytic nano- or pigment sized particles in the film surface will quickly degrade when exposed to UV-light which causes the particles to separate from the film, i.e. chalking. This effect has been interpreted as self-cleaning due to the constant renewal of the surface but it has some serious disadvantages as the film rapidly loses its protective properties. Furthermore as a result of a high chalking rate such a film would constantly release particles to its surroundings. The effect of photocatalytic nano-particles on people has not yet been fully studied but investigations suggest they may have adverse photo-toxicological effects [8]. Microspheres on the other hand are embedded much deeper in the film so although the binder is degraded at the surface UV-light doesn't reach the binder-particle interface deeper in the film. A thin gap has been observed to form around the particles in the surface but nevertheless the particles do not separate from the film prematurely. The glass particles therefore provide an area for the photocatalysis to take place which is unaffected by the reaction. Furthermore due to the exceptionally short lifetime of the OH radical [9] it is impossible for it to diffuse away from the site of creation and attack binder which isn't in direct contact with the photocatalyst.

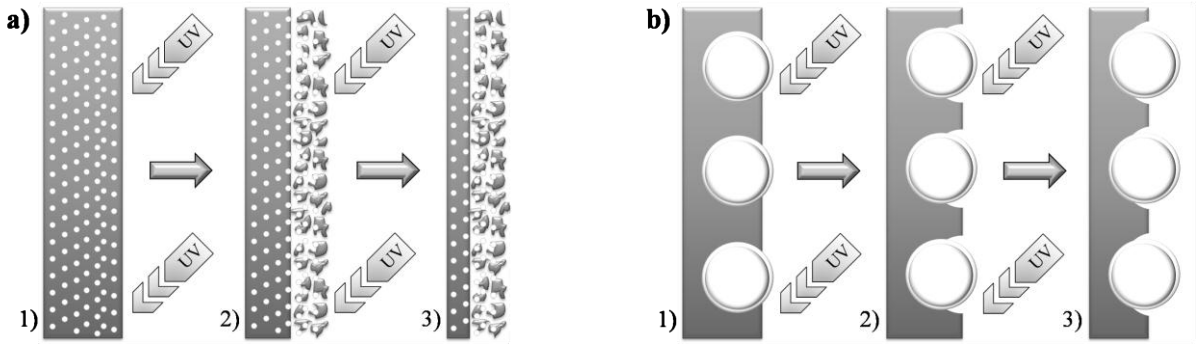

Fig. 7-1 a) shows a film with nano-particles constantly eroding from 1) to 3). b) shows a film with photocatalytic carrier particles 1) Fresh film, 2) After initial exposure chalking has occurred, 3) Chalking has nearly ceased as UV radiation no longer reaches carrier particle/binder interface and the much slower photochemical degradation of the binder becomes the predominant process. The figures do not represent the full film thickness.

In order to make the surface sufficiently self-cleaning it is necessary to have a large concentration of coated microspheres in the surface so they need to be a substantial part of the formulation volume. This work was done to investigate the performance of such paint films during outdoor exposure.

7.2 Experimental

7.2.1 Materials and equipment

Three different types of hollow glass microspheres (HGMS) were used in the paint formulations. iM30K and S38 glass bubbles from 3M and Sphericel 110P8 from Potters Industries. The microspheres are from borosilicate glass. The average density of the iM30K microspheres is 0,6g/cm^3 and the average particle size 15,5µm. The S38 spheres have an average density of 0,38 g/cm^3 and an average size of 40µm and the 110P8 an average density of 1,1 g/cm^3 and an average size of 11µm. The size distribution of the microspheres can be seen in Fig. 7-2.
The titanium-tetraisopropoxide (TTIP) used to coat the microspheres was VERTEC® TIPT, 97+% from Alfa Aesar.
Artificial weathering of samples was done in a Q-lab QUV artificial weathering chamber, equipped with QUV-A340 UV lamps, according to EN 927-6:2006 where the samples were exposed to alternating periods of 2,5 hours of UV exposure and 0,5 hours water spray for six days followed by 1 day of water condensation.
Electron microscopy was done using a JEOL model JSM-5900 electron microscope with a LaB_6 filament and a FEI model Inspect S electron microscope with a tungsten filament. The x-ray diffraction analysis was done using a Huber Guinier G670 diffractometer with $Cu_{K\alpha 1}$ radiation and particle size was measured with a Malvern Mastersizer 2000.

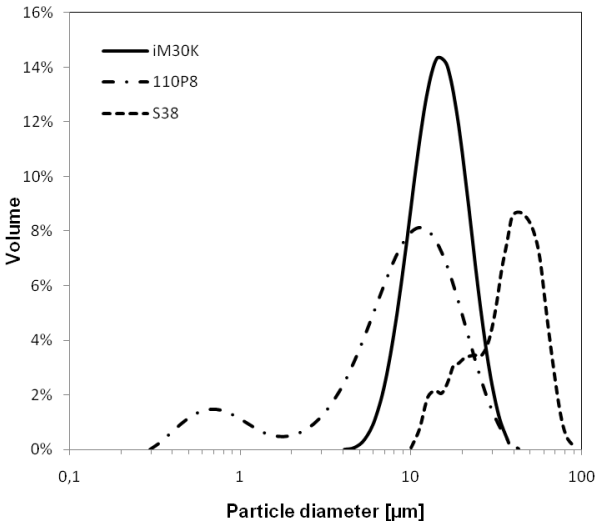

Fig. 7-2 Particle size distribution of iM30K, 110P8 and S38 HGMS.

7.2.2 Coating process

The HGMS were coated using the method described below. The microspheres were pre-treated at 150°C for 24 hours to remove physically adsorbed water. TTIP, see Fig. 7-3, was mixed with isopropanol with a ratio of 1:10 and stirred for 20 minutes. 1g (iM30K) or 1,8g (110P8) or 1,6g (S38) of microspheres was added to the solution for every 10 ml isopropanol and the mixture stirred for 20 minutes. Then de-ionized water, 1 ml for every 1ml of TTIP, was added to the solution and stirred for 10 minutes. The solution was filtered to remove most of the isopropanol and then heated to 70°C and continuously stirred to avoid agglomeration while the remaining isopropanol evaporated. Once dry the coated microspheres were calcined at 550°C for 5 hours to crystallize the TiO_2. The process was repeated once more to load more TiO_2 on the microspheres. After the second round of coating the microspheres were separated from all unbound TiO_2 by sonication.

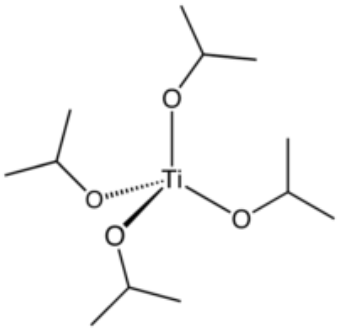

Fig. 7-3 Titanium tetraisopropoxide structure.

7.2.3 Paint formulations

Both opaque and transparent solvent borne air drying alkyd paints were formulated with different HGMS concentrations. The approximate formulations can be seen in Table 7-1 where “other solids”

represent binder, pigment and fillers. The paints were prepared by dispersing the microspheres in the binder at 1000rpm which was then mixed with the remaining ingredients such as pigment paste, solvents, additives etc.

Color	HGMS % of total solids	HGMS vol.%	Other solids vol%	Solvents and additives vol%
White	0	0,0	40,1	59,9
	5	2,1	39,3	58,6
	10	4,3	38,4	57,3
	20	9,1	36,5	54,4
	30	14,7	34,2	51,1
	40	21,1	31,7	47,2
Transparent	0	0,0	36,0	64,0
	10	3,9	34,7	61,4
	30	13,4	31,2	55,4

Table 7-1 Approximate paint formulations in vol.%.

7.2.4 Outdoor exposures

The panels with the S38 microspheres were exposed outdoors in Søborg, Denmark, for 10 months from June to April. During exposure the panels were facing south at a 45°angle.
The panels with iM30K and 110P8 microspheres were exposed outdoors in Miami, USA, for 10 months from November to September at the Atlas South Florida Test Service. There the panels were exposed to a difficult climate with intense sunlight, high temperature and high humidity. During exposure all panels were facing south at a 45°angle except for three panels which were facing north at 90°.
The paints were applied on 9x30x2cm Scots Pine (Pinus Sylvestris) sapwood panels in two layers and the ends of the panels sealed.
Chalking was evaluated according to ASTM D4214-2007 (Method A) and cracking was evaluated according to ASTM D661-93 2005. Gloss was measured according to ASTM D523-2008 using a BYK-Gardner Micro-TRI-Gloss glossmeter at an angle of 60° and color measurements were made with a X-Rite Color i7 spectrophotometer with a 6 inch integrating sphere according to ASTM E1331-2009. The CIE Lab color scale was used and the changes in color calculated according to ASTM D2244.

7.2.5 Water permeability test

The water permeability of paint films with coated Sphericel 110P8 microsphere concentrations of 0, 10, 20 and 30% of the solid volume was measured by the cup method according to ISO 7783:2008. 0,7mm thick pinewood veneer was used as a substrate for the paint films. The formulated paints were transparent (un-pigmented) to decrease the UV stability of the samples. This was done to shorten the exposure time needed to measure changes in the film properties as it is limited how long such a thin substrate can withstand the rapid temperature and relative humidity changes. Great care was taken to spread the film evenly on the veneer and the film thickness was controlled by

measuring the weight of the paint applied to a known area. The films were allowed to dry for 2 weeks at 23°C and 50%RH before being exposed to UV radiation in a QUV chamber for 0, 10, 20 and 30 days. After the exposure the paint films were kept in a climate chamber at 23°C and 50%RH for 4 days before testing began. Uncoated veneer samples were also measured to determine the permeability of the substrate. Three specimens were measured for each sample.
The cups used were made from standard 1 ¼" x 40mm PVC adapter unions with PVC plugs which were sealed with glue. The cups were filled with de-ionized water up to a rim 1,7cm from the paint film. 5cm diameter samples were cut from the veneer and placed in the cups with the painted side inside the cup. The exposed area of the samples was 3,2cm in diameter. The cups were kept in a climate chamber at 23°C and 50%RH and weighed twice per week to keep track of water evaporation. The cups were placed downwards on a wire mesh with the water in contact with the paint films to measure the liquid water permeability.

7.3 Results and discussion

7.3.1 TiO_2 coating

The coated iM30K microspheres were characterized by SEM, EDS and XRD. Figure F5 shows the coating on the surface of a broken microsphere. The coating is approximately 150nm thick with large clusters randomly placed on the surface.

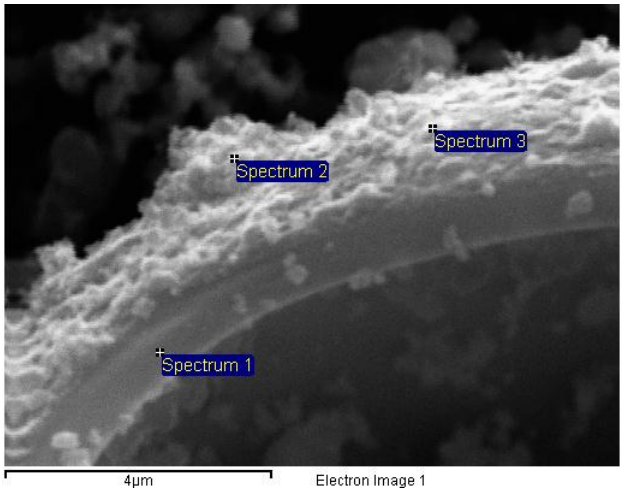

Fig. 7-4 Broken iM30K microsphere with TiO_2 coating on surface.

Spectrum	O w%	Na w%	Si w%	Ca w%	Ti w%
1	43.82	2.67	35.72	10.40	7.39
2	40.27	2.20	13.74	2.91	40.89
3	42.62	2.22	21.79	5.47	27.89

Table 7-2 EDS analysis of coated microsphere shown in Fig. 7-4

The results of the EDS analysis of the coating in Fig. 7-4 is shown in Table 7-2. Spectrum 1 as expected shows a high content of the elements found in borosilicate glass. Spectrum 2 and 3 show a high Ti and O content indicating an oxide of titanium on the microsphere surface. This was confirmed with an XRD analysis of the coated microspheres compared with uncoated spheres. The microspheres were found to be amorphous while the coated spheres were crystalline. The spectra can be seen in Fig. 7-5 where the peak positions of anatase are represented by vertical broken lines. The peaks match an anatase TiO_2 structure and a Rietveld refinement of the spectrum indicated a crystal size of 14nm.

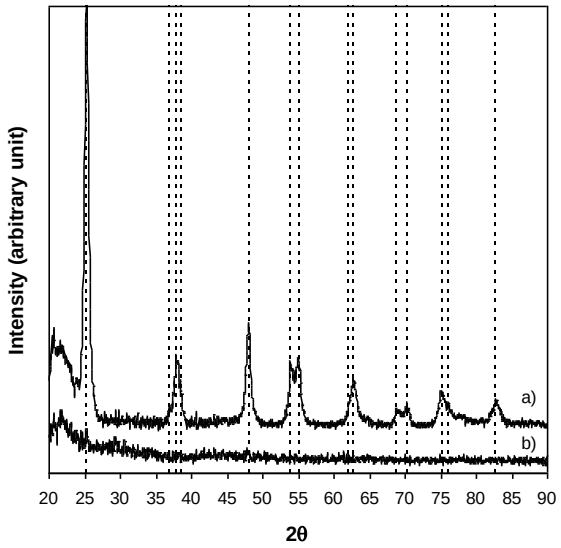

Fig. 7-5 XRD spectrum of a) coated iM30K microspheres and b) uncoated iM30K microspheres. The broken lines represent anatase TiO_2 peak positions.

7.3.2 Outdoor exposure of films with S38 microspheres

The paints tested were the standard with and without UV absorbers, standard with 30% coated S38 microspheres both with and without UV absorbers and the standard with 30% uncoated S38 microspheres and with UV absorbers. Fig. 7-6 shows the films after 10 months of exposure which started in June and ended in April.

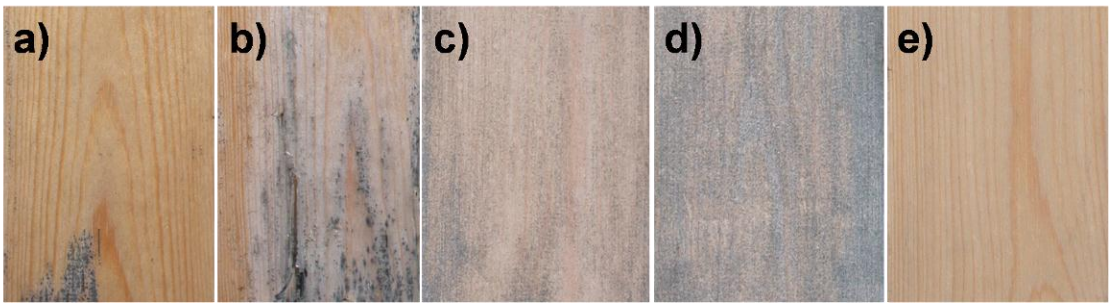

Fig. 7-6 Transparent paint films after 10 months of exposure in Denmark. a) Standard with 0% microspheres, b) standard with 0% microspheres and no UV absorber, c) with 30% coated S38 microspheres, d) with 30% coated S38 microspheres and no UV absorber e) with 30% uncoated S38 microspheres.

The films with uncoated microspheres, Fig. 7-6 e), were free of cracks and micro-organisms and were therefore found to be the most durable. The standard sample with UV absorbers, Fig. 7-6 a), had areas with cracks and areas where micro-organisms had gained a foothold whereas the standard without UV absorbers, Fig. 7-6 b), had large cracks and large areas where the film had lost adhesion and was flaking off. The films with coated microspheres and UV absorbers, Fig. 7-6 c) did not have any visible cracks but the entire panel was covered with micro-organism. The films with coated microspheres and without UV absorbers, Fig. 7-6 d) had areas with small cracks and the entire surface was densely covered with micro-organisms. The UV absorbers clearly have a strong influence on the durability of the film as can be seen by comparing Fig. 7-6 a) to Fig. 7-6 b) and Fig. 7-6 c) to Fig. 7-6 d). Furthermore the microspheres were found to improve the cracking resistance of the films which will be discussed in further detail below. More surprisingly though the photocatalytic paint films had the lowest resistance to micro-organisms. An investigation of the film surface revealed that the micro-organisms tend to grow very close to large microspheres or microsphere clusters as shown in Fig. 7-7 and Fig. 7-8. The S38 microspheres have an average size of 40µm and an effective top size of 85µm which is very large compared to the paint film thickness which is approximately 50-60µm. This means that the largest microspheres can be in contact with the substrate and still be exposed in the surface. The gap that forms around the spheres due to photocatalytic activity can result in high water permeability and seems to promote favourable conditions for micro-organisms. It is therefore necessary to use a smaller particle size to ensure lower permeability of the paint film.

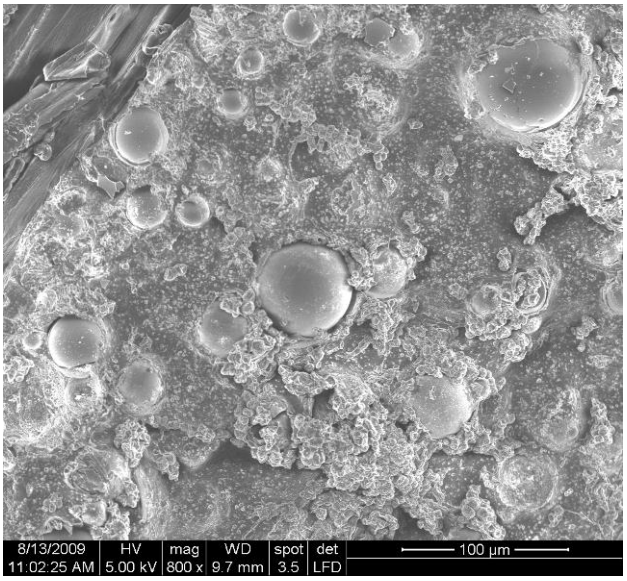

Fig. 7-7 Paint film with micro-organisms growing around coated S38 microspheres.

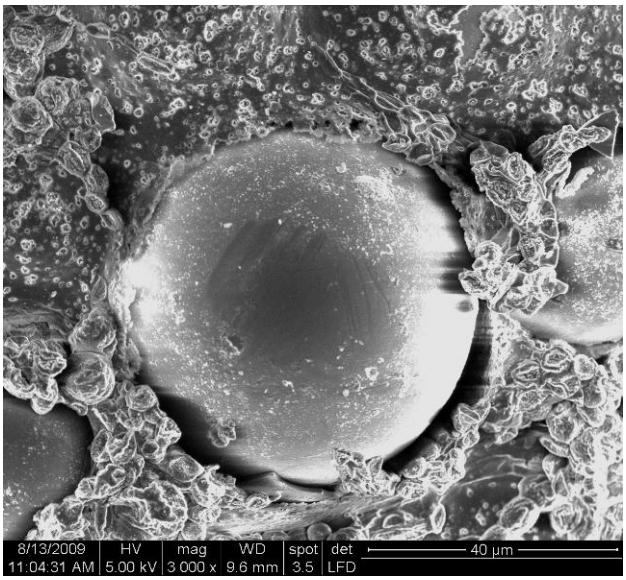

Fig. 7-8 Coated S38 microsphere in paint film surface with micro-organisms surrounding it.

7.3.3 Outdoor exposure of films with iM30K and 110P8 microspheres

After observing the rapid failure of the paint films formulated with coated S38 microspheres new formulations were made with iM30K and 110P8 microspheres. All the transparent films contained UV absorbers. Both transparent and opaque paints were prepared and applied on panels, see Table 7-1, which were exposed in Florida, USA, for 10 months. Due to the aggressive conditions present there 10 months can be considered as significantly "longer" exposure than 10 months exposure in the Danish climate.

				Dry film microsphere volume					
	HGMS	Surface	Color	0%	5%	10%	20%	30%	40%
Primer	iM30K	Coated	White	x		x		x	
		Coated	Transparent	x		x		x	
No primer	iM30K	Coated	White	x	x	2x	x	2x	x
		Coated	Transparent	x		x		x	
		Uncoated	White	x	x	x	x	x	x
	110P8	Uncoated	White	x		x		x	
		Uncoated	Transparent	x		x		x	

Table 7-3 Paint systems tested in outdoor exposure.

Fig. 7-9 illustrates some of the transparent paint samples after 1, 5, 7, 9 and 10 months of exposure. Formulating the paints with smaller microspheres clearly improved the performance of the films with coated microspheres. Comparing the panels after 10 months of exposure it can be seen that the film with 30% coated microspheres, Fig. 7-9 c), has nearly no growth on the surface and the film with 10% coated microspheres, Fig. 7-9 b), has very little. The films with 10% and 30% uncoated microspheres, Fig. 7-9 d) and e) respectively, have more growth and the standard, Fig. 7-9 a), by far the most. The degree of cracking of the paint films was evaluated every month and the results can be seen in Table 7-4. No cracking was detected the first five months. Very little growth was

detected on the standard panels until after 9 months of exposure where they are totally covered. This coincides with cracks first being detected on the same panels after 9 months of exposure which suggests that once the film begins to develop cracks micro-organisms are able to reach the wood substrate. Furthermore the micro-organisms seem to be more concentrated on the light coloured areas of the wood which are made up of earlywood whereas the dark areas are latewood. Earlywood is the wood created in the early part of a trees growth cycle where the growth is fast compared to the later period and the wood therefore less dense. Earlywood expands far more due to moisture changes than latewood which means the paint film covering those areas is exposed to higher strains. Cracks therefore tend to form on earlywood or at the earlywood/latewood interface. The connection between crack development and micro-organisms for the microsphere containing films is however not as evident. The self-cleaning films begin to crack earlier but are nowhere near as much affected by micro-organisms which suggests that the photocatalyst is effective in combating them. The same can be said about the films containing uncoated microspheres which are not affected to the same degree as the standard samples although far more than the self-cleaning films. The reason for this has been found to be due to differences in the way cracks propagate in the material which will be discussed in further detail in section on water permeability.
Despite the seemingly good durability of the self-cleaning films the colour change of the films is unacceptable as seen in Fig. 7-9. Both films have gotten a bluish colour most likely due to a light scattering effect related to the microspheres and surface roughness. It may therefore be impractical to use coated microspheres in a transparent system

Paint system	Months of exposure				
	6	**7**	**8**	**9**	**10**
Standard	10	10	10	A7	A6
Standard	10	10	10	A8	A6
Standard w/primer	10	10	10	A7	A6
iM30K(C)10%	10	10	A7	A6	A6
iM30K(C)10% w/primer	10	10	A6	A6	A6
iM30K(C)30%	10	10	A7	A6	A6
iM30K(C)30% w/primer	A7	A7	A6	A6	A6
110P8(U)10%	10	10	10	A8	A7
110P8(U)30%	10	10	10	10	A9

Table 7-4 Evaluation of degree of cracking of transparent paint films. The films are evaluated on a scale from 0-10 where 10 = None, 8 = trace, 6 = slight and the capital letter represents the crack shape, A = long line. (C) indicates coated microspheres and (U) uncoated.

Fig. 7-9 Transparent paint films after 1, 5, 7, 9 and 10 months (left to right) of exposure in Miami, USA. a) Standard with 0% microspheres and primer, b) with 10% coated iM30K microspheres and primer, c) with 30% coated iM30K microspheres and primer, d) with 10% uncoated 110P8 microspheres and e) with 30% uncoated 110P8 microspheres. The top part of the 1 month images shows an unexposed area.

Fig. 7-10 shows the gloss development of the transparent films during exposure. The initial gloss level of films containing microspheres is much lower than the standard films due to the spheres increasing the surface roughness. The gloss reduction due to the iM30K microspheres is larger than

due to the 110P8 type because of a larger particle size. Furthermore films with coated microspheres lose a larger percentage of gloss as a result of surface roughening than any of the other films. It therefore seems that high gloss is unattainable using microspheres.

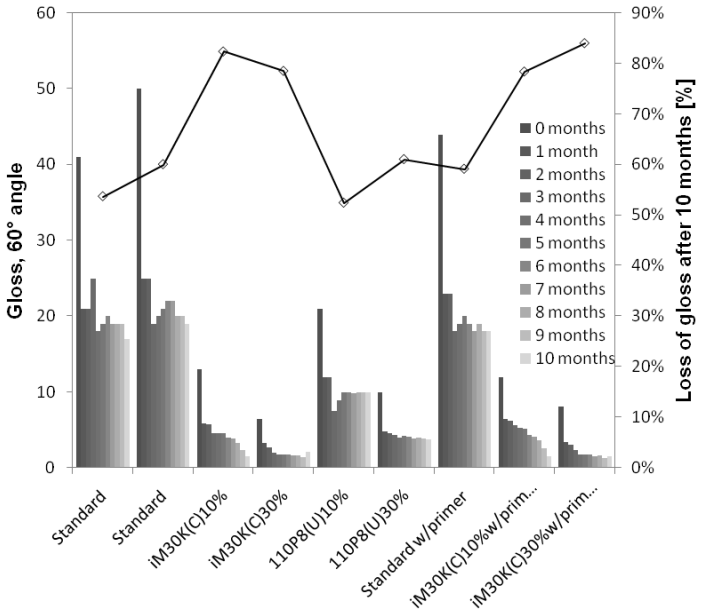

Fig. 7-10 Gloss change (60°angle) of transparent paints. The line shows the loss of gloss in percentage after 10 months of exposure. (C) indicates coated microspheres and (U) uncoated.

Fig. 7-11 shows some of the opaque paint films after 1, 5, 7, 9 and 10 months of exposure. The films are clearly more durable than the transparent films which can be attributed to added UV stability due to pigmentation. Very few signs of micro-organisms can be found. After 10 months of exposure cracking was only detected on three panels. The standard film shown in Fig. 7-11 a) had a rating of A9 on a scale from 0-10 where 9 represent only a trace and the letter A represent a crack shape described as a long line. A film with 30% uncoated 110P8 microspheres also had a rating of A9 and a film with 40% coated iM30K microspheres had a rating of A8. Furthermore chalking, a rating of 9 on a 0-10 scale, was only detected on three panels. Two of them with 30% coated iM30K microspheres and one with 30% uncoated 110P8.

Fig. 7-12 shows the gloss development of the standard films compared to the films with coated microspheres and Fig. 7-13 the films with uncoated microspheres and the ones facing north during exposure. As seen with the transparent films the initial gloss of films containing microspheres is a lot lower than the standard samples. The gloss of the 5% samples is roughly half of the standard film and it is further reduced as the concentration increases. Interestingly the gloss reduction of the north facing panels is roughly the same as for the panels facing south. The films with uncoated microspheres have somewhat better gloss retention than the films with coated ones. The color change, in terms of ΔE according to the CIE Lab standard, of the same samples during exposure is shown in Fig. 7-14 and Fig. 7-15. During the first 8 months of exposure the differences in color development are small. The change is in ΔE is mostly from a reduction of the L value, or darkening of the film, and reduction of the b value, or more blue. After 9 and 10 months however the films with a high concentration of coated microspheres show a large increase in ΔE which can be traced to a reduction of the L value. This is neither observed for the standard films nor the films with uncoated microspheres. This change is believed to be explained by the first layer of microspheres beginning to separate from the surface resulting in the film losing hiding power. This can be seen in

Fig. 7-11 e) where the structure of the wood substrate has become more visible after 10 months of exposure.

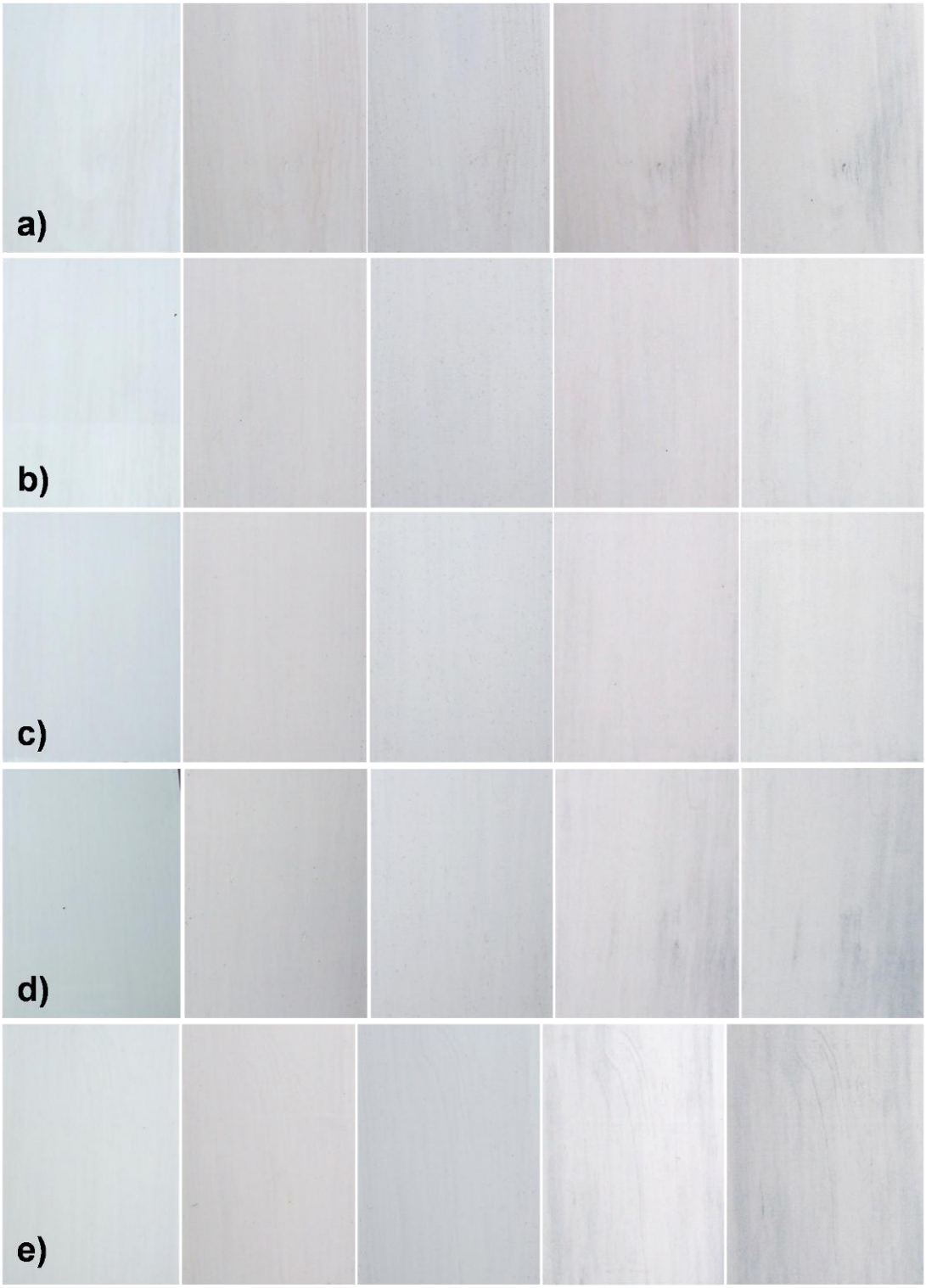

Fig. 7-11 Opaque paint films after 1, 5, 7, 9 and 10 months (left to right) of exposure in Miami, USA. a) Standard with 0% microspheres, b) with 5% coated iM30K microspheres, c) with 10% coated iM30K microspheres, d) with 20% coated iM30K microspheres and e) with 30% coated iM30K microspheres.

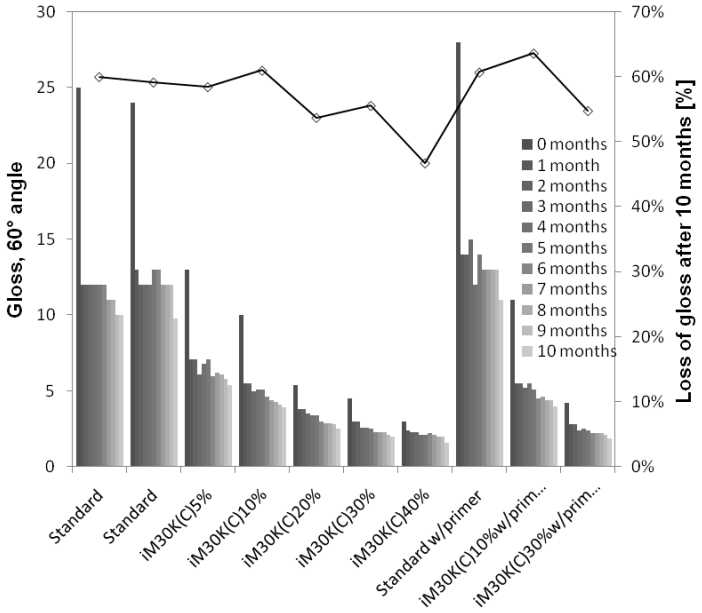

Fig. 7-12 Gloss change (60°angle) of opaque paints with coated microspheres (C). The line shows the loss of gloss in percentage after 10 months of exposure.

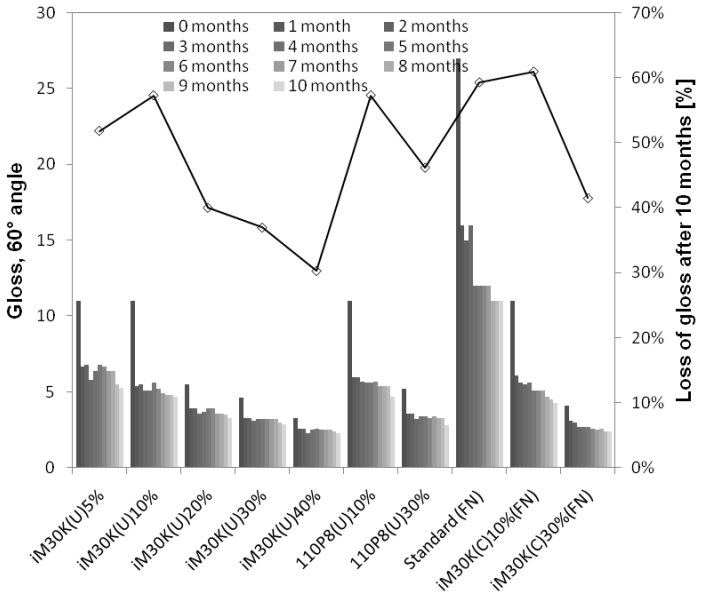

Fig. 7-13 Gloss change (60°angle) of opaque paints with uncoated microspheres (U) and opaque paints with coated microspheres (C) facing north (FN) during exposure. The line shows the loss of gloss in percentage after 10 months of exposure.

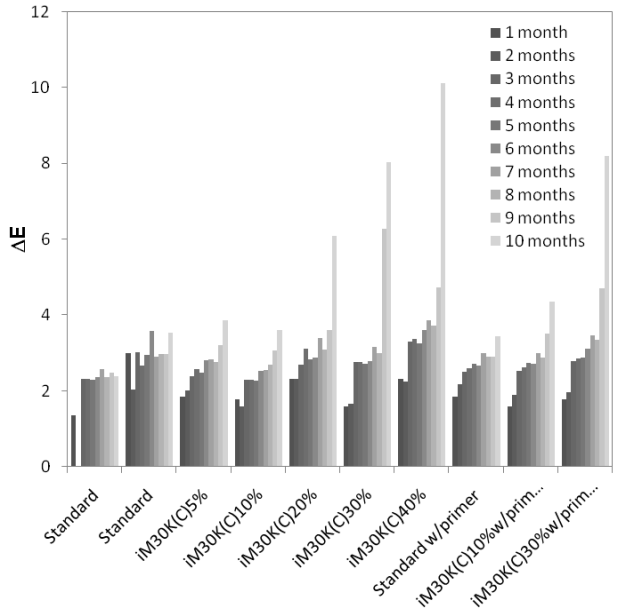

Fig. 7-14 Color change of opaque paints with coated microspheres (C).

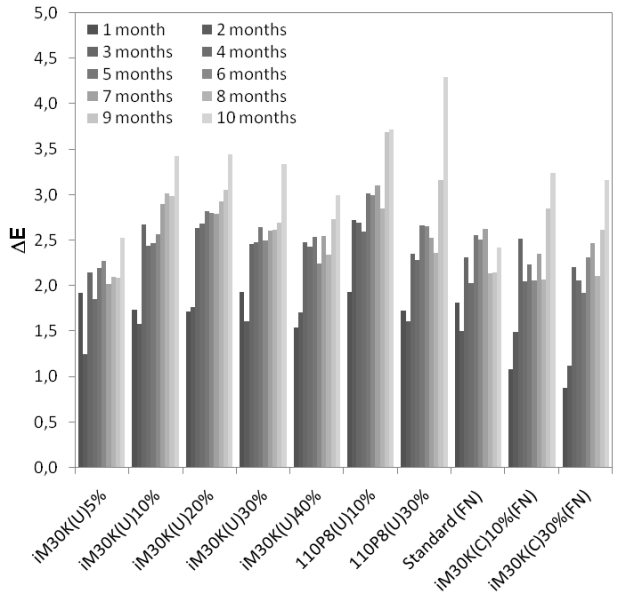

Fig. 7-15 Color change of opaque paints with uncoated microspheres (U) and opaque paints with coated microspheres (C) facing north (FN) during exposure.

7.3.4 Water permeability

The cup test measures the steady state permeability of a paint film. The driving force for the permeation is the difference in partial pressure on both sides of the film and the barrier consists of different resistances such as the coating, substrate and external air gap. If the cup is kept in a climate chamber there is no resistance due to an external air gap [10].
The water transmission rate of the coating, V_c, can be described by the equation

$$V_c = \frac{G_{cs} \cdot G_s}{(G_s - G_{cs}) \cdot A}$$

Equation 7-1

where A is the area of permeation, G_s is the mass change per time measured for the substrate and G_{cs} is the mass change per time for a coated substrate. The permeability coefficient, δ, is then calculated with the equation

$$\delta = \frac{V_c \cdot d}{\Delta p}$$

Equation 7-2

where d is the coating thickness and Δp is the vapour pressure difference between the inside and outside of the cup. The Δp was calculated to be 1320Pa.
The liquid water permeability coefficients are shown in Fig. 7-16. It was not unexpected to initially measure lower permeability coefficients for the films with microspheres as the effective diffusion length for water molecules is longer with a higher concentration of impermeable particles. It was however originally believed that the permeability of the filled films would quickly become higher than for the 0% film because of degradation caused by the photocatalyst. The fact that these films maintain lower permeability coefficients after all stages of UV exposure however indicates good UV stability of the films. What is most interesting though is the sudden increase in permeability of the 0% films after 30 days of QUV exposure. A SEM analysis of the films revealed that after 30 days large cracks had formed in the 0% films while the microsphere films had small superficial cracks covering a large part of the surface as seen in Fig. 7-17. Some of the cracks in the 0% film reached all the way down to the substrate revealing the wood fibers as seen in Fig. 7-17 c). Once cracks are initiated in the 0% films they can propagate relatively unhindered and therefore become long and deep. This allows micro-organism to gain a foothold which will lead to the wood rotting and ultimately disbondment of the paint film. In the 30% films on the other hand crack propagation is different due to crack front pinning [11][12][13][14]. Crack front pinning occurs when a propagating crack hits a rigid particle and can not continue to grow in the same direction. The crack must therefore bow out past the particle effectively lengthening the crack and thereby increasing the crack surface which requires more energy. This mechanism results in numerous small and, judging from the relatively small increase in permeability, superficial cracks being formed rather than a few large ones. The mechanical energy from stresses in the film is released over a much larger area so the film retains more of its protective properties and doesn't expose the substrate. This is in good agreement with the observations made on the panels shown in Fig. 7-9 where the 0% films were covered with micro-organisms shortly after cracks developed in the films which was not the case for the self-cleaning films.

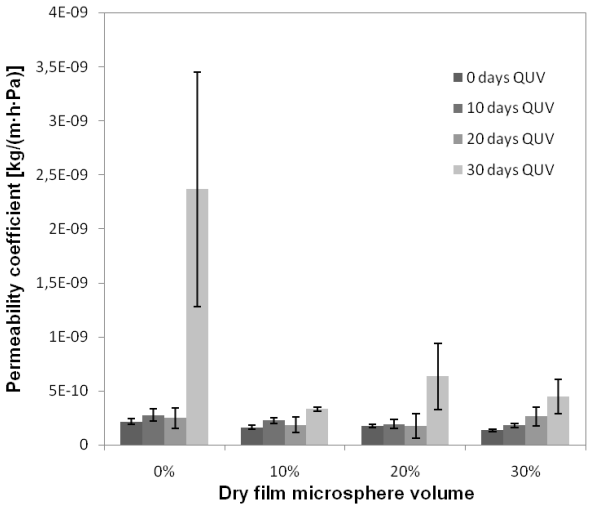

Fig. 7-16 Liquid water permeability coefficients of paint films with different concentrations of coated microspheres after different QUV exposure times. The error bars show the standard deviation.

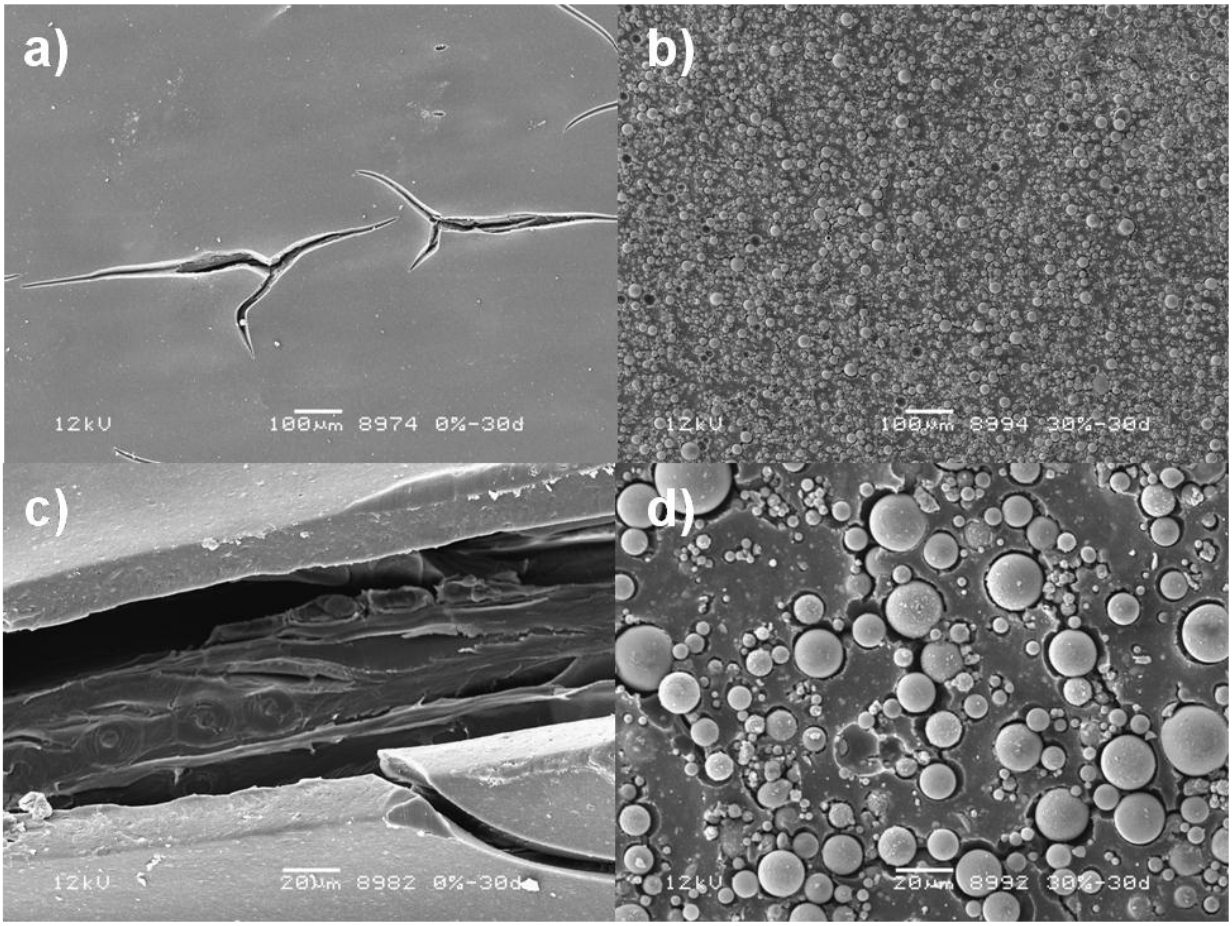

Fig. 7-17 Illustrates the surface of transparent alkyd films painted on veneer after 30 days of exposure in QUV, a) and c) 0% film with large cracks in surface, b) and d) film with 30% 110P8 microspheres with small cracks over entire surface. Both films are shown with the same magnification.

7.4 Conclusion

It has been shown that photocatalytic self-cleaning organic paints where the photocatalyst is introduced as a coating on hollow glass microspheres are durable and effective in keeping micro-organisms from immobilising on the surface. This is due to the photocatalytic properties of anatase coated microspheres which further contribute to the durability of the film by decreasing water permeability. The water permeability is lower because of the barrier effect of the microspheres and the films were also found to better maintain low permeability due to a different mechanism controlling crack propagation in the binder. The gloss and colour retention of the self-cleaning paint films were however found to be inferior to films without microspheres.

Acknowledgements

The authors would like to express their gratitude to the evaluations team at the Atlas South Florida Test Service and to Nina Axelsen and Bent Samuelsen of Dyrup A/S. Furthermore we thank Dyrup A/S and the Danish Agency for Science and Innovation for financial support.

References

[1] A. Mills, A. Lepre, N. Elliott, S. Bhopal, I. P. Parkin, and S. A. O'Neill, "Characterisation of the photocatalyst Pilkington Activ(TM): a reference film photocatalyst?," *Journal of Photochemistry and Photobiology A: Chemistry*, vol. 160, no. 3, pp. 213-224, Aug. 2003.

[2] I. P. Parkin and R. G. Palgrave, "Self-cleaning coatings," *Journal of Materials Chemistry*, vol. 15, no. 17, p. 1689, 2005.

[3] N. S. Allen, M. Edge, G. Sandoval, J. Verran, J. Stratton, and J. Maltby, "Photocatalytic Coatings for Environmental Applications¶†," *Photochemistry and Photobiology*, vol. 81, no. 2, pp. 279-290, Mar. 2005.

[4] A. E. Jacobsen, "Titanium Dioxide Pigments: Correlation between Photochemical Reactivity and Chalking.," *Industrial & Engineering Chemistry*, vol. 41, no. 3, pp. 523-526, Mar. 1949.

[5] G. KAEMPF, PAPENROT.W, and R. HOLM, "DEGRADATION PROCESSES IN TIO2-PIGMENTED PAINT FILMS ON EXPOSURE TO WEATHERING," *JOURNAL OF PAINT TECHNOLOGY*, vol. 46, no. 598, pp. 56-63, 1974.

[6] U. Gesenhues, "Al-doped TiO2 pigments: influence of doping on the photocatalytic degradation of alkyd resins," *Journal of Photochemistry and Photobiology A: Chemistry*, vol. 139, no. 2-3, pp. 243-251, Mar. 2001.

[7] P. A. Christensen, A. Dilks, T. A. Egerton, E. J. Lawson, and J. Temperley, "Photocatalytic oxidation of alkyd paint films measured by FTIR analysis of UV generated carbon dioxide," *Journal of Materials Science*, vol. 37, no. 22, pp. 4901-4909, 2002.

[8] W. G. Wamer, J.-J. Yin, and R. R. Wei, "Oxidative Damage to Nucleic Acids Photosensitized by Titanium Dioxide," *Free Radical Biology and Medicine*, vol. 23, no. 6, pp. 851-858, 1997.

[9] W. A. Pryor, "Oxy-Radicals and Related Species: Their Formation, Lifetimes, and Reactions," *Annual Review of Physiology*, vol. 48, no. 1, pp. 657-667, Oct. 1986.

[10] Charles M. Hansen, "Potential Errors in Water/Water Vapor Permeation Measurements Using the Cup Method," *Färg och Lack*, vol. 39, no. 3, pp. 57-60, 1993.

[11] A. G. Evans, "The strength of brittle materials containing second phase dispersions," *Philosophical Magazine*, vol. 26, pp. 1327-1344, Dec. 1972.

[12] F. F. Lange and K. C. Radford, "Fracture energy of an epoxy composite system," *Journal of Materials Science*, vol. 6, pp. 1197-1203, Sep. 1971.

[13] D. J. Green, P. S. Nicholson, and J. D. Embury, “Fracture of a brittle particulate composite,” *Journal of Materials Science*, vol. 14, pp. 1413-1420, Jun. 1979.
[14] D. J. Green, P. S. Nicholson, and J. D. Embury, “Fracture of a brittle particulate composite,” *Journal of Materials Science*, vol. 14, pp. 1657-1661, Jul. 1979.

8 Conclusion

It has been demonstrated that TiO_2 coated microspheres give organic paint films self-cleaning properties without causing severe degradation of the binder. The coated microspheres improve the durability of the paint films both in accelerated weathering test and during outdoor exposure. The self-cleaning films are found to increase the films resistance to micro-organisms due to the photocatalytic activity and through improved crack resistance and lower water permeability.

Heat treating the microspheres before coating them was found to drastically improve the adhesion of the coating to the glass. It was concluded that this was due to physically adsorbed water occupying the main adsorption sites for the titanium precursor. Removing the adsorbed water allows the precursor to react with hydroxyl groups on the glass surface and form a covalent bond with the surface. Furthermore it was found that during the crystallisation of the coating the calcining temperature should be as close to the temperature tolerance of the microspheres as possible to optimise the photocatalytic activity.

The photocatalytic activity of the paint films was found to be highly dependent on the concentration of microspheres in the surface. Pigmented films containing coated microspheres exhibited excellent UV stability which caused the surface concentration to remain relatively low compared to the volume concentration for the entire duration of the QUV testing period. The surface concentration in transparent films on the other hand quickly becomes high due to their lower UV stability. Coated microspheres are however not found to be suitable for use in transparent paint systems due to negative effects on film colour after extended periods of exposure. Uncoated microspheres are however found to impart better properties mainly due to the improved cracking resistance of the films and are therefore suggested as a substitute in transparent films.

The particle size of the microspheres is one of the key properties when designing the paint system and the optimal size is in the range of 5-20µm. If the spheres are too large the permeability of the film will be too high and if the particles are too small they may separate from the film prematurely. Small particles however have the advantage of giving better surface coverage relative to volume concentration as compared to large particles.

The effect of the microspheres on the viscosity profiles of both solvent borne and water borne paint systems is found to be minimal and it should therefore be possible to adjust the viscosity to that of the standard by minor adjustments of the formulations.

The mechanical properties of films containing microspheres are found to generally become poorer with increased concentrations of spheres. At high concentrations the films become less elastic, the elongation to break is less, stress relaxation becomes slower and the creep recovery is significantly poorer. Nevertheless the mechanical performance of the films during exposure is improved due to a different mechanism for crack propagation in the film.

The microspheres are found to reduce the gloss of paint films which makes incorporation into high gloss systems difficult or altogether impossible.

9 Future work

One of the major challenges in advancing the project is the limited availability of hollow glass microspheres coated with TiO_2. Currently there is no known industrial scale production of such particles. In order to commercialise the project it is therefore necessary to develop an economical industrial process preferably through collaboration with an industrial partner specialised in TiO_2 deposition. The most promising process for production is believed to be deposition by controlled hydrolysis of titanium oxychloride or titanium oxysulfate in aqueous solution followed by spray drying to avoid agglomeration.
The anti-microbial properties of the self-cleaning coating have not been fully studied and although the films seem effective in battling micro-organisms the contribution of the photocatalytic effect versus the improved barrier properties is not fully understood yet.
Hollow glass microspheres are a relatively expensive raw material for paint intended for wood protection. Coating the microspheres with TiO_2 further increases the price and considering the large concentration needed for adequate surface coverage the coated microspheres may be too costly to achieve commercial success. Coating the TiO_2 on a cheaper substrate such as mica, as previously suggested, may therefore increase the likelihood of success. Not only is mica a much cheaper material but less volume is needed for high surface coverage due to the plate like particle shape. Pearlescent pigments are not suitable due to their colour but they can however be made colour neutral by a slight modification of the TiO_2 coating. Initial investigations of the use of such particles showed promising results but further study is needed to confirm that a film comprising TiO_2 coated mica is sufficiently UV stable. This would include a more thorough study of the degradation of the binder during UV exposure and an investigation of how much exposure the films can withstand before the particles begin to separate from the film. A more detailed study of the self-cleaning efficiency is also necessary to determine whether the film is sufficiently self-cleaning and whether it can prevent micro-organisms from immobilising on the surface.

10 Patent application

SELF-CLEANING COATING COMPOSITION
EP patent application nr. 08 17 1810.8

Technical field of the invention
The current invention relates to compositions with self-cleaning properties. More particularly, the invention concerns coatings or paints comprising particles coated with a catalytically active composition.

Background of the invention
There is a need in the art for compositions related to coatings or paints providing self-cleaning properties. Such properties can e.g. be mediated by electromagnetic radiation, such as sunlight, for example by the use of heterogeneous photocatalysis, a process in which a solid catalyst semiconductor both absorbs light and acts as a catalyst. Such a process can e.g. be utilized to oxidize organic compounds and has been used for applications such as cleaning water. It is believed that when a photocatalytic semiconductor is exposed to light with sufficiently short wavelength (i.e. sufficiently high energy) to promote an electron from the valence band to the conduction band of the photocatalyst, which depends on the band gap of the photocatalyst, a positive "hole" is created. The electron and the positive hole can diffuse to the surface where the electron generally reduces oxygen and the hole oxidizes adsorbed molecules for example water or some organic material. If an absorbed water molecule is oxidized an OH radical, which has an extremely high oxidation potential, is formed and can then further oxidize an organic molecule.

This effect is well known and has been utilized in self cleaning products such as Pilkington Activ™ window glass and in some types of paints, such as silicone paints. Silicone binders are believed to be resistant to the photocatalytic effect because a protective layer of SiO_2 is formed when the binder is oxidized, but they are relatively expensive compared to other organic binders. Silicone based paints appear only suitable for a limited range of applications. For wood these paints will be too open for water vapor transmission and in many instances not flexible enough which may result in cracking and flaking.

Commonly, an organic binder will not form a protective layer when oxidized and therefore organic binders are not as resistant. Environmental effects and/or weathering will cause the film to decompose making the film chalk, i.e. pigment particles loose adhesion to the film due to binder decomposition. Therefore photocatalytic activity in paint comprising organic binders is considered undesirable, so photocatalytic pigments such as TiO_2 are generally coated with other oxides such as Al_2O_3 and/or SiO_2 to reduce the photocatalytic activity of TiO_2 in order to reduce chalking of the paint film.

The chalking effect is used in some cases to make paint films self cleaning. That means that the chalking rate of the paint film is controlled by adding nano-sized photocatalytic particles into the film so the surface will constantly renew itself because the film constantly erodes. However, this solution does not provide a durable film and also introduces another potentially more serious problem, namely a high release of photocatalytic nano-particles to the environment. The photo-toxicological effect of highly photocatalytic material is believed to be very dangerous, especially if photocatalytic particles come into contact with e.g. the skin. If photocatalytic particles are in contact with skin and exposed to sunlight, or any UV-radiation source for that matter, the extremely

powerful oxidation process will attack skin cells. This can be especially dangerous if the size of the photocatalytic particles is in the nano range because they can easily diffuse through the top skin layers and reach healthy living cells. Photocatalytic nano-particles are believed to be a possible carcinogenic. Therefore it is necessary to develop a technology where photocatalytic material is used to give organic coatings self cleaning properties without causing the film to chalk too fast and release nano-sized particles to the environment.

It is an objective of the present invention, to provide a self-cleaning paint which addresses one or more of the above-mentioned issues.

US 6 110 528 concerns a method for the preparation of fine hollow glass spheres coated with TiO_2.
US 5 616 532 concerns a photocatalyst composition containing a substantially non-oxidizable binder.
WO2004/060555 pertains to a photocatalytically-active, self-cleaning coating compositions and methods.
Srinivasan et al. (1994) relates to the interaction of titanium isopropoxide with surface hydroxyls on silica.
Linsebigler et al. (1995) relates to the principles and mechanisms of photocatalysis on TiO_2 surfaces.
Lachheb et al. (2002) relates to photocatalytic degradation of various types of dyes including methylene blue.
Portjanskaja et al. (2004) relates to photocatalytic oxidation of humic substances with TiO_2-coated glass micro-spheres.

Summary of the invention
In a first aspect, the invention relates to a self-cleaning coating composition and/or self cleaning paint comprising micro-sized particles coated with a functional layer, wherein the micro-sized particles are hollow or solid beads, or any combination/ratio of hollow and solid beads, wherein the beads comprise one or more material(s) selected from ceramic material(s); polymeric material(s); cermet material(s); metallic material(s); pigmented material(s); light-absorbing and/or light reflecting material(s); including any combination thereof.

A second aspect of the invention concerns a self-cleaning surface comprising a dried layer (paint film) derived from a self-cleaning paint, such as a paint comprising micro-sized particles coated with a functional layer, wherein the micro-sized particles are hollow or solid beads, or any combination/ratio of hollow and solid beads, wherein the beads comprise one or more material(s) selected from ceramic material(s); polymeric material(s); cermet material(s); metallic material(s); pigmented material(s); light-absorbing and/or light reflecting material(s); including any combination thereof.

A third aspect of the invention pertains to a method of cleaning a surface according to claim, comprising the step of exposing said self-cleaning surface to electromagnetic radiation, wherein said electromagnetic radiation comprises radiation with a wavelength in the range of 200-400 nm and/or 400-800 nm, wherein said radiation is provided by the sun (e.g. daylight, reflected sunlight, twilight, moonlight), or by an artificial source.

A fourth aspect of the invention relates to a use of a self-cleaning coating composition (paint) for providing a self-cleaning surface on wood, brick, concrete, cement, asphalt, natural or artificial

stone, clay, glass, plastic, metal, fiber glass, carbon fibers, (wall) paper, painted surface, glued surface, composite material, or any combination thereof, such as a surface on an item, wall, building, structural element, bridge, building element, building block, window, door, floor, ceiling, roof (sheathing), smoothed and/or plastered surface, furniture, house hold equipment, medical equipment, sanitary equipment, car, (motor)bike, truck, container, bus, aircraft, rocket, ship, train, locomotive, wind mill, or solar panel.

A fifth aspect of the invention concerns one or more micro-sized particles coated with a functional layer, wherein the micro-sized particles are hollow or solid beads, or any combination/ratio of hollow and solid beads, wherein the beads comprise one or more material(s) selected from ceramic material(s); polymeric material(s); cermet material(s); metallic material(s); pigmented material(s); light-absorbing and/or light reflecting material(s); including any combination thereof.

A sixth aspect of the invention relates to a method for providing one or more micro-sized particles coated with a functional layer, wherein the micro-sized particles are hollow or solid beads, or any combination/ratio of hollow and solid beads, wherein the beads comprise one or more material(s) selected from ceramic material(s); polymeric material(s); cermet material(s); metallic material(s); pigmented material(s); light-absorbing and/or light reflecting material(s); including any combination thereof.

Brief description of the drawings

Figure 1. Schematic representation of a cross section of a surface painted/coated with a paint comprising beads coated with photocatalytic material. (A) Shortly after application to surface; (B) after considerable wear and/or weathering; (C) after severe wear and/or weathering.
(1) Environment; (4) Interface between paint film and substrate; (5) Substrate; (10) Predominantly binder; (12) Paint film surface; (20) Active coated bead; (21) Inactive coated bead; (25) Active photocatalytic material; (26) Inactive photocatalytic material.
Figure 2. Schematic representation of the reaction when a titanium precursor reacts with a glass surface and a covalent bond between the glass and titanium is formed.
Figure 3.SEM images of hollow glass microspheres (HGMS) uncoated and coated with anatase TiO_2.
Figure 4. XRD analysis of commercially available anatase powder and glass bead coating.
Figure 5. Concentration change vs. irradiation time plot showing the decomposition of a methylene blue solution with and without TiO_2-coated HGMS.
Figure 6. SEM images of alkyd paint films comprising TiO_2-coated HGMS after different exposure times in a QUV chamber.
Figure 7. SEM images of alkyd paint films after different exposure times in a QUV chamber.
Figure 8. SEM images of polyurethane paint films comprising TiO_2-coated HGMS after different exposure times in a QUV chamber.
Figure 9. SEM images of polyurethane paint films after different exposure times in a QUV chamber.
Figure 10. SEM images of polyurethane paint films comprising anatase TiO_2 nano-particles after different exposure times in a QUV chamber.
Figure 11. Results of a self cleaning test made with an alkyd paint film comprising TiO_2-coated HGMS and an alkyd paint film comprising uncoated HGMS.
Figure 12. Irradiance vs. wavelength plot of UVA-340 lamps.

Definitions

In the context of the present invention, the following definitions may apply to the terms listed below, unless specified otherwise:

The terms “titanium dioxide”, “TiO_2” and/or “TiO2” are meant to comprise oxides of titanium, and can be used interchangeably. Titanium dioxide can also comprise different crystal forms known in the art, such as anatase, rutile, brookite, and the like, including any mixtures between one or more crystal forms. Alternatively, titanium dioxide can also be present in one or more amorphous forms (i.e. non-crystalline form), including any mixture between said one or more amorphous forms. Furthermore titanium dioxide can be present in any mixture between one or more amorphous forms, and one or more crystalline forms.

Unless specified otherwise, chemical compositions are either p.a. (*pro analysii*), in pure form (i.e. usually more than 99% or 99.9% (weight/weight or volume/volume (vol./vol.) purity), almost pure form (i.e. usually more than 90% or 95% (weight/weight or vol./vol.) purity), or in technically pure form, such as a purity, which is common, generally known and/or accepted in the art.

The terms “bead” or “particle” can be used interchangeably, and are meant to comprise a particle or piece of material/composition having virtually any three-dimensional shape, including spherical, near-spherical, rotational symmetrical, octahedral, prismatic. Bead(s) or particle(s) can also be of irregular shape, and/or of irregular cross section. The term “bead” can also be meant to comprise filler material that can be added to paint in volume concentration of e.g. 10% or more of the volume of solids of a dried paint film, without severely affecting the rheological properties of the paint.

The term “equivalent diameter” is meant to comprise the diameter of a bead, if it were a sphere with equal volume as said bead. Thus a bead, not of spherical shape, with a volume of $\pi/6$ μm^3 would have an equivalent diameter of 1 µm as a sphere of equal volume.

The term “layer” is meant to comprise a film or coating of any material on a surface, thus comprising paint, coating compositions etc., but also e.g. any material deposited or associated with a particle or bead, such as photocatalytic material coated onto a bead. It can also refer as to a paint film, which can be wet, in the process of drying, or dry or dried. The latter can also be referred to as “dried layer”.

The terms “material(s)” and “composition(s)” can be used interchangeably.

The terms “polymeric” and “polymeric material/composition” can be used interchangeably and are meant to comprise material/composition which is made up of repeating subunits of organic, inorganic and/or organo-metallic materials including any combination and/or mixture thereof.

The terms “ceramic” and “ceramic material/composition” can be used interchangeably and are meant to comprise inorganic non-metallic material(s) and/or compositions which comprise e.g. oxides, nitrides, borides, carbides, silicides and sulfides including any combination and/or mixture thereof. Ceramic materials can be non-crystalline (glass or glass-like), partially crystalline, or fully crystalline.

The terms “metallic” and “metallic material/composition” can be used interchangeably and are meant to comprise metal(s) or metalloid(s) according to the periodic system of elements including

alloys and intermetallics and any combination and/or mixture thereof. Metallic materials can be non-crystalline (glass), partially crystalline or fully crystalline.

The terms “cermet” and “cermet material/composition” can be used interchangeably and are meant to comprise composite material(s) comprising ceramic and metallic material as defined above. Cermet materials can be non-crystalline (glass), partially crystalline or fully crystalline.

The term “light absorbing material(s)/composition(s)” is meant to comprise material(s) and/or composition(s) that can absorb electromagnetic radiation, such as electromagnetic radiation in the range ~300-800 nm.

The term “light reflecting material(s)/composition(s)” is meant to comprise material(s) and/or compositions that can reflect electromagnetic radiation, such as electromagnetic radiation in the range ~300-800 nm.

The terms “photocatalyst” and “photocatalytic material(s)/composition(s)” can be used interchangeably and are meant to comprise material(s)/ composition(s) that can accelerate the oxidation of organic material/composition, such as by creating electron-hole pairs when exposed to electromagnetic radiation

The terms “pigment” and “pigmented material(s)/composition(s)” can be used interchangeably and are meant to comprise material(s)/composition(s) with light absorption properties, comprising electromagnetic radiation with wavelengths in the range of visible light, such as ~380 -750nm, optionally altered by the addition of another material/materials such as one or more pigment(s).

The term hollow glass bead is meant to comprise beads comprising a glass shell and a void under the shell comprising essentially air, gas and/or vacuum.

The terms “self cleaning”, “self cleaning surface” and “self cleaning layer” can be used interchangeably and are meant to comprise surfaces/layers that through e.g. heterogeneous photocatalysis, hydrophilicity and/or hydrophobicity are resistant dirt and/or contamination, or can prevent, remove or disintegrate organic and/or inorganic dirt/undesired material and/or micro-organisms from adhering/contaminating the surface/layer.

The term “wetting” is meant to comprise a liquids capability to wet a solid surface, where high or good wetting is represented by a low contact angle between liquid and solid, and low or poor wetting represented by a high contact angle.

The term “abrasion resistance” is meant to comprise resistance to mechanical wear.

The term “weather resistance” is meant to comprise resistance to environmental factors, such as weather, sunlight, UV radiation, rain, moisture, temperature and wind.

The term “chalking” is meant to comprise a process, where the binder in the surface of a paint film is degraded, often as a result of weathering, causing pigment particles to become loose.

The term “co-catalyst” is meant to comprise a catalyst that can accelerate e.g. oxidation of organic material on the surface of a photocatalyst.

The term “band gap” is meant to comprise the energy difference between the bottom of the conduction band and the top of the valence band of a material/composition.

The term “BET surface area” is meant to comprise the measured surface area of particles according to the BET (Brunauer-Emmet-Teller) adsorption theory.

The term “crystal size” is meant to comprise the measured crystal size of material/composition/particle using e.g. the method of powder diffraction and calculated with the Debye-Scherrer formula and/or the Stokes and Wilson expression.

The term “index of refraction” is meant to comprise the index of refraction measured at the sodium D-line at approximately 589nm. When the term is used e.g. for hollow beads, it can be used to only refer to the shell material and not the air, gas and/or vacuum inside the hollow space.

The terms “nano-particle(s)” and “nano-sized particle(s)” can be used interchangeably and are meant to comprise particles that have a diameter and/or equivalent diameter around or below 1 µm, often in the range of around 1 -1000nm.

The terms “micro-particle(s)” and “micro-sized particle(s)” can be used interchangeably and are meant to comprise particles that have a diameter and/or equivalent diameter around or below 1 mm, often in the range of around 1 -1000µm.

The terms “coating”, “coating composition”, “paint”, and/or “paint composition” can be used interchangeably, and are meant to comprise any fluid, liquid, gel, powder, liquefiable, or mastic composition - which after application to a substrate or surface in a layer of a certain thickness - is converted to an essentially solid, or semi-solid film. Commonly, paint is liquid and comprises one or more of:

- pigment,
- binder (also called resin),
- solvent (also called vehicle), and
- filler.

Optionally, paint can comprise one or more additives.

Pigment

Pigments are granular solids incorporated into the paint to contribute color and opacity. Furthermore they will for wood stains contribute to the UV-protection. Alternatively, some paints contain dyes instead of or in combination with pigments. Other paints contain no pigment at all. Pigments can be classified as either inorganic or organic pigments. Inorganic pigments include e.g. titanium dioxide, carbon black or red and yellow ironoxides. The group of organic pigments comprises synthesized and/or modified organic compounds with chromatic properties, e.g. phthalo blue, phtalo green and chinacridone. A pigment according to the invention may also comprise one or more pigments disclosed in Industrial Inorganic Pigments, 3rd, Completely Revised and Extended Edition, Gunter Buxbaum and Gerhard Pfaff (Editors),
ISBN: 978-3-527-30363-2 (2005); and/or Industrial Organic Pigments: Production, Properties, Applications, 3rd, Completely Revised Edition

Willy Herbst, Klaus Hunger, ISBN: 978-3-527-30576-6 (2004); both of which are herewith incorporated by reference.

Filler
The filler serves to thicken the film, support its structure and simply increase the volume of the paint and lower the cost. Fillers are usually comprised of cheap and inert materials, such as on or more of talc, calcium carbonate, kaolin, lime, baryte, clay, etc. Paints that will be subjected to abrasion may even contain fine quartz sand as filler. Not all paints include fillers. On the other hand some paints contain large proportions (more than 10, 20, 30, 40 or 50% (vol/vol) of filler.

Binder
The binder or resin can be described as the actual film forming component of paint. The binder imparts adhesion, binds the pigments together, and strongly influences such properties as gloss potential, exterior durability, flexibility, and toughness. Binders include synthetic or natural resins such as acrylics, polyurethanes, polyesters, melamine resins, epoxy, alkyds, modifications of these or oils.
Binders can be categorized according to drying, or curing mechanism used commonly for paints. Common principles are solvent evaporation, oxidative cross-linking, (catalyzed) polymerization, and coalescence. The term organic binder relates to organic polymeric material.

Solvent
A major purpose of the solvent (or vehicle) is to adjust the viscosity of the paint. It can also control flow and application properties, and affect the stability of the paint while in liquid state. Its main function is as the carrier for the non volatile components. Solvents are generally more or less volatile. Water is the main vehicle for water based paints. Organic solvent-based, also called oil-based paints can consist of one or more solvents, such as one or more of aliphatic solvent, aromatic solvent, alcohol, ketone, petroleum distillate, ester, and glycol ether, and the like. Optionally, paints can comprise a volatile low-molecular weight synthetic resins also serve as diluents.

Additives
A paint can comprise one or more miscellaneous additives, which are usually added in smaller amounts (e.g. less than 5%, 1%, 0.1%, or 0.01% (vol./vol.) and yet give a very significant effect on the product. Additives can comprise one or more of catalyst, thickener, stabilizer, emulsifier, texturizer, adhesion promoter, UV stabilizer, flattener (de-glossing agent), biocide to fight microbial and/or plant growth, agent to modify and/or control surface tension, agent to improve and/or control flow properties, agent to improve the finished appearance, agent to increase wet edge, agent to improve pigment stability, agent to impart anti-freeze properties, agent to control foaming, agent to control skinning, agent to catalyze drying.

Drying and curing
Drying and curing can be regarded as two different processes. Drying generally refers to evaporation of vehicle, whereas curing refers to polymerization of the binder. The result of the drying and/or curing of the paint can be a dried layer or paint film.
Depending on chemistry and composition of the paint, any particular paint may undergo either drying or curing or both processes. Thus, there are paints that dry only, those that dry then cure, and those that do not depend on drying for curing. Paints that dry by simple solvent evaporation usually contain a solid binder dissolved in a solvent; this forms a solid film when the solvent evaporates, and the film can re-dissolve in the solvent again. Classic nitrocellulose lacquers fall into this

category, as do non-grain raising stains composed of dyes dissolved in solvent. Latex paint is a water-based dispersion of sub-micrometer (μm) polymer particles. The term "latex" in the context of paint simply means an aqueous dispersion; latex rubber (the sap of the rubber tree that has historically been called latex) is usually not a paint ingredient. These aqueous dispersions are prepared by emulsion polymerization. Latex paints cure by a process called coalescence where first the water, and then the trace, or coalescing, solvent, evaporate and draw together and soften the latex binder particles together and fuse them together into irreversibly bound networked structures, so that the paint will not re-dissolve in the solvent/water that originally carried it. Residual surfactants in the paint as well as hydrolytic effects with some polymers can cause the paint to remain susceptible to softening and, over time, degradation by water.
Paints that cure by oxidative cross-linking are generally single package coatings that when applied, the exposure to oxygen in the air starts a process that crosslinks and polymerizes the binder component. Classic alkyd enamels would fall into this category.

Paints that cure by catalyzed polymerization are generally two package coatings that polymerize by way of a chemical reaction initiated by mixing resin and hardener, and which cure by forming a hard plastic-like structure. Depending on composition they may need to dry first, by evaporation of solvent. Examples of paints that cure by catalyzed polymerization include epoxy- and polyurethane paints.

Still other films are formed by cooling of the binder. For example, encaustic or wax paints are liquid when warm, and harden upon cooling. Often, they can re-soften and/or liquefy if reheated.

Environmental requirements can restrict the use of volatile organic compounds, and alternative means of curing have been developed, particularly for industrial purposes. In UV-curing paints, the solvent is evaporated first, and hardening is then initiated by ultraviolet light. In powder coatings there is little or no solvent, and flow (film) and cure are produced by heating of the substrate after application of the dry powder.
Apart from the definitions given herein, further definitions concerning the present invention may apply, such as definitions provided in e.g. “Coatings Formulation”, Bodo Muller and Ulrich Poth, 2006, Vincentz Network; ”Organic Coatings: Science and Technology”, 3rd Ed., Zeno W. Wicks, Jr., Frank N. Jones, S. Peter Pappas, and Douglas A. Wicks, 2007, Wiley – Interscience; and “BASF Handbook on Basics of Coating Technology”, Artur Goldschmidt and Hans-Joachim Streitberger, 2003, Vincentz Network, which are herewith incorporated by reference.

Detailed description of the invention

Self-cleaning coating composition

In a first aspect of the current invention, a self-cleaning coating composition (“paint”) is provided, such as a self-cleaning paint and/or a paint providing a self-cleaning surface. A suitable self-cleaning coating composition may comprise one or more micro-sized particles (“particles”) coated with a functional layer.

According to an embodiment of the invention, a coating and/or coating composition is provided according to “Coatings Formulation”, Bodo Muller and Ulrich Poth, 2006, Vincentz Network; ”Organic Coatings: Science and Technology”, 3rd Ed., Zeno W. Wicks, Jr., Frank N. Jones, S. Peter Pappas, and Douglas A. Wicks, 2007, Wiley – Interscience; and “BASF Handbook on Basics of Coating Technology”, Artur Goldschmidt and Hans-Joachim Streitberger, 2003, Vincentz Network,

further comprising a micro-sized particles ("particles") coated with a functional layer, such as any particle(s) coated with a functional layer according to the current invention.

According to an embodiment, the paint comprises one type of micro-sized particles, or two or more types of micro-sized particles, optionally coated with a similar or different functional layer.

According to an embodiment of the invention, the paint comprises micro-sized particles, such as hollow, partially-hollow; or solid beads, or any combination/ratio thereof, such of hollow, partially hollow, and solid beads.

According to an embodiment of the invention, the paint comprises beads comprising one or more material(s) selected from e.g. ceramic material(s); polymeric material(s); cermet material(s); metallic material(s); pigmented material(s); light-absorbing and/or light reflecting material(s) etc.; including any combination thereof.

It is believed that the size of the beads used may be related to the desired thickness of a dry paint film, and is preferably less than the film thickness. According to an embodiment of the invention, the particles/beads should also not be too small, as the ratio of area of contact between photocatalytic coating and binder vs. volume of beads increases as the beads become smaller.

According to an embodiment of the invention, more than 10, 20, 30, 40, 50, 60, 70, 80, 85, 90, 92.5, 95, 97, 98, 99, 99.5, 99.9, 99.95, or 99.99% of the micro-sized particles of one or more type(s) have an equivalent diameter in the range of around 0.1-2000µm, 1-1000µm, 1-900µm, 1-800µm, 1-700µm, 1-600µm, 1-500µm, 1-400µm, 1-300µm, 1-200µm, 1-100µm, 2-1000µm, 2-900µm, 2-800µm, 2-700µm, 2-600µm, 2-500µm, 2-400µm, 2-300µm, 2-200µm, 1-100µm, 5-1000µm, 5-900µm, 5-800µm, 5-700µm, 5-600µm, 5-500µm, 5-400µm, 5-300µm, 5-200µm, 5-100µm, 10-1000µm, 10-900µm, 10-800µm, 10-700µm, 10-600µm, 10-500µm, 10-400µm, 10-300µm, 10-200µm; 10-100µm, 1-20µm, or 10-200µm.

When the paint comprises more than one type of micro-sized particles, these may be identical, similar, or different in size and/or equivalent diameter.

The size and/or density of beads can be normally distributed or the size distribution and/or the density distribution of the beads can be asymmetrical around the mean. The term percentile can be meant to comprise the size and/or density which a certain percent, "the percentile", of measured beads of a sample are equal to or lower. For example, if the 10th percentile is 1µm and/or 0.1g/cm^3, it means that 10% of the measured sample are 1µm or smaller in size and/or 0.1g/cm^3, or less dense.

According to an embodiment of the invention, the mean size and/or density of the beads can be between the 40th percentile and the 60th percentile, the 30th percentile and the 70th percentile, or the 20th percentile and the 80th percentile. The 10th percentile value of bead size and/or bead density can be between 30%-70%, 20%-80% or 10%-90% of the mean bead size and/or bead density. The 50th percentile value of bead size and/or bead density can be between 70%-130%, 60%-140% or 50%-150% of the mean bead size and/or bead density. The 90th percentile value of bead size and/or bead density can be between 130%-170%, 120%-180% or 110%-190% of the mean bead size and/or bead density.

According to an embodiment of the invention, the size distribution and/or the density distribution of the beads can be so small that the size difference and/or density difference between the 10th percentile bead size and/or bead density and the mean bead size and/or mean bead density is less than 10% and/or the size difference and/or density difference between the 90th percentile bead size and/or bead density and the mean bead size and/or mean bead density is less than 10% of the mean bead size and/or mean bead density.

According to an embodiment of the invention, the paint comprises one, two, three, four, five, or more than five types of micro-sized particles.

According to an embodiment of the invention, the paint comprises micro-sized particles which are hollow glass beads, such as hollow glass micro spheres (HGMS).

According to an embodiment of the invention, the self-cleaning paint comprises beads or particles coated with a photocatalytic layer providing photocatalytic activity, said layer and/or photocatalytic activity providing e.g. one or more of:

a. reduction in growth of (micro)organisms, such as one or more of: bacteria, algae, lichen, yeasts and/or moulds; and/or
b. increase in adhesion strength between an organic binder and a bead by chemical bonding; and/or
c. increase in abrasion resistance of the paint film; and/or
d. increase in weather resistance and/or UV-stability, such as one or more of: (i) reduction of chalking of an organic binder; (ii) reduction of decomposition of an organic binder; and/or (iii) reduction of release of (photocatalytic) material and/or material with a particle size of less than 1 μm; and/or
e. decomposition and/or oxidation of undesired organic matter and/or dirt; and/or
f. improvement of wetting property of the paint; and/or
g. any combination of a – g.

The coating can also be designed to have various other properties depending on what is needed for a given paint system. Without being bound by any single theory then according to an embodiment of the invention, an improved adhesion between the beads and the binder is achieved. This improved adhesion could e.g. be achieved by creating covalent bonds between the coated beads and the binder or due to high affinity of the binder to the coated beads. This is believed to improve the mechanical properties of the paint film, making it more resistant to cracking.

According to an embodiment of the invention, the self-cleaning paint comprises a layer, such as a photocatalytic layer, wherein said layer comprises e.g. one or more of:

a. a photocatalyst and/or n-type semiconductor having a band gap in the range of 1.8-10.3, 2.5-6.2 or 3.1-4.1 eV; and/or
b. a photoconductive material/composition; and/or
c. a photocatalytic material/composition; optionally comprising one or more catalyst(s) selected e.g. from the group consisting of: TiO_2, ZnO, WO_3, SnO_2, CaTiO3, Bi_2S_3, Cu_2O, Fe_2O_3, ZrO_2, SiC and $Ti_xZr_{(1-x)}O_2$ ($0 < x < 1$), and any combination thereof; optionally doped with one or more co-catalyst(s), wherein the co-catalyst is selected e.g. from the group consisting of palladium, platinum, rhodium, ruthenium, tungsten, molybdenum, gold, silver, copper, including any of their oxides and/or any of their sulfides, and any combination/mixture/ratio of two or more of palladium, platinum,

rhodium, ruthenium, tungsten, molybdenum, gold, silver, copper, including any of their oxides and/or any of their sulfides; wherein the molar ratio of co-catalyst(s) to catalyst is optionally less than 1 ppm, 1 ppm - 0.1%; 0.1-1%, 1-10%, or more than 10%; and/or wherein said co-catalyst covers optionally less than 10%, 5%, or 1% of the surface area of the photocatalytic layer; and/or wherein said co-catalyst covers optionally between 0.001-3%, or 0.01-2% of the surface area of the photocatalytic layer; and/or

d. any combination of a.-c.

According to an embodiment of the invention, the self-cleaning paint comprises micro-sized particles comprising a photocatalytic layer comprising a photocatalyst and/or n-type semiconductor, wherein the photocatalyst and/or n-type semiconductor has a band gap in the range 1.8-6.2 eV (~200-700 nm), ~3.1-10.3 eV (~120-400 nm), ~3.1-6.2 eV (~200-400 nm), ~2.5-4.1 eV (~300-500 nm), ~1.8-4.1 eV (~300-700 nm), less than 1.8 eV (~ > 700 nm) or more than 6.2 eV (~ < 120 nm). Said photocatalyst and/or n-type semiconductor can be doped with e.g. one or more of N-, S-, and F-atoms, including any combination and/or ratio thereof.

According to an embodiment of the invention, a photocatalytic layer comprising a photocatalyst and/or n-type semiconductor is provided, wherein the photocatalyst and/or n-type semiconductor has a band gap of around 1.8-6.2 eV (~200-700 nm), ~3.1-10.3 eV (~120-400 nm), ~3.1-6.2 eV (~200-400 nm), ~2.5-4.1 eV (~300-500 nm), ~1.8-4.1 eV (~300-700 nm), less than 1.8 eV (~ > 700 nm) or more than 6.2 eV (~ < 120 nm). According to a further embodiment, the band gap is between ~1.8-2.5 eV, 2.5-3.1 eV, 3.1-4.1 eV, 4.1-6.2 eV, or ~6.2-10.3 eV. In yet a further embodiment, the band gap is ~ 3,2 eV (~388 nm).

According to an embodiment of the invention, the self-cleaning paint comprises micro-sized particles comprising a photocatalytic layer, wherein:
(i) the photocatalytic material is covalently bound to said beads/micro-sized particles; and/or
(ii) the photocatalytic material coated on the beads/micro-sized particles has a crystal size of 1 - 150nm; and/or
(iii) the photocatalytic material coated on the beads optionally has a specific surface area (e.g. BET surface area) in the range of 0.01-100; 0.1-100, 1-100, 10-100, 0.01-50, 0.1-50, 1-50, 10-50, 0.01-30, 0.1-30, 1-30, 0.01-10, 0.1-10, or 1-10 m^2/g; and/or
(iv) any combination of (i)-(iii).

In an embodiment of the invention, alternatively, the BET surface area of a bead or particle, optionally with or without coating or (photocatalytic) layer, can be less than 0.01 m^2/g, or greater than 100 m^2/g. Said BET surface area can also be in the range of 0.01-100; 0.1-100, 1-100, 10-100, 0.01-50, 0.1-50, 1-50, 10-50, 0.01-30, 0.1-30, 1-30, 0.01-10, 0.1-10, or 1-10 m^2/g.

According to an embodiment of the invention, the weight of the bound photocatalyst in average is more than 0.001%; 0.0025%; 0.005%; 0.01%; 0.025%; 0.05%; 0.1%; 025%; 0.5%; 1%; 2,5%; 5%; or 10% of the weight of the bead.

According to an embodiment of the invention, the self-cleaning paint comprises micro-sized particles comprising a photocatalytic layer, wherein the photocatalytic layer comprises TiO_2 in the crystal form of rutile and/or anatase.

According to an embodiment of the invention, the self-cleaning paint comprises micro-sized particles comprising a photocatalytic layer, wherein more than 90%; 99%; or 99.9% (weight/weight) of the TiO_2 in the photocatalytic layer is in the catalytic active form of anatase. According to another embodiment, said particles are glass spheres or a hollow glass sphere (e.g. HGMS) coated with TiO_2. According to a further embodiment, more than 50%; 75%; 80%; 90%; 95%; 99%; or 99.9% of said TiO_2 is in the photocatalytically active form of anatase.

In one embodiment of the invention, the self-cleaning coating composition (paint) comprises particles, e.g. hollow glass spheres, where more than 95% of particles have diameter between 10 and 200 µm. In a further embodiment, essentially all particles, or more than 99%, 95%, or 90 % of the particles have a diameter of less than 10µm; 25µm; 50µm; 100µm; 250µm; 500µm; or 1000µm; alternatively all particles, or more than 99%, 95%, or 90 % of the particles have a diameter between 1 and 20µm; between 10 and 25µm; between 20 and 40µm; between 35 and 55µm; between 45 and 75 µm; between 70 and 105µm; between 100 and 300 µm; between 250 and 600 µm; or between 500 and 1100µm. In another embodiment, all particles, or more than 99%, 95%, or 90 % of the particles have a diameter of more than 10µm; 25µm; 50µm; 100µm; 250µm; 500µm; or 1000µm.

According to an embodiment of the invention, the self-cleaning paint comprises micro-sized particles comprising a photocatalytic layer comprising anatase, wherein in average 10^5-10^{10}; and/or at least 10^2, 10^5, 10^{10} or more individual anatase crystals are bound per bead/particle (in average); and/or wherein the weight of the bound anatase is more than 0.001%; 0.01%; 0.1%; 1%; or 10% of the weight of the particle/bead (in average). According to a further embodiment of the invention, at least 1, 10, 10^2, 10^3, 10^4 10^5, 10^6, 10^7 10^8, 10^9, 10^{10}, 10^{11}, 10^{12}, 10^{13}; 10^{14}, 10^{15}, or more individual anatase crystals are bound per bead/particle (in average). According to another embodiment, the weight of the bound anatase is less than 0.001%, or more than 10% of the weight of the particle/bead (in average).

According to an embodiment of the invention, the TiO_2 and/or anatase crystal size associated with a photocatalytic layer is in average around 1-200 nm, 5-100 nm, 10-80 nm. According to another embodiment, said crystal size is in average less than ~1nm, around ~1-10, ~10-20, ~20-30, ~30-40, ~40-50, ~50-60, ~60-70, ~70-80, ~80-90, ~90-100, ~100-120, ~120-150, ~150-175, ~175-200, ~200-250, or ~250-300 nm, or more than ~300 nm.

According to an embodiment of the invention, and photocatalytic layer is provided with a thickness (in average) of around less than ~1 nm, ~1-300 nm, ~20-160 nm, or more than ~300 nm. According to another embodiment of the invention, the average thickness of the photocatalytic layer is ~1nm, around ~1-10, ~10-20, ~20-30, ~30-40, ~40-50, ~50-60, ~60-70, ~70-80, ~80-90, ~90-100, ~100-120, ~120-150, ~150-175, ~175-200, ~200-250, or ~250-300 nm, or more than ~300 nm. According to a further embodiment, the thickness of the photocatalytic layer corresponds to the average size of the TiO_2 and/or anatase crystals associated and/or bound to the particle(s) or bead(s).

According to an embodiment of the invention, the self-cleaning paint comprises less than 1%; 0.5%; 0.25%; 0.1%; 0.05%; 0.025%; 0.01%; 0.005%; 0.0025%; 0.001%; 0.0005%; 0.00025%; 0.0001%;0.00005%; 0.000025%; or 0.00001% anatase particles not bound to micro-sized beads; and/or derived/released from the micro-sized beads, determined e.g. as weight/weight of non-covalently bound anatase per total amount of anatase, or per total amount of TiO_2.

Table 1. Typical generic examples of paint formulations.

Type		Basis	Solvent	Resin	Pigment	Filler	Additive
Alkyd	Paint	Organic	~20-70	~10-30	~0-35	~0-50	~0.1-10
		Water	~45-70	~1-30	~0-35	~0-50	~0.1-10
	Wood stain	Organic	~10-90	~5-80	~0-25	~0-20	~0.1-10
		Water	~40-90	~5-40	~0-25	~0-20	~0.1-10
Acrylic	Paint	Water	~45-70	~1-30	~0-35	~0-50	~0.1-10
	Wood stain	Water	~45-90	~1-30	~0-35	~0-20	~0.1-10
Polyurethane	Paint	Water	~45-70	~1-30	~0-35	~0-50	~0.1-10

Compositions are given % (weight/weight)

According to an embodiment of the invention, the self-cleaning paint can be essentially an alkyd-, acryl-, polyurethane-, epoxy-, and/or co-polymer-based paint or painting composition. Typical (generic) examples of paint formulations are given e.g. in Table 1. Further examples can be found in e.g. in one or more of "Coatings Formulation", Bodo Muller and Ulrich Poth, 2006, Vincentz Network; "Organic Coatings: Science and Technology", 3rd Ed., Zeno W. Wicks, Jr., Frank N. Jones, S. Peter Pappas, and Douglas A. Wicks, 2007, Wiley – Interscience; and "BASF Handbook on Basics of Coating Technology", Artur Goldschmidt and Hans-Joachim Streitberger, 2003, Vincentz Network.

According to an embodiment of the invention, a method is provided for providing or integrating photocatalytically active material into paint, while limiting, reducing or avoiding undesired activity of the photocatalyst, such as oxidation of the binder, e.g. film breakdown, when exposed to the environment, such as light, including UV-radiation. This can be achieved by coating the photocatalytic material onto micro-sized (carrier) particles, such as particles with an equivalent diameter smaller than e.g. 200µm; 500µm; or 1000µm, instead of mixing the photocatalytic particles directly into the paint. By coating the photocatalyst on (inert) carrier particles the photocatalytic reaction is believed to take place at a surface which is inert, i.e. not oxidized by the reaction, and contact between the photocatalyst and binder is minimized.

According to an embodiment of the invention, the amount of photocatalytic material released from a paint film over time is reduced, compared to paint film, where the photocatalytic material is not bound to carriers/particles. Without wanting to be bound by any theory, it is believed that this can be achieved because the photocatalytic material(s) is/are immobilized on larger particles that are much deeper embedded in the film than e.g. a photocatalytic particle in nano-size would be.

According to an embodiment of the invention, a healthier and/or less toxic paint composition and/or (dried) paint film is provided. Without wanting to be bound by any theory, it is believed that larger particles, such as e.g. > 5 micron, do not diffuse into skin as easily as smaller particles, making them much easier to wash off if skin is contaminated.

According to an embodiment, a benefit of using inert particles according to the invention is provided, as carriers after some weathering of a paint film (surface), the concentration of inert material in the surface will be increased giving the overall effect of increased weather stability of the paint film.

According to an embodiment of the invention, the photocatalytic coating can also be a multifunctional coating, providing e.g. (improved) adhesion between the binder and the carrier particles, whereby the overall film becomes more resistant to cracking.

Self-cleaning surface

According to a second aspect of the invention, a self-cleaning surface is provided comprising a dried layer (paint film) derived from a self-cleaning paint, such as a self-cleaning paint according to the first aspect of the invention.

According to an embodiment of the invention, a self-cleaning surface is provided on e.g. one or more of wood, brick, concrete, cement, asphalt, natural or artificial stone, clay, glass, plastic, metal, fibre glass, carbon fibres, (wall) paper, painted surface, glued surface, composite material, or any combination thereof, such as a surface on an item, wall, building, structural element, bridge, building element, building block, window, door, floor, ceiling, roof (sheathing), smoothed and/or plastered surface, furniture, house hold equipment, medical equipment, sanitary equipment, car, (motor)bike, truck, container, bus, aircraft, rocket, ship, train, locomotive, wind mill, or solar panel; including any combination thereof.

According to an embodiment of the invention, a similar, constant or near constant ratio can be provided or obtained of paint film surface area (without (coated) micro-sized particles) to surface of coated micro-sized particles (e.g. TiO_2-coated HGMS) through the lifetime of the paint file (painted/coated surface). Thereby, a self-cleaning surface is provided during the lifetime of the painted/coated surface.

Without wanted to be bound by any theory, examples of surface ratios of the environment-exposed surfaces of paint surface (without coated micro-sized particles) and coated micro-sized particle (e.g. TiO_2-coated HGMS) surface may comprise the range of 1:100 to 1:10; 1:10 to 1:1; 1:1 to 10:1; or 10:1 to 100:1. These ratios are determined, assuming a flat and horizontal surface of the paint film (without particles) and a spherical surface of the surface-exposed particles (micro-sized particles) HGMS.

HGMS are used as a common filler material in paints. It is thus believed that such particles are a suitable (micro-sized) particle according to the invention. Different volume percentage of HGMS can be added to paint, approximately up to 40%, which gives a large surface area coated with anatase. In one embodiment of the invention, a paint or paint film comprises 1-50 %, 10-45%, 20-40% or 30-40% (volume / volume) HGMS.

According to an embodiment of the invention, a paint system is provided wherein (photocatalytic) degradation of e.g. one or more of binder(s), pigment(s), and/or chemical compound(s)/composition(s) in the paint or paint film is reduced, inhibited, delayed, prevented in the paint/painted surface/coating, by the use of micro-sized particles comprising a photocatalytic coating compared to similar coatings comprising photocatalytic nano-particles instead of micro-sized particles comprising a photocatalytic coating.

According to the invention, a painted surface such as e.g. a paint film is provided with self-cleaning properties, such as the capability of maintaining the painted surface essentially free of organic

and/or inorganic dirt, filth, debris and the like, providing e.g. a cleaner appearance. This can reduce or avoid discoloring/staining of the painted surface. Furthermore, a paint composition providing a self-cleaning painted surface has the potential or capability to reduce growth of one or more of microorganism, bacterium, mould, yeast, alga, lichen and plant. This could e.g. be due to the lack of nutrients, and/or the production of one or more toxic and/or aggressive chemical compound.

According to an embodiment of the invention, the photocatalytic activity of the painted surface/coating is maintained essentially unchanged during the total life span of the painted film (painted surface).

Method of cleaning a surface

According to a second aspect of the invention, a method of cleaning a surface is provided.

According to an embodiment of the invention, such a method for cleaning a surface may comprise exposing a self-cleaning surface, such as a self-cleaning surface according to the 2nd aspect of the invention, to electromagnetic radiation, wherein said electromagnetic radiation comprises radiation with a wavelength in the range of 200-400 nm and/or 400-800 nm, wherein said radiation is provided by the sun (e.g. daylight, reflected sunlight, twilight, moonlight), or by an artificial source.

According to an embodiment of the invention, the method of cleaning a surface comprises irradiation with a wavelength comprising 388 nm or less, and/or a wavelength corresponding to the band-gap of the photocatalyst and/or n-type semiconductor, or a wavelength shorter than the band-gap of the photocatalyst and/or n-type semiconductor.

According to an embodiment of the invention, the paint film inhibits growth of microorganisms, e.g. by killing them on the surface through reaction products derived from the highly oxidative photocatalytic process taking place on the coated beads. It is believed that microorganisms will not be able to survive on the surface of a paint film according to the invention, and thereby prevent said microorganisms from penetrating the paint film and reaching e.g. a painted substrate, such as wood substrate.

According to one embodiment of the invention, the coated particles comprised in a paint composition and/or paint film are Hollow Glass Micro Spheres (HGMS), e.g. coated/coupled with anatase and/or one or more other compounds and or compositions. An embodiment of a coating/painted surface according to the invention comprising HGMS coated with anatase is illustrated in **Figure 1.**

Figure 1 shows a cross section of a surface or substrate 5 painted/coated with paint according to the invention. The paint comprises beads, such as hollow glass microspheres (HGMS) 20, 21 which are coated with TiO_2 in the photocatalytic active form of anatase 25, 26. The thickness of the coating/paint 10 deposited on the surface 5 exceeds the diameter of the TiO_2-coated HGMS 20, 21. Upon application of the paint and drying of the paint, a population of TiO_2-coated HGMS will be embedded in the surface, whereby anatase will be exposed to the environment. Other TiO_2-coated HGMS will be covered and/or embedded in a layer of paint. **Figure 1 A** shows a newly painted surface. With time, the thickness of a painted layer can decrease (**Figure 1 B**), e.g. through one or more of degradation, weathering, erosion, abrasion and the like. Consequently, e.g. after prolonged periods of weathering, TiO_2-coated HGMS close to the surface can become loose and fall of. Such a

TiO_2-coated HGMS is illustrated with an arrow. This process can continue as seen in **Figure 1 C**, where the thickness of the paint/coating has decreased further, and more TiO_2-coated HGMS have been lost. However, there will still be TiO_2-coated HGMS present protruding the surface, exposing photocatalytically active anatase.

In an embodiment of the invention, all, or a fraction of the anatase-coated HGMS can be covered by the paint composition (without glass beads), e.g. shortly upon providing a paint film. It is believed that during natural decay of the painted/coated surface, e.g. through degradation of the binder, gradually, the coating surface will have a larger percentage of glass in it and therefore the degradation of the paint film should be decreased. Particles, such as beads and/or spherical particles can be added to paint in significant amounts without making the paint too viscous. Consequently, a large fraction or proportion of the surface can comprise beads, such as TiO_2–coated HGMS which are often more weather resistant than the binder, and which also may contribute to providing a self-cleaning surface which does not decompose as a result of e.g. a photocatalytic effect. Dirt from the environment will sit on the glass and be oxidized when subjected to sunlight. The OH radicals created by the photocatalysis are believed to be extremely short lived, half life of approximately 10^{-9}s. It is assumed that OH radicals will decay before they can reach/diffuse to the binder.

According to an embodiment of the invention, anatase on the side of the HGMS that is embedded and/or in contact with the paint/film, i.e. non-surface-exposed anatase, will not be active or show reduced activity, e.g. due to lower levels of (UV-)light or reduced availability of water molecules. This can inhibit, prevent or reduce the formation of radicals, thereby preventing and/or reducing degradation of the paint/film.

Without being bound by a single theory, it is believed that anatase-catalyzed photochemical reaction(s) will occur, whereby OH-radicals and/or peroxy-radicals are formed from e.g. water and/or oxygen. These radicals are believed to be highly reactive, and to possess a very short life span. Due to the short life span of the radicals, it is assumed that they are unlikely to move away from the site of creation, e.g. by diffusion. Consequently, the highly reactive radicals that otherwise would be very damaging for e.g. a filler or pigment present in a paint, will remain close to the site of creation. These radicals will be created where anatase absorbs light, such as UV light, in the presence of water at the surface of a painted/coated surface according to the invention.

By the use of TiO_2 in the catalytic active form of anatase coupled to particles, such as HGMS, the location of the anatase crystals is confined to the exterior of the particles, to which they are bound/coupled/attached to. Thereby, occurrence of unbound anatase crystals in the paint is avoided. The presence of unbound anatase crystals in the paint is not desired, as it is believed that their presence has a negative influence on essential components of the paint, such as binder, pigment and/or additives.

According to an embodiment of the invention, a surface comprising particles (e.g. glass) and photocatalytic/functional layer/composition (e.g. anatase) is provided, where the light-induced catalytic property of the photocatalytic/functional layer/composition (e.g. anatase) is physically separated / spaced from e.g. the binder, pigment and/or additive. This system is believed to be active for an extended period of time.

It is also believed that the lifetime of a coated/painted surface provided with paint according to the current invention is significantly longer compared to a paint comprising e.g. anatase dispersed in the paint, i.e. non-coupled/conjugated/ attached to particles, such as HGMS.

Use of a self-cleaning coating composition

A fourth aspect of the invention concerns the use of a self-cleaning coating composition, such as a self-cleaning coating composition (paint) according the first aspect of the invention for providing a self cleaning surface, such as a self cleaning surface according to the second aspect of the invention.

According to an embodiment of the invention, a self-cleaning coating composition (paint) is used for providing a self-cleaning surface e.g. on one or more of wood, brick, concrete, cement, asphalt, natural or artificial stone, clay, glass, plastic, metal, fibre glass, carbon fibres, (wall) paper, painted surface, glued surface, composite material, or any combination thereof, such as a surface on an item, wall, building, structural element, bridge, building element, building block, window, door, floor, ceiling, roof (sheathing), smoothed and/or plastered surface, furniture, house hold equipment, medical equipment, sanitary equipment, car, (motor)bike, truck, container, bus, aircraft, rocket, ship, train, locomotive, wind mill, or solar panel, including any combination thereof.

Micro-sized particles coated with a functional layer

In a fifth aspect, the current invention pertains to micro-sized particles coated with a functional layer, such as any micro-sized particle(s) according to the first aspect of the invention.

According to an embodiment of the invention, micro-sized particles comprise one or more of hollow beads, partially hollow beads, solid beads, or any combination/ratio of hollow-, partially hollow, and solid beads, wherein the beads comprise e.g. one or more material(s) selected from ceramic material(s); polymeric material(s); cermet material(s); metallic material(s); pigmented material(s); light-absorbing and/or light reflecting material(s); including any combination thereof.

According to an embodiment of the invention, beads are colored/pigmented to match the desired color of the paint film. This can be achieved by adding pigment to the bead material or by coating the beads with a material which yields the desired color before coating the beads with the photocatalytic material. The pigments may include inorganic and/or organic pigments e.g. phtalo blue, phtalo green, chinacridone, naphthol and azo. According to an embodiment of the invention, a paint, coating, or composition comprises one or more organic and/or inorganic pigment(s) disclosed in disclosed in Industrial Inorganic Pigments, 3rd, Completely Revised and Extended Edition, Gunter Buxbaum and Gerhard Pfaff (Editors), ISBN: 978-3-527-30363-2 (2005); and/or Industrial Organic Pigments: Production, Properties, Applications, 3rd, Completely Revised Edition Willy Herbst, Klaus Hunger, ISBN: 978-3-527-30576-6 (2004).

According to an embodiment of the invention, a paint or paint film comprises a mixture of micro-sized particles coated with a functional layer to non-coated micro-sized particles (e.g. TiO_2-coated HGMS to TiO_2-coated HGMS) of less than 1:100, 1:100 - 1:10; 1:10 - 1:1; 1:1 - 10:1; 10:1 - 100:1, or more than 100:1.

According to an embodiment of the invention, carrier particles, such as micro-sized particles according to the invention, can be fully or partially coated with one or more photocatalytic materials. This may comprise any combination of photocatalytic materials that e.g. under

illumination and in the presence of air are capable of accelerating oxidation of one or more organic compounds. Photocatalytic materials may comprise, but are not limited to one or more of: TiO_2, ZnO, WO_3, SnO_2, MoO3, CaTiO3, Bi_2S_3, Cu_2O, Fe_2O_3, ZrO_2, SiC and $Ti_xZr_{(1-x)}O_2$ (where x is a number between 0 and 1); including any combination thereof.

It is believed that doping the surface and/or bulk of a photocatalyst with one more elements, such as metals, can increase, alter, or reduce the efficiency or the working range (e.g. nm) of a photocatalyst according to the invention.

In one embodiment of the invention the coated beads are doped, preferably on the surface instead of in the bulk, with co-catalysts able to accelerate the oxidation process that yields self cleaning properties. Said co-catalysts include any one or a combination of palladium, platinum, rhodium, ruthenium, tungsten, molybdenum, gold, silver, copper and oxides or sulphides thereof, preferably in amounts of 0,001; 0,01; 0,1-1; 2; 5 weight% of the photocatalyst.

According to an embodiment of the invention, the beads comprise one or more metallic materials. The term metal may be used for both pure metals and alloys.

According to an embodiment of the invention, the beads comprise one or more cermet materials. The term cermet may be used for materials which are composites of metals and ceramics.

According to an embodiment of the invention, the beads are believed to be acting at least in part as a waveguide, and internally reflect light, such as sunlight back to the photocatalytic coating. The beads can be hollow and may possess an index of refraction e.g. between 1.4-1.6; 1.2-1.6; 1.4-2.0; or 2.0-2.7. The photocatalytic coating material can have an index of refraction of e.g. 2.5-2.75; 2.0-4.0; 2.0-3.0 or 1.5-3.0. Without wanting to be bound by any theory, it is believed that in the case the beads are hollow, it could be beneficial, if the photocatalytic coating material has a substantially higher index of refraction than the bead. When e.g. sunlight hits a coating, which has a much higher index of refraction than air, the light is refracted and according to Snell's law, it will have a low angle of refraction compared to the angle of incidence, which in essence guides the sunlight closer to the centre of the bead. When the sunlight is again refracted in the bead material the angle of refraction is increased. When light passes from a material with a high index of refraction to one with a lower index of refraction there is a critical angle, calculated from the indices of refraction of the two materials, where all the light is reflected. This phenomenon is also called total internal reflection. When the sunlight hits the air in the hollow space of the bead a substantial fraction can be totally reflected back up to the photocatalytic coating. This means that less sunlight will pass through the bead. This can be advantageous, because due to (total) internal reflection, more light can be absorbed in the photocatalytic coating at the surface of the paint film, thereby increasing the yield of the self cleaning effect. Furthermore, it is believed that (total) internal reflection may contribute to reducing potential damage to the paint film, due to reduction of light-induced activation of the photocatalytic material comprised and/or enclosed in the paint film (i.e. not exposed to the surface).

According to an embodiment of the invention, the beads are pigmented to match the desired color of the paint film. This can be done to avoid discoloring of the film, e.g. when the beads become exposed on the surface of the paint film. Even though the beads are so small that they are nearly not visible to the human eye, it is believed that a large concentration of beads in the surface can affect

the optical properties. For example white beads in a dark colored paint film could have a "bleaching" effect because of the countless small white dots in the surface of the film.

According to an embodiment, hollow or solid beads according to the invention comprise, consist of, or consist essentially of one or more ceramic material(s), such as glass, borosilicate glass. The beads can be, and may be coated with a photocatalytic material. According to another embodiment, said beads comprise, consist of, or consist essentially of one or more polymeric material(s), such as e.g. a tough and ductile organic polymer or silicone. According to a further embodiment, if necessary, e.g. in order to protect the polymer from a (photo)catalytic action of the photocatalytic layer, the beads are provided with a protective and/or intermediate layer of a suitable material that is not oxidized by e.g. a (photo)catalytic reaction, such as for example materials like SiO_2 or Al_2O_3.

According to an embodiment of the invention, the binding strength of the bound photocatalytic layer, such as bound anatase crystals, is so high that the amount of loose photocatalytic layer (e.g. anatase crystals) after sonicating the coated beads for half an hour in distilled water is less than 10, 5, 2, 1, 0.5, or 0.1% of the total weight of the coated beads.

In an embodiment of the invention, the coated beads improve the abrasion resistance of the paint film.

In an embodiment of the invention, the coated beads improve the weather resistance of the paint film.

In one embodiment of the invention, the coated beads improve the UV stability of the paint film by acting as UV-stabilizers.

Providing micro-sized particles

A sixth aspect of the current invention concerns one or more methods for providing micro-sized particles, such as micro-sized particles according to the first and/or fifth aspect of the invention.

According to an embodiment of the invention, photocatalytic material is e.g. covalently bonded to the beads, whereby release of nano-sized photocatalytic particles to the environment or paint composition is reduced or avoided. Suitable coating processes may comprise e.g. Physical Vapour Deposition (PVD), Plasma Enhanced Physical Vapour Deposition (PE-PVD), Chemical Vapour Deposition (CVD), Plasma Enhanced Chemical Vapour Deposition (PE-CVD), Metal Organic Chemical Vapour Deposition (MO-CVD), Atomic Layer Deposition (ALD) and/or "wet chemistry" using a metal-organic precursor, such as e.g. a metal-alkoxide dissolved in alcohol.

According to an embodiment of the invention, TiO_2-coated and/or anatase-coated (hollow) glass spheres are provided by coating hollow glass microspheres with a CVD process. The titanium precursor used in the process can be an organic-titanate, titanium alkoxide, e.g. titanium-tetraisopropoxide (TTIP), and/or Titanium-tetrachloride ($TiCl_4$). To achieve covalent bonding between the glass surface and the anatase TiO_2 coating, it is believed that the titanium precursor must be easily hydrolyzed. It is believed that the reaction comprises that OH groups on the glass surface hydrolyze the titanium precursor, whereby a covalent bond between the glass surface and

the titanium atom is provided (see **Figure 2**). The process can e.g. be divided into the following steps:

1. The hollow glass microspheres are pre-treated by heating them up to 110-200°C to evaporate physically adsorbed water of the surface.
2. The titanium precursor is evaporated by applying heat and/or vacuum.
3. Inert gas, e.g. nitrogen, argon etc., e.g. with less than 10ppm H_2O is used to carry the evaporated precursor into a reaction chamber, where the hollow glass microspheres are continuously being stirred e.g. mechanically or fluidized by the carrier gas. The temperature in the reaction chamber can be in the range 0-800°C
4. The titanium precursor reacts with the glass surface, when it comes into contact with OH groups on the glass surface, which hydrolyze the precursor, creating a covalent between the titanium atom and the glass bead (**Figure 2**).
5. Inert gas with 0.01-50% relative humidity is blown through the hollow glass microspheres to hydrate the surface while e.g. stirring or fluidizing.
6. Steps 2 through 5 are repeated to build up a thicker layer.
7. The coated microspheres are heated to temperatures in the range 100-800°C for a period ranging from a few seconds to several hours to crystallize the anatase.

According to an embodiment of the invention, TiO_2-coated and/or anatase-coated (hollow) glass spheres are provided by coating hollow glass microspheres with a ALD process. The titanium precursor used in the process can be an organic-titanate, titanium alkoxide, e.g. titanium-tetraisopropoxide (TTIP), and/or Titanium-tetrachloride ($TiCl_4$). To achieve covalent bonding between the glass surface and the anatase TiO_2 coating, it is believed that the titanium precursor must be easily hydrolyzed. It is believed that the reaction comprises that OH groups on the glass surface hydrolyze the titanium precursor, whereby a covalent bond between the glass surface and the titanium atom is provided (see **Figure 2**). The process can e.g. be divided into the following steps:

1. The hollow glass microspheres are pre-treated by heating them up to 110-200°C to evaporate physically adsorbed water of the surface.
2. The titanium precursor is evaporated by applying heat and/or vacuum.
3. Inert gas, e.g. nitrogen, argon etc., e.g. with less than 10ppm H_2O is used to carry the evaporated precursor into a reaction chamber, where the hollow glass microspheres are continuously being stirred e.g. mechanically or fluidized by the carrier gas. The temperature in the reaction chamber can be in the range 0-800°C
4. The titanium precursor reacts with the glass surface, when it comes into contact with OH groups on the glass surface, which hydrolyze the precursor, creating a covalent between the titanium atom and the glass bead (**Figure 2**).
5. Inert gas with 0.01-50% relative humidity is blown through the hollow glass microspheres to hydrate the surface while e.g. stirring or fluidizing.
6. Steps 2 through 5 are repeated to build up a thicker layer.
7. The coated microspheres are heated to temperatures in the range 100-800°C for a period ranging from a few seconds to several hours to crystallize the anatase.

The following contemplations are at lest(there is some typo here. I am not quite sure which word should be here) in part of more theoretical nature, and are not to be construed as limiting to the current invention:

Without wanting to be bound to any theory, it is believed that e.g. the photocatalyst is coated onto beads to minimize contact between the photocatalytic material and the binder of the paint film. If the same volume of coated microspheres or photocatalytic nano-particles are introduced into a paint formulation then clearly the area of contact between the photocatalytic material and the binder is much less in the case of coated microspheres as compared to photocatalytic nano-particles because the nano-particles have a much larger surface area per volume. More importantly when the photocatalytic material is coated on inert material such as hollow glass microspheres, which protrude from the paint film surface, the photocatalysis, i.e. the self cleaning effect, takes place on an inert surface which is not in contact with the binder material. Due to the size of the microspheres, e.g. UV-radiation will not penetrate deep enough into the paint film to activate the part of the coated microsphere which is within the paint film whereas a nano-particle is so small that if it is at the paint film surface, essentially all its surface area can be activated and therefore all the organic binder adhering the particle to the film can be degraded causing the nano-particle to fall out of the film.

Likewise, it is further contemplated that the coated beads that are located close to the surface, are completely or partially covered with a very thin layer of binder, for example 2µm or less, upon "painting", i.e. in a fresh film. The paint film will absorb UV-radiation based on which binder is used and the amount and type of UV-stabilizers used in the paint formulation. Paint formulations generally comprise UV-stabilizers because protecting a substrate from UV-radiation is a typical function of paint. Therefore only the coated beads closest to the surface will become photocatalytically active and affect the thin film covering them. This will cause the thin film covering the beads to loose adhesion and with weathering and wear the thin film will be removed. This will leave a part of the coated beads exposed in the surface of the paint film giving it self cleaning properties. The degradation of the binder, due to the photocatalytic effect, will stop or be severely reduced at this point as the UV-radiation reaching the photocatalytic material is exclusively or predominantly where the binder has been removed. This means the self cleaning effect (photocatalysis) takes place on the inert surface of the bead without contact with the binder. The photocatalytic material that is in contact with the binder is much deeper in the film where very little or no UV-radiation reaches it.

It is also believed that after application of the paint film to a substrate the concentration of coated beads in the surface will increase as the paint film is subjected to wear and/weathering and then remain stable throughout the lifetime of the film as shown in **Figure 1** from **a)** to **c)**. A high concentration of coated beads in the surface of the film will increase the wear and weathering resistance of the film because a bead made of inert material is much more resistant than an organic binder. This will lengthen the service life of the paint film and along with the self cleaning effect make a painted surface maintenance free for a much longer period than a paint film without coated beads.

One benefit of the invention can be that release of photocatalytically active material to the environment is significantly reduced compared to e.g. paint comprising photocatalytic nano-particles. This is not only because the degradation of the paint film is slowed down, because of the positive effect of the coated beads on the wear and weathering resistance of the paint film, but also because the beads are embedded much deeper in the film and therefore much more paint has to be degraded for the beads to be released than for nano-particles. This difference is e.g. illustrated in **Figure 1**. Nano-particles have very high activity due to their high surface area and are therefore

interesting for this application. There is however not enough known about the effect of nano-particles on the human body but research indicates that photocatalytic nano-particles that come into contact with skin and are exposed to sunlight can be extremely dangerous and possibly carcinogenic. Therefore a paint film comprising a binder degradable by photocatalytic material with highly active photocatalytic nano-particles is a possible health hazard. This is however not the case with this invention because the release of photocatalytic material is by far less and also because the photocatalytic material is prevented from reaching living skin cells below the stratum corneum of the epidermis because it is coated onto much larger particles that do not diffuse as easily through the top skin layers as nano-particles and are therefore much easier to wash off.

EXAMPLES

The following Examples are not to be construed as limiting to the current invention.

Example 1

This example provided evidence that photocatalytic material such as anatase TiO_2, can be coated onto hollow glass microspheres.

Photocatalytic TiO_2 was coated onto S38 hollow glass microspheres, produced by 3M, with an average/mean size of 40µm and an average/mean density of 0.38g/cm^3, by treating the microspheres with Vertec XL110, a titanium-tetraisopropoxide (TTIP), produced by Johnson Matthey Catalysts, followed by calcining the product afterwards to crystallize the titanium. The coating procedure was essentially as follows:

TTIP was dissolved in isopropanol and the ratio of isopropanol to TTIP was 10:1 by volume. After stirring for 20 minutes the S38 hollow glass microspheres were added to the solution in the ratio 1g glass spheres to 1ml TTIP and stirred for 20 minutes. Next distilled water was added to the solution in the ratio 1ml distilled water to 1g glass spheres and the solution stirred for 10 minutes. The solution was then filtered using a filter paper, such as a Schleicher & Schuell filter nr. 589/1, which retains particles larger than 12µm, to separate the glass beads from the liquid and afterwards the glass spheres were heated to dryness at 110°C. After all the alcohol had been evaporated the coated glass beads were then heated at 550°C for 5 hours. The same coating process was then repeated once and then the coated glass spheres were sonicated in distilled water and separated from any anatase powder in the solution. Finally the coated spheres were heated to dryness at 110°C. The photocatalytic coating can be seen in **Figure 3** which shows a comparison of a coated and uncoated glass bead.

Figure 4 shows x-ray diffraction patterns, measured with a Huber G670 Guinier diffractometer with a 0,005° measurement step of commercial grade anatase TiO_2 provided from Sigma Aldrich, and anatase from coated beads according to Example 1. The comparison indicated that the coating was essentially anatase because both spectra have peaks at the same angles. The spectrum for the anatase provided from Sigma Aldrich was shifted up in Figure 4 so both spectra could be clearly seen and compared and both spectra include a tape background which the powder was attached to during the measurement. The high peaks of the commercial grade anatase indicated that the material was highly crystalline and much more than the other spectrum indicated. The wide peaks of the anatase from the coated beads indicated that the crystal size of the material was very small and much smaller than the Sigma Aldrich anatase.

Example 2

This example provides evidence that hollow glass microspheres coated with anatase TiO_2, as described in Example 1, can accelerate the decomposition/oxidation of an organic material.

The photocatalytic activity of the beads was tested by preparing a dilute solution of an organic dye, methylene blue (MB), and mixing the coated glass beads into the solution. Thereto, 60mg of coated beads were mixed into 30ml of dilute MB solution in a 100ml beaker. After the mix had reached equilibrium in the dark it was exposed for 20 minutes to UV radiation using a Dymax 5000-EC UV lamp where the irradiated area in the 100ml beaker was around 16.6cm^2. The irradiance of the lamp was about 225mW/cm^2 and the output wavelength mainly between 350 and 400nm. The MB concentration was determined by making a calibration curve using a Shimadzu UV-mini 1240 photospectrometer and measured in a 1 cm cuvette. The initially determined MB concentration of the mixture was approximately 80µmol/litre. **Figure 5** summarizes the results of said experiment. After 20 minutes the measured MB concentration had decreased about 76µmol/litre to 4µmol/litre, i.e. the blue color of the solution had almost totally disappeared. A MB solution without any glass beads was also irradiated under the same conditions for 20 minutes. The measured concentration change was only 4µmol/litre which means very little difference could be seen in the solution color showing that the coated beads accelerated the oxidation of MB.

Example 3

This example provides evidence that a self-cleaning paint film can be provided comprising photocatalytic material, without the film being severely degraded as a result of photocatalytic activity.

To test the effect of the coated beads on a paint film a typical alkyd paint formulation comprising ~40% resin, ~28% coated HGMS, ~2% pigment, ~29% solvent and ~1% additives was prepared, to which coated glass beads prepared according to Example 1 were added to the formulation so that 40% of the volume of solids of a dried paint film was coated glass beads. Several 200µm thick paint films (wet thickness) were applied on panels and placed into a Q-lab (i.e. an accelerated weathering test chamber), where the films were subjected to cycles of 4 hours of UV-radiation, where the temperature was maintained at 60°C, followed by 4 hours moisture condensation, where the temperature was maintained at 50°C. QUV-A340 UV lamps were used in the QUV chamber and the wavelengths emitted from the UV lamps were in the range of essentially 290-450nm with the highest intensity at 340nm. **Figure 12** shoes the emission characteristics of the UVA-340 lamps used in the QUV chamber. The films were analyzed using scanning electron microscopy before and after exposure in the QUV chamber. **Figure 6** shows the alkyd paint with coated glass beads after different exposure times. The images show that before any exposure the coated beads near the surface of the paint film were fully or partially coated with a thin layer of binder. After some exposure the photocatalytic coating on the beads had removed the thin layer of binder on top of the beads so the beads became exposed and available for the self cleaning effect. There was no indication of the binder in between the beads being affected by the photocatalyst and actually it was found that the reference sample (the same alkyd formulation without glass beads), seen in **Figure 7**, was further degraded indicating that the coated beads improve the weather resistance of the paint film. After having been exposed for 2200 hours in a QUV chamber, roughly correlating to 5 years outdoor exposure, a thin clearance was seen having formed around many of the coated glass beads as a result of photocatalytic activity but as before the rest of the binder is not affected. This did however not cause the beads to fall out of the film even after a long period of exposure. This shows that the photocatalytic coating is not active where it is deeply embedded in the paint film, presumably because the UV radiation does not penetrate so deep into the paint film.

Example 4
A similar experiment as described in Example 3 was performed with a typical polyurethane formulation, according to table 1, to test the effect of the coated beads on a UV resistant binder. The formulation comprised coated glass beads as 40% of the volume of solids of a dried film. The results of the experiment, shown in **Figures 8** and **9**, were comparable to the results obtained in Example 3. The binder between the beads appeared not affected by the coated beads. Furthermore, the coated glass spheres remained retained/embedded in the paint film even after prolonged exposure to UV radiation.

Example 5
This example provides evidence that an organic paint with photocatalytic nano-particles is not as durable as an organic paint according to the invention, such as paint according to Example 3.

A typical polyurethane paint, according to **Table 1**, comprising nano-sized anatase TiO_2 powder was formulated for comparison. Several 200µm thick paint films (wet thickness) were applied on panels and put into a QUV test chamber where the films were subjected to cycles of 4 hours of UV-radiation, where the temperature is maintained at 60°C, followed by 4 hours moisture condensation, where the temperature is maintained at 50°C. The wavelengths emitted from the UV lamps in the QUV chamber were in the range of 290 -450nm with the highest intensity at 340nm. Emission characteristics of the UVA-340 lamps used in the QUV chamber and the wavelengths emitted and the intensity can be seen in **Figure 12**.

A polyurethane binder was chosen because of its far better UV stability than an alkyd binder. **Figure 10** shows the difference before UV exposure and after 1500 hours exposure. Even though a far more UV resistant binder than alkyd was chosen the film was literally disintegrated after 1500 hours in a QUV chamber and the chalking of the film was so heavy that the surface of the film appeared more as loose fine powder than a solid paint film.

Example 6
This example provides evidence that a typical alkyd paint film (Table 1), comprising hollow glass microspheres coated with anatase TiO_2, as described in example 1, provides a self cleaning surface.

To test the self cleaning effect of a paint system designed according to the invention, the surface of a typical alkyd paint, comprising coated glass beads according to Example 1, added as 40% of the volume of solids in a dried paint film, and another sample of the same paint, with essentially the same amount of uncoated glass beads, were contaminated with a solution of methylene blue and allowed to dry. The paint panels were then exposed to UV-radiation and humidity in a QUV chamber. The results are shown in Figure 11. The same amount of methylene blue was applied to both panels, but presumably due to the hydrophilic nature of the TiO_2-coating on the beads, the methylene blue solution was spread over a much larger area on the paint film with coated beads. After only 28 hours of exposure in a QUV chamber the stain on the film with coated beads had almost totally disappeared (Figure 8). This clearly demonstrates that the coated beads greatly accelerate the decomposition of methylene blue, providing support for the self cleaning effect of the paint film.

Example 7

This example provides evidence for a method for determining/quantifying the binding strength of a bound photocatalytic layer.

According to an embodiment of the invention, the photocatalytic material coated on the bead material has a high binding strength to the bead to ensure low release of nanoparticles. To test and/or quantify the release of photocatalytic anatase TiO_2 from hollow glass microspheres (HGMS), 10 grams of coated beads provided according to Example 1, are stirred into 250ml of distilled water in a 250ml beaker. The beaker is placed in a sonicator, such as a Bronson 1210 sonicator, and the mixture sonicated for a defined period of time, e.g. 40Hz , such as 30 minutes, using a defined power setting. While the mixture is sonicated it is lightly stirred for 30 seconds every 5 minutes. After sonication, the mixture is centrifuged to separate the coated HGMS and loose anatase powder and the weight of the loose anatase powder and coated HGMS measured.

List of References

Lachheb, Hinda; Puzenat, Eric; Houas, Ammar; Ksibi, Mohamed; Elaloui, Elimame; Guillard, Chantal; Herrmann, Jean-Marie. "Photocatalytic degradation of various types of dyes (Alizarin S, Crocein Orange G, Methyl Red, Congo Red, Methylene Blue) in water by UV-irradiated titania". Applied Catalysis B: Environmental, Vol. 39, 2002, 75-90.

Linsebigler, Amy L.; Lu, Guangquan; Yates, John T. "Photocatalysis on TiO2 Surfaces: Principles, Mechanisms, and Selected Results".
Chemical Review, Vol. 95, 1995, 735-758.

Portjanskaja, Elina; Krichevskaya, Marina; Preis, Sergei; Kallas, Juha.
"Photocatalytic oxidation of humic substances with TiO2-coated glass micro-beads".
Environmental Chemistry Letters, Vol. 2, 2004, 123-127.

Srinivasan, S.; Datye, A. K.; Smith, M. H.; Peden, C. H. F. "Interaction of Titanium Isopropoxide with Surface Hydroxyls on Silica". Journal of Catalysis, Vol. 145, 1994, 565-573.

BASF Handbook on Basics of Coating Technology, Artur Goldschmidt and Hans-Joachim Streitberger, 2003, Vincentz Network

Coatings Formulation, Bodo Muller and Ulrich Poth, 2006, Vincentz Network

Organic Coatings: Science and Technology, 3rd Ed., Zeno W. Wicks, Jr., Frank N. Jones, S. Peter Pappas, and Douglas A. Wicks, 2007, Wiley - Interscience

Industrial Inorganic Pigments, 3rd, Completely Revised and Extended Edition; Gunter Buxbaum and Gerhard Pfaff (Editors); ISBN: 978-3-527-30363-2 (2005)

Industrial Organic Pigments: Production, Properties, Applications, 3rd, Completely Revised Edition; Willy Herbst, Klaus Hunger, ISBN: 978-3-527-30576-6 (2004)

Claims

1. A self-cleaning coating composition (paint) comprising micro-sized particles coated with a functional layer, wherein the micro-sized particles are hollow or solid beads, or any combination/ratio of hollow and solid beads, wherein the beads comprise one or more material(s) selected from ceramic material(s); polymeric material(s); cermet material(s); metallic material(s); pigmented material(s); light-absorbing and/or light reflecting material(s); including any combination thereof.

2. A self-cleaning paint according to claim 1, wherein more than 95% of the particles have an equivalent diameter in the range of 1-1000µm, 1-500µm, 10-200µm or 1-20µm; optionally wherein the particles are hollow glass beads, such as hollow glass micro spheres (HGMS).

3. A self-cleaning paint according to claim 1 or 2, wherein the beads or particles are coated with a photocatalytic layer providing photocatalytic activity, said layer and/or photocatalytic activity providing one or more of:
    a. reduction in growth of (micro)organisms, such as one or more of: bacteria, algae, lichen, yeasts and/or moulds;
    b. increase in adhesion strength between an organic binder and a bead by chemical bonding;
    c. increase in abrasion resistance of the paint film;
    d. increase in weather resistance and/or UV-stability, such as one or more of: (i) reduction of chalking of an organic binder; (ii) reduction of decomposition of an organic binder; and/or (iii) reduction of release of (photocatalytic) material and/or material with a particle size of less than 1 µm;
    e. decomposition and/or oxidation of undesired organic matter and/or dirt and/or
    f. improvement of wetting property of the paint.

4. A self-cleaning paint according to any one of the preceding claims, wherein the layer comprises one or more of:
    a. a photocatalyst and/or n-type semiconductor having a band gap in the range of 1.8-10.3, 2.5-6.2 or 3.1-4.1 eV;
    b. a photoconductive material/composition; and/or
    c. a photocatalytic material/composition; optionally comprising one or more catalyst(s) selected from the group consisting of: TiO_2, ZnO, WO_3, SnO_2, CaTiO3, Bi_2S_3, Cu_2O, Fe_2O_3, ZrO_2, SiC and $Ti_xZr_{(1-x)}O_2$ ($0 < x < 1$), and any combination thereof; optionally doped with one or more co-catalyst(s), wherein the co-catalyst is selected from the group consisting of palladium, platinum, rhodium, ruthenium, tungsten, molybdenum, gold, silver, copper, including any of their oxides and/or any of their sulfides, and any combination/mixture/ratio of two or more of palladium, platinum, rhodium, ruthenium, tungsten, molybdenum, gold, silver, copper, including any of their oxides and/or any of their sulfides; wherein the molar ratio of co-catalyst(s) to catalyst is optionally less than 1 ppm, 1 ppm - 0.1%; 0.1-1%, 1-10%, or more than 10%; and/or wherein said co-catalyst covers optionally less than 10%, 5%, or 1% of the surface area of the photocatalytic layer; and/or wherein said co-catalyst covers optionally between 0.001-3%, or 0.01-2% of the surface area of the photocatalytic layer.

5. A self-cleaning paint according to any one of the preceding claims, wherein the photocatalyst and/or n-type semiconductor has a band gap of around ~3,2 eV (~388 nm), and/or wherein the photocatalyst and/or n-type semiconductor is doped with one or more of N-, S-, and F-atoms, including any combination and/or ratio thereof.

6. A self-cleaning paint according to claim 4 or 5, wherein the photocatalytic material is covalently bound to said beads/particle; wherein the photocatalytic material coated on the beads optionally has a crystal size of 1 -150nm; and wherein the photocatalytic material coated on the beads optionally has a specific surface area (e.g. BET surface area) in the range of 0.01-100; 0.1-50; 0.1-30, or 0.1-10 m^2/g.

7. A self-cleaning paint according to any one of claims 4-6, wherein the photocatalytic layer comprises TiO_2 in the crystal form of rutile and/or anatase.

8. A self-cleaning paint according to claim 7, wherein more than 90%; 99%; or 99.9% (weight/weight) of the TiO_2 in the photocatalytic layer is in the catalytic active form of anatase.

9. A self-cleaning paint according to claim 7 or 8, wherein in average 10^5-10^{10}; and/or at least 10^2, 10^5, 10^{10} or more individual anatase crystals are bound per bead/particle; and/or wherein the weight of the bound anatase is more than 0.001%; 0.01%; 0.1%; 1%; or 10% of the weight of the particle/bead.

10. A self-cleaning paint according to any one of claims 7-9, wherein the coating composition (paint) comprises less than 1%; 0.1%; 0.01%; 0.001%; 0.0001%; or 0.00001% anatase particles not bound to micro-sized beads; and/or derived/released from the micro-sized beads, determined as weight/weight of non-covalently bound anatase / total amount of anatase.

11. A self-cleaning paint according to any one of the preceding claims, wherein the paint is alkyd-, acryl-, polyurethane-, epoxy-, and/or co-polymer-based., wherein said paint comprises:

12. A self-cleaning surface comprising a dried layer (paint film) derived from a self-cleaning paint according to any one of claims 1-11.

13. A method of cleaning a surface according to claim 12, comprising the step of exposing said self-cleaning surface to electromagnetic radiation, wherein said electromagnetic radiation comprises radiation with a wavelength in the range of 200-400 nm and/or 400-800 nm, wherein said radiation is provided by the sun (e.g. daylight, reflected sunlight, twilight, moonlight), or by an artificial source.

14. A method of cleaning a surface according to claim 12, wherein said wavelength comprises 388 nm or less, and/or a wavelength corresponding to the band-gap of the photocatalyst and/or n-type semiconductor, or a wavelength shorter than the band-gap of the photocatalyst and/or n-type semiconductor.

15. Use of a self-cleaning coating composition (paint) according to any one of claims 1-14 for providing a self-cleaning surface on wood, brick, concrete, cement, asphalt, natural or artificial stone, clay, glass, plastic, metal, fibre glass, carbon fibres, (wall) paper, painted surface, glued surface, composite material, or any combination thereof, such as a surface on an item, wall,

building, structural element, bridge, building element, building block, window, door, floor, ceiling, roof (sheathing), smoothed and/or plastered surface, furniture, house hold equipment, medical equipment, sanitary equipment, car, (motor)bike, truck, container, bus, aircraft, rocket, ship, train, locomotive, wind mill, or solar panel.

Abstract

The current invention relates to compositions with self-cleaning properties. More particularly, the invention concerns coatings or paints comprising particles coated with a catalytically active composition. In particular, a self-cleaning coating composition (paint) is provided, comprising micro-sized particles coated with a functional layer, wherein the micro-sized particles are hollow or solid beads, or any combination/ratio of hollow and solid beads, wherein the beads comprise one or more material(s) selected from ceramic material(s); polymeric material(s); cermet material(s); metallic material(s); pigmented material(s); light-absorbing and/or light reflecting material(s); including any combination thereof.

Figures

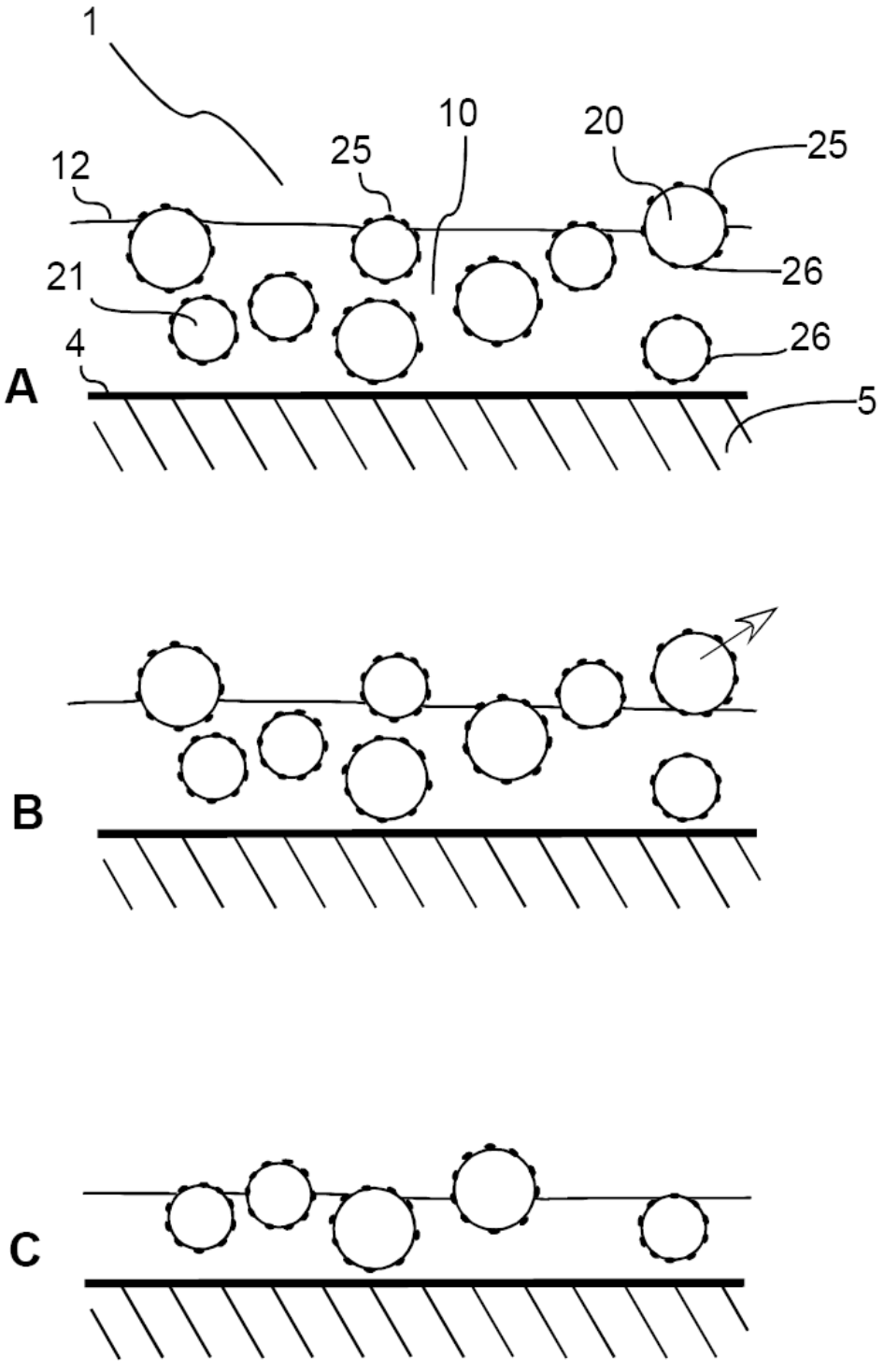

Figure 1

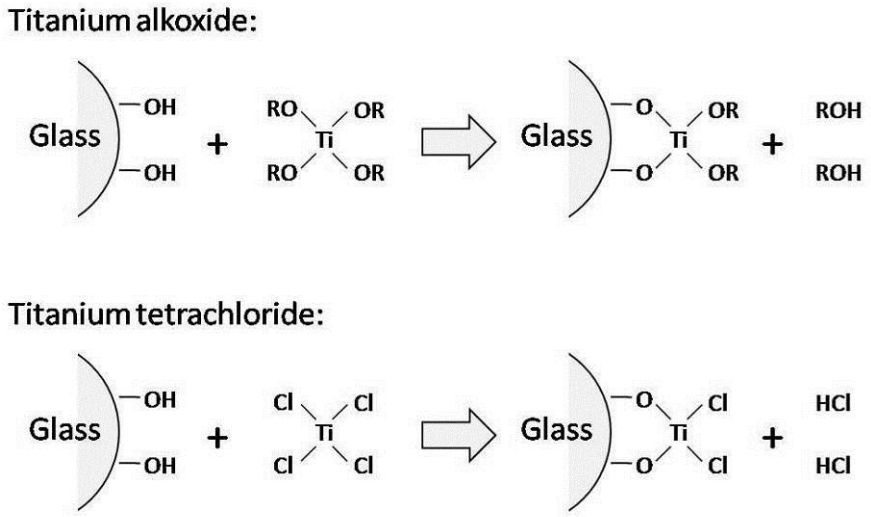

Figure 2

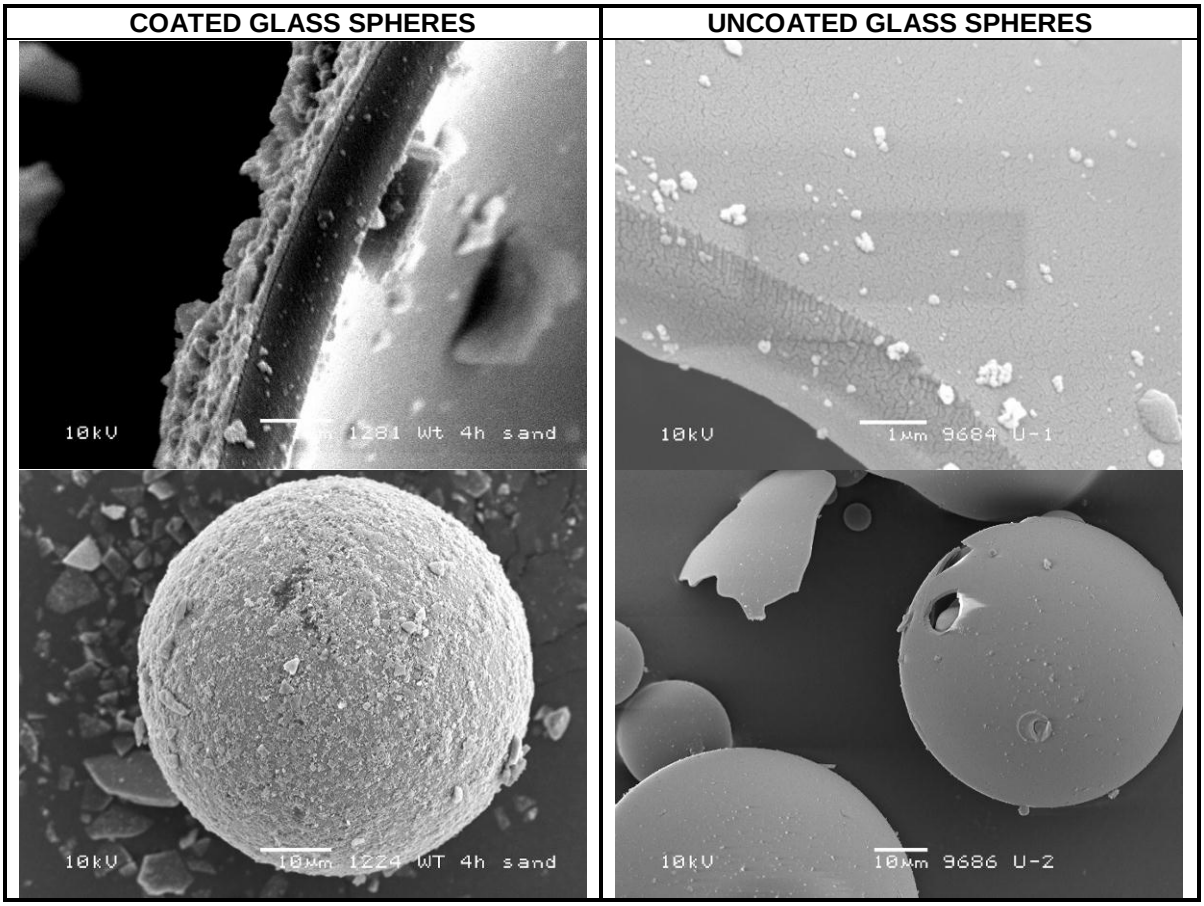

Figure 3

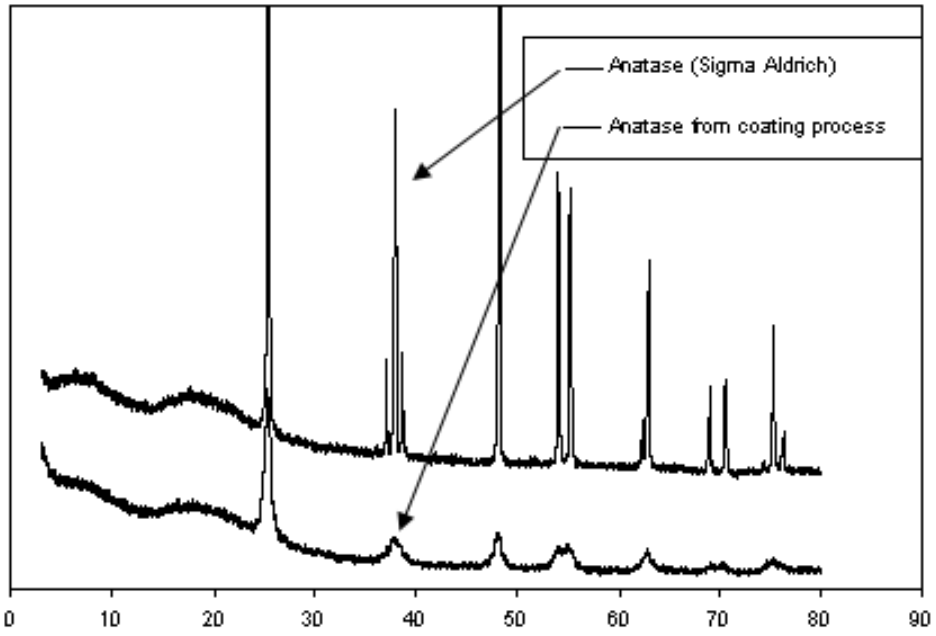

Figure 4

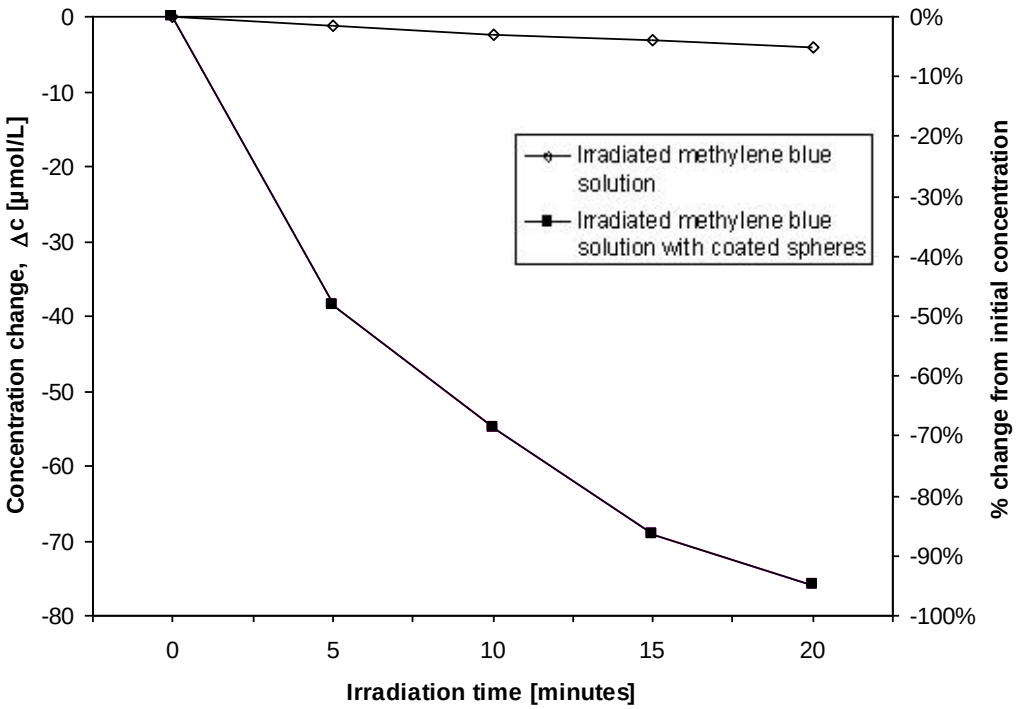

Figure 5

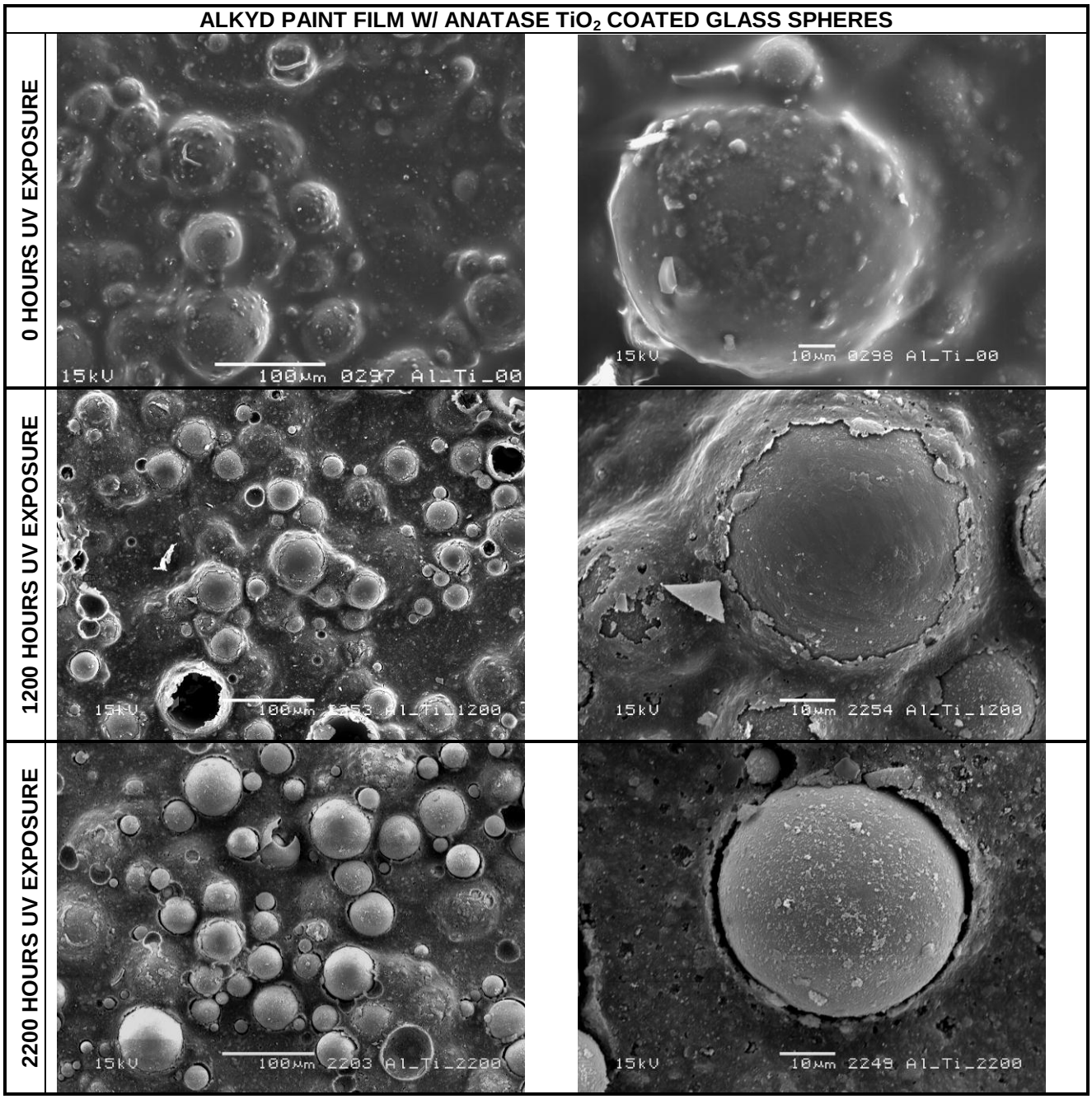
ALKYD PAINT FILM W/ ANATASE TiO2 COATED GLASS SPHERES
0 HOURS UV EXPOSURE
1200 HOURS UV EXPOSURE
2200 HOURS UV EXPOSURE
15kV 100µm 0297 Al_Ti_00
15kV 10µm 0298 Al_Ti_00
15kV 100µm 2253 Al_Ti_1200
15kV 10µm 2254 Al_Ti_1200
15kV 100µm 2203 Al_Ti_2200
15kV 10µm 2249 Al_Ti_2200

Figure 6

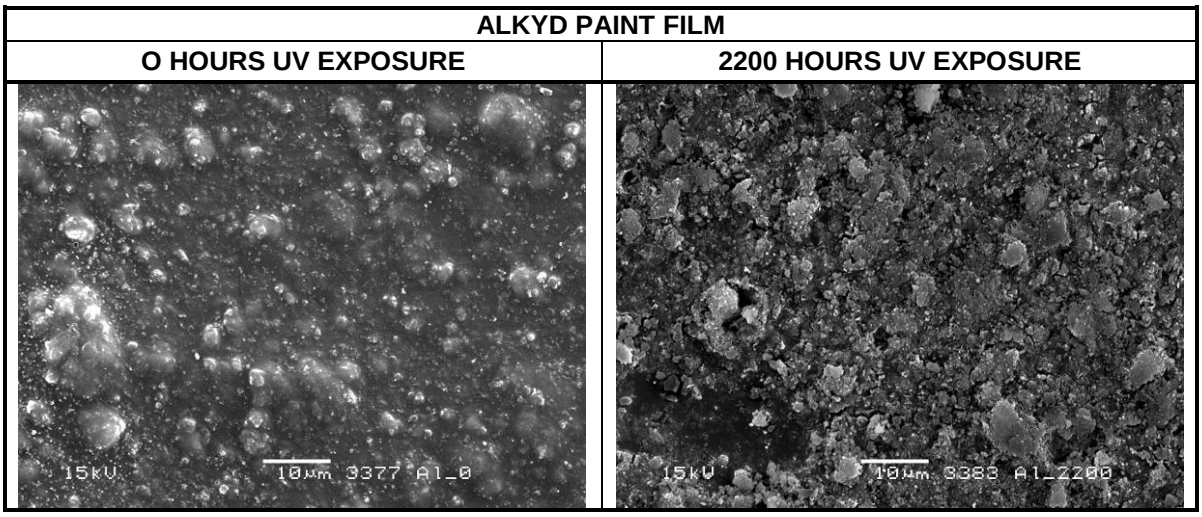
ALKYD PAINT FILM
O HOURS UV EXPOSURE
2200 HOURS UV EXPOSURE
15kV
10µm 3377 Al_0
15kV
10µm 3383 Al_2200

Figure 7

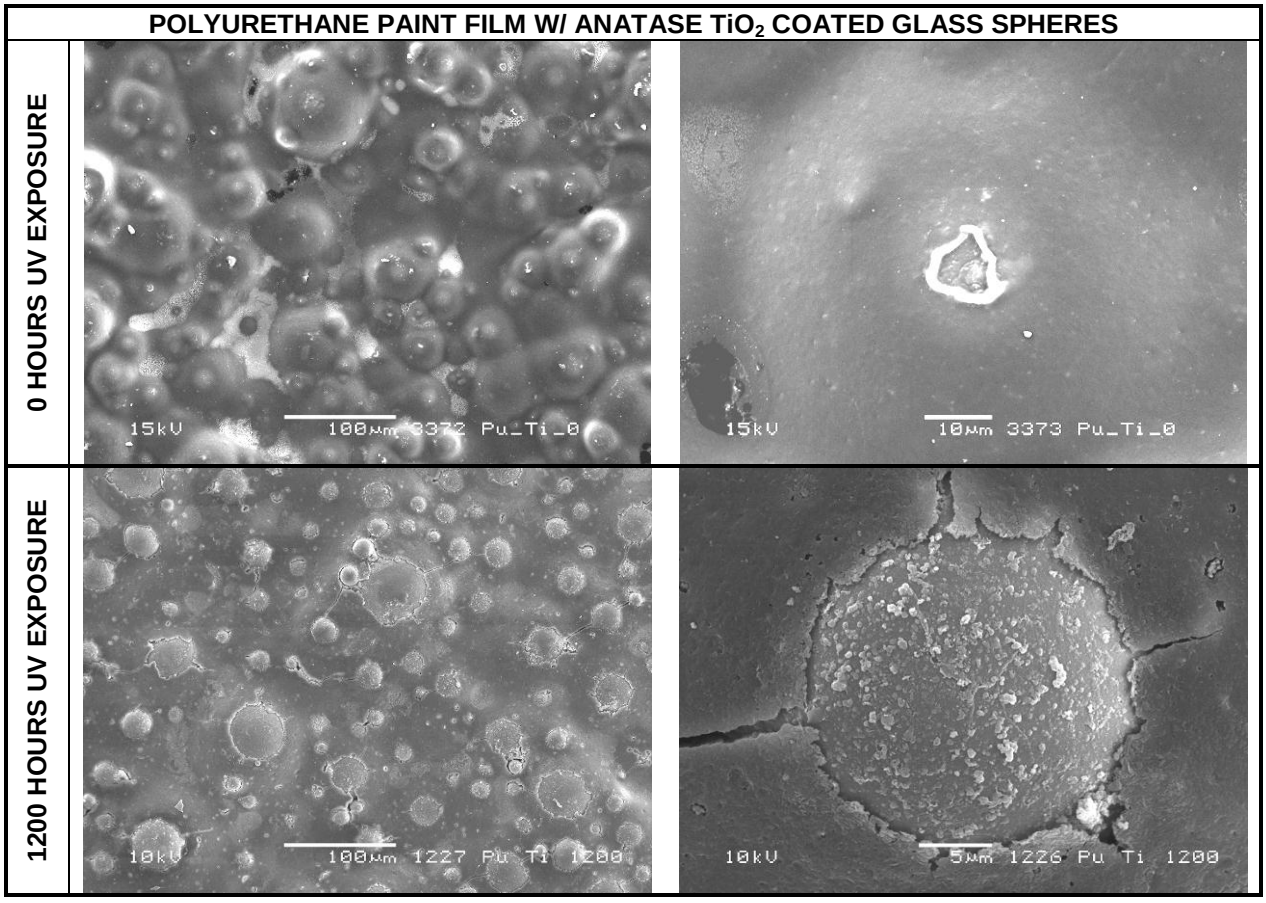
POLYURETHANE PAINT FILM W/ ANATASE TiO2 COATED GLASS SPHERES
0 HOURS UV EXPOSURE
1200 HOURS UV EXPOSURE
15kV
100µm 3372 Pu_Ti_0
15kV
10µm 3373 Pu_Ti_0
10kV
100µm 1227 Pu Ti 1200
10kV
5µm 1226 Pu Ti 1200

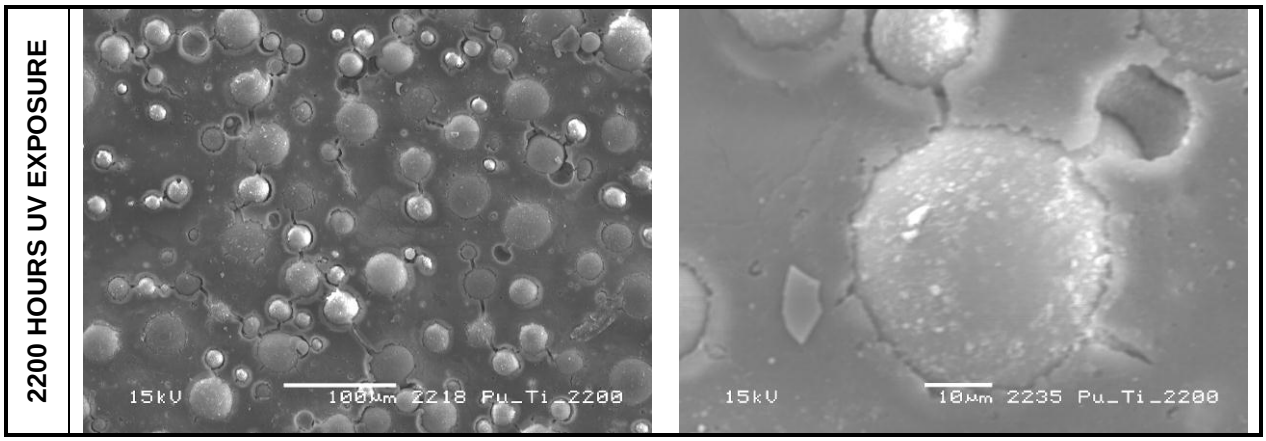

Figure 8

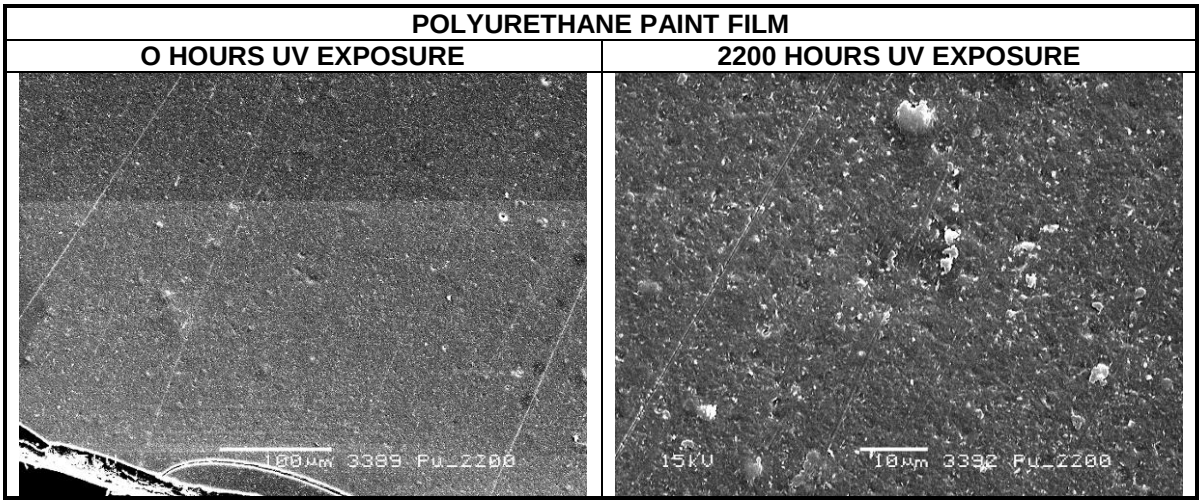

Figure 9

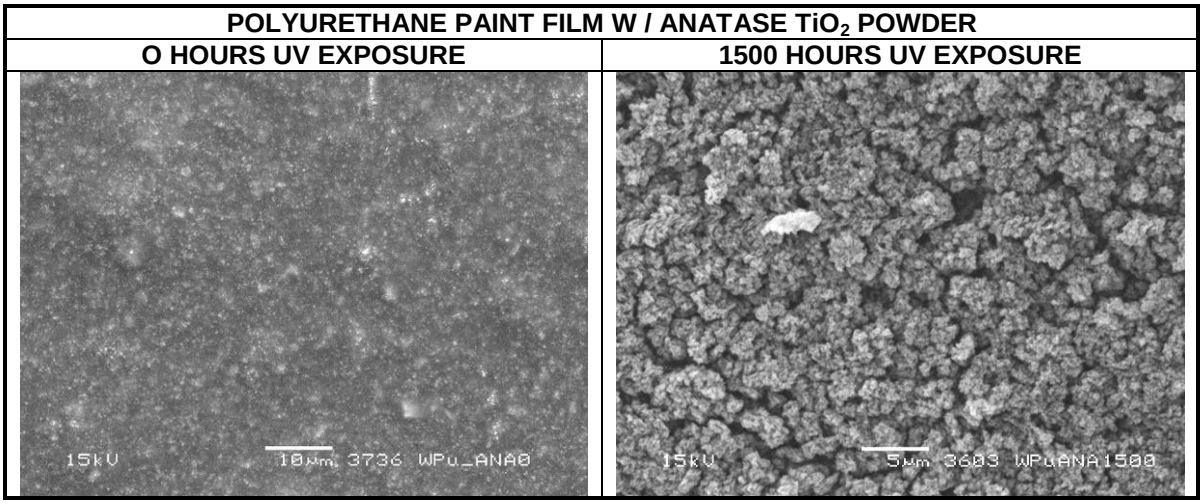

Figure 10

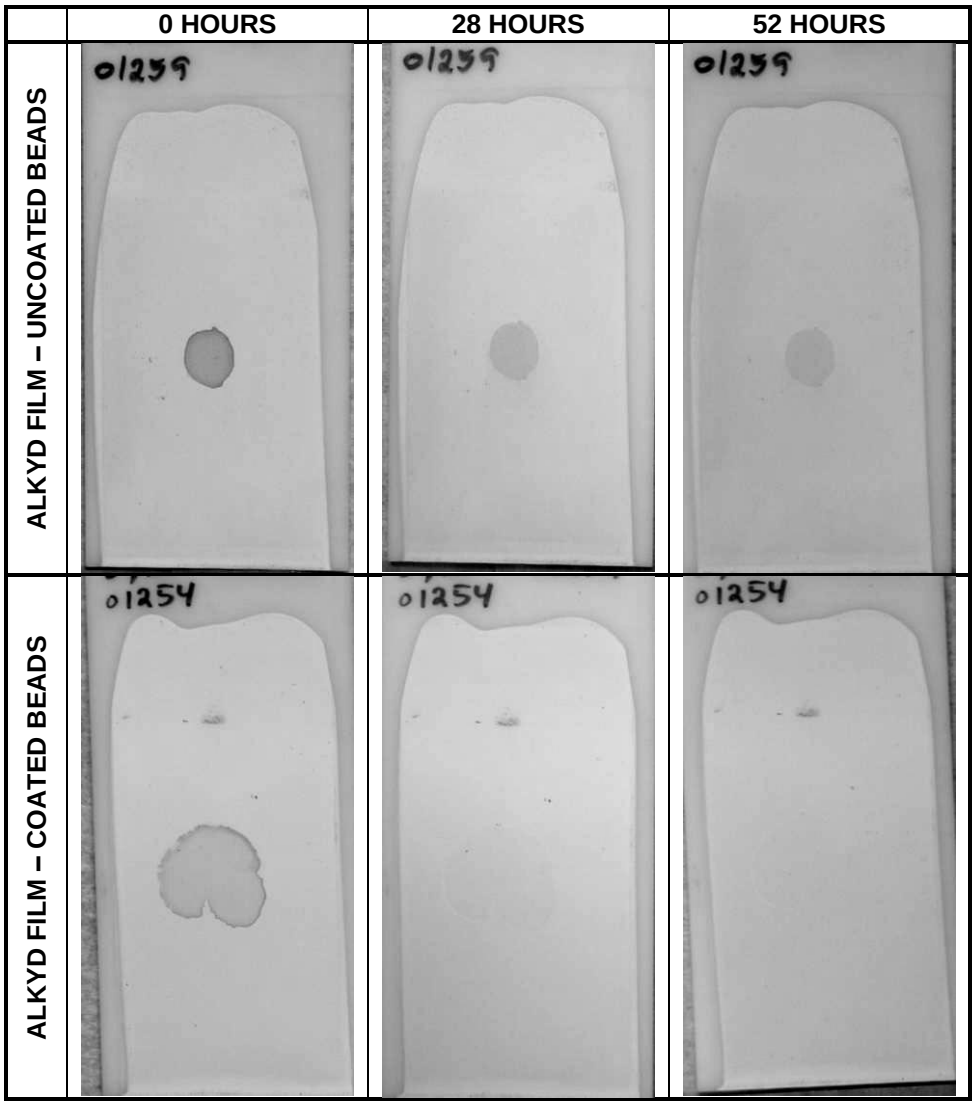
0 HOURS
28 HOURS
52 HOURS
ALKYD FILM – UNCOATED BEADS
ALKYD FILM – COATED BEADS
01259
01254

Figure 11

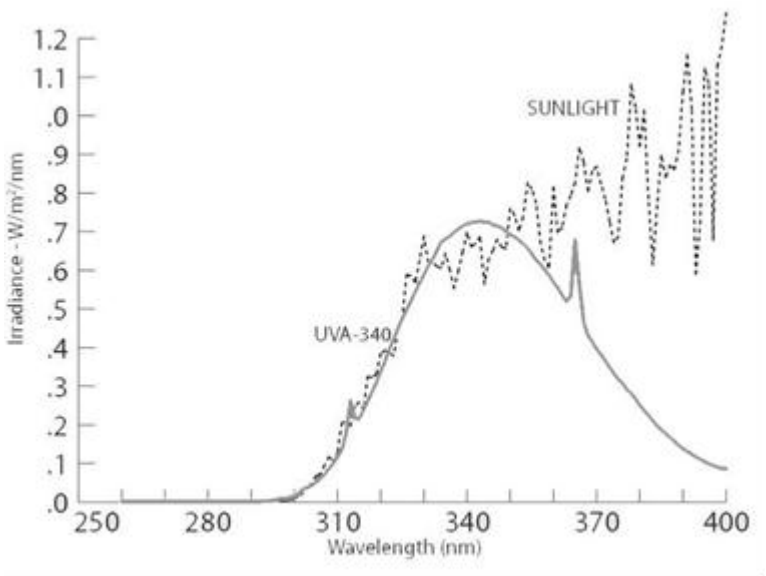
1.2
1.1
.0
.9
.8
.7
.6
.5
.4
.3
.2
.1
.0
Irradiance - W/m²/nm
SUNLIGHT
UVA-340
250
280
310
340
370
400
Wavelength (nm)

Figure 12